Distinct functional roles of microRNA-23b and microRNA-26a in breast cancer pathogenesis

BY

LOREDANA PELLEGRINO

A thesis submitted for the degree of Doctor of Philosophy

at Imperial College London

Faculty of Medicine,

Department of Oncology, 1st floor ICTEM

Imperial College London

Hammersmith Hospital, Du Cane Road

London, W12 0NN

Supervisor: Prof Justin Stebbing

Co-supervisor: Dr Leandro Castellano

Dedicated to…

my boyfriend Ale…

for having taken care of all the "housewife" stuff during the whole writing up stage,

for having made me laugh when I only wanted to cry,

for your tireless support and encouragement,

for your infinite patience,

for you being you,

My One.

my parents and my sister…

for your constant comfort and support, despite being far away,

for knowing how to deal with my stubbornness,

for having made this possible,

for always believing in me.

Statement of originality

All the experimentation presented in this thesis has been conducted by myself, aside from the following:

Results section 3.1: Bioinformatic analyses were performed by Dr Leandro Castellano. Plots showed in Figure 31C were carried out by Dr Matthew Caley; analysis of the phase-contrast time lapse cell tracking assays was conducted by myself.

Chromatin immunoprecipitation (ChIP) assays and relative primer design were performed by Dr Leandro Castellano.

Human breast cancer MDA-MB-231 cells isolated from metastatic loci in immunocompromised mice were kindly provided by Prof Harikrishna Nakshatri.

Primary breast cancer and lymph node metastatic samples were acquired from surgery undertaken by members of the Breast Surgical Department at Imperial College London, specifically Miss Jacqueline Lewis. The samples were analysed and histopathologically characterised by Prof Sami Soushi, the lead breast cancer pathologist at Imperial College.

Total RNA extraction from these tissue samples was performed by Dr Jonathan Krell; real time RT-qPCR assays on total RNA extracted from tissue samples were conducted by Dr Leandro Castellano and myself and data analysis was performed by Dr Leandro Castellano.

In vivo animal studies were conducted by Dr Leandro Castellano, Dr Adam Frampton, Dr Manikandan Periyasamy and myself. Immunohistochemistry and histopathological analysis of tissue samples isolated from mammary primary tumour and metastatic lymph nodes formed in nude mice was performed by Dr Mona Elbahrawy. Quantification and statistical analysis were performed by Dr Leandro Castellano and myself.

Results section 3.3: RNA-sequencing was carried out by Genomic Laboratories, MRC Clinical Sciences Centre, London UK. RNA-sequencing and relative bioinformatic analyses were conducted by Dr Leandro Castellano.

I am appreciative of the help from the aforementioned.

Loredana Pellegrino

Copyright declaration

Aknowledgements

I would like to express my most sincere gratitude to my boss, Prof Justin Stebbing, for giving me the opportunity to be part of his prestigious lab and taking me under his wing throughout this unique experience. Thank you for being an unlimited source of patience, knowledge and inspiring ambition.

I would like to thank my supervisor, Dr Leandro Castellano for helping me establish a scientific mindset, for his immense expertise and knowledge, for always knowing the answer and for his essential role in the evolving of this project.

I would like to specially thank all my lab colleagues, who have created the best working environment I could have ever asked for.

Jimmy Jacob… You welcomed me in the lab as you knew me for ages; you have been and still are the most trustworthy and unconditionally giving person; you made the difference in my PhD and "London" experience; you… thank you, friend.

Laura Roca-Alonso, my Laurita. You brought the female support that I was looking for in our initially boy-dominant lab. Your sparkling energy, your pure sensitivity and your exhilarating personality grew on me very quickly and fast-forwarded our friendship.

Dr Adam Frampton, for being a very enjoyable guy, despite his very busy schedule. Thank you for your support in teasing Jimmy, your countless advices and your ever-lasting encouragement.

Dr Jonathan Krell, for having brought the "muscle" in the lab, for his peculiar sense of humour and for his kind support.

Alex De Giorgio, for always telling intriguing facts, for his passionate interest in science and not only, for the critical reading of my thesis.

Dr Victoria Harding, Toey, for being so contagiously humorous and caring, for being always helpful and for the critical reading of my thesis.

I would also like to thank Dr George Giamas for his precious advices and support. And a big thank you to Dr Hua Zhang, Dr Andy Photiou, Lit Lei Cheng, Arnhild Gothey, Yichen Xu, Dr

Ylenia Lombardo and Dr Monica Faronato for having made each day (and weekend) in the lab joyful and unique.

A particular thank you to Dr Ana Gomes, Joao Nunes and Nair Bonito, for their countless advices, for always being genuine and offering a comforting smile or a drink (at off working hours of course).

Thank you to all the people in the department for having greatly contributed to the nice time I have had in all these years.

A thank you to my special friends Dario Di Biase and Cecile Guillaume, for always encouraging me and spoiling me with awesome dinners and feasts.

Abstract

Tumour formation and metastasis are distinct processes that arise from cumulative alterations of genomic and epigenetic regulation. Uncontrolled modulation of cell cycle-related genes is crucial to tumour growth and additional genetic modifications provide cancer cells with motile and invasive phenotypes, leading to metastatic dissemination.

The cytoskeleton constitutes the structural support to cell motility, invasion and adhesion. Among the best-characterised cytoskeletal modulators are the p21-activated kinases (PAKs). In breast cancer (BC), the HER2 pathway controls the cytoskeletal dynamics and cell motility via PAK activation, through distinct downstream signaling mechanisms.

MicroRNAs (miRNAs) are small, non-coding RNAs that modulate gene expression post-transcriptionally. MiRNAs dysregulation can contribute to tumorigenicity, cell motility and metastasis by affecting relevant signaling pathways.

We identified PAK2 as target of both miR-23b and miR-26a, implicating a direct role for these miRNAs in cytoskeletal remodeling. Experimentally, expression of miR-23b and miR-26a in BC cells promotes focal adhesions and cell spreading on substrates, but miR-23b alone controls cell-cell junctions and lamellipodia formation.

Despite sharing the same target, the two miRNAs show additional distinct functions. MiR-26a overexpression in BC leads to formation of aneuploid cells associated with higher tumorigenicity. On the other hand, miR-23b inhibition enhances BC cell migration, invasion and metastasis *in vivo*. Clinically, low miR-23b levels correlate with metastatic development in BC patients. Mechanistically, growth factor-mediated signal transductions activate the transcription factor AP-1 and we show that this transcriptionally reduces miR-23b expression thus releasing PAK2 from its translational inhibition. The distinct cellular phenotypes described by the two miRNAs indicate that their global functions depend upon all the genes they regulate. Using RNA-sequencing and luciferase reporter assays, we validated a subset of genes as direct targets of either the two miRNAs. These genes are crucial to distinct molecular pathways and contribute to elucidate the observed phenotypes induced by miR-23b and miR-26a modulation.

CONTENTS

LIST OF FIGURES

LIST OF TABLES

ABBREVIATIONS

αPIX: PAK-interacting exchange factor alpha
µg: Microgram
µl: Microliter
23b: hsa-miR-23b
26a: hsa-miR-26a
ABL2: Abelson tyrosine kinase-protein 2
AIIt: Annexin II tetramer
AJ: Adherens junction
ANAPC10: Anaphase-promoting complex subunit 10
ANXA2: Annexin 2
AP-1: Activator protein-1
APC/C: Anaphase-promoting complex or cyclosome
ARHGEF6: Rac/Cdc42 guanine nucleotide exchange factor 6
ARP2: Actin-related protein 2
ARP3: Actin-related protein 3
BC: Breast cancer
BCL2: B-cell lymphoma 2
BRCA1: Breast cancer 1
BSA: Bovine serum albumin
BUB1: Budding uninhibited by benzimidazoles 1 homolog
BUB1B: Budding uninhibited by benzimidazoles 1 homolog beta
BUB3: Budding uninhibited by benzimidazoles 3
c-MET: MET or MNNG HOS Transforming gene or hepatocyte growth factor receptor
CB: Cathepsin B
CCNB1: Cyclin B1
CCNB2: Cyclin B2
CCND3: Cyclin D3
CCNE1: Cyclin E1
CCNE2: Cyclin E2
CDC20: Cell division cycle 20
CDC42: Cell division cycle 42
CDK1: Cyclin-dependent kinase 1
CDK2: Cyclin-dependent kinase 2
CDK6: Cyclin-dependent kinase 6
CDKN1A: Cyclin-dependent kinase inhibitor 1A
CDKN2B: Cyclin-dependent kinase inhibitor 2B
CDKN2C: Cyclin-dependent kinase inhibitor 2C
CDKN2D: Cyclin-dependent kinase inhibitor 2D
CFL2: Cofilin 2
CHFR: Checkpoint with forkhead and ring finger domain, E3 ubiquitin protein

ChIP-seq: ChIP-sequencing
ChIP: Chromatin immunoprecipitation
CIN: Chromosomal instability
COOL: Cloned out of library
CSC: Cancer stem cell
CTC: Circulating tumour cell
CTDSP: Carboxy-terminal domain, RNA polymerase II, polypeptide A small phosphatase
CTNNB1: Catenin beta 1
CUP: cancer of unknown primary origin
d: Days
DAVID: Database for annotation, visualisation and integrated discovery
ddH20: Double distilled water
del: Deleted
DGCR8: DiGeorge syndrome critical region 8
DTT: Dithiothreitol
ECL: Enhanced chemiluminescence
ECM: Extracellular matrix
EDTA: Ethylenediaminetetraacetic acid
EGF: Epithelial growth factor
EGFP: Enhanced green fluorescent protein
EGFR: Epithelial growth factor receptor
EGTA: Ethylene glycol tetraacetic acid
EMT: Epithelial to mesenchymal transition
ENA/VASP: Enabled/Vasodilator-stimulated phosphoprotein
ENAH: Enabled Homolog (Drosphila)
ERBB: Erythroblastic leukemia viral oncogene homolog
EZH2: Enhancer of zeste homolog 2
FA: Focal adhesion
FACS: Fluorescence activated cell sorter
FAK: Focal adhesion kinase
FCS: Fetal calf serum
FX: Focal complexe
FZD7: Frizzled-7
g: Gram
GAP: GTPase activating protein
GDP: Guanosine diphosphate
GEF: Guanine exchange factor
GID: Guanosine nucleotide dissociation inhibitor
GLS: Glutaminase
GO: Gene ontology
GSK3β or **GSK3B**: Glycogen synthase kinase 3 beta

GSK: Glycogen synthase kinase
GTP: Guanosine (guanine) triphosphate
h: Hours
HCC: Hepatocellular carcinoma
IL6: Interleuchin 6
JNK: c-JUN N-therminal kinase
KEGG: Kyoto Encyclopedia of Genes and Genoms
LARP1: La Ribonucleoprotein domain family, member 1
LIMK1: LIM (Lin-11, Isl-1, and Mec-3) Domain Kinase 1
LIMK2: LIM (Lin-11, Isl-1, and Mec-3) Domain Kinase 2
LMO7: LIM domain only protein 7
LNA: Locked nucleic acid
M: Molar
MACF7: Microtubule-actin cross linking factor 1
MAD1L1: Mitotic arrest deficient, yeast, homolog-like 1
MAD2L2: Mitotic arrest deficient, yeast, homolog-like 2
MAP3K1: Mitogen-activated protein kinase kinase kinase 1, E3 ubiquitin protein ligase
MAPK: Mitogen-activated protein kinase
MCL1: Myeloid cell leukemia sequence 1
MET: Mesenchymal to epithelial transition
mg: Milligram
miRNA: MicroRNA
ml: Milliliter
MLC: Myosin light chain
MLCK: Myosin light chain kinase
MLCP: Myosin light chain phosphatase
mM: Millimolar
MMP: Metalloproteinase
MTDH: Methaderin
mut: Mutated
MYH9: Non-muscle, myosin heavy chain 9
MYL9: Myosin light chain 9
NF-κB: Nuclear factor kappa-light-chain-enhancer of activated B cells
nM: Nanomolar
NRAS: Neuroblastoma RAS viral oncogene homolog
nt: Nucleotide
ON: Overnight
PA: Plasminogen activator
PAGE: Polyacrilamide gel electrophoresis
PAK1: p21-activated kinase 1
PAK2: p21-activated kinase 2

PAK: p21-activated activated kinase
PBS: Phosphate-buffered saline
PCKε: Protein kinase C epsilon
PFA: Paraformaldehyde
PI3K: Phosphatydilinositol-3 kinase
PIK3R3: Phosphoinositide-3-kinase, regulatory subunit 3
PKC: Protein kinase C
Pol II: Polymerase II
PPP1R12A1: Protein phosphatase 1, regulatory subunit 12A
PTEN: Phosphatase and tensin homologue
PVRL1: Poliovirus-receptor-like 1
PVRL2: Poliovirus-receptor-like 2
qPCR: Quantitative polymerase chain reaction
RAP1A: RAS-related protein Krev-1 A
RAP1B: RAS-related protein Krev-1 B
RAP2C: RAS-related protein RAP-2c
RB1: Retinoblastoma 1
RISC: RNA-induced silencing complex
RLC: Regulatory light chain
RLC: RISC-loading complex
RNA-seq: RNA-sequencing
RNAi: RNA interference
ROCK: RHO-associated protein kinase threonine kinase
RPKM: Read per kilobase per million
RT: Room Temperature
SAC: Spindle assembly checkpoint
SDS: Sodium dodecyl sulphate
SEM: Standard error of the mean
siRNA: small interfering RNA
SNARE: SNAP (Soluble NSF Attachment Protein) receptor
Sp-23b: MiR-23b-sponge
Sp-26a: MiR-26a-sponge
SRB: Sulforhodamine B
SSH2: Slingshot homolog 2 (Drosophila)
STX2: Sintaxin 2
TBS: Tris-buffered saline
TBST: Tris-buffered saline and Tween® 20
TGFRβ or **TGFRB**: Transforming growth factor receptor beta
TJ: Tight junction
TJP1: Tight junction protein 1
TLN2: Talin 2

TP53: Tumor protein p53
tPA: Type plasminogen activator
TRE: TPA (12-O-tetradecanoylphorbol-13-acetate)-responsive element
Tris: Tris(hydroxymethyl)aminomethane
TSS: Transcription starting site
TU: Transcription unit
UCSC: University of California at Santa Cruz
UK: United Kingdom
uPA: Urokinase-like plasminogen activator
uPAR: Urokinase-like plasminogen activator receptor
UTR: Untraslated region
v: Volume
VAMP8: Endobrevin
VCL: Vinculin
w: weight
WASF2: Putative Wiskott-Aldrich syndrom protein family member 4
WASP: Aldrich syndrome protein
WAVE: WASP family verprolin homology protein
YWHAE: Tyrosine 3-monooxygenase/tryptophan 5-monooxygenase activation protein, epsilon polypeptide
°C: Celsius degrees

CHAPTER 1

INTRODUCTION

1.1 Cancer

1.1.1 Cancer is a leading cause of disease and death

Cancer is a major public health problem with an estimated 12.7 million people having been diagnosed with cancer worldwide in 2008. The cancer burden on the global population is so severe that about 14% of all deaths that occurred worldwide in 2008 were caused by cancer[1]. Due to persistent demographic growth and aging, cancer-related deaths are predicted to increase from 7.6 million in 2008 up to an estimated 13.2 million cases by 2030 across the world[2].

In the United Kingdom more than one in four deaths is due to cancer. 324,579 individuals were diagnosed with cancer in the UK in 2010 and 157,275 cancer-related deaths were estimated in the same year. Despite small increases in cancer incidence, mortality rates are decreasing in the UK. Since early 1990s, the number of people that died from cancer started to fall over the time and cancer mortality rates are predicted to decrease of a further 17% between 2011 and 2030[3-5] (**Figure 1**).

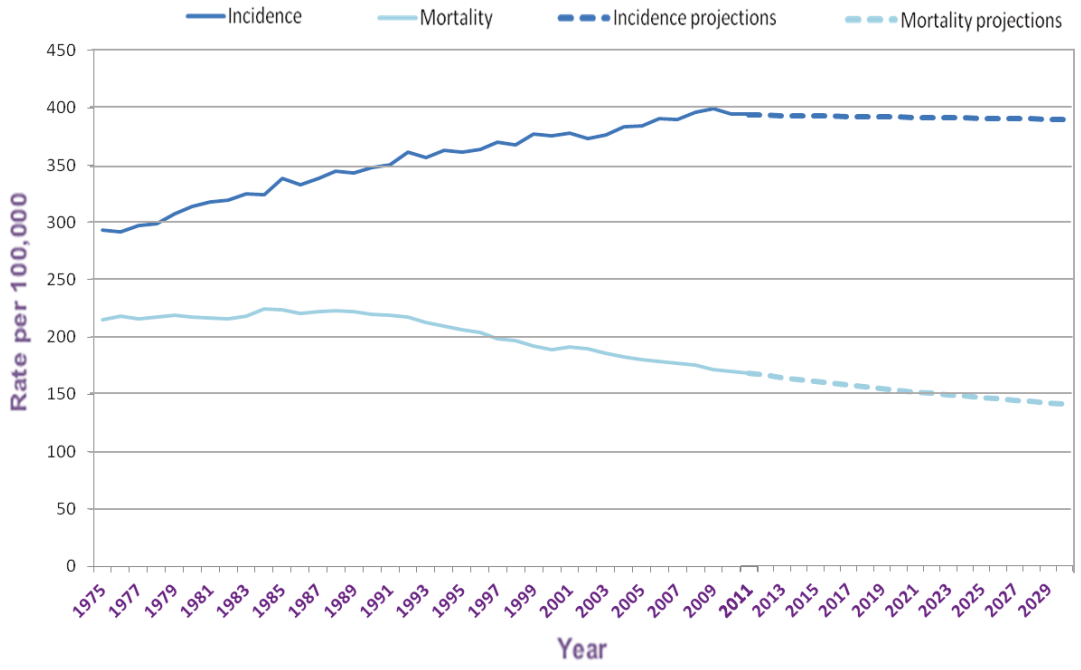

Figure 1: Cancer statistics in the UK. All cancers, European age-standardized incidence and mortality rates (1975-2010) and projections for both (2011-2030), Persons, UK. Modified from[4-7].

1.1.1.1 Breast cancer

For women, breast cancer (BC) is the most common malignancy seen across the world with 1.38 million cases diagnosed each year, representing the 23% of all cancers afflicting women worldwide[8]. Female BC is by far the most prevalent cancer in Western Countries with over 45,000 and 200,000 new cases estimated in 2010 in the UK and in the United States, respectively, representing the 31% and 28% of all cancers diagnosed in women in these populations[4, 8]. While fewer than 1% of BC diagnoses each year are male, one out of eight women will develop BC in her life time in the UK, a highly significant gender bias[9]. Over the past three decades, BC incidence rates have increased progressively, partly due to improved public awareness of BC disease and implemented BC screening programs, which allow earlier diagnosis and treatment. Along with these factors, advances in research and the development of more effective treatments, which combine improved surgery techniques, radiotherapy approaches and use of adjuvant endocrine therapies, have led to a marked decline of BC-associated mortality rates. Indeed, compared to mid-1980s, when BC-related deaths peaked in the UK, the mortality rates have decreased by about 39% in 2008-2010, with 12,000 women dying of BC in the UK each year[5] [10]. The major cause of mortality in BC patients resides in tumour progression and metastasis at distant sites, with a specific dissemination pattern involving the regional lymph nodes, lungs, bones and liver. BC metastasis is frequently associated with *de novo* or acquired resistance to therapies and/or secondary manifestations following relapse[10]. Thus development of new therapies directed to impede early steps of BC progression and dissemination to different organs is of crucial importance in order to abolish BC-associated mortality.

1.1.2 The hallmarks of cancer

In 400 BC, Hippocrates, a Greek physician and father of the Western medicine, gave cancer its name. He described chronic ulcers or growths that resembled malignant tumours as moving crabs and referred to them with the Greek words “carcinos” (from the Ancient Greek karkinos: crab) and “carcinoma”. He believed that cancer originated from a systemic excess of black bile, one of the four bodily humors (blood, phlegm, yellow and black bile)[11]. This simplistic view of cancer as humoral imbalance remained in force for the next 1400 years. It was only in the 19th century that Rudolph Virchow, father of the modern cellular pathology,

with his theory that all cells derive from other cells, led to the concept that cancer arises from a disordered multiplication of cells[12].

Nowadays, technological advances mean we are able to detect the exact localisation of molecules of about 20 nanometers in size inside a human cell and yet, a holistic understanding of cancer biology remains beyond our reach. Nevertheless, the scientific community has been able to define human tumour pathogenesis as a multistep process characterised by several hallmark traits that enable a normal cell to become cancer. These include:

- uncontrolled proliferative capabilities;
- adapting energy metabolism (to sustain cell proliferation);
- escape from tumour suppressor signals;
- resistance to cell death;
- unlimited replicative immortality;
- stimulation of the formation of new vessels (neoangiogenesis);
- accumulation of genome instability and mutation;
- tumour-promoting immune system stimulation (inflammation);
- overcome immune surveillance and
- activating invasion and metastasis.

Focusing on the main scope of this thesis, we will here elaborate some aspects of cancer pathogenesis, particularly highlighting the metastatic process and outlining the main features of chromosomal instability and aneuploidy. We will then introduce microRNAs (miRNAs), illustrating their biological features and their functional relevance in cancer development and progression.

1.2 Metastasis

Metastasis accounts for 90% of cancer-associated mortality, yet it remains the most poorly understood component of cancer pathogenesis. The formation of metastases is a highly complex, multistep process that requires the movement of tumour cells from one organ (the primary site) to a distant location and the development into a metastatic lesion[13].

Although it is believed that metastatic dissemination occurs in advanced steps of cancer progression, systematic spread of tumour cells was recently detected during the earliest pre-invasive phases of tumourigenesis both in mice and humans[14]. In rare cases (2 to 5% of all cancer cases), the primary tumour is no longer detectable at initial presentation so that the derived metastastic lesions are considered cancers of unknown primary site (CUPs)[15].

The molecular basis for traits such as invasiveness and metastatic dissemination has yet to be fully understood. The model of the clonal selection suggests that progressive accumulation of mutations in a given cell results in a clonal expansion, subject to microenvironmental pressures that select for tumour cells expressing traits advantageous for the primary tumour[16]. However, the discovery that populations of cells within a tumour are organised hierarchically, similar to normal tissues, led to the formulation of the cancer stem cell (CSC) model[17]. CSCs are distinguished by their capacities of self-renewal, tumourigenesis, and operationally defined as that subset capable of regenerating populations of cancer cells when xenografted into immunocompromised mice[18]. Their inherent resistance to chemotherapies and tumour seeding abilities may explain the high recurrence rates observed in many cancers; accordingly, specific targeting of this population has become an area of focus in basic research and drug development. As only a subset of cancer cells can overcome the numerous challenges encountered during metastatic progression, metastasis is generally an inefficient process[19, 20].

Simplistically, the metastatic cascade goes through a sequence of different steps[21] (**Figure 2**) that include:

- cancer cell motility, invasion and infiltration into the surrounding tissue;
- intravasation into blood or lymphatic vessels;
- survival and transit in the colonised vessels;
- arrest and extravasation;
- colonisation at a new site.

Tumour cells, at the origin site, start to locally invade the surrounding tissue moving along the extracellular matrix (ECM). Subsequently, intravasation occurs when tumour cells penetrate the capillary system (heamatogenous or lymphatic) and transit in the systematic circulation as circulating tumour cells, (CTCs). CTCs that are capable of surviving extravasate into the parenchyma of surrounding tissues at distant sites and form micrometastasis that may eventually grow into macroscopic secondary tumours[13] (**Figure 2**).

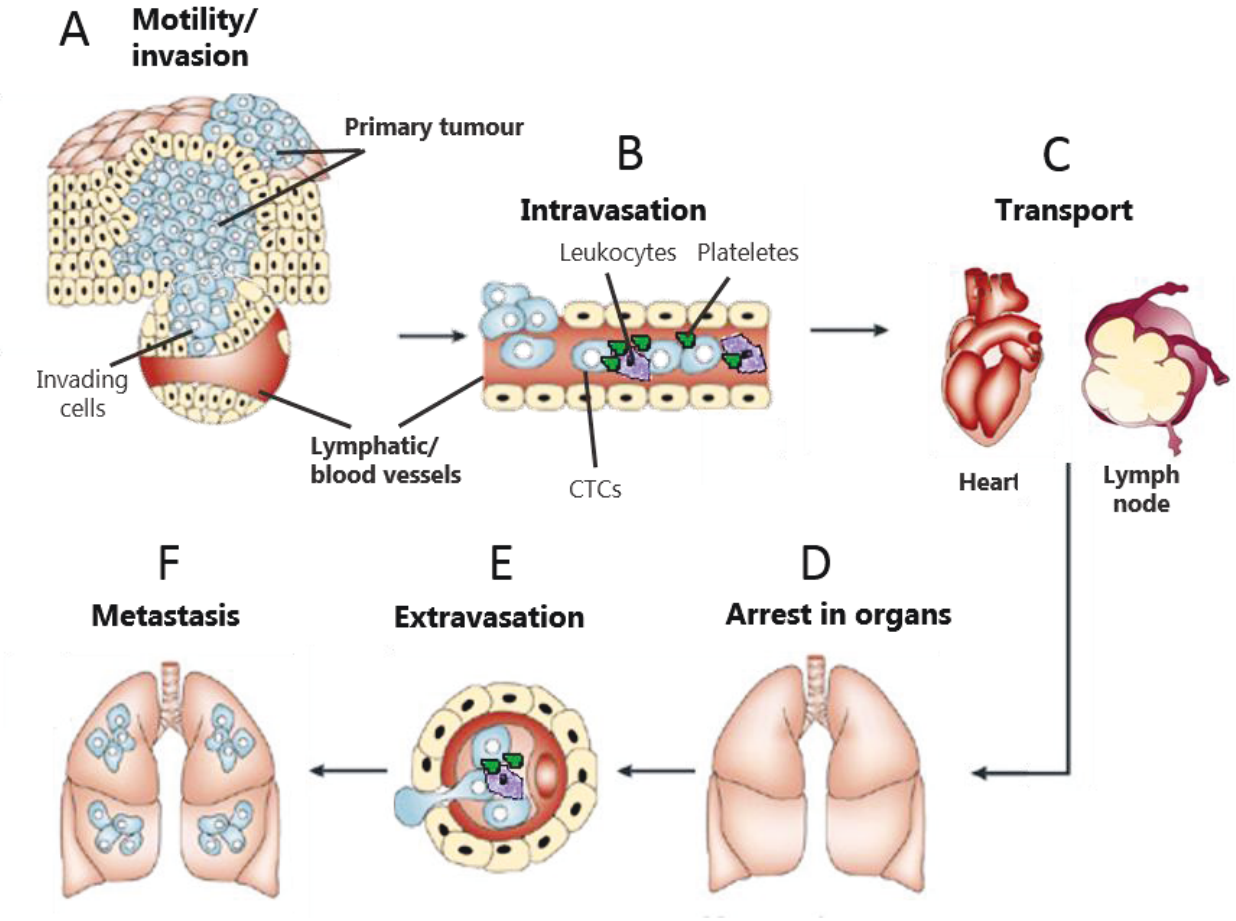

Figure 2: The metastatic cascade. **A,** Motility and invasion of primary tumour cells into the surrounding tissue and attraction towards nearby blood or lymphatic vessels. **B,** Intravasation into the lumen of the colonised vessels, where circulating tumour cells (CTCs) can interact with circulating host cells including leukocytes and platelets. **C,** Transport of tumour cells via hematogenous or lymphatic route. **D-E,** Arrest in the capillary beds of a distant organs and subsequent extravasation by eventual formation of micro emboli due to interaction with host cells. **F,** Colonisation of the distal organ and metastatic formation (here illustrated in the lung). Figure adapted from[22]

1.2.1 Step by step overview of the metastatic process

To unravel the complexity that lies behind each step of the metastatic process, it is essential to understand the biology and environment of tumour cells. As the majority (~85%) of cancer cases is represented by carcinomas that arise from epithelial tissues, we first elucidate the structural traits of a normal epithelium.

1.2.1.1 General structure of a normal epithelium

The epithelium is formed of coherent multicellular sheets called epithelia. Epithelial tissues can be constituted of a single epithelium or be stratified; some can cover the external surface of an organism, such as the epidermal covering of the skin, and others line internal organs and cavities, such as the acini in the mammary gland[23, 24]. A prototypic monolayer epithelium (**figure 3**), as well as its individual cells, is structurally characterised by an apical-basal polarisation. The apical region of the epithelia faces the outer surface or the lumen (generally filled by extracellular fluid) in case of epithelial cavities; on the other side, epithelia are anchored to the underlying tissue through the mechanical support of a heterogeneous mixture of extracellular matrix (ECM) material that includes:

- **The basement membrane :** a semi-permeable layer of an acellular mixture composed of laminin, nonfibrillar amorphous collagen (mostly type IV), heparan sulphate proteoglycans, and other glycoproteins, which are secreted by both the epithelial and the underlying mesenchymal cells[25] (**Figure 3**);
- **The stroma** (from the Greek word for "bed" or "bed covering")**:** also referred as mesenchymal connective tissue, is a supportive framework of ECM consisting of a ground substance, a porous, well-hydrated gel made of proteoglycan aggregates, tangled to a network of connective tissue fibers, such as collagen type I (the most abundant), elastic and collagen type III (reticular) fibers. Various types of cells are freely embedded in the stromal ECM, among these are fibroblasts, immune and inflammatory cells as well as nervous elements. The stromal tissue is also infiltrated by blood and lymphatic vessels that permit the rapid diffusion of nutrients, wastes and other chemicals between the local blood supply and the epithelium[26] (**Figure 3**).

The characteristic polarised orientation of epithelial cells is essential to guarantee the main function of the epithelium: they form effective barriers that protect from pathogens and separate the fluid that bathes their basal side from the chemically different fluid (or the external environment) on their apical side[24]. During the assembly of the epithelial layer, individual cells start to instate adhesive contacts between each other or with the underlying ECM that contribute to the establishment of the apico-basal polarisation. The successive maturation of these adhesions leads to the typical packed morphology of the epithelia, responsible for the scant mobility of the epithelial cells and their characteristic polygonal shape, in which vertices are points of contacts between two or more cells, and edges are contacts between adjacent cells[27]. The epithelial adhesive contacts show demarcated differences in morphology, structure and physical function, thus they are commonly distinguished in cell-cell adhesions, including tight junctions (TJs), adherens junctions (AJs) and desmosomes, and cell-matrix adhesions, amongst which focal adhesions (FAs) and hemidesmosomes are the most important ones.

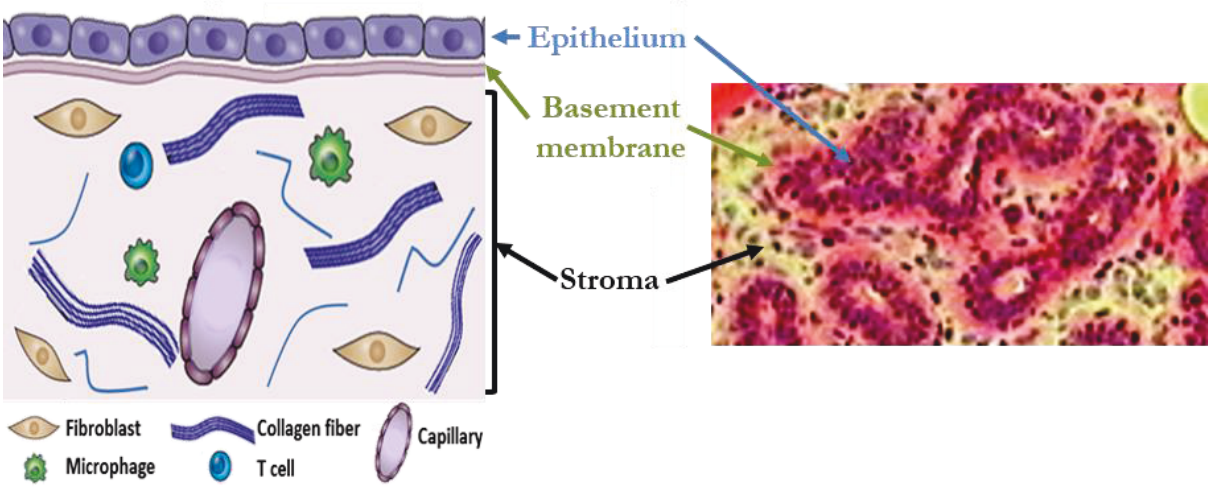

Figure 3: The normal epithelium and its environment. Schematic representation of a prototypical epithelium separated from the stromal compartment by the basement membrane (left panel). Different cell types are highlighted along with structural elements (modified from [28]). On the right, hematoxylin and eosin (H&E) staining of nuclei (purple) and protein rich structures (pink), respectively, of normal breast epithelial acini. Modified from[29] .

1.2.2 Cell motility and invasion

Cell motility encompasses cell invasion and together represent the first hallmark of metastasis. The ability of cells to migrate underlies varied physiological process, including embryogenesis, wound healing, inflammation and tissue regeneration. Despite that, deregulated migration contributes to several pathological processes, such as vascular disease, osteoporosis, chronic inflammation, mental retardation and cancer[29, 30]. Indeed, aberrant migration and acquired invasive capability allow cancer cells to break away from the primary tumour, make their way through the surrounding tissue and penetrate the capillary vessels during the first steps of the metastatic process (**Figure 4**). Thus, identification of signalling events, temporal triggers and/or spatial cues that modulate cell migration and invasion during metastasis is critical for the development of new therapeutic strategies.

Over the past decade, great progress has been made in understanding how tumour cells move in their physiological conditions *in vivo*. Until then, the cell migration model, derived from *in vitro* studies on different 2-dimensional (2D) cell cultures, was conceived as a cyclic process of coordinated steps required to migrate. These include: (1) extension of protrusion at the leading edge of the cell, (2) formation of adhesion to the substratum, (3) focalised proteolysis and degradation of ECM and (4) retraction of the trailing edge[30].

Development of new experimental approaches in the study of cell migration/invasion have highlighted important differences between the way in which tumour cells move *in vivo* compared with *in vitro*. Analysis of stimulated 3-dimensional (3D) cancer cell cultures and intravital imaging of primary tumours in live animals have shown that tumour cells can adopt different strategies of cell migration/invasion with increased speed and persistent directionality as compared to their slow, random mode of migration *in vitro*. These differences may be explained by the production of chemotactic signals (i.e., growth factors) by the tumour microenvironment and by the presence of specific ECM components that provide optimal adhesive substrates for cancer cell migration in physiological conditions[31].

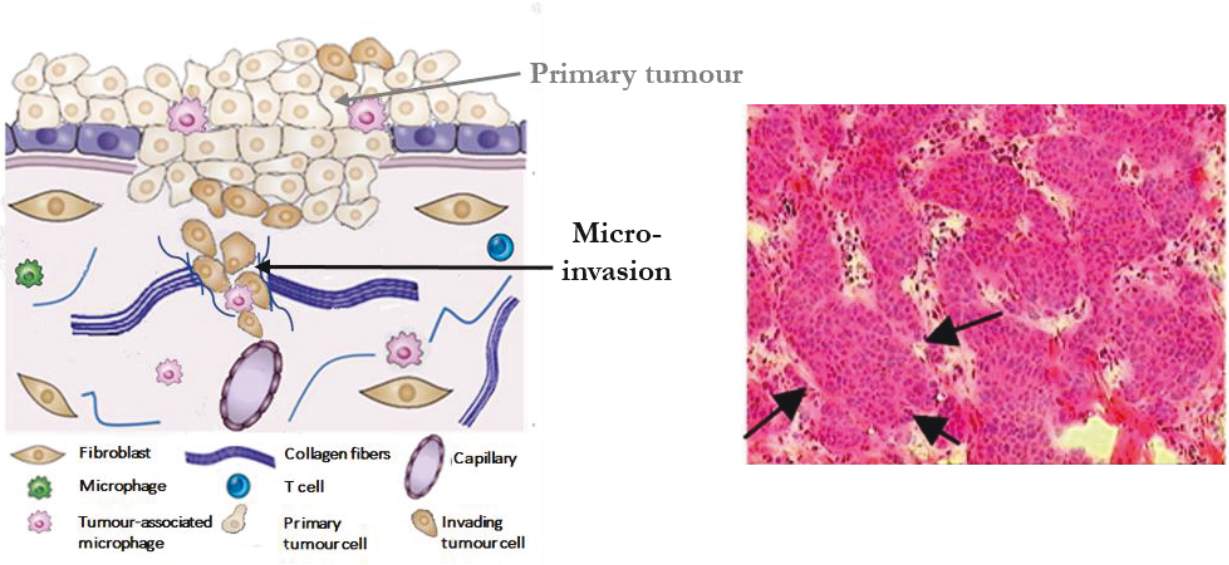

Figure 4: Invasion of primary tumour cells into the surrounding tissue. Schematic representation of invasive tumour cells into the underlining stroma (modified from [28]). On the right, hematoxylin and eosin (H&E) staining of nuclei (purple) and protein rich structures (pink), respectively, of invasive breast ductal carcinoma (black arrows) [29]

1.2.2.1 Different modes of invasive cell migration

Tumour cells move and invade either collectively or individually[32] (**Figure 5**).

In tumours, two morphological and functional variants of collective invasive migration have been described (**Figure 5A**). The first is protruding sheets and strands of tumour cells that maintain contact with the primary site, yet generate local invasion (**Figure 5A**). The second consists in cluster of cells that detach from their origin and extend along stromal tissue gaps (**Figure 5A**). Both the variants of cohesive movement are based on the same biomechanical model: cells in inner and trailing regions of the strand/cluster maintain cell-cell contacts and are passively dragged behind a subset of highly motile cells. These cells extend anterior protrusions (invadopodia–like) that attach and degrade the ECM and generate migratory traction at the leading edge[33].

Single-cell migration also can occur in two different morphological variants, amoeboid and mesenchymal types (**Figure 5A**). Amoeboid migration commonly refers to the movement of rounded cells characterised by blebs/pseudopodia protrusions that typically lack mature cell-matrix adhesions and actin-stress fibers. Rounded, blebby cells in fact do not adhere or pull on the substrate, but rather use high contractility to squeeze through the ECM in a propulsive,

pushing migration mode[34, 35] (**Figure 5A**). Mesenchymal cancer cells adopt a polarised, fibroblast-like shape and typically move via the multistep migration cyclic model. At the leading edge of the cells, the extension of membrane protrusions, such as lamellipodia and filopodia, is stabilised by assembly of new cell adhesion on the ECM (i.e., focal adhesions, FAs) and associated with stress fibers. Integrins, metalloproteinases (MMPs) and other proteases, such as the urokinase-type plasminogen activator (uPA), co-localise at FAs to execute pericellular proteolysis. Thus, ECM-cell contacts and ECM degradation allow the cell to retract the cell body by actomyosin-based contractility. Finally, the cell retracts its trailing edge by disassembly the adhesions at the rear.[36, 37] (**Figure 5A** and **B**).

Collective migration is a common feature of many different types of cancer, including both carcinomas (i.e., melanoma and BC) and tumours of the connective tissue, such as rhabdomyosarcoma and fibrosarcoma[38]. Individual motile tumour cells can originate from most solid stromal tumours, such as sarcomas[39] and gliomas[40], from leukemias and lymphomas[41], as well as from epithelial tumour sources, such as *in situ* carcinomas or multicellular sheets or clusters in cohesive migration[32]. This dual capacity can explain the observation that both collective and single migrating cells are simultaneously present in *vivo*, and that individual and collective migration modes are interconvertible. As a matter of fact, after departing from the primary site, tumour cells can adopt a different migration mode to suit modifications in the microenvironment or in their molecular scenario[42]. A well-studied model of tumour cell plasticity is represented by the process of epithelial-to-mesenchymal transition (EMT).

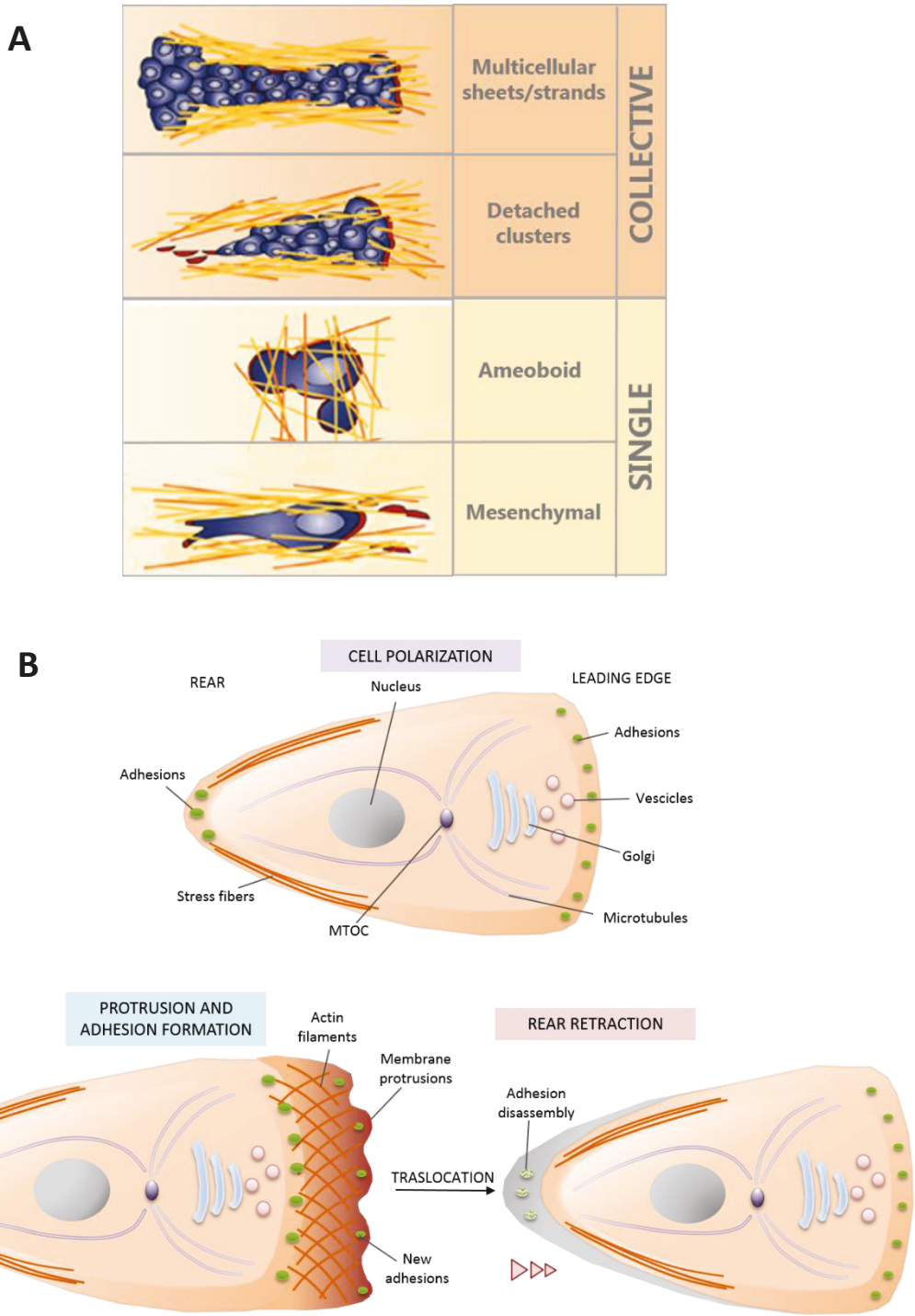

Figure 5. Different modes of cell migration. A, Mechanisms of collective migration as multicellular strands or detached clusters, and mechanisms of single-cell migration: amoeboid and mesenchymal[31]. **B,** Mesenchymal migration occurs via a multistep cyclic model: firstly, cell polarisation defines the leading edge and a rear tail of the migrating cell; secondly, membrane protrusions and formation of new adhesions at the leading edge allows the cell to pull the cell body and translocate after consecutive rear retraction via adhesion disassembly. Modified from[30].

1.2.2.1.1 Epithelial-mesenchymal transition

The epithelial-to-mesenchymal transition (EMT) describes a complex program through which epithelial cells lose their cell-cell contacts and switch from a collective migration pattern to a single cell mode of migration[36]. One of the characteristic findings in EMT is the loss of cell-cell adhesion with decreased expression of E-cadherin, the main cell-cell adhesion molecule[43]. E-cadherin expression is regulated by several transcription repressors, such as the zinc finger E-box-binding homeobox proteins 1 (ZEB1) and 2 (ZEB2), TWIST and the Snail family of zinc finger proteins SNAIL and SLUG[44-48]. In the process of EMT, SNAIL and ZEB2 initiate downregulation of E-cadherin whose repression is then maintained by SLUG and ZEB1 activity[49]. Various signal pathways, such as transforming growth factor (TGF)-β, the Wingless-int (Wnt) cascade and phosphatidylinositol 3‘‟kinase-serine/threonine kinase (PI3K/AKT) axis are connected with these transcriptional repressors of E-cadherin[50, 51]. TGF-β stimulation activates the PI3K/AKT axis and transcription factors of the SMAD family leading to expression of ZEBs, TWIST and SNAILs. The Wnt cascade releases β-catenin from degradation which can enter in the nucleus where it up-regulates SLUG and SNAIL. Alongside a cell‟‟s loss of epithelial properties, required in order to initiate an EMT, there is also the acquisition of a mesenchymal phenotype. In fact cancer cells undergoing to EMT *de novo* express several mesenchymal markers such as N-cadherin, Vimentin, and Fibronectin[52].

EMT has a major role in the initial step of the metastatic cascade: once tumour cells have spontaneously differentiated into a of single-cell state of migration, metastatic dissemination is promoted, resulting in poor prognosis[43]. In line with EMT as event of cancer cell plasticity in the initiation of metastatic spread, a process termed mesenchymal-to-epithelial transition (MET) has been proposed for tumour cells at later stages of the metastatic process. Studies have shown that tumour cells in the secondary organ can undergo „‟redifferentiation‟‟ to an epithelial phenotype and form metastases with similar histological characteristics as the primary tumour[53]. The tendency of disseminated cancer cells to undergo MET likely reflects the local microenvironment that they encounter after extravasation, i.e., the absence of the heterotypic signals responsible for the induction of EMT in the first site after departing from the primary tumour[41].

1.2.2.2 Proteolytic degradation of ECM

During the metastatic process, the ECM constitutes a mechanical support allowing malignant cells to adhere and migrate and, at the same time, serving as a physical barrier that prevents cell invasion of the surrounding tissue. Migrating cells overcome the ECM obstacle using different approaches depending on the type of migration modes adopted and the molecular and cellular composition of the 3D environment.

Typically, both mesenchymal and collectively migrating cells, as well as stromal cells, upregulate multiple protease systems that mediate proteolytic degradation of the ECM. Two major protease systems are represented by matrix metalloprotinases (MMPs) and the serine protease, plasmin, that requires activation by two proteases: the urokinase-like plasminogen activator (uPA) and the tissue-type plasminogen activator (tPA)[54] . Membrane-type MMPs (MT-MMPs) and uPAs are heavily found at focal adhesion sites to promote pericellular proteolysis during mesenchymal migration *in vitro* and *in vivo*[55-57]. On the other side, multicellular migrating clusters are led by motile cells that are associated with high proteolitic activity, mainly mediated by membrane type 1 metalloprotease (MT1-MMP) and metalloproteinase-2 (MMP-2)[58]. MMPs, plasmin and uPAs catabolise contact-dependent proteolysis of different ECM proteins, including fibrillar and nonfibrillar collagens, fibronectin, laminins. For example, *in vivo,* MT-MMP1 is essential for degradation and redistribution of collagen fibers generating tube-like matrix gaps that allow single cells to move in collagen-rich interstitial tissues. Further collagen proteolysis leads to remodelling of existing matrix gaps in larger tracks that accommodate collective invasion of multicellular clusters[59]. In contrast, ameoboid type migration is generally promoted in microenvironments with low collagen fiber concentrations. Amoeboid cells do not require proteolytic activity, as they squeeze through collagen fibers by filling available spaces with their body. Eventual increase of collagen density can either block migration of amoeboid cells through the ECM or induce them to adopt a proteolytic approach to invasion, switching for example from amoeboid to mesenchymal migration mode[60]. The presence of stromal cells in the tumour microenvironment supports degradation and remodelling of the ECM, thereby assisting cancer cell migration. Stromal cells, such as fibroblasts and microphages, in fact, express a proteolytic repertoire, responsible for the formation of migration tracks between the tumour and the nearby vessels; once formed, these tracks can be followed by tumour cells lacking of intrinsic proteolytic activity, further promoting tumour cell dissemination[61].

1.2.2.2.1 Plasmin activation cascade and its implication in cancer metastasis

Plasmin is a serine protease that mediates proteolytic degradation of a wide spectrum of ECM components, including fibronectin, vitronectin and fibrin. It is secreted by cells as inactive precursor called plasminogen (or zymogen), produced mainly by the liver, and it is found at high levels in the plasma and also in interstitial fluids that surround most of the tissues[62]. Plasminogen is locally converted into active proteinase plasmin by proteolitic cleavage mediated by either of two plasminogen activators (PA): the protease urokinase-like PA (uPA) and tissue-type PA (tPA) (**Figure 6**). uPA is expressed and secreted into the extracellular environment by various tumour cells and tumour-associated stromal cells, in a pro-enzymatic form, pro-uPA, that is activated by proteolysis by plasmin itself and other proteases, such as cathepsin B[63]. Secreted pro-uPA and uPA bind to cell-surface uPA receptor (u-PAR), which localises at focal adhesion sites at the leading edge of migrating cells (**Figure 6**)[64]. u-PAR accumulates protease uPA at these regions where it catalyses activation of plasminogen into plasmin, promoting proteolysis of the ECM and tumour cell invasion. Increased expression and secretion of uPA correlates with metastasis in many types of cancer and predicts poor survival and high risk of relapse in BC[64, 65]. Consistent with this concept, inhibition of uPA activity has been shown to abrogate BC invasion and metastasis *in vivo*[66].
The other pathway that leads to activation of plasminogen into plasmin implies the function of tPA and its binding receptor annexin II (**Figure 6**)[67] [68]. Along with its involvement in thrombolysis, tPA has been also clinically implicated in neoplastic transformation and invasive phenotypes of different tumours, including BC[69]. tPA is secreted by endothelial cells and tumour cells of various types and interacts with its cell surface receptor annexin II (**Figure 6**). Annexin II is a phospholipid-binding protein that exists on the cell surface as both a monomer and a heterotetramer, the latter called annexin II tetramer (AIIt). AIIt is composed of two annexin II molecules and two molecules of an 11-kDa regulatory subunit known as the p11 light chain (**Figure 6**)[68]. AIIt functions as a protein scaffold for the localisation of serine preoteases, such as tPA, plasminogen and the inactive form of the cysteine protease cathepsin B (pro-cathepsin B [pro-CB])[70]. AIIt-bound tPA converts pro-CB into active CB and plasminogen into plasmin. This activates a proteolytic cascade which results in plasmin/CB-mediated uPA activation, ECM degradation and proteolytic activation of pro-metalloproteinases (pro-MMPs) (**Figure 6**)[70, 71]. In addition, AIIt interacts on the cell surface with collagen I fibers, known to regulate cell migration, and the ECM protein tenascin C (TNC), which is found in sites of active tissue regeneration and migration, as is also found in

a large variety of tumours[72]. By offering docking sites to several protease systems and matrix molecules, AIIt not only participates to cell-ECM interaction, but provides also a structural linkage between proteases and matrix components at the cell surface, thereby facilitating extracellular matrix remodelling. As annexin II has been found overexpressed in many tumours, including BC, its function in mediating localised proteolytic activity at the surface of tumour cells largely correlates with increased invasiveness and metastatic potential[73] [74].

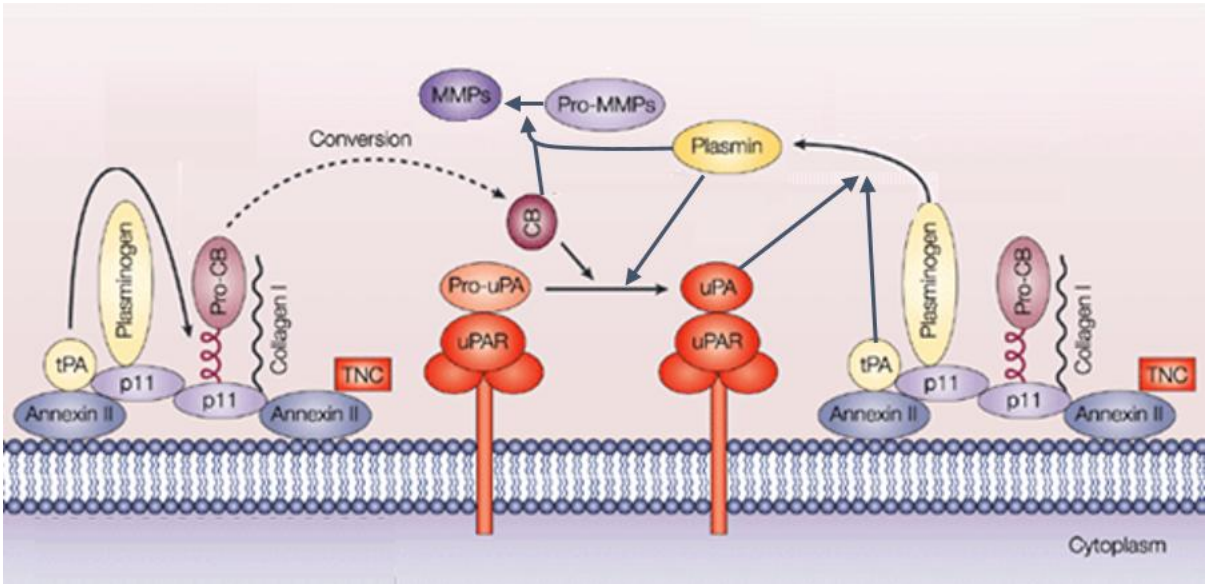

Figure 6: Plasmin activation cascade. The phospholipid-binding protein annexin II forms a heterotetramer AIIt at the cell surface which serves as scaffold for the interaction of tPA, pro-cathepsin B (Pro-CB), plasminogen, collagen I and tenascin C (TNC). tPA converts pro-CB into cathepsin B (CB). The urokinase-lyke plasminogen activator receptor (uPAR) accumulates uPA proenzyme (Pro-uPA) that is converted into uPA by CB. uPA and tPA catalyses proteolityc cleavage of plasminogen which results in the formation of the serine protease plasmin. Plasmin enhances activation of uPA and, together with CB, converts pro-metalloproteinases (Pro-MMPs) into active MMPs. Modified from[67]

1.2.3 Cancer cell dissemination

After migration and invasion into the surrounding of the primary tumour, malignant cells need to spread throughout the body in order to reach distant sites and form metastatic colonies. Cancer cell dissemination can occur through three major routes: blood circulation, lymphatic vessels and serosal surfaces. Metastatic spread established via these three routes is referred to as hematogenous, lymphatic and transcoleomic, respectively[75].

Lymphatic and the hematogenous dissemination is facilitated by reinforced vascularisation of the primary tumour, a process known as angiogenesis that correlates with metastatic occurrence and worsening prognosis[76]. Angiogenesis is the result of the increased expression of angiogenic factors induced by cancer cells to promote tumour progression. The family of vascular endothelial growth factors (VEGFs) represents the major proangiogenic component produced by the tumour. VEGFs are expressed and deposited by cancer cells in the ECM, where they stimulate "de novo" formation of blood or lymphatic vessels (neoangiogenesis) or outgrowth of preexisting ones. The loosely-formed structure of these newly formed vessels renders them weak barriers for invading tumour cells to overcome. Tumour-associated vessels are in fact characterised by a discontinuous basement membrane, a lack of surrounding perycite barrier, and insufficient cell-cell contacts in the endothelial walls. Lymphatic vessels lack also of tight junction formation between their endothelial cells, which confers them a leakier phenotype compared to blood vessels. This may explain why cancer cells derived from carcinomas commonly enter the lymphatic system to disseminate into distant sites. Carcinomas in fact form initial metastases in the lymph nodes, which represents an early prognostic marker of invasiveness and metastatic progression[77]. In later stages, carcinomas achieve colonisation of other organs through distal hematogenous dissemination. This occurs as result of both blood vessel intravasation by cancer cells at the primary site and cancer cell transport from the colonised lymphatic system to the hematogenous circulation. However, other types of malignancies, such as sarcoma, metastasise to distant sites via hematogenous spread, without prior dissemination into local lymph nodes. These evidences suggest that hematogeneous dissemination is required for the metastatic colonisation of distant organs (lymph node excluded)[78].

Along with the weak nature of tumour-associated vessels, others factor contribute to facilitate the mechanical intravasation of cancer cells, including invasive membrane protrusions, and assistance from stromal cells (**Figure 7**). Proteolytic cell protrusions, such as invadopodia, allow migrating cancer cells to degrade the basement membrane surrounding vessels and breach the endothelial wall to intravasate into the systematic circulation[79]. On the other side, tumour-associated macrophages (TAMs) enhance tumour cell invasion and intravasation by secreting paracrine factors, such as epithelial growth factors (EGFs) and colony-stimulating factor 1 (CSF1)[80]. Moreover, TAM-derived EGFs have been shown to promote invadopodia formation and recruitment of BC cells at blood vessels[79].

Cancer cells can also disseminate via transcoleomic spread by invading the serosal membrane of an organ. This can occur either by a primary cancer established within the cavity of the

organ, such as lungs and ovary (pleural an pelvic cavities, respectively) or as result of systemic metastasis derived from hematogenous and lymphatic dissemination of a primary cancer, e.g. advanced BC [81]. Indeed, a large variety of BC cell lines commonly used for *in vitro* experimentation have been established from patients‟ pleural effusions [82].

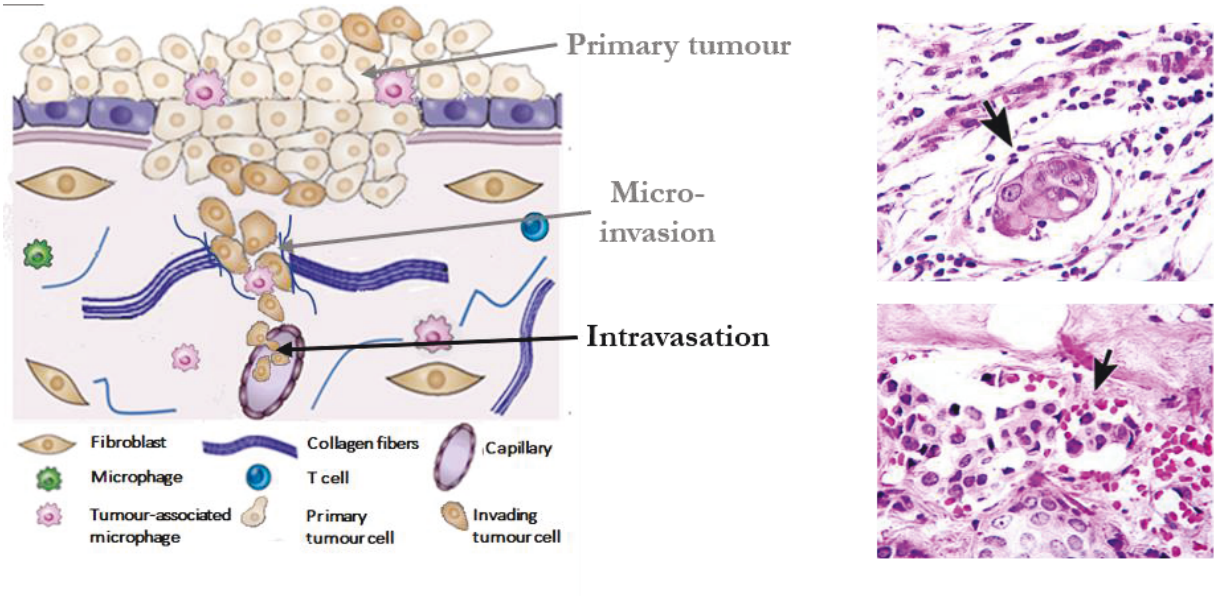

Figure 7: Intravasation of primary tumour cells. Schematic representation of intravasation of primary tumour cells into the capillary system after invasion into the surrounding tissue (left panel). Different cell types are highlighted along with structural elements (modified from [28]). On the right, lymphatic vascular colonisation (top) and blood vessel intravasation (bottom) of BC cells are indicated by black arrows in BC specimens stained with hematoxylin and eosin (H&E). Modified from [83].

1.2.4 Survival in the circulation

Successful conquest of the systematic circulation confers malignant cells the ability to virtually reach any part of the body. However, circulating tumour cells (CTCs) encounter stressful conditions, including physical damage, shear forces, lack of cell-matrix contacts and the immune surveillance [84]. Thus, survival of CTCs can be a very inefficient event with less than 0.01% of cells successfully initiating a secondary tumour over the several million cells that can spread from a gram of tumour daily into the circulation[85, 86]. The population of CTCs increases with disease progression and is associated with poor prognosis[87].

1.2.4.1 Anoikis

Among the stresses that affect tumour cells in the circulation system is loss of adherence to the substratum. In normal conditions, integrin-mediated anchorage to the ECM ensures both survival and viability of epithelial cells[88]. Absent or inappropriate cell adhesion lead cells to undergo to a cell death program, called anoikis. Anoikis is a specialised form of apoptosis that occurs when cells are deprived of their substratum and are maintained in suspension[89]. Metastatic cells, streaming along with the circulation flow, experience abnormal physiological conditions that favorite anoikis. In order to resist to anoikis and survive during their dissemination journey, metastatic cells deregulate crucial apoptotic modulators by adopting different strategies. Among these, overexpression of the anti-apoptotic protein B-cell lymphoma 2 (BCL2), observed in many types of cancer, was early shown able to prevent cell apoptosis in absence of anchorage to the substratum[90]. Resistance to anoikis is accomplished also through activation of pro-survival signals, such as the phosphatidylinositide 3-kinase (PI3K)-AKT pathways, expression of a different pattern of cell-surface integrins that protect cells from anoikis by providing survival signals and overexpression of the neurotrophic tyrosine kinase receptor TrkB, that has been shown to be a key mediator in anoikis suppression[89, 91]. Ectopic expression of TrkB in intestinal epithelial cells is able not only to prevent anoikis, but also to confer transforming and metastatic capabilities to these cells that are normally non tumourigenic[91]. This evidence is a fine illustration of the tight association between resistance to anoikis, tumourigenicity and ultimately metastasis. Indeed, most cell lines derived from solid tumours are able to grow in anchorage-independent conditions, such as soft agar or suspension cultures[92]. Moreover, abolition of the ability to overcome anoikis in transformed cells is able to inhibit their tumourigenic and metastatic potential both *in vitro* and *in vivo*[93, 94].

1.2.5 Arrest, extravasation and colonisation at a new site

Having endured the adverse conditions of the systematic circulation, CTCs must escape the vasculature in order to colonise distal organs and develop a secondary tumour. Theoretically, CTCs are able to reach a wide variety of organs, which suggests that arrest in the capillary beds of a specific organ may be a passive event determined by anatomy and haemodynamics of the vasculature at that site. Indeed, physical constraints imposed by

reduced blood vessels size impede passage of CTCs and force their arrest in certain distant organs, a case frequently observed in the liver, where its more restricted microvessels physically trap colorectal carcinoma cells directly drained into this organ by the portal vein[95]. Another possibility is that passive arrest in the capillary bed at a certain site results from aggregation of CTCs with leukocites and platelets forming micro-emboli that obstruct vessels. Following arrest in the capillary, tumour cell growth can occur into the intravascular space until disruption of the capillary wall allows dissemination into the surrounding parenchyma[96]. Despite mechanical arrest into the vasculature can occur in all organs, CTCs frequently exhibit the capacity to actively home to a specific pattern of organs. For example, BC preferentially metastasises to lung, bone, liver and brain, whereas colorectal cancer cells disseminate to liver and lungs[97]. Organ-specificity in tumour cell homing has been widely investigated and experimental evidences suggest that various mechanisms can determine where tumour cells will arrest and disseminate. Chemokine receptors-mediated chemotaxis represents one of these mechanisms: surface chemokine receptors expressed by tumour cells respond to chemotattic signals (i.e stromal cell-derived factors) secreted by fibroblasts of the local tissue, thus determining the localisation of metastasis of certain tumour types. Using several models of mouse metastasis, it has been observed that primary tumours are able to distally modulate the microevironment of distant sites in order to accommodate circulating tumour cells. Indeed, factors secreted by the primary tumour (e.g., VEGF and placenta growth factor, PIGF) can induce the formation of premetastatic sites by recruiting bone marrow-derived cells at the relative organ prior the tumour cell arrival. Cell within „premetastatic niches" then release chemokines (e.g., stromal cell-derived factor-1, SDF-1, and the calprotectin S100A8/9) that direct chemotaxis of disseminating tumour cells[98, 99]. Furthermore, gene expression profile studies have revealed that changes in gene expression patterns can contribute to organ-specific homing of tumour cells. For example, the human breast cancer MDA-MB-231 cell line, originally isolated from the pleural effusion of a metastatic patient, expresses a set of 54 genes that determine eventual BC metastasis to the lungs[100].

Following arrest in the circulation at a certain distant site, CTCs need to extravasate in order to gain access to the organ parenchyma. Extravasation, the physical passage of tumour cells out the vessel lumina is facilitated by vasculature hyperpermeability. This can be either an intrinsic characteristic of the capillary system, i.e loose cell-cell interactions of certain microvessel walls allow "diffusion" of tumour cells, or induced by tumour cells themselves through proteolytic action of metalloproteinases expressed at the tip of invadopodia or

secretion of factors, like angiopoietin-like proteins, that disrupt endothelial cell-cell junctions thus increasing vasculature permeability[101].

After extravasation into the parenchyma of a new organ, tumour cells encounter a microenvironment physiologically different compared to the one where they originated. Depending on their ability to create favorable conditions for their survival and proliferation, tumour cells in metastatic sites can either undergo a quiescent, nonproliferative state (dormancy), form small lesions (micrometastases) or develop sites of high proliferation called macrometastases[13].

1.3 Cytoskeletal remodelling drives cancer cell migration and invasion

1.3.1 Membrane protrusions

Motile cancer cells are characterised by plasma membrane protrusions that are the prerequisite for recognition, binding and degradation of the ECM and the maintenance of cell migration modes[32]. Cell protrusions can originate in response of chemoattractive signals that cells detect in their microenvironment (chemotaxis) or as guide-sensors in case of random cell migration (i.e., 2D cell cultures). They form from local extension of the plasma membrane, a process that is driven by spatial and temporal organisation of the actin cytoskeleton. Depending on their morphology, molecular structure and function, cell protrusions are distinguished in lamellipodia, filopodia, plasma membrane blebs/pseudopodia and invadopodia[36].

Lamellipodia are broad, flat, sheet-like membrane protrusions characterised by high content in actin filaments that form a branched dendritic network[102] (**Figure 8**). They are commonly observed at the leading edge of cells migrating on 2D substrates *in vitro*[79]. Their formation is initiated by active actin polymerisation that pushes the plasma membrane forward. Behind this highly dynamic region is the lamella, a more stable area with mature FAs where myosin II-mediated contractility generate the force to pull the cell body forward[103].

Filopodia are long, thin protrusions that function as exploratory sensors to help migrating cells investigating the surround (**Figure 8**). They originate from actin polymerisation in long, parallel bundles of actin filaments stabilised by the actin-bundling protein fascin[104], whereas

their elongation is mediated by members of the formin family, such as mammalian Diaphanous-related formins (mDia)[105].

Plasma membrane blebs or pseudopodia (**Figure 8**) are considered the functional analogues of lamellipodia but they are preferentially observed in 3D contexts *in vitro* and *in vivo*[31]. They are tiny protrutions formed upon local disruption of the actin filament cortex that allows cytoplasmic flow to push outwards the plasma membrane. Polymerisation of the actin cortex in the elongated bleb provides then sufficient force for the stabilisation of the resulting pseudopod. Actomyosin contractility has a major role in plasma membrane blebbing: it induces the rupture of the actin cortex required for generation of the focal hydrostatic pressure that initiates the membrane blebbing and also for the retraction of the pseudopodia after elongation[106].

Invadopodia are actin-rich protrusions that form ventrally in cells attached to the substratum [107] (**Figure 8**). They share most of the molecular scenario that orchestrates actin polymerisation in lamellipodia and filopodia, but are distinguished for their high content in matrix-degrading proteases. These proteolytic enzymes are actively localised at the plasma membrane of the invadopodium through delivery in exocytotic vescicles[108]. Indeed, invadopodia constitute proteolytic structures by which migrating cells degrade the basement membrane, the underlying stroma and the capillary barriers during metastatic intravasation/extravasation[109].

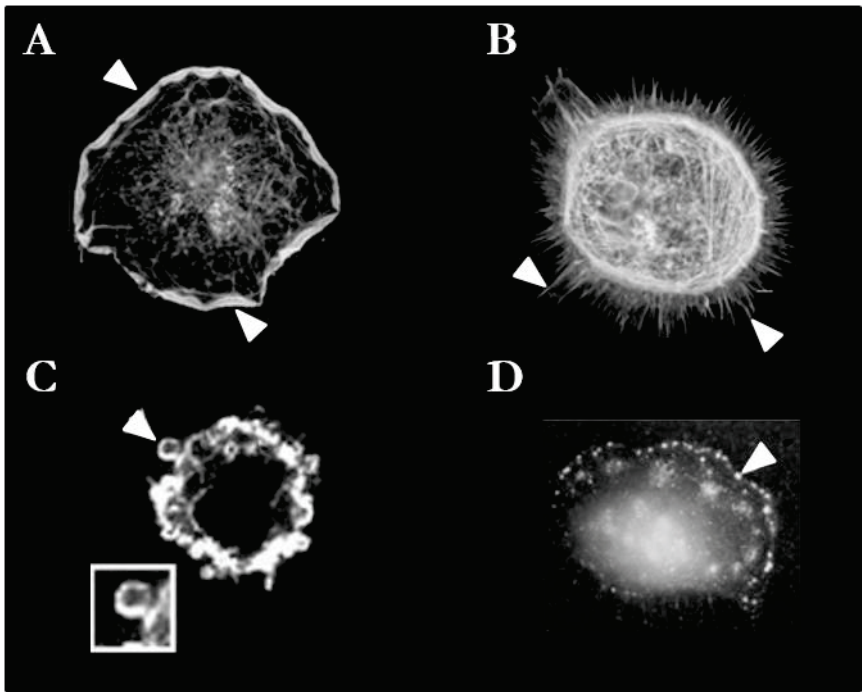

Figure 8: Different types of membrane protrusions. A-B, Actin filament (F-actin) visualisation with rodhamine phalloidin highlights formation of lamellipodia (**A**) and filopodia (**B**) protrusions in Swiss 3T3 fibroblasts (arrow heads). Scale: 1 cm = 25 μm[110]. **C,** F-actin stained with TRITC-phalloidin localises as a ring around membrane blebs in Ltk fibroblasts (arrow heads and insert)[111]. **D,** Immunostaining by antibody A27 against invadopodia visualises sites of invadopodial complexes (arrow head) formed in human melanoma RPMI-7951 cells transfected with MT-MMP and cultured on fibronectin-gelatin films for 3 h[112].

1.3.1.1 Cytoskeleton remodelling in membrane protrusions

Extension of plasma membrane protrusions is driven by the actin cytoskeleton, whose dynamics are tightly regulated by the RHO-family[113]. RHO, RAC and cell division cycle 42 (CDC42) are the three members of the highly conserved RHO family of small GTPases, a subgroup of the Ras superfamily. They cycle between an activated state (GTP-bound form) and an inactive state (GDP-bound conformation). Guanine exchange factors (GEFs) and GTPase activating proteins (GAPs) promote and inhibit small GTPases activity, respectively. Once activated, they interact with a large variety of molecular effectors that mediate downstream signalling leading to cytoskeleton remodelling, critical for formation of both cell protrusions and cell adhesions[114].

RHO family-activated actin polymerisation is required for the extension of filopodia, lamellipodia, invadopodia and the later stages of pseudopodia elongation[115-117]. Actin is a

globular protein (G-actin) that polymerises in a helical fashion to form a polarised actin filament (F-actin) with a fast pointed "barbed" end and a slow growing "pointed" end. Polymerised actin appears under different forms, such as highly dynamic, dendritic network typical of lamellipodia, long, parallel actin bundles found in lamella and filopodia and thick myosin II-conjugated actin bundles called stress fibers, localised in central and rear regions of migrating cells[118]. Actin polymerisation is orchestrated by the actin-related protein 2 (ARP2) and ARP3 complex (ARP2/3 complex), an actin nucleation factor whose upregulation has been shown to enhance cell invasion and metastasis *in vitro* and *in vivo*[119]. ARP2/3-mediated actin nucleation is promoted by its interaction with both Wiscott-Aldrich syndrome proteins (WASPs) and WASP family verprolin homology proteins (WAVE)[120], direct downstream effectors of RAC and CDC42 (**Figure 9**). CDC42 is known to activate the WASP-ARP2/3 axis and is the main RHO GTPase involved in formation of filopodia and invadopodia[121]; whereas actin polymerisation via the WAVE-ARP2/3 nucleation machinery is orchestrated by RAC, essential for lamellipodia protrusion[122] (**Figure 9**). RHO also contributes to actin polymerisation with a major role in filopodia elongation[105]. RHO activates mammalian Diaphanous homolog (mDia) formins, that promote actin nucleation by barbed-end elongation; in addition, RHO phosphorylates and activates LIM kinase (LIMK) which in turn inactivates by phosphorylation the actin-binding protein cofilin, responsible for the disassembly of actin filaments into monomeric G-actin[123] (**Figure 9**). LIMK function has been shown to be crucial for the maintenance of migratory and invasive phenotypes of BC cells[124]. In addition to activation by RHO, LIMK is also activated by p21/RAC1/CDC42-activated kinases (PAKs), considered major players in cytoskeleton dynamics, cancer motility and invasion[125] (**Figure 9**). In mammals, the PAK kinases family comprehends 6 members, PAK1-6 [126]. Among them, PAK1 seems to have a major role in the regulation of actin polymerisation by activating LIMK during lamellipodia formation at the front of the cell. PAK1 induces LIMK-mediated cofilin phosphorylation that ensures cofilin recycling back to the leading edge where it produces free barbed end for the polymerisation of new actin filaments at this site. Nevertheless, uncontrolled cofilin activity leads to an accelerated F-actin turnover that results in widening of the lamellipodium[127-129]. Thus, PAK1 controls formation of lamellipodia and limits their extent through negative regulation of cofilin activity.

Finally, extension of plasma membrane blebs is mainly controlled by RHO[130]. RHO and its downstream effector, the RHO-associated serine/threonine kinase (ROCK) induce bebbling by increasing actomyosin contractility which requires myosin II activity. Myosin II is an actin-bundling protein composed of two heavy chains, two regulatory light chains (RLCs) and two essential light chains, and its activity is regulated by phosphorylation of the Thr18 and Ser19 of its RLC [131]. Myosin II phosphorylation state is regulated by ROCK via two mechanisms: direct phosphorylation of the myosin RLC and inhibition of dephosphorylation of myosin RLC by phosphorylation and inactivation of the MLC phosphatase (MLCP)[132] (**Figure 9**). ROCK-mediated phosphorylation of the RLC allows actin-bundled myosin II to move antiparallel stress fibers past each other. This sliding movement generates the contractile force required for tail retraction during the migration cycle and bleb protrusion/retraction[130, 133]. After bleb is formed, RAC-driven actin polymerisation leads to actin cortex formation that sustains bleb extrusion[134].

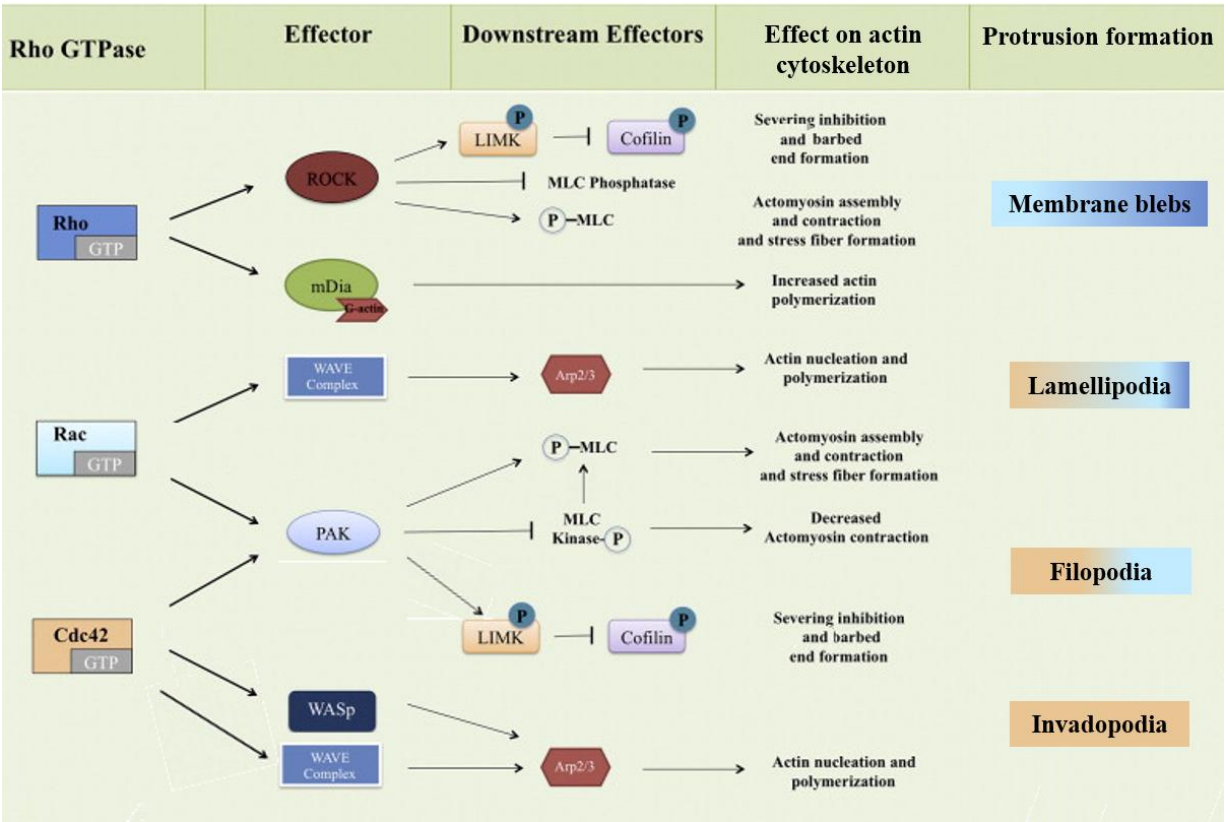

Figure 9. RHO GTPases in actin remodelling and cell protrusion formation. Arp, actin-related protein; LIMK, LIM kinase; mDia, mammalian homologue of the Drosophila diaphanous protein; MLC, myosin light chain; MLCK, MLC kinase; MLCP, MLC phosphatase; P, phosohorylated; PAK, p21 activated kinase; ROCK, RHO kinase; WASP, Wiskott-Aldrich syndrome protein; WAVE, WASP family verprolin-homologous protein. Modification from[135] .

1.3.2 Cell adhesion in cell migration

1.3.2.1 Adherens junctions in collective migration

During collective migration, adhesive cell-cell coupling within multicellular migrating strands/clusters is mediated by existing cell-cell contacts, known as adherens junction (AJs). Adherens junctions (AJs), as well as TJs and desmosomes, are cell-cell adhesions that are established on the lateral surfaces of epithelial cells during morphogenesis of the epithelia[24]. AJs anchor cytoskeletal actin elements of two adjacent cells to each other through the interplay of a large number of transmembrane adhesion proteins and cytoplasmic molecules (**Figure 10**). Nectins and cadherins, both cell-cell adhesion molecules (CAMs), are the most important transmembrane protein families involved in the assembly of AJs. In humans, nectins is a group of four members (Nectin1-4) that contain a cytoplasmic tail, a transmembrane region and an extracellular (EC) one[136]. During the formation of nascent AJs, nectins homo-dimerise on the lateral surface of the cell and then *trans*-interact with nectin clusters on the lateral surface of the adjacent cell through Ca^{2+}-independent heterophilic binding of their EC domain (**Figure 10**). Simultaneously, on the cytoplasmic side, the C-terminus of the nectin tail binds to afadin, a large cytoplasmic protein that interacts directly with actin filaments [137]. These so-formed nectin-based scaffolds serve as structural platforms for the following assembly of cadherin adhesive structures. Among the more than 100 members of the cadherin family, epithelial cadherin (E-cadherin or Cadherin-1) is expressed in most epithelial tissues and is commonly used as marker of fully developed AJs[24]. E-cadherin forms *cis* and *trans*-homophilic dimers through its EC domain that are internally stabilised by aggregating to nectin-based complexes via catenin molecules such as catenin p120, β-catenin and α-catenin (**Figure 10**). β-catenin binds the intracellular tail of E-cadherin and interacts with the adaptor protein α-catenin, which in turn binds to F-actin[138]. Vinculin and α-actinin, other two actin-bundling molecules, then associate directly with α-catenin, thus connecting E-cadherins to the actin cytoskeleton[139]. Following, two afadin-binding proteins, ponsin and afadin DIL domain-interacting protein (ADIP), localise at the nascent AJ and connect nectin-afadin clusters to cadherin-based units via binding vinculin and α-actinin, respectively[140]-[141]. At the later stage of the AJs assembly, the LIM domain only protein 7 (LMO7), an afadin and α-actinin interacting protein, localises at the AJ site to connect nectin-afadin to cadherin-catenin units cluster through α-actinin[142] (**Figure 10**). The progressive

association of these membrane peripheral molecules to the nascent adhesion sites, called "punctates", contributes to stabilise and strengthen the cell-cell adhesive capabilities of E-cadherin. Maturation of the AJs is accompanied by ARP2/3-mediated actin polymerisation, following RAC activation by E-cadherin at the punctated sites[143] (**Figure 10**). RHO-activated myosin II accumulates then at the newly formed actin filaments and generates contractile force that brings two adjacent cadherin-based clusters together and maintain the junctional tension[144] (**Figure 10**). Moreover, myosin II-mediated tension at the AJs procures conformational changes in various adhesion proteins, such as vinculin, that allow them to interact and recruit further adhesion molecules at the developing AJ. Therefore myosin II contributes to AJ maturation by promoting clustering of E-cadherin and recruitment of anchor molecules[145] [146].

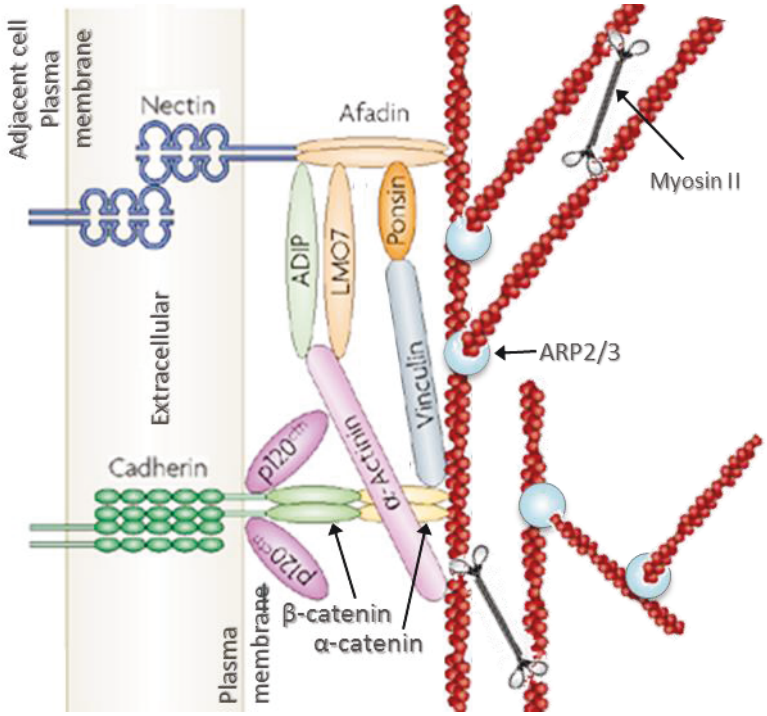

Figure 10: Molecular structure of adherens junctions (AJs). During the assembly of AJs, the nectin-afadin complex is linked to the cadherin-catenin (p120catenin, β- and α-catenin) unit by protein connectors, such as ponsin/vinculin and ADIP/LMO7/α-actinin. The F-actin-bundling proteins, afadin, vinculin, α-catenin and α-actinin interact with ARP2/3-induced polimerized actin branches that are stabilised by activated myosin II molecules. Modified from [147].

1.3.2.2 Cell-matrix contacts: Focal adhesions

Migrating cells need to attach to the substratum in order to stabilise membrane protrusions and gain traction support over which they pull their bodies forward.

Cell adhesion to the ECM is predominantly mediated by focal adhesions (FAs), adhesive complexes that anchor the actin cytoskeleton inside the cell on the ECM. FAs are flat, elongated structures that usually assemble near the periphery of a spreading or moving cell from adhesion precursors. When migration process begins, nascent adhesions are firstly established at the leading edge of the cell upon interaction between the ECM and the integrin transmembrane receptors. Integrins constitute a large family of heterodimeric receptors, consisting of 18 α and 8 β subunits able to assemble in 24 distinct functional variants in mammals[148]. They represent the major cellular component found in FA structures and mediate physical connection between the cytoskeleton and the ECM (**Figure 11**)[149]. The extracellular domains of both α and β subunits in fact associates with various ECM components, depending on different binding affinities, e.g. $\alpha_v\beta_3$ integrin specifically interacts with fibronectin, whereas $\alpha_1\beta_1$ binds collagen and laminin[150, 151]. Integrin interaction with the ECM determines activation of the RHO GTPases which induce a sequential accumulation of cytoplasmic proteins at the nascent adhesions. Over 50 different proteins are involved in the assembly and maturation of FAs, including integrin-binding proteins, adaptor proteins, and enzymes (**Figure 11**)[152]. Talin and paxillin first interact with the cytoplasmic tail of β-integrin subunits, followed by the actin-bunding proteins vinculin, α-actinin and tensin (**Figure 11**). Simultaneously, ARP2/3-mediated actin polymerisation takes place in the emerging lamellipodium, leading to assembly of an actin dendritic network that is sooner recruited at the nascent adhesions. Actin filaments are in fact linked to the integrin-based site via talin, vinculin, α-actinin and tensin[143] (**Figure 11**). Nascent adhesions can either disassemble (turnover) or mature in larger adhesion sites, called focal complexes (FXs). These result from the involvement of other proteins that function as adaptors for the association with actin bundles at the boundary of the lamellum and lamellipodium. For example, paxillin, a β integrin-binding protein, serves as scaffold for structural proteins, such as vinculin, and different signalling kinases, including SRC, focal adhesion kinases (FAKs) and PAKs (**Figure 11**). FAKs directly associate with β-integrins and paxillin and reinforces integrin-actin bundles connection by recruiting additional talin molecules[153, 154]. PAKs co-localise with paxillin via an adaptor complex, comprehensive of the paxillin kinase linker

(PKL) and PAK-interacting exchange factor alpha/cloned out of library (alphaPIX/COOL) (**Figure 11**)[155]. AlphaPIX/COOL, also known as ARHGEF6, is a member of the RHO GTPase guanidine exchange factor (GEF) family and along with its function in activating RHO small GTPases, is essential for PAK localisation at FA sites [156]. PAKs differentially regulate turnover and maturation of the FX (**section 1.3.2.2.1**). After integrin-actin aggregation is achieved, FXs either disassemble or evolve into elongated and more stable FAs, a process that requires the association with stress fibers and actomyosin contractility. Association of FX complexes with stress fibers is mediated by the activity of α-actinin and Enabled/vasodilator-stimulated phosphoprotein (Ena/VASP) proteins: both recruit zyxin molecules that directly associate with the termini of stress fibers (**Figure 11**)[157]. The second is conferred by binding of active myosin II between adjacent stress-fibers-integrin clusters thus providing contractile force to bring them closer to one another[158]. Persistent focal adhesion-associated contractility at the leading edge provides the cell with sufficient force to pull its body and slide along the ECM[159]. At the opposite site of the cell, disassembly of FAs allows retraction of the trailing edge through actomyosin contraction.

High heterogeneity in size and dynamics of adhesion complexes has been observed in migrating cells, which depends on cell type, composition of the substratum and stimulation by external signals. These determine in turn which membrane protrusions, forces and speed rates are being generated during migration. For example, FAs are associated with slow migration and they are hardly observed in cells migrating in 3D. On the contrary, nascent adhesions and FXs are observed in highly motile cells, due to their fast turnover rates[160].

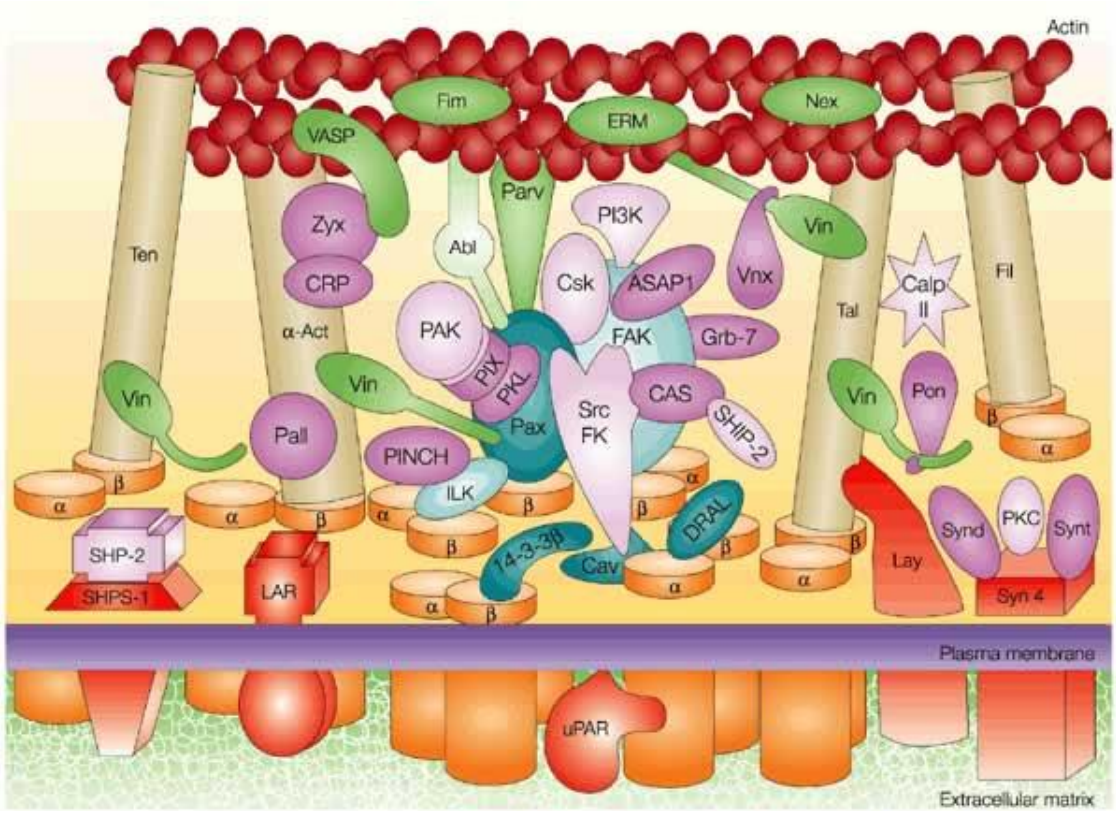

Figure 11: Molecular composition of focal adhesions. Heterodimeric (α and β) integrins are the primary adhesion receptors (orange cylinders). Additional membrane-associated molecules enriched in these sites (red) include syndecan-4 (Syn4), layilin (Lay), the phosphatase leukocyte common antigen-related receptor (LAR), SHP-2 substrate-1 (SHPS-1) and the urokinase plasminogen activator receptor (uPAR). Proteins that interact with both integrin and actin include α-actinin (α-Act), talin (Tal), tensin (Ten) and filamin (Fil) (golden rods). Integrin-associated molecules in blue include: focal adhesion kinase (FAK), paxillin (Pax), integrin-linked kinase (ILK), down-regulated in rhabdomyosarcoma LIM-protein (DRAL), 14-3-3β and caveolin (Cav). Actin-associated proteins (green) include vasodilator-stimulated phosphoprotein (VASP), fimbrin (Fim), ezrin–radixin–moesin proteins (ERM), Abl kinase, nexillin (Nex), parvin/actopaxin (Parv) and vinculin (Vin). Other proteins, many of which might serve as adaptor proteins, are coloured purple and include zyxin (Zyx), cysteine-rich protein (CRP), palladin (Pall), PINCH, paxillin kinase linker (PKL), PAK-interacting exchange factor (PIX), vinexin (Vnx), ponsin (Pon), Grb-7, ASAP1, syntenin (Synt), and syndesmos (Synd). Adhesion-associated enzymes are presented in light shades: SH2-containing phosphatase-2 (SHP-2), SH2-containing inositol 5-phosphotase-2 (SHIP-2), p21-activated kinase (PAK), phosphatidyl inositol 3-kinase (PI3K), SRC-family kinases (SRC FK), carboxy-terminal SRC kinase (Csk), the protease calpain II (Calp II) and protein kinase C (PKC)[161].

1.3.2.2.1 Regulation of actin cytoskeleton in cell-matrix adhesion

RHO, RAC and CDC42 are also involved in the regulation of cytoskeletal dynamics during FA formation by directly controlling the balance between actin-mediated protrusion and actomyosin contraction. RAC and CDC42 stimulate the formation of nascent adhesion and FXs by inducing ARP2/3-mediated actin polymerisation at the initial site of adhesion. On the other side, focal adhesion assembly and stabilisation is provided by RHO activation as well as myosin II-dependent contractility[162]. Turnover and maturation of FAs is controlled by several FAs-associated proteins, such as paxillin, FAK/SRC and PAK. Phosphorylation of paxillin by the FAK/SRC complex correlates with the turnover of existing FAs and increased motility[163], whereas PAKs differentially regulate both assembly and maturation of FA. PAKs exhibit the dual potential to inhibit and promote myosin II activity, necessary for the maturation of FAs. PAKs can phosphorylate MLCK, leading to its inhibition and decreased MLC phosphorylation[164]. At the same time, they can activate myosin II-mediated contractility by direct phosphorylation of the MLC subunit[165-167]. Recent evidences suggest that PAKs may contribute to both assembly and maturation of FAs in an isoform-specific way. Using siRNAs in breast carcinoma cells, Coniglio et al. demostrated that both PAK1 and PAK2 promote BC invasion, by playing opposite roles in the regulation of MLC phosphorylation and FAs stabilisation[129]. In particular, they observed that silencing of PAK1 in BC cells inhibits MLC phosphorylation, suggesting that PAK1 may directly phosphorylate MLC; while the depletion of PAK2 enhances MLC phosphorylation, by stimulating the RHOA/ROCK axis. Moreover, the observation that FAs do not increase in size in PAK1-depleted BC cells suggested that PAK1 may play a role in promoting focal adhesion maturation, at least in part, by stimulating MLC phosphorylation. The depletion of PAK2, instead, led to increased FAs size, likely due to the higher myosin II activation, on one side; on the other, loss of PAK2 inhibited the assembly of new FAs that may reflect a direct requirement of PAK2 to focal adhesion generation,. Thus, PAK1 and PAK2 cooperate to ensure optimal focal adhesion generation and maturation during BC cell migration.

1.3.3 Signalling to cytoskeletal remodelling, cell motility and metastasis

1.3.3.1 Regulation of RHO GTPases

Small RHO GTPases are master regulators of spatial and temporal cytoskeletal re-organisation that is required for various cellular processes including cell-cell interaction, cell polarity, cell adhesion, proliferation and chemotaxis[36].

RHO GTPases function as molecular switches that cycle between an active (GTP-bound) and inactive (GDP-bound) conformations[168]. The cyclic switch between GDP and GTP is regulated by two classes of cytoplasmic molecules, the guanine nucleotide exchange factors (GEFs) and GTPase activating proteins (GAPs). GEFs and GAPs control the cyclic switch of RHO GTPases between inactive and active forms. GEFs activate RHO GTPases by promoting exchange of GTP for GDP, whereas GAPs inactivate RHO GTPases by enhancing the intrinsic GTP-hydrolysis activity. In addition, guanine-nucleotide-dissociation inhibitors (GIDs) sequester GDP-bound RHO GTPases, preventing their translocation at plasma membrane sites where they are usually activated[168] (**Figure 12**).

Activation of RHO GTPases occurs in response to external stimuli that can be both chemical, including growth factors and cytokines and physical, such as adhesion to extracellular matrix or other cells and mechanical stresses. External stimuli are detected and captured by plasma membrane receptors that consist mainly of three classes: (1) receptor tyrosine kinases (RTK), i.e., epithelial growth factor receptor (EGFR), hepatocyte growth factor receptor (HGFR/cMet), and transforming growth factor receptor (TGFR), (2) G protein-coupled receptors, such as lysophosphatidic acid receptor (LPA-R) and sphingosine-1 phosphate (S1P) receptor, and (3) integrins[169] (**Figure 12**). After stimulation, they initiate intracellular transduction of external signals to RHO GTPases through activation of GEFs via different mechanisms. As result, GEFs undergo to conformational changes that relieve them from autoinhibitory mechanisms, changing their subcellular localisation to increase the chance of interaction with RHO GTPase substrates. A common mechanism of GEF regulation used by RTKs and GPCRs is the activation of the phosphatidylinositide 3-kinase (PI3K) (**Figure 12**). Activated PI3K leads to production of phosphatiylinhositol 3,4,5-triphosphate (PI[3,4,5]P3) which acts as second messenger to activate membrane-associated GEFs, owing to its high affinity for the GEF authoinhibitory domain. GEFs activity can also be stimulated by direct phosphorylation by membrane RTKs and via heterodimeric G proteins that after activation of

GPCR are released in the intracellular space where they interact with GEFs or activate PI3K[170, 171] (**Figure 12**). Moreover, RHO family GEFs are activated downstream signalling pathways triggered by integrin-mediated cell adhesion to the ECM. In this respect, after paxillin-mediated recruitment at FA sites, FAK is activated by SRC and this results in phosphorylation and activation of CAS scaffolding proteins. CAS is a docking protein that once activated form a complex with the adaptor protein CRK and together recruit and activate RHO family GEFs[135] (**Figure 12**).

Over 60 mammalian RHO family GEFs have been identified and their functional investigation has revealed a complex regulatory network for these proteins, including upstream receptor-specific activation/inactivation pathways and downstream RHO GTPase-specific regulation[169].

Among these, the αPIX (alpha PAK-interacting exchange factor) member of the RHO family GEFs exhibit a particularly complex mode of action in controlling RHO GTPases activity and downstream effects. αPIX, also known as COOL2 (Cloned out of library 2) or ARHGEF6 (RAC/CDC42 guanine nucleotide exchange factor 6), is a GEF member specific for RAC and CDC42, because it binds to the RAC/CDC42 target PAK. It can be activated by PI3K following upstream stimulation of both RTKs and GCPRs, by G protein subunits derived from G protein activation and by integrin-based focal adhesions, where αPIX localises in complex with PAK via interaction with GIT-paxillin. Activation of αPIX through all these different mechanisms has been shown to be essential for both RAC and CDC42 function[170, 172, 173]. αPIX activity as GEF highly depends on its cytosolic conformation. It can exist in fact as either homodimer and in this state it functions as RAC-specific GEF, or in a monomeric form which acts as a GEF for either RAC or CDC42, but the molecular mechanisms that mediate the switch between its dimeric and monomeric states and vice versa are still unclear [174]. It is known that PAK interaction with αPIX is required for the monomeric form to exhibit GEF activity, but it is not sufficient to stimulate the dissociation of dimeric αPIX into monomers[175]. In addition, αPIX interaction and localisation of PAK at focal adhesion sites induces PAK activation through local stimulation of RAC and CDC42. Moreover, αPIX is frequently found in integrin-based adhesion clusters and its overexpression dramatically promotes lamellipodia and protrusion formation during integrin-mediated cell spreading, as result of αPIX-induced activation of RAC and CDC42[176].

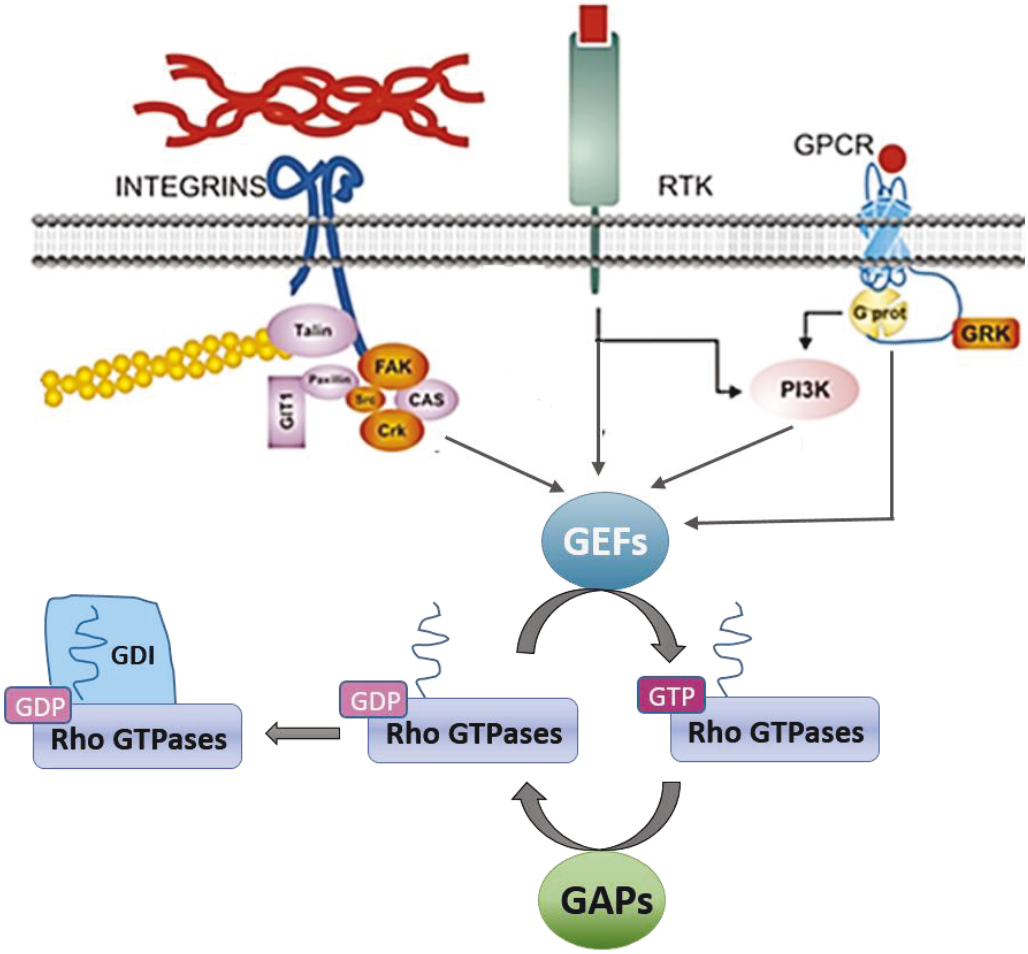

Figure 12: Signalling regulating RHO GTPases. In response to external stimuli, plasma membrane receptors, including integrins, receptor tyrosine kinases (RTKs) and G protein-coupled receptors (GPCRs) trigger different signalling pathways that lead to activation of small RHO GTPases. Integrin-mediated complexes recruit proteins such as CAS and CRK that activate guanine nucleotide exchange factors (GEFs); RTKs can activate GEFs either by direct phosphorylation or through activation of phosphatidylinositid-3 kinases (PI3K); along with RTKs also GPCRs used PI3K and G proteins for the activation of GEFs. GEFs in turn activate RHO GTPases by exchanging GTP for GDP, whereas GTPases-activating proteins (GAPs) enhance intrinsic GTP hydrolytic activity, thus inactivating RHO GTPases (GDP-bound), creating a cyclic mechanism that control RHO GTPases active/inactive state. Inactive RHO GTPases can be sequestered by guanine-nucleotide-dissociation inhibitors (GIDs) preventing their activation and traslocation to the plasma membrane. Modified from[177]

1.3.3.2 EGFR and HER2 drive pro-metastatic signalling cascades in BC

Epidermal growth factor receptor (EGFR) and human epithelial growth factor receptor 2 (HER2) belong to the erythroblastic leukemia viral oncogene homolog (ERBB) family of RTKs that play important roles in cell proliferation, survival, motility and development. Nevertheless, deregulation of ERBB receptors and their downstream signalling pathways is frequently observed in cancer and is critical for cellular transformation and tumour progression[178]. EGFR and HER2 have been implicated in the development of a number of cancers, where genetic alterations such as gene amplification result in receptor overexpression, or somatic mutations lead to constitutive receptor activation. Particularly, overexpression of HER2 is detected in about 20-30% of human breast tumours and correlates with increased metastatic aggressiveness such that it is clinically used as prognostic and predictive marker for BC, as well as a therapeutic target[179].

In mammals, the ERBB family includes ERBB1 (also called EGFR), ERBB2 (also known as HER2 or c-NEU), ERBB3 (also named HER3) and ERBB4 (or HER4). As RTKs, they comprise an extracellular ligand binding domain, a transmembrane region and a cytoplasmic tail with tyrosine kinase activity. Binding of the ligand to the extracellular domain induces homo- or heterodimerisation of ERBB receptors which is essential to initiate intracellular signal transduction[180]. The ERBB receptors respond to multiple ligands that exhibit a receptor-dependent binding specificity. They include: epithelial growth factor (EGF), transforming growth factor (TGF)-α, amphiregulin and epigen which bind specifically to EGFR; betacellulin (BTC), heparin-binding EGF, and epiregulin which show dual specificity by binding both to EGFR and ErbB4; neuregulins (NRGs)/heregulins which bind to ErbB3 and ErbB4. HER2 lacks ligand binding activity and its function depends on its dimerisation with other ligand-bound ErbB receptors. When overexpressed, HER2 is preferentially selected for ErbB receptor heterodimerisation and HER2-containing heterodimers exhibit the most potent downstream signalling responses[181, 182].

After binding of the ligand, ErbB dimerisation stimulates the intrinsic receptor tyrosine kinase activity which results in autophosphorylation and *trans*-phophorylation of tyrosine residues in the cytoplasmic tail of each dimerised receptor (**Figure 13**). These phosphotyrosines serve as docking sites for the recruitment of various adaptor molecules or enzymes containing specific SRC homology 2 (SH2) domains (phosphotyrosines binding domains), such as SRC, SHC, growth factor receptor–bound protein 2 (GRB2), PI3K, non-catalytic region of tyrosine

kinase adaptor protein (NCK) and regulatory subunits of the phosphatidyl inositol 3-kinase (PI3K), which include p85α, p55α, p50α, p85β, p55γ (**Figure 13**). These adaptors transduce the RTK-captured signal via simultaneous activation of multiple signalling cascades resulting in proliferative, survival and migratory outcomes[183].

EGFR/HER2 heterodimers has been shown to be the favorable dimeric combination for induction of BC motogenic and invasive phenotypes[184]. In fact, constitutive expression and activation of EGFR and HER2 are responsible for the high transendothelial invasiveness of BC cells where tyrosine phosphorylated-EGFR and HER2 are found to be localised in areas of high membrane protrusion activity. Moreover, overexpression and increased intrinsic tyrosine kinase activity of HER2 is critical for formation of lung metastases from mammary gland primary tumours in transgenic mice models[185]. Notably, only EGF stimulation and EGFR/HER2 heterodimer formation are able to induce a sufficient HER2 tyrosine phosphorylation to recruit SHC, GRB2 and PI3K onto its cytoplasmic tail (**Figure 13**). Activated EGFR/HER2 dimers induce sustained cytoskeletal re-organisation and confer motogenic and invasive properties at both cytoplasmic and nuclear levels through several downstream pathways[186].

Firstly, EGFR/HER2-mediated recruitment of PI3K through its SH2-containing p38 subunit links RTKs to RHO GTPases regulation. EGF-stimulated lamellipodia formation requires PI3K activity which leads to activation of RAC or CDC42 [187].These in turn activates PAK which form a complex with LIMK resulting in phosphorylation and activation of the latter. Activated LIMK then phosphorylates cofilin leading to inhibition of cofilin-mediated actin filament severing[188]. Activation of small RHO GTPases and their downstream signalling effectors by EGF stimulation can also occur through EGFR-mediated direct recruitment and phosphorylation of RHO GEFs, such as the VAV family which activates RAC and RHO leading to cytoskeletal rearrangements[189], and the RAC/CDC42 GEF αPIX which is essential for EGFR/HER2-induced activation of PAK function (**Figure 13**)[190].

In addition, tyrosil-phosphorylation of HER2 triggers recruitment of SHC and GRB2 adaptor proteins, which directly transmit RTK stimulation to the RAS GTPases family and indirectly to small RHO GTPases. HER2-activated SHC in fact recruits GRB2 which is constitutively associated with Son of Sevenless (SOS), a guanyl nucleotide exchange factor for RAS GTPases[188]. Coupling of SOS whith HER2 through GRB2 leads to SOS-mediated GTP-loading of RAS and subsequent activation of RAS effectors, such as PI3K and rapidly accelerated fibrosarcoma (RAF) kinases (**Figure 13**)[188]. RAF initiates then a cascade of phosphorylation events that results in activation of the mitogen-activated protein kinase

(MAPK) pathway through the MAPK/ extracellular signal regulated kinase (ERK)-activating kinases (MEK). Stimulated MAPKs translocate to the nucleus where their function in the phosphorylation of a variety of proteins, including the transcription factors c-MYC, c-JUN and c-FOS. The activated c-JUN and c-FOS then interact with each other to form a functional transcription complex called activator protein-1 (AP-1) (**Figure 13**)[191]. EGFR-mediated downstream formation of AP-1 transcription factor can also take place through another signalling cascade which is initiated via recruitment of the NCK adaptor protein. NCK is able to associate with PAKs, thus bringing them in proximity of their EGFR-activated RAC and CDC42 regulators on one hand; on the other hand, NCK itself directly activates PAKs, and this regulation is essential for PAK1 and PAK2 to induce JNK (c-JUN N-terminal kinase) activation, through sequential phosphorylation of MAP/ERK kinase kinase 1 (MEKK1) and MAP kinase kinase 4/7 (MKK4/7)[192, 193]. Once activated, JNK enters in the nucleus where it specifically phosphorylates c-JUN, thus leading to its dimerisation with c-FOS to form the active AP-1 complex (**Figure 13**).

AP-1 is a transcription factor complex which forms upon homo- or heterodimerisation of FOS- and JUN-family proteins which include c-FOS, FRA1, FRA2, FOS B and c-JUN, JUN B, JUN D, respectively, as well as activating transcription factor (ATF) and musculoaponeurotic fibrosarcoma (MAF) protein families[191]. These proteins exhibits transcriptional gene regulation activity by binding to consensus DNA sequences usually present in gene promoter regions. The typical nucleotide sequence recognised by AP-1 factors is the 12-*O*-tetra-decanoylphorbol-13-acetate (TPA)-responsive element (TRE) (fig), which is preferentially bound by AP-1 dimers formed by the two main AP-1 proteins, c-JUN and c-FOS[191]. Growth factor-stimulated AP-1 activity has been largely associated with cytoskeletal remodelling, increased invasiveness and metastatic spread of BC[194] [195] [196] [197]. Indeed, owing to its activity in transcriptionally regulating gene expression, AP-1 has been shown to orchestrate a multigenic invasion program by both up-regulating and down-regulating a large number of genes that differentially participate to cytoskeletal dynamics, cell-cell and cell-ECM adhesion, motility, invasion, angiogenesis and transcriptional regulation of all these processes [198]. Amongst the genes strongly up-regulated by AP-1 are several metalloproteinases, such as *uPA*, *MMPs* and cathepsins and cytoskeletal regulators, such as *ARP2/3 p16 subunit* and the *SCAR2* member of the WASP family. Notably, AP-1 is able to induce transcriptional expression of its component *c-JUN* in response to EGF stimulation, by interacting with TREs sequences present in its gene promoter (**Figure 13**)[199].

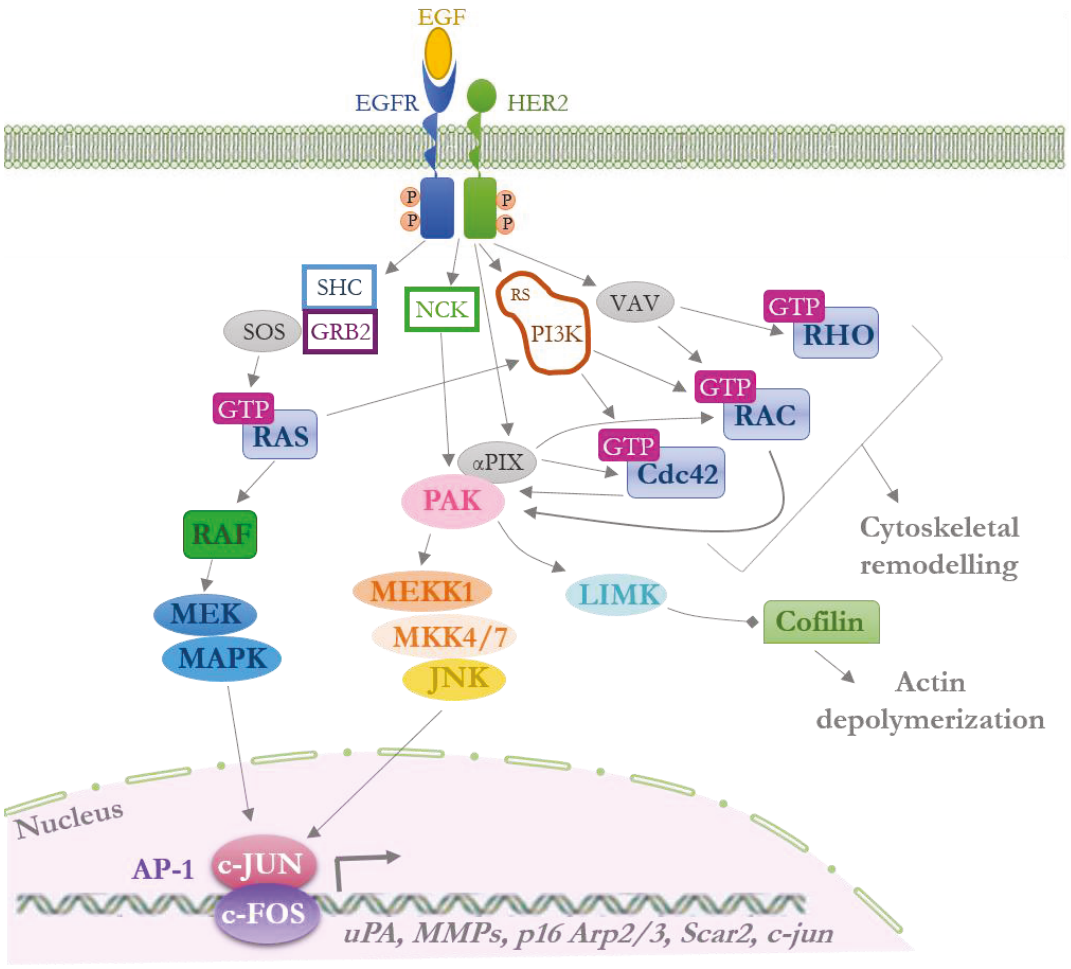

Figure 13: EGFR/HER2-activated signalling cascades regulating cytoskeletal re-organisation, cell motility and invasion. Binding of epithelial growth factor ligand to the extracellular domain of EGF receptor (EGFR) leads to heterodimerisation of EGFR and human epithelial groth factor receptor 2 (HER2) which activates auto- and transphosphorylation of their intracellular tyrosine kinase domains. Activated EGFR/HER2 triggers a series of intracellular signalling cascades through recruitment of adaptor proteins (line-coloured shapes), including SHC, GRB2 (growth factor receptor–bound protein 2), the regulatory subunit (RS) of PI3K (phosphatidyl inositol 3-kinase), NCK (non-catalytic region of tyrosine kinase adaptor protein). These signalling can activates guanyl exchange factors (GEFs) (in grey ovals), such as SOS (Son of Sevenless), VAV and αPIX (p21-activated kinase-interacting exchange factor alpha), which activate their primary regulators (GTP-labelled boxes): RAS, CDC42, RAC and RHO. Several RAS and RHO GTPases effectors are involved in EGF-stimulated signalling cascades: RAF (Rapidly Accelerated Fibrosarcoma), MAPK (mitogen-activated protein kinase), MEK (MAPK/ERK [extracellular signal regulated kinases]-activating kinase), PAK (p21-activated kinase), LIMK (LIM-kinase), cofilin, MEKK1 (MAP/ERK kinase Kinase 1), MKK4/7 (MAP Kinase Kinase 4/7), JNK (c-JUN N-terminal kinase), and AP-1 (activating protein-1) formed by c-JUN and c-FOS. AP-1 activates transcriptional expression of *uPA* (urokinase-like plasminogen), *MMPs* (metalloproteinases), the *p16 of ARP/2/3 (actin-related protein 2/3)* subunit, *SCAR2* and *c-JUN*.

1.4 Aneuploidy

Every species is characterised by a distinct karyotype (chromosome complement) that is referred as to euploidy. The successful perpetuity of all multicellular organisms relies on maintainance of the euploid genomic state during transmission of genetic information to daughter cells. Almost all mammals are diploid, such that they contain two copies (2n) of each autosomal chromosome (haploid complement); for instance, in humans the 2n basic chromosome number is 46. A balanced ploidy state requires maintanance of an equal number of each chromosome, thus ensuring the possession of an equal copy number of genes present in different chromosomes[200]. Deviation from the euploid kariotype caused by changes in the copy number of specific genes, entire or parts of chromosomes leads to a state of aneuploidy. The term aneuploidy refers to any karyotype containing a chromosome number that differs from the haploid complement and its multiples (polyploidy). Aneuploidy can arise form either gain or loss of entire chromosomes due to chromosome segregation defects, known as "whole-chromosome" aneuploidy, or by deletion, amplification or translocation of sub-chromosomal fragments, so-called "partial" or "segmental" aneuploidy[201]. As aneuploid cells are stricken by either an excess or deficit of gene copies located in the affected chromosomes, occurring of aneuploidy is generally poorly tolerated in nature, a sweeping consequence of the impairment in growth and reproductive fitness caused to the organism. Autosomal aneuploidy derived from chromosome mis-segregation during meiosis is indeed responsible for impaired fertility, causing 30% of human miscarriages and detrimental embryonic development[202]. When aneuploidy is not lethal, it results in severe defects in the progeny, such as mental retardation. Indeed a well characterised example of viable aneuploidy is trisomy 21 in humans, a genetic condition, responsible for Down syndrome, in which individuals stably possess three copies of the chromosome 21[200]. Nevertheless, aneuploidy often encompasses chromosomal instability (CIN), a condition in which cells experience ongoing chromosome segregation defects, leading to continuous changing of the aneuploid set. Cells affected by CIN are always aneuploid due to accumulation of new karyotype alterations[203]. CIN and consequently aneuploidy are widely found in many solid tumours and cancer cell lines, and are believed to be contributive events during the process of tumourigenesis[204].

1.4.1 Causes of whole-chromosome aneuploidy

1.4.1.1 Chromosome segregation

Whole-chromosome aneuploidy arises from defects in the processes that orchestrate chromosome segregation during different steps of the cell cycle, resulting in gain or loss of an individual chromosome (or few of them). Accuracy of these processes is essential for proper mitotic spindle assembly, kinetochore-microtubules attachment and dynamics, and centrosome number[205].

To better understand how aberrant chromosome repartition in the two daughter cells can occur, we here summarise the main steps of chromosome segregation (**Figure 14A**). During the synthesis phase (S phase) of the cell cycle, the mother cell undergoes DNA replication and duplication of the centrosome, a cytoplasmic organelle responsible for the assembly of the mitotic spindle. The centrosome is composed by two barrel-shaped structures, the centrioles, embedded in a proteinacious substance called the pericentriolar material (PCM), which orchestrate microtubule nucleation essential for spindle maturation[203]. Mitosis begins with entrance of the cell into prophase, when replicated DNA condensates into sister chromatids which are held together each with its own kinetochore linked to the other by cohesin ring structures[206]. Almost simultaneously, the duplicated centrosomes migrate to opposite poles of the dividing cell, where they form spindle fibers by emanating microtubules that, after nuclear membrane breakage, attach to each kinetochore of the sister chromatids. In metaphase, the sister chromatids are oriented at the equator of the cell, where they aligned to form the so called metaphase plate, due to pulling forces generated by opposite kinetochore microtubules. A mitotic checkpoint mechanism, known as spindle-assembly checkpoint (SAC) prevents chromosome mis-segregation by halting cell cycle progression until every sister chromatid pair is correctly attached to spindle microtubules [207]. Components of the SAC machinery senses the presence of incorrectly attached or empty kinetochores and delays mitosis in metaphase: they inhibit activity of the anaphase-promoting complex or cyclosome bound to its activating subunit CDC20 (APC/C-CDC20), required for metaphase-to-anaphase transition. Once all the kinetochores are properly attached, SAC inhibition is disrupted, and APC-CDC20 leads to activation of the protease separase: it induces degradation of both securin, the separase inhibitory subunit, and Cyclin B, the latter resulting in inhibition of cyclin-dependent kinase 1 (CDK1) activity which leads to separase dephosphorylation and

activation. Active separase then cleaves cohesion rings, thus promoting detachment of the sister chromatids and chromosome segregation[208].

1.4.1.2 Different mechanisms of chromosome mis-segregation lead to aneuploidy

Multiple errors occurring during mitosis can give rise to chromosome mis-segregation and therefore aneuploidy. Defects in the mitotic checkpoint signalling due to compromised SAC functions or APC-CDC20 hyperactivation inevitably lead to formation of aneuploid daughter cells lacking or gaining one or few chromosomes, as result of their faulty attachment to the spindle (**Figure 14B**). An impaired mitotic checkpoint due to mutations in the genes of the SAC machinery is highly associated to increased CIN and aneuploidy occurrence. Nevertheless, mutations that completely inactivate the mitotic checkpoint function are accompanied by massive chromosome mis-segregation and are highly detrimental to cell fate[204].

Production of aneuploid cells can also occur despite functional mitotic checkpoint signalling. Aberrant attachments of the spindle microtubules to the chromatid kinetochores represent an additional example of mitotic defects with clear aneuploid outcomes. Premature loss of sister chromatid cohesion, due to impaired cohesin function or hyperactivation of separase, can result in attachment of individual sister chromatids by microtubules from the same spindle pole, thus leading to random chromosome segregation (**Figure 14C**)[206]. Since kinetochore-microtubule connection occurs, no delay signals are generated by the SAC machinery. This principle is valid also when the kinetochore of paired-sister chromatids is anchored by microtubules from both spindle poles, a condition known as merotelic attachment (**Figure 14D**)[209]. The improper attachment is usually corrected before anaphase entry, but in some cases culminates with a median lagging chromosome that is either excluded from both daughter cells during cytokinesis or accurately segregated into one of them, where it is confined in a micronucleus[210]. Merotely occurrence can be promoted by formation of multipolar spindles, which derives from the presence of more than two centrosomes or fractured centrosomes within the mitotic cell. In this situation, efficient cytokinetic events can generate a progeny of multiple aneuploid cells; on the other hand, aberrant cytokinesis results in polyploidisation (**Figure 14E**)[204, 208]. Supernumerary centrosomes causing multiple spindles are generated by several mechanisms, including cytokinesis failure; cell fusion; endoreduplication (DNA duplication without following mitosis); and mitotic slippage, a

condition in which, after long-term mitotic arrest, a cell exit from mitosis generating one tetraploid G1 cell[200]. Acquisition of multiple centrosomes can also occur due to aberrant regulation of the protein machinery that control centriole duplication and separation. The CDK2 kinase is required to initiate centrosome duplication in S phase and promotes centriole maturation and separation together with Polo-like kinase 1 (PLK1), Aurora A kinase and the microtubule-molecular motor Kinesin family member 22 (KIF22) at the G2 and M phases[203, 211]. Constitutive activation of CDK2 promotes aneuploidy by inducing centrososme amplification; similarly, mis-regulation of PLK1, Aurora A and KIF22 expression or activation is a major cause of chromosome instability and aneuploidy, by promoting formation of multiple centrosomes and spindle disorganisation. A crucial regulator that maintains homeostasis of these proteins is checkpoint with forkhead and ring finger domains, E3 ubiquitin protein (CHFR), a checkpoint protein that delays entry in mitosis in response to mitotic stresses, to ensure chromosome stability. CHFR is an E3-ubiquitin ligase that promotes degradation of PLK1, Aurora A and KIF22, preventing their excessive accumulation and functional activity. Loss of CHFR produces severe CIN, arisen from centrosome amplification, spindle mis-organisation and cytokinesis failure[211-213].

By contrast, failure of centrosome duplication or separation due to mutation, inhibition or depletion of central players of these processes is responsible for establishment of monopolar spindles (**Figure 14F**)[214]. Cells containing only one centrosome generally undergo to prolonged mitotic checkpoint-dependent arrest, triggered by presence of at least a few unattached chromosomes. Although it is not clear what determines the fate of these cells, under these conditions cells either die following a sustained mitotic arrest or survive by adaptation. This is a poorly understood process that occurs when cells adapt to exit mitosis after prolonged mitotic arrest skipping the cytokinesis and karyokinesis (nuclear division) steps to generate a tetraploid G1 phase cell that still contains unattached chromosomes (**Figure 14F**). In cases where these abnormalities are accompanied by impaired mitotic checkpoint pathway at individual kinetochore, the cells escape from mitotic arrest at earlier steps and have more chances to survive[204]. Viable tetraploid cells then can succeed in cell division, leading to formation of high grade aneuploid cells, due to abnormal centrosome number and increased chromosome instability.

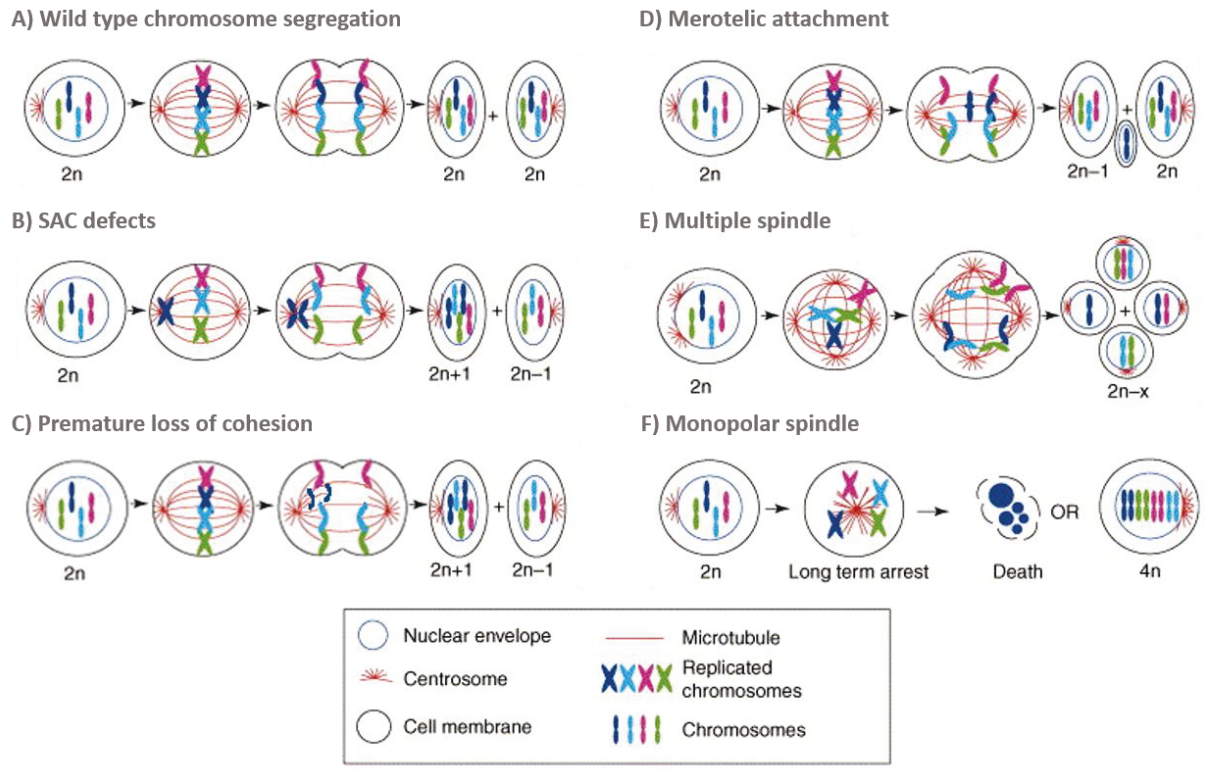

Figure 14: Mitotic defects inducing aneuploidy. A, Wild type chromosome segregation during mitosis produces two identical diploid daughter cells hypothetically containing four chromosomes. Gain or loss of one or few chromosomes due to chromosome mis-segregation in mitotic cells is caused by: **B,** Defects of the spindle-assembly checkpoint (SAC) determining improper kinetochore attachment by microtubules; **C,** Premature loss of cohesion that results in attachment of individual sister chromatids by microtubules from the same spindle; **D,** Merotelic attachment causing lagging chromosomes generally expelled upon cytokinesis; **E,** Multipolar spindle and consecutive cytokinesis that generates a progeny of multiple aneuploidy cells. **F,** Cells containing monopolar spindle undergos to either cell death or mitosis exit producing a tetraploid G1 cell. Modified from [204]

1.4.2 Aneuploidy: cause of cancer?

More than a century ago, Theodor Boveri described a link between aneuploidy and malignant transformation, proposing that chromosomal instability is the causal trigger for uncontrolled cell proliferation and tumour formation[215]. Although proving that aneuploidy is a direct cause of tumourigenesis is still a challenging matter, aneuploidy is widely recognised as a common feature of cancer. Effectively, more than 90% of solid tumours and 75% of hematogenous cancers show heterogenous degrees of aneuploidy. Indeed, most cancers contain near-diploid cells that exibit not only an unbalanced number of chromosomes but also different chromosome numbers from one another (usually between 60 and 80). However, a significant proportion of solid tumours shows near-tetraploid karyotypes, which derives from

cells that after tetraploidisation events (such as failure of cytokinesis) have mis-segregated individual chromosomes[204]. Ongoing gain or loss of one or few whole chromosomes during mitosis, which determines harbouring of the aneuploid state, is an inevitable consequence of chromosomal instability (CIN), another feature shared by many types of cancer. Moreover, tumour cells frequently harbor a series of genetic alterations, such as mutations, amplifications and deletions, a consequence of the genomic instability that is a hallmark of cancer. Targets of genomic instability events commonly found in a variety of solid tumours are oncogenes and tumour-suppressor genes such as *KRAS*, tumour protein p53 (*TP53*), phosphatase and tensin homologue (*PTEN*), retinoblastoma 1 (*RB1*), breast cancer 1 (*BRCA1*), and others, with inevitable impact on cell proliferation and survival[208]. How CIN and therefore aneuploidy causatively contribute to malignant transformation in addition to the action of genomic instability, is still unaddressed. The hypothesis is that the property of a cell population to rearrange whole chromosome distribution can elicit tumourigenesis, by possibly causing loss of heterozygosity (LOH) of a tumour suppressor gene, present in the lost chromosome. Conversely, this ability might lead to amplification of an oncogene by duplicating the chromosome in which the mutated allele is embedded[216].

Mitotic defects causing chromosome mis-segregation and aneuploidy have been shown to promote malignant transformation. Evidence for this arises from *in vivo* and *in vitro* studies where CIN was induced by engineered mutations or deregulation of genes involved in different steps of chromosome segregation. For example, transgenic mice that overexpress or carry a heterozygotic mutation in individual SAC genes, such as Budding uninhibited by benzimidazoles 1 homolog (*BUB1*), mitotic arrest deficient,yeast, homolog-like 1 (*MAD1L1*) and mitotic arrest deficient,yeast, homolog-like 2 (*MAD2L2*), exhibit increased tumour incidence, as result of impaired mitotic checkpoint signal and consequent increased CIN and aneuploidy[217]. Additionally, aberrant cohesion or separation of the two sister chromatids is associated with tumourigenic outcomes. Indeed, inactivating deletion or mutations of *STAG2* gene, encoding a cohesin subunit, result in defective chromatid separation and are a cause of aneuploidy in different tumour types[218]. In addition to defective mitotic spindle checkpoint and chromatid cohesion, abnormal centrosome number has been implicated in tumourigenesis. In this respect, amplification and experimental overexpression of *Aurora A* has been reported to yield centrosome amplification, resulting in CIN, aneuploidy and malignant transformation in *in vivo* BC models[219]. Moreover, *CHFR* deficiency in mice greatly increases incidence of spontaneous tumour formation, and promotes CIN through mis-regulation of Aurora A. CHFR is a tumour suppressor that ensures chromosomal stability by

regulating the expression levels of crucial centrosome components, such as Aurora A, PLK1 and KIF22[211-213]. A tumour suppressive function of CHFR has also been demonstrated in BC, where *CHFR* exhibits low or null expression[220]. Stable downregulation of CHFR in immortalised mammary cell lines resulted in the acquisition of multiple malignant phenotypes, including increased aneuploidy and anchorage-independent cell growth.

Finally, primary breast carcinomas display chromosome instability and aneuploidy, associated with lack of *PTEN* expression[221]. The tumour suppressor PTEN controls proliferation and survival by inhibiting the proliferative activity of the phosphatydilinositol-3 kinase (PI3K)/AKT pathway. Loss of PTEN in BC results in hyperactivation of AKT, which induces phosphorylation, degradation and reduced nuclear localisation of CHK1, a DNA damage checkpoint kinase that control mitosis entry and prevent chromosome instability.

1.4.3 Cytokinesis failure as a precursor of aneuploidy and cancer

1.4.3.1 General mechanisms of cytokinesis

Cytokinesis is the final step of cell division responsible for the physical separation of two distinct daughter cells, ensuring proper inheritance of the segregated chromosomes, the cytoplasmic content, and the plasma membrane. Thus, it is essential for maintenance of euploidy during organismal development, adult life and reproduction, and to avoid the development of disease, particularly cancers[222].

In animal cells, cytokinesis is accomplished through a series of key events that include formation of the central spindle, assembly and contraction of an actomyosin ring that allows cleavage furrow ingression, and abscission via membrane fusion (**Figure 15**).

Establishment of the division plane or central spindle (**Figure 15**) begins at the anaphase onset, when a set of microtubules between the segregated chromosomes becomes bundled during anaphase in an antiparallel fashion to provide a docking scaffold for key regulators of cytokinesis. These include the centralspindlin complex, a heterotetramer consisting of a kinesin, MKLP1 and a RHO family small GTPase-activating protein (GAP), CYK-4. After release from Cyclin B/CDK1-mediated inhibition, centralspindlin accumulates at the mid-zone between the nascent daughter nuclei by interacting with bundled microtubules of the central spindle[223]. Localisation and clustering of centralspindlin complexes is tightly coordinated by Aurora B kinase and 14-3-3 proteins. The latter sequester cytoplasmic MKLP1

allowing Aurora B to activate by phosphorylation clustering and stable accumulation of centralspindlin at the spindle mid-zone[224]. Active centralspindlin then associates with a RHO GTPase guanine exchange factor (GEF), ECT2, which promotes local activation of the small RHO GTPase RHOA, critical for the production of the functional actomyosin ring[223]. In its active, GTP-bound form, RHOA triggers multiparallel signalling pathways that result in actin nucleation and polymerisation via formin activity, and myosin light chain phosphorylation (see 1.3.1.1). The resulting actin filaments and active myosin coordinate the arrangement of a contractile actomyosin ring that associates with the inner face of the plasma membrane (**Figure 15**). Actomyosin contractility then drives shrinkage of the ring that causes furrowing of the plasma membrane, thus progressively reducing the cytoplasmic space that still connects the two daughter cells[222, 223]. As ingression of the cleavage furrow proceeds, the microtubule bundles in the spindle midzone are compacted in an intercellular bridge, which consists of a midbody ring derived from the actomyosin ring and cross-linked midzone proteins (**Figure 15**). Final separation, or abscission, is accomplished through coordinated disruption of the intercellular bridge and resolution of the two daughter cells‟ plasma membranes[222, 223] (**Figure 15**). The intercellular bridge is disrupted by clearance of microtubule bundles via breaking and severing events and by dissociation of the actomyosin ring that requires RHOA inactivation. In this respect, 14-3-3 proteins and protein kinase C epsilon (PCKε) are critical for completion of cytokinesis. PCKε activation upon binding by 14-3-3 protein dimers is required to limit RHOA function at the midbody during late cytokinesis, which in turns allows dissociation of the actinomyosin ring during final separation[225]. Ultimately, resolution of an independent plasma membrane for each daughter cell is achieved via delivery of membrane vescicles at the midzone where they bridge the space remaining after maximal furrow ingression via fusion mechanisms. Different cellular machineries are involved in the process of membrane separation, including members of the v-SNARE vescicle trafficking and fusion machinery, such as Sintaxin 2 (STX2) which mediates membrane fusion for successful cytokinesis completion[226]; and RAB family GTPases, such as RAB21, which associates with integrins and ensures their proper trafficking/recycling to and from the membrane furrow, necessary for a proper abscission[227].

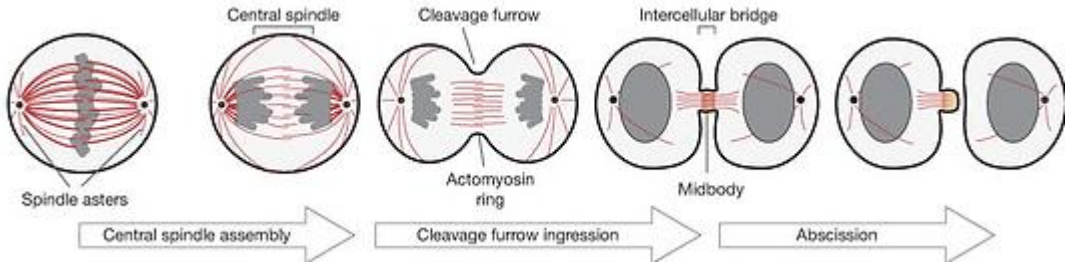

Figure 15: Main steps of cytokinesis. Cytokenisis begins with assembly of the central spindle via microtubule (red) bundling and proceeds with formation of an actinmyosin ring of which contraction allows ingression of the cleavage furrow. Maximal membrane furrowing culminates with formation of an intercellular bridge containing the midbody, of which disruption enables abscission of the plasma membrane that separates the two daughter cells. Modified from[228].

1.4.3.2 Cytokinesis failure as prelude to aneuploidy and tumourigenesis

Accuracy in spatial and temporal coordination of distinct steps of the cytokinesis process is necessary for proper inheritance of genetic information and cytoplasmic content of the two daughter cells. Misregulation of several cytokinetic proteins can compromise the progression of cytokinesis, resulting in generation of binucleated or multinucleated cells, with enhanced genomic instability and implications for tumourigenesis.

For instance, localisation of the centralspindlin complex at the midzone microtubules is essential for proper central plane formation and successful cytokinesis. In this respect, aberrant regulation of Aurora B, 14-3-3 proteins and CDK1 expression or activity causes incorrect accumulation of centralspindlin components at the central spindle and cytokenisis defects[224, 229] [230]. Additionally, abnormalities in pathways regulating actinomyosin dynamics can slow ring closure making cells incompetent for completion of cytokinesis and therefore causing furrow regression and formation of binucleated cells. For example, disruption of PCKε-14-3-3 complex is accompanied by RHOA hyperactivation, which leads to delay of actinomyosin ring dissociation and consequently to cytokinesis failure[225]. Moreover, complete abscission that separates the two daughter cells can be compromised by abortive cleavage furrow ingression and impaired membrane fusion. In the first case, inhibition of RAB21, a RAS small GTPase that control integrin endo/exocytosis, is known to produce binucleated and multinucleated cells, due to reduced trafficking of integrin at the cleavage furrow where integrin-mediated adhesion is required for anchoring and furrowing of the plasma membrane[227]. In the second case, it has been shown that inhibition of members of

the SNARE fusion machinery, such as Syntaxin 2, affects later steps of the abscission event, impeding complete separation and fusion of the daughter cells" membranes[231].

An inevitable result of a failed cytokinesis process is the production of a tetraploid cell. In addition to impaired or unattempted cytokinesis or monopole spindle occurrence as seen before, failure of karyokinesis (nuclear division) can also leads to tetraploidisation. Karyokinesis failure can occur following defective mitotic spindle formation associated with impaired mitotic checkpoint activity with a similar mechanism to that seen in monopolar spindle formation (**Figure 14F**), or in the failed separation of sister chromatids, which is usually caused by defects in key regulators of this process, such as APC/C and separase[217].

Tetraploidisation, a form of euploidy in which a cell possesses 4 sets of homologous chromosomes, has been largely associated with tumourigenesis. Indeed, tetraploid cells exibit genomic instability and are believed to elicit a high aneuploidy state, thus contributing to malignant transformation. This is consistent with the observation of tetraploid or near-tetraploid cells in many types of cancer, such as carcinomas of the breast and the cervix[216, 232]. Moreover, chromosomal abnormalities associated with tetraploidisation, such as centrosome amplification, have been observed in cancer. About 80% of invasive breast carcinomas display aberrant structure and/or number of centrosomes associated with aneuploidy and chromosomal instability[233].

A critical feature of tetraploid cell is, in fact, the presence of two centrosomes. With the entrance in a new cell cycle, these centrosomes likely duplicate and produce multipolar spindles with three or four poles, which would lead to generation of aneuploid progeny during a subsequent mitosis with successful cytokinesis (**Figure 16**)[204]. Propagation of tetraploid cells can be compromised by the intervention of a "tetraploidy checkpoint", a mechanism believed to sense centrosome amplification and to prevent inheritance of errors of late mitosis and enhanced aneuploidy by affecting viability of tetraploid cells[232]. A "tetraploidy checkpoint" mechanism was observed upon induction of cytokinesis failure via drug-induced inhibition of furrow ingression, when the resulting tetraploid cells undergo to cell cycle arrest in G1 phase in a p53-dependent manner[234]. Tetraploid cells generated after transient block of cytokinesis are able to promote tumourigenesis in p53-null mice, due to enhanced whole-chromosome mis-segregation[235]. However, tetraploid cells frequently exhibit the ability to succeed cell cycle progression without undergoing to arrest or delay in G1, thus questioning the existance of the "tetraploid checkpoint" that monitors centrosome and chromosome number. It seems more likely that tetraploids arrest in G1 phase is a consequence of p53 activation in response to cellular stresses associated with drug treatments or to aberrant

centrosome duplication[232]. In addition to cell cycle arrest, tetraploid cells can undergo to cell death by activation of pro-apoptotic pathways. Consistently, defective apoptosis due to mis-regulation of BCL2 (B cell lymphoma 2) family members leads to spontaneous generation of tetraploid cells that are able to induce malignant transformation associated with ploidy abnormality[236].

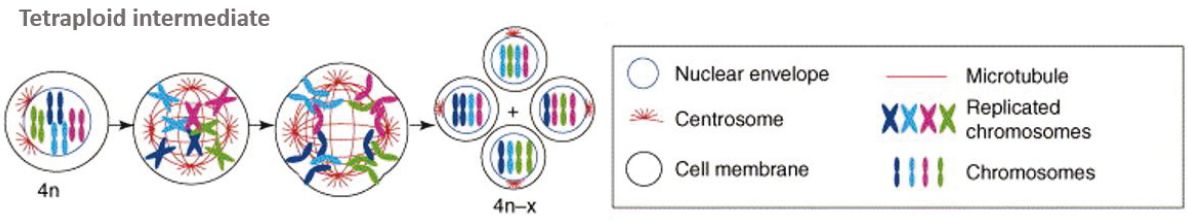

Figure 16: Tetraploid intermediate derived from unattemped or failed cytokinesis. A tetraploid cell generated by failure of cytokinesis contains two centrosome form multipolar spindles with four poles, resulting in the formation 4 aneuploid cells following successful mitosis and cytokinesis. Modified from [228].

1.5 MicroRNAs

MicroRNAs (miRNAs) are a class of endogenous, non-coding, single stranded RNAs ranging in size from 18 to 26 nucleotides. They play an important role in the regulation of gene expression, mainly at the post-transcriptional level, thus representing a unique mechanism of epigenetic control.

The first description of miRNAs dates from 1993, when two research groups simultaneously identified *lin-4*, as a gene necessary for the postembryonic development of *Caenorhabditis elegans*[237]. They found that *lin-4* gene codifies for a ~22-nts non-coding RNA that negatively regulates the protein level of *lin-14*, creating a temporal gradient of this protein, necessary for the developmental transition from the first larval stage (L1) to the second one (L2). They also demonstrated that this small RNA is complementary with conserved elements located in the 3′ untranslated region (3′UTR) of *lin-14* mRNA, suggesting that *lin-4* negatively modulates its translation by base-pairing with these sites in the *lin-14* 3‟UTR. Almost 7 years later, the second miRNA, *let-7*, was identified also in *C. elegans*. *Let-7* encodes a temporally modulated 21-nts non-coding RNA that negatively controls the expression pattern of a subset of genes, fundamental for the later developmental stages, in a similar way as for *lin-14* regulation by *lin-4*[238]. Homologs of let-7 were soon identified throughout many metazoans, including flies and humans, thus pinpointing *let-7* small RNAs as evolutionary conserved regulators of the latest developmental stages [239]. A large number of different small, endogenous RNAs were successively found in worms, flies and humans, associated with a cell-specific rather than a time-specific pattern of expression[240] [241]. This implicated a broader role in the cell physiology for this novel class of RNAs, that was commonly referred to as microRNAs.

To date, over 25,000 mature miRNAs have been sequenced from the genome of a wide number of plant and animal species, amongst which *Homo sapiens*‟ encodes more than 2500 small RNAs, although some of these need to be authenticated[242, 243]. On the other side, more than a half of all human protein-coding genes are evolutionarily selected as miRNA gene targets[244], supporting the miRNA potential in the control of the expression of most human proteins and their related pathways. Indeed, miRNA functions have been widely described in numerous physiological processes, including proliferation, differentiation, development, apoptosis and stress response[245]. More importantly, deregulated expression of miRNAs has been associated with tumourigenesis and metastasis, and implicated in other common diseases[246]. As our understanding of miRNA biology continues to improve, miRNA-based

therapy as an effective anti-cancer treatment is becoming a much more tangible possibility[247].

1.5.1 MicroRNA genes

Large-scale genomic mapping analysis have identified microRNA-coding sequences in all chromosomes, with the exception for the human Y chromosome[248].

Genomic organisation of miRNA genes can be distinguished as intergenic or intragenic.

Intergenic miRNAs are found in genomic regions that do not overlap with annotated genes; instead they originate from independent transcription units, carrying their own promoters and other regulatory elements. Intergenic miRNAs are generally transcribed by RNA Polymerase II (Pol II), thus exhibiting typical features of Pol II transcripts, such as capped 5‟ends and a polyadenylated tail (polyA) at the 3‟ends[249]. Intergenic miRNAs can be present as individual miRNAs or clustered in polycistronic units that encode a long primary transcript (~3-4kb) containing more than one miRNA[250].

Intragenic miRNAs reside in transcriptional units of host annotated genes as single or clustered miRNAs; approximately half of all miRNAs are localised in non-protein-coding genes[250], whereas the rest are found within the introns of protein-coding genes. Generally, intronic miRNA genes share the same promoter regulation as their host genes and consequently exhibit similar expression profiling as their host transcripts[251]. Nevertheless, it has been reported that intronic miRNAs can be under transcriptional control of their own promoters, such as the miR-17-92 cluster, which is localised in intron 3 of the *chromosome 13 open reading frame 25* (*C13orf25*) gene [252]. Intronic miRNAs are transcribed within the intron of their host messenger transcripts, from which they are processed following the classical pathway of miRNA biogenesis. In special cases, intronic miRNAs constitute the entire intron of a protein-coding gene and are therefore released upon splicing of the host gene mRNAs. These are known as mirtrons and typically bypass the first processing event during their maturation [253].

Very rarely, intragenic miRNA are found in regions that overlap an exon and an intron of non-protein-coding genes. These are known as exonic miRNAs and their expression is coordinated by their host gene promoters[254].

1.5.2 MicroRNAs biogenesis

The majority of mirRNAs go through a biogenesis model demarked by maturation events necessary for their ultimate function (**Figure 17**). MiRNA-coding sequences are generally transcribed by RNA polymerase II (Pol II), or less frequently by Pol III, yielding a long, primary miRNA transcript, called pri-miRNA[249] [255]. After transcription, pri-miRNA are capped and polyadenylated at the 5‟ and 3‟ end, respectively and fold in their characteristic conformation containing one or more stem-loop structures (hairpins) (**Figure 17**). Typically the pri-miRNA hairpin contains a ~33 base-pairs (bp) double-stranded stem formed by regions of imperfect complementarity, with flanking single stranded 5‟ and 3‟ ends[256]. One of the two strands of the pri-miRNA stem includes the mature miRNA sequence, which needs to be excised (**Figure 17**). Two processing events lead to the formation of the mature miRNA. The first takes place in the nucleus and is mediated by the so-called Microprocessor complex, which consists of the RNase III endonuclease DROSHA and the RNA-binding protein DiGeorge syndrome critical region 8 (DGCR8) (**Figure 17**)[257] After recognition and binding of the stem-loop structure of the pri-miRNA by the Microprocessor complex, DROSHA cleaves both strands of the pri-miRNA stem near the base of the hairpin, thus releasing a ~60-70-nt stem-loop intermediate, known as miRNA precursor (pre-miRNA) (**Figure 17**)[258]. However, a sub-class of miRNAs (such as intronic miRNAs called “mirtrons”) undergo a non-canonical maturation pathway that does not require a DROSHA/DGCR8-mediated cleavage event, but instead uses the cellular splicing machinery for the formation of the pre-miRNA[253, 259]. Pre-miRNAs consist of a >14 base pairs (bp) stem-loop region along with a 5‟phosphate and a 2-nt overhang at the 3‟end. This structure is essential for recognition by the nuclear transport receptor Exportin 5 (EXP5)[260], that, in complex with a RAN-GTP, exports the pre-miRNA to the cytoplasm via the nuclear pore complex (NPC) (**Figure 17**)[261].

The second processing event (maturation) occurs in the cytoplasm by the RNase III endonuclease DICER (**Figure 17**). DICER, first found to be implicated in the process of RNA interference (RNAi) by mediating the formation of the small interfering RNAs (siRNAs)[262], has also been shown to mediate miRNA maturation[263-265] . DICER recognises the 3‟end of the pre-miRNA and cleaves off the loop, generating a ~22-nt dsRNA duplex (miRNA-miRNA*) with 2-nt overhangs at both 3‟ends (**Figure 17**). This duplex is formed by a functional strand called the guide strand (miRNA) and a complementary strand, known as the

passenger strand (miRNA*). In the cytoplasm, DICER is part of a multiprotein complex, called the RNA-induced silencing complex (RISC) loading complex (RLC)[248]. This is assembled upon interaction of DICER with the dsRNA-binding proteins, TAR RNA-binding protein (TRBP)[266] and protein activator of protein kinase R (PACT) in mammals, and subsequently with a member of the Argonaute (AGO) protein family. TRBP and PACT facilitates DICER-mediated cleavage and the recruitment of AGO protein (**Figure 17**)[266, 267]. Following DICER-mediated cleavage, the RLC is disbanded through dissociation from the miRNA duplex of DICER and its partners, TRBP and PACT. The double-stranded duplex is then unwound by helicase activity (which may not be universal), into the passenger strand that undergoes degradation, and the guide strand which forms the active RISC complex (**Figure 17**)[268]. The mechanism that controls sorting of the two miRNA strands remains still unclear; although some evidences suggest that the thermodynamic stability of the base pairs at the two ends of the duplex may be determinant, so that the strand with less base pair stability at its 5‟end will become the guide strand[269]. This represents the mature miRNA that is loaded onto the RISC complex upon interaction of the RISC component AGO with both ends of the miRNA strand[270]. The mature miRNA then guides the RISC to a target messenger RNA (mRNA) by a mechanism of imperfect base pair complementarity (**Figure 17**)[271]. The mature miRNA interacts with specific sites commonly present in the 3‟untraslated region (3‟UTR) of the target mRNA through the so-called "*seed*" region[272]. This consists of nucleotides comprised between positions 2 to 8 from the 5‟end of the miRNA sequence and forms a perfect match with the site in the mRNA 3‟UTR. This interaction may be stabilised by base pairing of a less stringent degree of the 3‟end of the miRNA, whereas central bulges are commonly formed due to the presence of mismatches predominantly in the centre of the miRNA sequence. In rare cases, near-perfect complementarity is observed between the miRNA sequence and its target site[273], resembling the complete base-pairing occurring between the siRNA and its mRNA target during the process of RNA interference (RNAi) (**Figure 17**)[274, 275]. Depending on the degree of complementarity established after interaction between the miRNA and its target mRNA, a distinctive AGO composition of the RISC complex will be observed. In mammals, the AGO protein family consists of 4 members (AGO1-4), which all function in miRNA-mediated post-transcriptional repression of target mRNAs, whereas only AGO2 exhibits additional RNAse III endonuclease activity. In the majority of the cases, imperfectly matched miRNA-mRNA duplexes are formed upon interaction of the miRNA with its mRNA target, and any of the four AGO members can associates with these heteroduplexes. On the other hand, when a perfect miRNA-mRNA

annealing occurs only AGO2 is able to interact with duplexes of total complementarity. The difference in miRNA-mRNA interaction complementarity and specific AGO member involved determines a distinctive function of miRNAs[274].

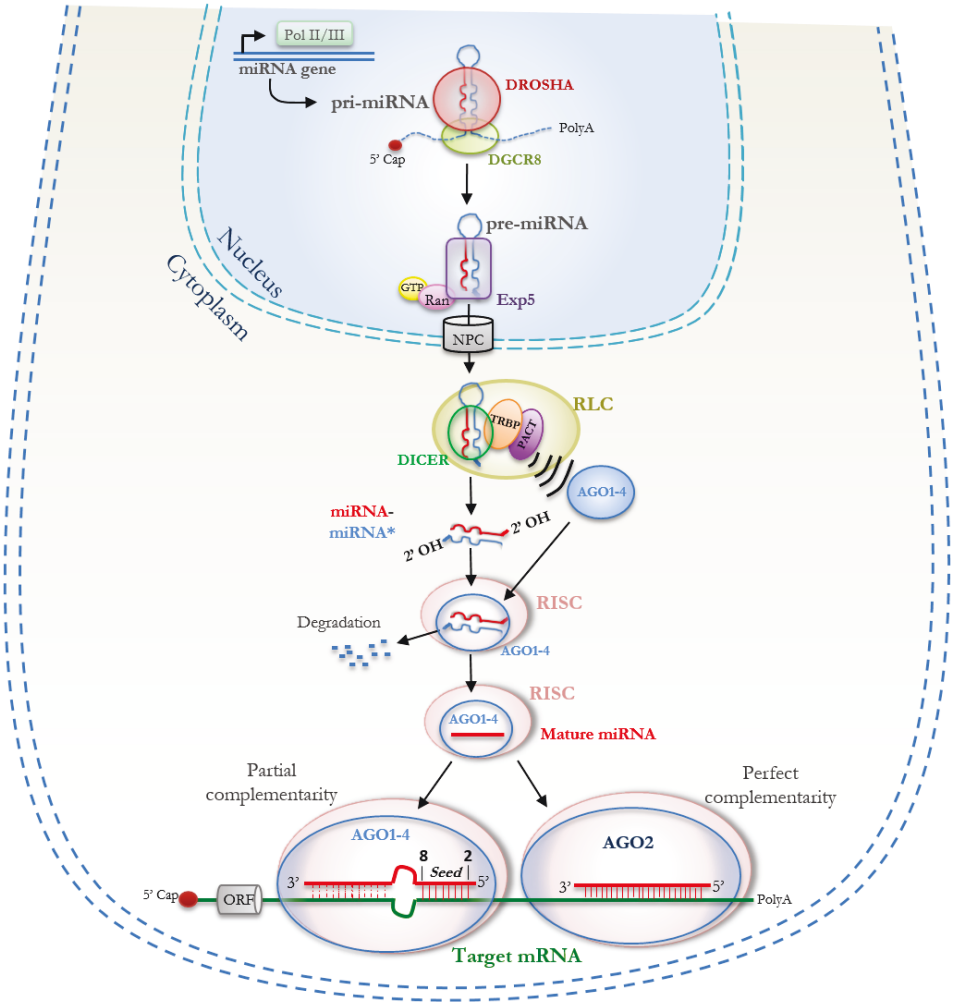

Figure 17: MicroRNA biogenesis model. MiRNA biogenesis begins with the transcription of the miRNA gene by Polymerase II or III (Pol/II/III) into a pri-miRNA. Pri-miRNAs are characterised by single stranded 5‟ and 3‟ ends, which are capped (5‟Cap) and polyadenylated (PolyA), respectively, which flank a stem loop region that is cleaved by the endonuclease DROSHA in complex with its mammalian partner DGCR8. The resulting miRNA precursor (pre-miRNA) is then engaged by Exportin 5 (Exp 5) which translocates it to the cytoplasm through the nuclear pore complex (NPC) in a Ran-GTP manner. The interaction between the pre-miRNA and the endonuclease DICER leads to RISC-loading complex (RLC) formation upon association of DICER with its co-factors TRBP and PACT; these facilitate DICER-mediated cleavage of the pre-miRNA into a miRNA-miRNA* duplex with 2‟ overhangs and recruitment of a member of the AGO protein family (AGO1-4). The miRNA duplex is then loaded onto the RISC complex and undergoes unwinding and strand selection. The passenger miRNA (miRNA*) is degraded, whereas the guide strand (mature miRNA) drives the AGO1-4-based RISC to selective recognition of a target mRNA: this is based on mechanisms of partial complementarity in which perfect match interaction occurs only between a region usually embedded in the 3‟UTR of the target mRNA and a “seed” sequence represented by positions 2 to 8 from the 5‟end of the mature miRNA. In rare cases, perfect complementarity is observed between the mature miRNA sequence and the target site and their interaction is mediated by AGO2.

1.5.3 MicroRNAs functions

MiRNAs are important physiological regulators of gene expression in plants and animals, thus their function has been demonstrated in a wide range of cellular processes[276].
Generally, miRNAs inhibit gene expression at the post-transcriptional level, by inducing either translational repression or degradation of their mRNA targets. The degree of complementarity in the miRNA-mRNA interaction determines one or other mechanism of inhibition. In the vast majority of the cases, poor base pair alignment is sufficient for the translational repression of miRNA targets. For this reason, it is not surprising that each miRNA is able to inhibit multiple genes, and one single mRNA can be targeted by several miRNAs[277]. On the other hand and in very few cases, highly matched mRNA targets preferentially undergo degradation induced by AGO2-mediated endonucleolytic cleavage.
MiRNA-mediated translational repression can occur through different mechanisms, which include: (1) inhibition of translation at the initiation stage; (2) block of translation at post-initiation stages; and (3) repression of translation by deadenylation and/or degradation of the target mRNA.
Translational inhibition at the initiation step was first observed after identification of a cap-binding-protein-like motif in human AGO2 proteins; AGO2 was found able to bind to the m^7G cap on a target mRNA, thus competing with the cap-binding protein eukaryotic translation initiation factor 4E (eIF4E) and subsequently inhibiting the initiation of translation of specifically capped mRNAs (**Figure 18**)[278]. Alternatively, translation initiation could be inhibited by the miRNA silencing machinery that impedes recruitment of the ribosomal subunits or formation of mature ribosomal complex at the 5‟end of the mRNA (**Figure 18**)[279].
Additionally, miRNAs have been found able to repress translation of their mRNA targets at post-initiation steps; a mechanism that was firstly suggested by the evidence that several mature miRNAs and AGO proteins co-localise with polysomal fractions both in mammals[280] and plants [281]. Various mechanisms of translational inhibition at post-initiation steps have been described. MiRNAs may impede elongation by either “dropping-off” translating ribosomes from the target mRNA, thus promoting premature termination[282], or inducing co-translational degradation of the nascent polypeptides (**Figure 18**)[283].
Finally, translational inhibition has been also shown to be achieved by miRNA-mediated mRNA degradation. By doing so, miRNAs affect target mRNA levels, thus decreasing their availability to the translational machinery. MiRNAs induce removal of the poly(A) tail at the

3‟end of the mRNA sequence by recruiting the deadenylation complex C-C chemokine receptor 4 (CCR4)-NOT1 (**Figure 18**)[284]. Deadenylase recruitment to the miRNA-silencing machinery is orchestrated by the AGO-interacting glycine-tryptophan [GW] repeat-containing protein of 182 kDa (GW182) which directly interacts with the complex NOT1[285]. Via GW182 interaction, the functional RISC is localised to specific foci within the cytoplasm, called processing bodies (P-bodies), where mRNA turnover occurs. In P-bodies, mRNA targets are in fact, decapped by decapping enzyme 1 and 2 (DCP1/DCP2) complexes[286], and therefore exposed to exonucleolytic digestion by the cytoplasmic 5‟-to-3‟exonuclease XRN1[248]. In cases of high-grade complementarity between the miRNA and the target sequence, AGO2 complexes within the RISC and directly induce mRNA degradation by endonucleolytic cleavage (**Figure 18**). Indeed, AGO2, also known as "slicer", cleaves the phosphodiester bond at the mRNA sequence corresponding to the tenth and eleventh nucleotides of the miRNA guide strand. AGO2-interacting GW182 brings the active AGO2-RISC to the P-bodies, where the cleaved mRNA is completely degraded (**Figure 18**): the 3' fragment of the mRNA is destroyed by the exonuclease XRN1, while the 5' fragment is degraded by the *exosome*, a complex composed by different exonucleases involved in 3'-5' RNA degradation[287].

Although miRNAs are universally recognised for their negative post-transcriptional regulation of gene expression, recent findings have raised the possibility of alternative functions of miRNAs, also at additional levels of gene expression. Indeed miRNAs can exhibit the ability to promote post-transcriptional translation, in the presence of certain conditions. An example of miRNA-mediated translational activity is given by miR-369-3: under serum starvation conditions, this miRNA interacts with the 3‟UTR of the tumour necrosis factor α (TNFα) mRNA via AGO2-RISC complex, which recruits the fragile X-related protein 1 (FXR1) and stimulates mRNA translation[288].

Moreover, recent evidence indicates a role for miRNAs in the nucleus at the transcriptional level, by either inhibiting or activating gene expression. For example, miR-320 has been shown to silence transcriptional expression of the cell cycle gene DNA-directed RNA polymerase III subunit RPC4 (POLR3D), by inducing recruitment of epigenetic mediators at the promoter of this gene in mammalian cells[289]. On the contrary, miR-373 is able to interact with complementary sites present in the promoter of the E-Cadherin and cold-shock domain-containing protein C2 (CSDC2) gene; this interaction is associated with Pol II enrichment at the transcription starting sites of these genes, which initiates their transcriptional

expression[290]. MiRNA nuclear activity has been also suggested by a possible retrograde transport of miRNAs from the cytoplasm into the nucleus[291].

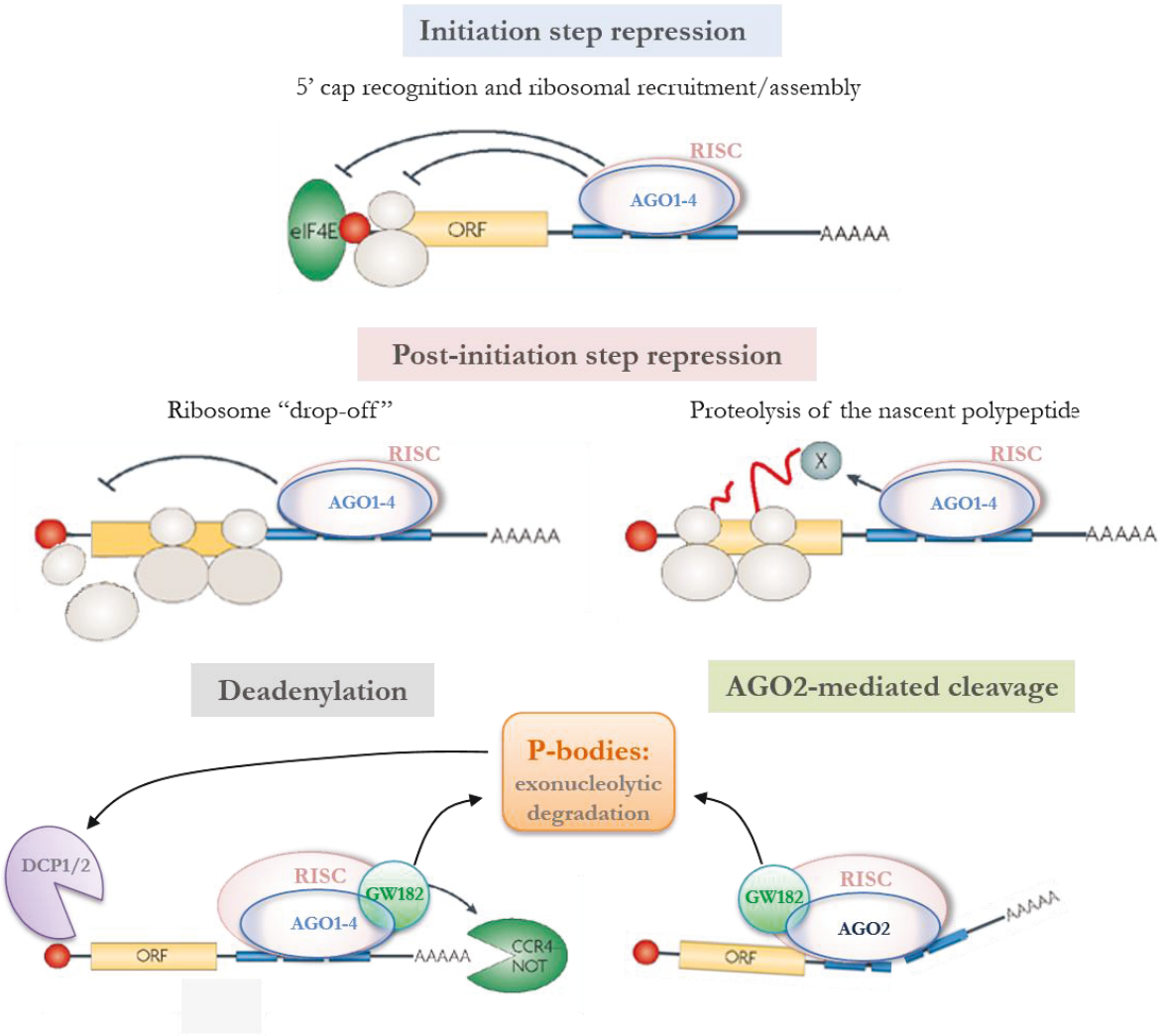

Figure 18: Mechanisms of post-transcriptional gene repression by microRNAs. MiRNAs complexed in the AGO-mediated RISC machinery can mediate repression of post-transcriptional expression of their target mRNAs via different mechanisms. In cases of imperfect complementarity base pair between the miRNA and the target mRNA, the RISC machinery can induce translation inhibition (i) at the initiation step: through inhibition of 5"Cap recognition and/or ribosomal recruitment/assembly; (ii) at the post-initiation step: by causing ribosome "drop off" which result in elongation inhibition or by stimulating proteolytic cleavage of the nascent polypeptide; (iii) or by inducing deadenylation of the target mRNA via recruitment of CCR4-NOT complex through the action of the RISC-associated cofactor GW182. This mediates target mRNA localisation to P-bodies where it undergoes to decapping due to DCP1/2 function and exonucleolytic degradation. In the rare cases of perfect matching between the miRNA and the target mRNA site, AGO2 mediates endonucleolitic cleavage of the miRNA followed by exonucleolitic degradation at the P-bodies. Modified from[271]

1.5.4 Regulation of miRNA biogenesis

The process of miRNA biosynthesis is subject to several control mechanisms that can be time-dependent, as seen for the temporal regulation of both lin-4 and let-7 expression, as well as organism/tissue-specific. Nonetheless, differential regulative control may apply only for a subset of miRNAs; more importantly, aberrant regulation of miRNA expression may contribute to pathogenesis, such as diseases and cancer.

There are three levels of regulation of miRNA biogenesis: pre-transcriptional, transcriptional, and post-transcriptional[292].

Many factors can affect miRNA expression at the pre-transcriptional level. Amongst them, genomic instability can lead to gain or loss of miRNA gene copy number; this has been widely observed in different types of cancers, as result of events of amplification, translocation or deletion of loci containing miRNA genes[293]. Additionally, miRNA gene expression is controlled by epigenetic mechanisms, such as DNA methylation and histone modification[292]. In fact, many miRNA genes are located in CpG islands, such as miR-127 which is silenced upon promoter hypermethylation in bladder cancer, and let7a-3, found to be highly methylated in normal lung tissues, but hypomethylated and up-regulated in lung cancer[294, 295].

MiRNA transcription is the most highly regulated step of the miRNA biogenesis process. Most of the miRNA genes are controlled by their own promoters which are transcribed by Pol II; this suggests that miRNA genes share the same transcription factors and other regulatory elements as the protein-coding genes. In fact, it has been shown for example that the transcription factor c-MYC directly induces expression of the miR-17-92 cluster during both B-cell proliferation and estrogen receptor (ER) activation in normal breast cells[296, 297]. On the other side, miRNA regulation by transcription factors has been amply associated to tumourigenesis. C-MYC-mediated activation of the miR-17-92 cluster or repression of several miRNAs, such as miR-15a, -29, -34, -23 and let-7 families leads to lymphoma initiation and progression[298] [299]. Another master-gene regulator, p53, controls the expression of many miRNAs[300], including miR-23, miR-26 and miR-34 families, the latter described as a key effector of the p53 tumour suppressor function[301, 302]. Furthermore, androgen receptor (AR) increases the abundance of miR-125b at the transcriptional level in prostate cancer cells[303] and the nuclear factor kappa-light-chain-enhancer of activated B cells (NF-κB**)** regulates miR-155 transcriptional regulation during lymphomagenesis[304].

In a similar way as for tumour suppressors and oncogenes, negative or positive regulation of miRNA expression by transcription factors can imply a state of cellular transformation that likely results in malignancy potential. Therefore, identification of putative miRNA regulators is of critical importance for the development of therapeutic strategies aimed to either restore silenced miRNAs or inhibit excessive miRNA expression. For this purpose, characterisation of miRNA promoters facilitates prediction of potential transcription factors that control the expression of specific miRNAs. Detailed information about promotor regions found in the entire human genome are provided by the ENCyclopedia of DNA Elements (ENCODE) Project and are available on the University of California, Santa Cruz (UCSC) Genome Browser[305]. Started in 2003, the ENCODE Project collects data from research groups worldwide about all functional elements in the human genome sequence. These include: histone modifications, transcriptional regulatory elements, Pol II and Pol III transcription starting sites (TSS) and binding positions for many transcription factors, such as c-MYC, c-FOS, c-JUN, E2F1, STAT1 and NF-κB identified in the whole genome by chromatin immunoprecipitation-sequencing (ChIP-seq) analysis in 27 human cell lines. From this tool, researchers can obtain preliminary information about possible regulatory mechanisms of a given miRNA that need to be experimentally validated [306].

After transcription, several steps of the miRNA maturation pathway can be exposed to external regulation. One example is given by miRNA-specific mechanisms that control DROSHA-mediated processing of the pri-miRNA. Although the DROSHA-DGCR8 Microprocessor complex processes many pri-miRNAs; a subset of miRNAs are maturated by a larger complex, which contains along with DROSHA and DGCR8, several additional factors[307]. Among these the RNA helicases p68 and p72 have been shown to be essential for the processing of specific pri-miRNAs[308]. Furthermore, the heterogeneous nuclear ribonucleoprotein A1 (hnRNP A1) binds specifically to pri-miR-18a increasing DROSHA processing rate[309].

Secondly, miRNAs are regulated at the DICER processing step. For example, pre-miR-138 is expressed ubiquitously but its mature form is restricted just to certain cell types, indicating tissue-specific DICER processing of this miRNA[310]. Additional regulatory mechanisms of miRNA formation were identified after observation that LIN-28 is a stem-cell-specific regulator of let-7 post-transcriptional maturation at both DROSHA and DICER level. In the nucleus, LIN-28 inhibits Microprocessor-mediated cleavage of pri-let-7[311], by competing with DROSHA[312, 313]. In the cytoplasm, LIN-28 is able to inhibit DICER-mediated cleavage of the pre-let-7 family member [314] by recruiting a terminal uridylyl transferase (TUTase) to

the precursor. The uridylated pre-let-7 (up-let-7) cannot be processed by DICER and is degraded by an unidentified nuclease[315]. Furthermore, Trabucchi *et al*. linked the KH-type splicing regulatory protein (KSRP) to the machinery regulating miRNAs maturation. They showed that KSRP is part of both DROSHA and DICER complexes and regulates the biogenesis of a subset of miRNAs in mammalian cells. KSRP binds with high affinity to the terminal loop of the target miRNA precursors and promotes their maturation. This mechanism of regulation provides differential expression patterns of target mRNAs that affect specific biological programs, including proliferation, apoptosis and differentiation [316].

1.5.5 Bioinformatic prediction and experimental validation of miRNA targets

MiRNA function is mediated by repressing translation of target mRNAs, thus identification of the targets is of crucial importance in understanding the biological role(s) of a miRNA. Target recognition by a miRNA is determined predominantly by the degree of complementarity between the miRNA-binding site contained in the target 3'UTR and the miRNA "*seed"* region, with less contribution from the 3' region of the miRNA[272, 317]. Based on the complementarity prerequisite and other determinants of miRNA-mRNA interactions, several research groups have elaborated various computational algorithms for the prediction of miRNA targets. These *in silico* systems base their predictions on the following three criteria: (1) perfect alignment between the miRNA *seed* and the 3'UTR of the target mRNA; (2) structural and thermodynamic stability of miRNA-target duplex, and (3) degree of evolutionary conservation of miRNA target sites. Examples of algorithm search for miRNA target prediction are *TargetScan, PicTar, RNAhybrid, DIANA-MicroT miRanda, and miRbase*, which are freely accessible on the web and are widely used to identify putative miRNA targets[318-320]. Despite being based on the same parameters, these methods use different approaches in elaborating computational predictions based on sequence alignments; for this reason, different algorithms give variable outputs of putative target sites for a specific miRNA, with plausible false positive production[321]. Therefore, predicted targets need to be experimentally validated in order to identify the true mRNA target(s) and elucidate miRNA functional roles[322].

Experimental validation of putative miRNA targets can be assessed in several different ways. Firstly, reporter systems are widely used in assessing for interaction of a given miRNA with its cognate mRNA. They consist of cloning the entire 3'UTR of the predicted target in a

plasmid vector downstream of the open reading frame of a reporter gene, such as a luciferase, and co-expressing the reporter vector and the miRNA of interest into a cellular system. Assayed reduction of reporter activity/expression is evidence of interaction between the miRNA and its predicted binding site[318]. Concomitant use of appropriate controls, such as vectors with mutated miRNA-binding sites, proves direct interaction and also eliminate any non-functional miRNA binding site that have been predicted for one or more target mRNAs.

For this interaction to happen in physiological conditions, it is necessary that both miRNA and its putative target(s) are co-expressed in the same cell models or tissue samples. Expression profiles of miRNAs and relative gene targets are usually obtained by quantitative real-time polymerase chain reaction (qPCR), Northern blotting and *in situ* hybridization assays.

Further, experimental validation of true miRNA targets is achieved by using both miRNA gain and loss of function approaches. In the first case, increase in miRNA levels is obtained by transient overexpression of a synthetic miRNA mimic in a cell model expressing the target mRNA. Consistent with miRNA-induced repression of target translation, decrease in the amount of protein encoded by the target mRNA is expected and can be quantified by Western blot analysis. Nevertheless, it has been demonstrated that reduction of target protein levels by miRNAs is variable and relatively mild, probably depending on the intracellular abundance of the target product and on the fact that a single miRNA can simultaneously target several genes[323]. Since miRNAs are also able to promote destabilisation and turnover of target mRNAs[284], predictable changes in the abundance of target messengers can be quantified (i.e., by real-time qPCR).

Nevertheless, gain of function experiments alone for the validation of miRNA targets are not an ideal approach, since the robust intracellular increase of a given miRNA induced by ectopic overexpression of a miRNA mimic could result in regulation of a subset of genes that are normally not targeted by this miRNA, when it is expressed at physiological levels. Therefore, experimental miRNA inhibition would increase the chance of identifying true target mRNAs. In fact, silence of the activity of a given miRNA leads to the up-regulation of specific genes that represent its physiological targets, because their up-regulation is the direct result of the impaired miRNA-mediated repression, caused by the experimental inhibition of the endogenous miRNA activity. Nevertheless, it has been shown that the distinct gene targets found repressed after engineered overexpression of a given miRNA are found with high similarity also after inhibition of the same miRNA[323], indicating that miRNA over-expression experiments may be still reliable. Therefore, combination of these two

experimental approaches would allow identification of the true physiological miRNA targets with a higher probability than each approach would do alone.

MiRNA loss of function (inhibition) is achieved by using miRNA inhibitors, such as synthetic oligonucleotides (anti-miRNAs) and miRNA-sponges. Both methods silence miRNA function by preventing assembly of functional miRISC, which is reflected in an increase of miRNA targets levels. Anti-miRNAs are oligonucleotides with miRNA-specific reverse complement sequence and anneal to the mature miRNA, thus competing with target mRNAs for binding[324]. MiRNA-sponge vectors encode transcripts expressed from strong promoters (Pol II promoters) containing multiple, tandem miRNA binding sites in their 3'UTR, that sequester intracellular mature miRNA from interaction with its target mRNAs. MiRNA-sponge systems have been shown to induce equal or higher degree of miRNA silencing compared to anti-miRNA activity[325]. Moreover, miRNA-sponge vectors expressing miRNA inhibitors in conjunction with reporter genes (i.e. luciferase or green fluorescent protein [GFP]) allow sorting of sponge-treated cells, as well as prolonged miRNA silencing from stable chromosomal integration of these sponge-transgenes. This represents a great advantage since maximal effect of miRNA-mediated target repression is usually observed after prolonged miRNA inhibition[326]. Therefore, miRNA-sponges constitute a reliable method for investigation of tissue-specific miRNA function *in vivo*[327].

Following validation of predicted miRNA targets, it is necessary to determine the impact of this regulation on biological processes in which the validated targets are involved. Commonly used experimental approaches are assays of cell proliferation/apoptosis, cell differentiation, cell migration/invasion, signalling pathways and *in vivo* experimental procedures, depending on the target protein involved. However, large-scale miRNA target predictions may complicate investigation of the biological function of a given miRNA, as an excessive number of predicted targets imply a potential role for a given miRNA in numerous cellular processes. Web-based bioinformatics resources, such as the Database for Annotation, Visualisation and Integrated Discovery (DAVID)[328] and the Gene Ontology (GO)[329] databases, are able to process large lists of genes giving outputs of biological meanings, such as cellular pathways enriched for a subset of genes. Use of these resources provides a more stringent approach in large-scale analysis of the physiological function of a specific miRNA.

1.5.6 MicroRNAs and cancer

Under normal physiological conditions, miRNAs take their part in the complex regulatory machinery that maintains the cell "in shape". MiRNAs are present when a cell proliferates, tries to survive or must die; they help the cell fight against external enemies or evolve and differentiate; they work for a cell to find its place in the environment and communicate with other cells.

As for protein-coding genes, alterations in the normal expression pattern of miRNAs disrupt the intracellular equilibrium, thus establishing favorable conditions for diseases and cancer.

Dysregulation of miRNAs is a very common feature in cancer. As mentioned before, miRNA genes are under the control of genetic and epigenetic mechanisms, such as transcription factors, promoter modifications and events of genomic instability, that link miRNA deregulation to a state of malignancy[293, 294, 298]. Different types of cancer exhibit characteristic miRNA expression profiles, so much so, that miRNAs have been elected good markers for cancer classification, diagnosis and prognosis[330]. Although some miRNAs are overexpressed in cancer cells, such as the oncogenic cluster miR-21[331], an overall down-regulation is commonly observed[332]. This phenomenon is usually attributed either to overexpression or hyperactivation of oncogenic transcription factors, such as c-MYC, known to repress a plethora of miRNAs in different cancers[298], or to deregulation of the miRNA biogenesis machinery[333], both commonly observed in cancer. For example, *in vivo* studies have demonstrated that depletion of DICER1 and DROSHA impairs miRNA processing, resulting in cellular transformation and tumourigenesis[334]; accordingly, reduced DICER1 and DROSHA expression have been associated with poor prognosis of cancer patients[335].

Deregulation of individual or clustered miRNAs has a direct impact on cancer phenotypes, depending on their specific target repertoire and, therefore, on the cancer networks that miRNAs interact with. Indeed, oncogenic miRNAs negatively regulate tumour suppressors, whereas tumour suppressor miRNAs often target protein-coding oncogenes.

Generally, oncogenic miRNAs, known as oncomiRs, are positively regulated in order to repress pro-apoptotic, anti-growth and reprogramming signals, typically controlled by tumour suppressors. One such miRNA with a defined oncogenic function is miR-21, which shows aberrant expression in different types of cancer[336]. Mir-21 promotes tumourigenesis at different levels: by accelerating cell cycle and growth through repression of the tumour suppressor phosphatase and tensin homolog (PTEN)[337]; and by inducing neoplastic transformation and anchorage-independent growth of BC cells via repression of the program

cell death 4 (PDCD4) and the tumour suppressor Tropomyosin 1 (TMP1), respectively[338, 339]. Additionally, oncomiRs negatively regulate critical modulators of the cell cycle, including inhibitors of cell division kinases (CDK) or transcriptional repressors of the retinoblastoma (RB) family. By doing so, oncomiRs facilitate cell cycle entry and phase transition, thus contributing to tumour development[340].

On the other hand, inhibition of miRNA expression determines general up-regulation of protein-coding oncogenes, commonly associated with anti-apoptotic and pro-survival phenotypes. One of the best characterised oncosuppressor miRNA is the miR-34 family, which has been shown to mimic major functions of its positive regulator p53, including induction of growth arrest and apoptosis (reviewed in[341]). MiR-34 members regulate these processes by targeting several genes, such as the anti-apoptotic protein BCL2 and numerous cell cycle regulators, including the cell division kinases 4 and 6 (CDK4 and 6), cyclin E2 and the eukaryotic transcription factor E2F3[301]. It is clear how depletion of the miR-34 family, which occurs in a number of cancers, is critical for tumour initiation and progression[342].

Moreover, miRNAs exhibit tumourigenic potential by targeting components of the epigenetic machinery, such as DNA methyltransferases 3A and B (DNMT3A and B), repressed by miR-29 in lung cancer[343], and the histone methyltransferase EZH2, inhibited by miR-101 and miR-26a in prostate and BC, respectively[344]. This epigenetic regulation by miRNAs implies genome-wide changes that affect gene expression in a hereditable way; thus miRNAs indirectly contribute to cancer cell reprogramming[345].

Classification of miRNAs in view of their potential role during cancer pathogenesis is very often complicated by the observation that miRNAs can act as both oncogenes and tumour suppressors[245]. This discordance mainly depends on the cellular context in which miRNAs are expressed and the expression pattern of target mRNAs. This implies that miRNAs can participate in distinct pathways, thus differentially affecting cell proliferation, growth and survival pathways. An example of this controversial situation is offered by the miR-17~92 polycistron: in human B-cells, which overexpress c-MYC, this cluster functions as a tumour suppressor by inhibiting c-MYC-mediated cell proliferation via repression of E2F1; contrarily, miR-17~92 exhibits oncogenic activity in B-cell lymphoma where it cooperates with c-MYC to impede apoptosis[346]. Moreover, evidence demonstrates that individual members of the miR-17~92 polycistron (consisting in miR-17, -18, -19a, -20, -19b1, -92a1) have opposite roles in the tumourigenesis of the same type. In fact, in BC miR-17 impairs anchorage-independent cell growth by targeting the oncogenic nuclear receptor coactivator 3 amplified in breast 1 (AIB1), which cooperates with nuclear estrogen receptor in modulating

gene expression[347]. MiR-19, instead, repress expression of PTEN and function as an oncomiR in breast tumours[348]. This evidence suggests that despite their similarity in sequence, related miRNAs can differently contribute to cancer development by repressing distinctive pattern of gene targets.

MiR-23b and miR-26a represent another two examples of miRNAs with opposite roles in tumour initation and progression and they are further discussed in detail in 1.4.6.1 and 1.4.6.2, respectively.

1.5.6.1 MiR-23b in cancer

Mammalian miR-23b is a 21-nt microRNA, ubiquitously expressed, that belongs to the miR-23 family. This consists of two cluster paralogs that originated by ancient gene duplications: miR-23a~27a~24-2 cluster and its paralogous miR-23b~27b~24-1 cluster. The first is an intergenic cluster localised on chromosome 19p13 (*C19p13*), while the second is located on *C9q22* and is intronic[349].

The expression of the miR-23b~27b~24-1 cluster is controlled by a complex transcription unit (TU), *Chromosome 9 open reading frame 3* (*C9orf3*). The product of this gene is a unique primary transcript which is processed in three mature miRNAs: miR-23b, miR-27b and miR-24-1. Mature sequences of miR-23b and miR-27b differ by just one nucleotide from their paralogs miR-23a and miR-27a: the third nucleotide from the 3‟end in both cases; whereas mature miR-24-2 and miR-24-1 have the same sequence[350]. The high degree in sequence similarity, predominantly in the 5‟end where the seed region resides, suggests that miR-23b and miR-23a, as well as the other two couples of paralogs, can interact with the same patterns of target mRNAs. In fact, target prediction programs, such as TargetScan[351] extrapolate common targets of miR-23a and miR-23b and miR-27a and miR-27b.

The role of miR-23b in cancer initiation and progression has been largely investigated, but a clear function for miR-23b as either onco-miR or tumour suppressor has not yet been defined.

The first evidence of a miR-23b involvement in cancer indicated that the overexpression of miR-23b mimics in human colorectal cancer cells leads to inhibition of their proliferative and migratory capabilities. MiR-23b was found to induce these phenotypes by direct repression of the urokinase-type plasminogen activator (uPA) and the proto-oncogene c-MET[352]. uPA was subsequently confirmed to be a direct target of miR-23b in an additional two studies. In an elegant work based on high-throughput screens of miRNAs with a role in cell migration, miR-

23b was shown to negatively regulate tumour growth, invasion and angiogenesis in *in vivo* experimental human colon cancer metastasis, by inhibiting a cohort of pro-metastatic genes, including, *FZD7*, *MAP3K1*, *uPA* and *PAK2*[353]. This evidence confirmed a tumour suppressive role of miR-23b in human colorectal cancer. The third report validating uPA as miR-23b target revealed that experimental miR-23b overexpression reduces uPA levels, thus leading to reduced migration of human cervical cancer cells[354]. In the same study, it was also observed that loss of miR-23b expression correlates with HPV (human papilloma virus)-associated cervical cancer development: HPV reduces miR-23b synthesis via inactivation of p53, which was found to bind p53-specific binding sites in the promoter of miR-23b, thus resulting in its transcriptional activation. This work demonstrated that HPV-mediated inhibition of the p53/miR-23b/uPA pathway contributes to HPV-associated cervical cancer development.

Additional studies have reported a tumour suppressor activity for miR-23b also in prostate cancer. Dahiya *et al*.[355] showed that methylation-induced silencing of miR-23b in prostate cancer confers proliferative and invasive advantages, as miR-23b reconstitution inhibited proliferation, apoptosis, colony formation, EMT and migration/invasion of prostate cancer cells *in vitro* and *in vivo*. The functional effect of miR-23b was found to be mediated by coordinated repression of proto-oncogene SRC kinase and AKT, reduction of the mesenchymal markers Vimentin and Snail and increase of E-Cadherin. Moreover, miR-23b was reported to cooperate with miR-27b in suppressing migration, invasion and anoikis in highly metastatic prostate cells that manifested impaired activation of RAC1 and up-regulation of E-Cadherin following reconstituted miR-23b expression[356]. Further, as mentioned before, the oncogenic transcription factor c-MYC is able to transcriptionally repress miR-23b and miR-23a in human P-493 B lymphoma cells and PC3 prostate cancer cell line. c-MYC-mediated reduction of the two paralogs results in release from repression of their target protein, mitochondrial glutaminase (GLS), which enhances glutamine metabolism, a physiological process that provides energy to sustain tumour growth[299].

Finally, in a recent study Lin *et al*. described an oncogenic role for both miR-23b and miR-27b in the development and progression of BC[357]. They firstly observed that both miRNAs were up-regulated in BC patient samples compared to normal specimens. Then, they found that expression of miR-23b/27b is positively regulated by HER2/NEU, EGF, and TNFA through the AKT/NF-κB signalling pathway. Additionally, by using miRNA loss-of-function approaches, they demonstrated that suppression of miR-23b/27b activity in a highly metastatic BC cell line (MDA-MB-231-4175) impaired tumour growth and metastasis *in vivo*.

This effect was attributed to release from miR-23b/27b-mediated repression of Nischarin, a novel intracellular protein that shows preliminary functions in inhibiting migration. This role for miR-23b in BC is in contrast with observations that experimental suppression of miR-23b function was associated with increased migratory abilities of BC MCF-7 cells[353] and that expression of miR-23b/27b was down-regulated in HER2/NEU-transformed mammary epithelial cells[358]. Finally, we performed a detailed analyses of expression levels of three miR-23 family members (miR-23b, miR-27b and miR-23a) obtained from published data using the GEO2R software in Gene Expression Omnibus (GEO)[359]. This has revealed that none of these miRNAs is differentially expressed in metastatic versus primary tumour versus normal tissue/cell lines of breast origin; whereas they are significantly deregulated during colon and prostate cancer initiation/progression (**Table 1**).

Table 1. MiR-23b/27b/23a expression in tissutal or cellular samples of different tumour types from 8 Genome Expression Omnibus (GEO) datasets. *P* values and fold changes were calculated by using unpaired, two-tailed t tests by using Graph Prism software.

Tumour type	Dataset (GEO)	n	Samples	miR-23b	miR-27b	miR-23a
Breast	GSE26659	94	PT vs. normal tissues	NS	NS	NS
Breast	GSE39543	51	PT vs. normal tissues	NS	NS	NS
Breast	GSE32922	37	PT vs. normal tissues	NS	NS	NS
Breast	GSE45666	116	PT vs. normal tissues	NS	NS	NS
Breast	GSE37407	22 29 19 19 29	PT vs. normal tissues BM vs. PT tissues LM vs PT tissues SM vs. PT tissues LN vs.PT tissues	NS NS NS NS NS	NS NS NS NS NS	NS NS NS NS NS
Breast	GSE40056	10 8	A vs. LA cell lines LA. vs. I cell lines	NS NS	NS NS	NS NS
Colon	GSE35834	53 52	LM vs. PT tissues PT vs. normal tissues	NS Down, *P*=0.0003 fc:-0.5280	NS Down, *P*<0.0001 fc:-0.64313	NS Up, *P*<0.0001 fc:0.4113
Prostate	GSE35834	113 126	Met vs. PT tissues PT vs. normal tissues	Down, *P*<0.0001 fc:-1.909 Down, *P*<0.0001 fc:-0.6348	Down, *P*<0.0001 fc:-1.749 Down, *P*<0.0001 fc:-0.6793	Down, *P*<0.0001 fc:-0.8689 Down, *P*=0.0004 fc:-0.4139

Key: PT, primary tumour; BM, brain metastasis; LM, liver metastasis; SM, skin metastasis; Met, metastasis; fc, fold change; NS, non-significant; A, aggressive (MDA-MB-231, HS578T, BT549, SUM159); LA, less aggressive (BT474, MDA-MB-468, T47D, ZR75-1, MCF-7, SK-BR3); I, immortalised (MCF-10A, MCF-12A).

1.5.6.2 MiR-26a in cancer

Mir-26a is a ubiquitous 22-nt miRNA, and, along with miR 26b, is a member of the miR-26 family. Evolutionary events have determined localisation of the genomic loci of miR-26a and miR-26b within the introns of genes that encode for three members of the carboxy-terminal domain RNA polymerase II polypeptide A small phosphatase (CTDSPs) family: *CTDSPL* (CTDS phosphatase-like), *CTDSP1* and *CTDSP2*. Mature miR-26a derives from two miRNA precursor paralogs, pre-miR-26a-1 and pre-miR-26a-2, of which sequence resides in the fifth intron of *CTDSPL* and *CTDSP2* gene, respectively. The fourth intron of *CTDSP1* contains the pre-miR-26b, which is then processed to release mature miR-26b[360] [361]. The nucleotide region between nucleotides at position 1 and 9 is the same in both miR-26a and miR-26b mature sequences; therefore prediction of common targets is valid also for these two miRNA paralogs.

MiR-26a has been implicated in a large variety of cancers, exhibiting different roles depending on the tissue-context.

Two independent studies reported that miR-26a expression is reduced in hepatocellular carcinoma (HCC)[362] [363]. In a first report, recovered miR-26a expression in HCC cell lines was able to induce cell cycle arrest and apoptosis through repression of cyclins D1 and E2[362]. Similar phenotypes were observed in a second report, where miR-26a works synergistically with miR-26b, as well as their host genes CTDSP1/2/L, to block G1/S phase progression in HCC cells. Moreover, miR-26a/26b, concomitantly expressed with their host genes, were negatively regulated by c-MYC, accelerating HCC cell cycle[363]. Decreased levels of miR-26a in HCC compared to normal tissues were also confirmed by another clinical dataset as shown in **Table 2**.

C-MYC-mediated repression of miR-26a was also depicted in lymphoma cells and associated with lymphomagenesis. Accordingly, miR-26a was found to be down-regulated in primary human Burkitt lymphoma and its ectopic expression impairs cell proliferation of c-MYC-dependent cells, through down-regulation of the histone methyltransferase EZH2[364]. Further, decreased expression of miR-26a correlates with increased levels of EZH2 in rhabdomyosarcoma[365]. The same correlation was also observed in BC. Indeed, experimental overexpression of miR-26a in MCF-7 BC cells inhibits oncogenic EZH2 and methaderin (MTDH), resulting in cell cycle arrest, apoptosis and inhibition of colony formation *in vitro* and impaired tumourigenicity of these cells *in vivo*[366]. Accordingly, trastuzumab treatment of BC cell lines induces miR-26a expression, an event that induces cell cycle arrest in G1 phase

and apoptosis[367]. In addition, tumour suppressive function of miR-26a in BC is shown also by regulating proliferation, apoptosis, migration and colony formation via miR-26a-induced depletion of the anti-apoptotic myeloid cell leukemia sequence 1 (MCL1)[368]. Nevertheless, analyses of further clinical datasets available on GEO database reveals that miR-26a/26b are not found consistenly down-regulated in BC tissue samples and that miR-26a expression is higher in BC cell lines compared to immortalized normal cells (**Table 2**).

On the contrary, miR-26a has been shown to have oncogenic activity in other types of cancer. For example, it induces cholangiocarcinoma growth by targeting glycogen synthase kinase (GSK)-3β; miR-26a-mediated intracellular reduction of GSK-3β leads to activation of β-catenin, which in turn induces expression of oncogenic, proliferative genes, such c-MYC, Cyclin D1 and peroxisome proliferator-activated receptor δ (PPARδ)[369]. Furthermore, miR-26a is amplified in high grade glioma and enhances *in vivo* glioma initiation by inhibiting PTEN[370].

Table 2. MiR-26a/26b expression in tissutal or cellular samples of different tumour types from 8 Genome Expression Omnibus (GEO) datasets. *P* values and fold changes were calculated by using unpaired, two-tailed t tests by using Graph Prism software.

Tumour type	Dataset (GEO)	n	Samples	miR-26a	miR-26b
Breast	GSE26659	94	PT vs. normal tissues	Down *P*<0.0001 fc: -1.408	Up, *P*<0.0001 fc: 0.6561
Breast	GSE39543	51	PT vs. normal tissues	NS	NS
Breast	GSE32922	37	PT vs. normal tissues	Down, *P*=0.0180 Fc: -0.9863	Down, *P*=0.0047 Fc: -2.171
Breast	GSE45666	116	PT vs. normal tissues	Down, *P*<0.0001 fc: -2.907	Down, *P*<0.0001 fc: -5.109
Breast	GSE40056	10 8	A vs. LA cell lines LA. vs. I cell lines	Down, *P*=0.0108 fc:-1.163 Up, *P*=0.0396 fc:1.394	Down, *P*=0.0024 fc:-2.747 NS
Colon	GSE35834	52	PT vs. normal tissues	Down, *P*=0.0094 fc:-0.3821	NS
Prostate	GSE35834	123	PT vs. normal tissues	Down, *P*=0.0094 fc:-0.3423	NS

Key: PT, primary tumour; fc, fold change; NS, non-significant; A, aggressive (MDA-MB-231, HS578T, BT549, SUM159); LA, less aggressive (BT474, MDA-MB-468, T47D, ZR75-1, MCF-7, SK-BR3); I, immortalised (MCF-10A, MCF-12A).

1.5.6.3 MicroRNAs and metastasis

Along with their role in cancer initiation, miRNAs have been unraveled as important regulators of metastatic progression, insomuch as they are commonly referred as metastamirs [371]. MiRNAs are able to affect expression and function of genes involved in cell adhesion, cytoskeletal remodelling, and cell signalling pathways, known to direct multiple steps of the metastatic process[372].

Recent reports have shown that miRNAs can modulate formation and maintenance of cell-cell and cell-matrix adhesions, leading to outcomes of increased or reduced aggressiveness. For example, miR-9 abolishes the expression of the cell-cell adhesion mediator E-cadherin, thus promoting cell motility, invasion and metastatic potential of BC cells *in vitro* and *in vivo*[373]. Contrarily, members of the miR-200 family and miR-205 have been shown to restore epithelial phenotypes by targeting ZEB transcription factors, known transcriptional repressors of *E-cadherin*, thus impairing BC cell migration and invasiveness[374, 375]. Cell-matrix adhesion molecules, such as integrins, can be also amongst miRNA targets. For example, integrin α5 and integrin β3 are negatively regulated by miR-31 and let-7a, respectively, resulting in impaired cell invasion of BC[376] and melanoma[377].

Additionally, miRNAs widely modulate the complex machinery that drives cytoskeletal dynamics, from central leaders, such as RHO GTPases, to their regulators and downstream effectors. For example, mir-224 and miR-31 suppress BC cell invasion and metastasis by targeting CDC42 and RHOA, respectively[376, 378]. Furthermore, induced by the transcription factor Twist, miR-10b inhibits the homeobox D10 (HOXD10), resulting in increased RHOC expression and consequently inducing BC cell invasion and metastasis[379]. MiR-10b is able also to impair RAC1 activation, by targeting the RAC-specific GEF T lymphoma invasion and metastasis 1 (TIAM1), thus contributing to decreased BC migration and invasion[380]. On the contrary, miR-155 synergistically activates RHO, RAC and CDC42, by targeting ARHGDIA, a GDP dissociation inhibitor that inhibits ARHGEFs, resulting in hepatocellular carcinoma (HCC) metastatic spread[381].Furthermore, miR-139 can directly regulate the expression of the RHO-associated kinase ROCK2, leading to suppression of HCC cell migration and invasion[382]; whereas miR-7 down-regulates PAK1 protein translation in BC cells and, consequently, suppresses their motility, invasiveness and metastatic potential[383]. In addition, overexpression of miR-200 was shown to inhibit the invasive capabilities of prostate and BC cells, mediating the suppression of WAVE3, a member of the WASF family[384].

Numerous evidences implicate miRNAs function in direct or indirect regulation of metastatic signalling processes. A clear example is the hepatocyte growth factor (HGF)/c-MET signalling cascade which regulates cell growth, cell motility and morphogenesis. c-MET has been shown to be directly regulated by miR-1, miR-206, miR34a and miR-23b. MiR-1 and miR-206, can directly suppress c-MET expression and inhibit cell proliferation and migration of rhabdomyosarcoma[385]. MiR-34a decreases c-MET-induced phosphorylation of extracellular signal-regulated kinases 1 and 2 (ERK1/2) and inhibits HCC cells migration and invasion[386]. MiR-23b reduces proliferative and migratory abilities of HCC cells by inhibiting c-MET and urokinase-type plasminogen activator (uPA)[352]. Both epithermal growth factor receptor (EGFR) and phosphatidylinositol 3-kinase (PI3K) signalling cascades are also regulated by different metastamirs. EGFR expression is inhibited by BC metastasis suppressor 1 (BRMS1)-mediated up-regulation of miR-146a[387]; and miR-125a/miR-125b overexpression reduces ERBB2 and ERBB3 levels, leading to reduced migration and invasion capacities of BC cells[388]. The PI3K signalling cascade is controlled by the tumour suppressor lipid phosphatase PTEN, a direct target of miR-21[389], miR-221 and miR-222[390] which cooperate to induce HCC cell migration and invasion.

Amongst the miRNAs with a well-defined role in metastatic progression, very few stand out for their ability to control multiple metastatic genes, so that they are considered true metastamirs.

In a study aimed to discover BC metastasis-related miRNAs, Tavazoie *et al*. identified miR-355 as the first miRNA with a role in metastasis suppression[391]. MiR-355 was found to be selectively lost during BC cell dissemination to the lung and bones, and more importantly, its reintroduction suppressed metastasis of BC cells to different organs. Further analysis showed that miR-355 mediated its suppressive function by altering migration and morphology of BC cells, through synergistic repression of a cohort of pro-metastatic genes, namely SRY-box containing transcription factor (SOX4), receptor type tyrosine protein phosphatase (PTPRN2), c-MER tyrosine kinase (MERTK) and the ECM glycoprotein Tenascin C (TNC) [391]. MiR-335-mediated suppression of SOX4 and TNC was found to be critical for metastatic abolition induced by miR-355.

Additionally, in an elegant report, Valastyan *et al*. demonstrated that miR-31 plays a pleiotropic role in the regulation of different steps of BC metastasis[376]. They observed, in fact, that miR-31 supervises different malignant phenotypes, such as motility, invasion, resistance to anoikis, and metastatic colonisation at distant sites of BC cells. MiR-31 coordinates inhibition of a set of pro-invasive/metastatic genes, including the already

mentioned RHOA and integrin-α5 (ITGA5), and the cytoskeletal protein radixin (RDX), Frizzled-3 (FZD3), the metalloproteinase 16 (MMP16) and the myosin phosphatase RHO-interacting protein (M-RIP). MiR-31-induced suppression of metastasis was found to be mediated by repression of at least FZD3, RHOA, ITGA5 and RDX, as their knockdown abolished migration and invasion of BC cells.

Finally, miR-200 participates in metastatic progression by controlling two different regulatory networks associated with opposite metastatic roles. The miR-200 family was firstly described as a suppressor cluster of BC invasion and metastasis by targeting *ZEB1/2*, which results in de-repression of E-Cadherin that maintains the epithelial tumour phenotype. A contradictory role for miR-200 reveales that this miRNA family functions as an enhancer cluster of BC metastatic colonisation, through silencing of the *S. cerevisiae* 23 homolog A (*SEC23A*). SEC23A is a vesicles-associated protein, that mediates secretion of metastasis-suppressive proteins including insulin-like growth factor binding protein 4 (IGFBP4) and tubulointerstitial nephritis antigen-like 1 (TINAGL1), which were found to mediate suppression of BC metastasis to the lung[392].

MiR-355, miR-31 and miR-200 family are major examples of how miRNAs can act pleiotropically to regulate distinct molecular pathways that dictate the progression of cancer.

1.5.6.4 MicroRNAs in anticancer therapy

Increasing understanding of miRNA biology and their implication in cancer initiation and progression raises the possibility to use miRNA-based strategies in cancer therapy.

MiRNAs exhibit several key qualities that make them suitable candidates for the development of drug delivery-based anti-cancer therapies. Firstly, owing to their small size and low molecular weight, miRNAs are ideal for systemic dissemination and uptake by target cells. Secondly, they are biological antisense interactors, and hence their intracellular uptake is less likely to induce an immune response, thus limiting toxic effects[393]. Moreover, owing to the ability of miRNAs to simultaneously regulate multiple genes involved in the same biological process, the use of a single miRNA as therapeutic target or drug can function as a combinatorial therapy, resulting in a cumulative effect on a subset of targets at multiple level in the same pathway[247]. Once more, because miRNAs frequently show altered expression in cancer, it is likely that agents developed to either inhibit oncomiRs or restore tumour suppressor miRNAs could result in cancer-specific effects[294, 394]. Oncogenic miRNAs can be

inhibited by using anti-miRs and virus-associated sponge constructs[395]. Anti-miR-based strategies comprehend locked nucleic acids (LNAs) and antagomiRs, which are synthetic oligonucleotides complementary to the mature miRNA sequence, carrying chemical modifications that increase their stability *in vivo*, their specificity for the miRNA target and their uptake from cells[393]. For example, antagomirs are usually conjugated to cholesterol molecules that increase their affinity with the plasma membrane, thus facilitating their entry in the cell. Application of LNA-based oligonucleotides and antagomiRs has successfully resulted in inhibiting miRNA activity in experimental mouse tumour models[396]; in addition, the use of LNA against miR-122 in non-human primates is showing exciting promise in the treatment of the hepatitis C virus (HCV), and consequent reduction in HCV-related hepatocellular carcinoma[397]. Miravirsen, a 15-nt LNA complementary to miR-122 has been recently introduced in a clinical trial in patients with chronic HCV infection and it showed to induce dose-dependent reduction of the HCV RNA levels due to miR-122 repression[398].

By contrast, restoration of miRNA expression with evident tumour suppressor functions can be achieved by delivery of miRNA mimics or viral vectors[395]. Both of these strategies have produced positive results in experimental animal models of cancer[399] [362].

Delivery of miRNAs or miRNA inhibitors (sponge) via viral strategies, such as adeno-associated viruses (AAV) is highly promising for several reasons: it is efficient as it ensures continual miRNA expression or inhibition; it is relatively safe, because the virus does not integrate into the genome, thus it is non-mutagenic; and finally it can be achieved with a high degree of tissue-specificity, due to availability of a number of different AAV serotypes that show natural tropism for different organs[393].

Delivery of miRNA mimics or antagonists represents a major challenge. First, the use of chemically modified mimics or anti-miRs (cholesterol-conjugated) does not exclude a possible uptake of these agents by tissues that normally do not express the miRNA of interest or where its inhibition can cause unwanted phenotypes, resulting in potential indirect effects[400]. Moreover, only systemic administration into the circulation system allows miRNA-based agents to reach many pathological tissues that are not directly accessible, but "naked" RNA-compounds injected in the blood are rapidly excreted via renal infiltration due to their small size[401]. For these major reasons, systemic delivery of miRNA mimics/inhibitors can be achieved via incorporation into larger vehicles, such as lipid-based nanoparticles and other different carriers. Various pharmaceutical and engineering companies have been challenged by the development of miRNA formulations with the properties to (1) overcome the numerous physical barriers encountered *in vivo* (enzymatic degradation,

entrapment in the capillary system, crossing of the plasma membrane), and (2) access target cells with high tissue-specificity[401].

In April of this year, for the first time, use of miRNA mimics as anticancer therapeutics has reached clinical trial in humans[402]. Mirna Therapeutics (Texas) has launched a phase 1 trial recruiting patients with liver cancer and liver-associated metastatic cancer and treating with MRX34, a synthetic miRNA mimic of the endogenous miR-34, a known master tumour suppressor miRNA. MRX34 is a double-stranded oligonucleotide delivered using a liposome-formulation, called Smarticles, patented by Marina Biotech, Washington. The Smarticles technology has been formulated in order to prevent unwanted interactions with normal cells, and achieve maximal accumulation of the miRNA mimic into the tumour, using the tendency for liposomal accumulation within the liver.

Despite the numerous clinical tests that MXR34 needs to overcome on its way to become an effective and licensed drug agent, it represents an exciting start point for the development and the improvement of RNA-based therapeutic strategies with realistic clinical relevance.

1.6 Aims

At the time of starting this project there was little published research that described miRNAs as crucial regulators of cellular pathways relevant for the acquisition of metastatic potential. Therefore the initial aim of this study was to identify miRNAs with possible roles in the regulation of malignant traits leading to initiation and development of the metastatic process, with particular focus on BC progression. We aimed to:

- investigate the impact of miRNAs on cellular phenotypes that mark aggressiveness of tumour cells, such as cytoskeletal remodelling, migratory and invasive capabilities and their metastatic potential;
- gain insight into the molecular mechanism(s) that underlie the miRNA function in regulating gene targets involved in intracellular pathways relevant to these phenotypes;
- and evaluate the effect and therapeutic potential that manipulation of these miRNAs may entail on the progression of BC.

In order to identify candidate miRNAs and establish their functional regulatory networks, we aimed to:

i. adopt a bioinformatic approach by combining use of algorithms of miRNA target prediction and web-based resources for large-scale analysis of biological gene functions, to gain a preliminary understanding of the miRNA physiological role(s);
ii. use both miRNA gain- and loss-of-function strategies to experimentally investigate the potential miRNA roles predicted in aim (i); this is achieved by performing a variety of techniques that assess for cell proliferation/ apoptosis, cytoskeletal dynamics, such as cell-cell and cell-matrix adhesion, cell migration/ invasion, intracellular signalling pathways and transcriptional regulation in a number of BC cell models;
iii. identify putative miRNA gene targets by using available prediction tools and RNA-sequencing-based genome-wide screening strategies, and validate them by performing western blot and luciferase reporter assays;
iv. investigate the impact of miRNA perturbation on tumourigenic and metastatic potential of BC cell models *in vivo*;
v. establish the clinical relevance of the miRNAs of interest by examining their expression levels in a cohort of primary and metastatic samples derived from patients affected by invasive BCs.

CHAPTER 2

MATERIALS AND METHODS

2.1 Materials

2.1.1 Buffers and Solutions

Table 3. Lists of buffers and reagents

Reagent	Recipe	Storage
1M Dithiothreitol (DTT)	1.54g of DTT in total of 10ml of double distilled MilliQ water (ddH_20)	100µl aliquots at -20**°C**
1M Tris-HCl	60.5g Tris in total of 500ml ddH_20 and adjusted to desired pH with pure HCl	RT
Laemmli's buffer	50mM Tris-HCl pH 6.8, 15% glycerol, 0.1% (w/v) bromophenol blue, 4% SDS	RT
NP-40 lysis buffer	30ml of 5 M NaCl, 100 ml of 10% NP-40, 50 ml of 1M Tris (pH 8.0), and 820 ml of ddH_2O	4 °C
SDS loading buffer (2x)	125mM Tris-Cl pH 6.8, 20% glycerol, 4% SDS, 100mM DTT, 0.04% (w/v) bromophenol blue	500µl aliquots at 4°C
10x SDS-PAGE Running buffer	10g SDS, 30.3g Tris, 144.1g glycine dissolved in 1l of ddH_20	RT
10x Transfer buffer	30.3g Tris, 144,1g glycine dissolved in 1l of ddH_20	RT
TBS 10x (Tris-Buffered Saline)	24.23g Trizma HCl, 80.06 g NaCl dissolved in 1l of ddH_20 and adjusted pH to 7.6 with pure HCl	RT
TBST buffer (TBS/ Tween® 20)	100ml of TBS 10x, 900ml ddH20, 1ml Tween® 20 (BDH)	RT
Blocking buffer	5% dried skimmed milk powder in TBST	Prepared as required
pp-MLC 2 Ab Buffer	5% bovine serum albumin (BSA, Sigma-Aldrich, Dorset, UK) in TBST	10ml aliquots at -20°C
IFF	1% BSA, 2% FCS in PBS	50ml aliquots at -20°C
Solution 1	0.25% Triton-X-100, 10mM EDTA, 0.5mM EGTA, 10mM Tris-HCl ph8, 300µl Protease Inhibitors (Roche, Diagnostic Ltd, West Sussex, UK)	4 °C
Solution 2	0.2M NaCl, 1mM EDTA, 0.5mM EGTA, 10mM Tris-HCl ph8, 300µl Protease Inhibitors (Roche)	4 °C
ChIP buffer	0.01% SDS, 1.1% Triton-X100, 1.2mM EDTA, 16.7mM Tris-HCl, pH 8.1, 167mM NaCl	4 °C
0.075M KCL Hypotonic solution	559mg of KCl in 100 ml of ddH_20	RT
Fixative solution	3:1 Methanol:Acetic acid	Prepared as required
Gurr's buffer	0.469g NaH2PO4, 0.937g Na2HPO4 in 1l of dH_20	RT

2.1.2 Mammalian cell lines

Table 4. Lists of mammalian cell lines

Cell Type	Tissue	Morphology	Tumourigenicity
HCT116	Colon	Mesenchymal	Human colorectal carcinoma cell line
HeLa	Cervix	Epitheloid	Human cervical carcinoma cell line
MCF-7	Breast	Epithelial	Human cell line derived from a pleural effusion of adenocarcinoma
MDA-MB-468	Breast	Epithelial	Human tumorigenic cell line derived from a pleural effusions of adenocarcinoma
MDA-MB-231	Breast	Mesenchymal	Human Metastatic and high invasive cell line derived from pleural effusions of ductal carcinoma
pEGFP- MDA-MB-231	Breast	Mesenchymal	MDA-MB-231 cell line stably expressing pEGFP-C1 plasmid
miR-23b-Sponge-EGFP-MDA-MB-231	Breast	Mesenchymal	MDA-MB-231 cell line stably expressing pEGFP-C1 plasmid containing the miR-23b-sponge construct
miR-26a- Sponge -EGFP-MDA-MB-231	Breast	Mesenchymal	MDA-MB-231 cell line stably expressing pEGFP-C1 plasmid containing the miR-26a-sponge construct
T-MDA-MB-231	Breast	Mesenchymal	Tumour cell line derived from tumour developed after MDA-MB-231(p) injection into mice
AD-MDA-MB-231	Breast	Mesenchymal	Metastatic cell line derived from T-MDA-MB- 231 cells metastasised to murine adrenal gland
B-MDA-MB-231	Breast	Mesenchymal	Metastatic cell line derived from T-MDA-MB- 231 cells metastasised to murine bone
L-MDA-MB-231	Breast	Mesenchymal	Metastatic cell line derived from T-MDA-MB- 231 cells metastasised to murine lungs

Table 5. Normal growth media

Cell Type	Media	Additives	Storage
HCT116	McCoy's 5A medium (modified) (Gibco®, Life Technologies Ltd, Paisley, UK)	2mM Glutamine 50 units/ml Penicillin 50µg/ml Streptomycin 10% fetal calf serum (FCS)	4°C, used within one month

Cell Type	Media	Additives	Storage
MCF-7 **MDA-MB-468** **MDA-MB-231** **HeLa**	DMEM (Dulbecco"s Modified Eagle"s Medium)(Sigma-Aldrich, Dorset, UK)	2mM Glutamine 50 units/ml Penicillin 50µg/ml Streptomycin 10% FCS	4°C, used within one month
pEGFP-MDA-MB-231 **miR-23b- Sponge -EGFP-MDA-MB-231** **miR-26a- Sponge -EGFP-MDA-MB-231**	DMEM (Dulbecco"s Modified Eagle"s Medium)(Sigma-Aldrich)	2mM Glutamine 50 units/ml Penicillin 50µg/ml Streptomycin 10% FCS 500µg/ml G-418 (Roche Diagnostic Ltd, West Sussex, UK)	4°C, used within one month
T-MDA-MB-231 **AD-MDA-MB-231** **B-MDA-MB-231** **L-MDA-MB-231**	Advanced MEM (Minimum Essential Medium) (Gibco®)	2mM Glutamine 50 units/ml Penicillin 50µg/ml Streptomycin 10% FCS 10 nM insulin (Sigma-Alderich)	4°C, used within one month

Table 6. Transfection media and reagents

Transfection Media	Additives	Transfection reagent	Storage
Normal growth medium	No	HiPerFect Transfection Reagent (Qiagen, West Sussex, UK)	4°C
Opti-MEM® I Reduced Serum Medium(Gibco®)	No	Lipofectamine® 2000 Reagent (Invitrogen, Life Technologies Ltd, Paisley, UK)	4°C

2.1.3 Primers

All the primers were synthesised by Sigma-Aldrich (Dorset, UK).

Table 7. Primer sequences for plasmid constructs

Gene	Primer sequence (5' to 3')
Sponge-miR-23b	S1-AGCTCATAAGGTAATCCCCCGAATGTGATCGATGGTAATCCCCCGAATGTGATC AS1-ACGCGTGATCACATTCGGGGGATTACCATCGATCACATTCGGGGGATTACCTTAT S2-ACGCGTCATAAGGTAATCCCCCGAATGTGATCGATGGTAATCCCCCGAATGTGATC AS2-ACTAGTGATCACATTCGGGGGATTACCATCGATCACATTCGGGGGATTACCTTATG S3-ACTAGTCATAAGGTAATCCCCCGAATGTGATCGATGGTAATCCCCCGAATGTGATC AS3-GATCGATCACATTCGGGGGATTACCATCGATCACATTCGGGGGATTACCTTATG
Sponge-miR-26a	S1-AGCTCTATAAGCCTATCCTCTATACTTGAACGATAGCCTATCCTCT AS1-ACGCGTCTTCAAGTATAGAGGATAGGCTATCGTTCAAGTATAGAG S2-ACGCGTCATAAAGCCTATCCTCTATACTTGAACGATAGCCTATCC AS2-ACTAGTCTTCAAGTATAGAGGATAGGCTATCGTTCAAGTATAGAG S3-ACTAGTCATAAAGCCTATCCTCTATACTTGAACGATAGCCTATCC AS3-GATCCTTCAAGTATAGAGGATAGGCTATCGTTCAAGTATAGAGGA

Gene	Primer sequence (5' to 3')
Sensor-miR-23b	S1-CTAGTCGGAGGTAATCCCTGGCAATGTGATCGATGGTAATCCCTGGCAATGTGAT AS1-ACGCGTATCACATTGCCAGGGATTACCATCGATCACATTGCCAGGGATTACCTCCGA S2-ACGCGTACGGAGGTAATCCCTGGCAATGTGATCGATGGTAATCCCTGGCAATGTGAT AS2-ACTAGTATCACATTGCCAGGGATTACCATCGATCACATTGCCAGGGATTACCTCCGT S3-ACTAGTACGGAGGTAATCCCTGGCAATGTGATCGATGGTAATCCCTGGCAATGTGAT AS3-AGCTATCACATTGCCAGGGATTACCATCGATCACATTGCCAGGGATTACCTCCGT
Sensor-miR-26a	S1-CTAGTCGGAGCCTATCCTGGATTACTTGAACGATGCCTATCCTGGATTACTTGAA AS1-ACGCGTTTCAAGTAATCCAGGATAGGCATCGTTCAAGTAATCCAGGATAGGCTCCGA S2-ACGCGTACGGAGCCTATCCTGGATTACTTGAACGATGCCTATCCTGGATTACTTGAA AS2-ACTAGTTTCAAGTAATCCAGGATAGGCATCGTTCAAGTAATCCAGGATAGGCTCCGT S3-ACTAGTACGGAGCCTATCCTGGATTACTTGAACGATGCCTATCCTGGATTACTTGAA AS3-AGCTTTCAAGTAATCCAGGATAGGCATCGTTCAAGTAATCCAGGATAGGCTCCGT
PAK1-3'UTR	S-CGCACTAGTATCACTAACTCTCCAGCC AS-CGCACGCGTAATTTGTGCTGCAGAGGC
PAK2-3'UTR	S-CGCACTAGTATGGTCTGCATAACCTGAATGA AS-CGCACGCGTGAACTCAGGTGGCACTGCAGCT
PAK2-3'UTR-23b mut	S-GGAAGAAAAGTATTTGATTTTTACCTTTTTTAACAAAGAAAAAGT AS-CAAAATTTCTAAAACTGACTTTTTCTTTGTTAAAAAAGGTAAAAA
PAK2-3'UTR-26a mut	S-CTTTGGGGTATTTCCAATACTACTATGGCAGATTGGAGTTTTTC AS-GAAAAACTCCAATCTGCCATAGTAGTATTGGAATACCCCAAAG
ANXA2-3'UTR-23bmut	S-GTTGGAAGTGAAGTCTATGATGACTAACACTTTGCCTCCTGTGTACT AS-AGTACACAGGAGGCAAAGTGTTAGTCATCATAGACTTCACTTCCAAC
ARHGEF6-3'UTR-23bmut	S-AGCTGGCCAAGGCTTATTAAATGACTACCCAACTTTTCCCCAGG AS-CCTGGGGAAAAGTTGGGTAGTCATTTAATAAGCCTTGGCCAGCT
CFL2-3'UTR-23bmut	S-GCACTACAATGTATGTGATCGTCAATGACTATAGCTTAGAATACTGCAAAGGATAAG AS-CTTATCCTTTGCAGTATTCTAAGCTATAGTCATTGACGATCACATACATTGTAGTGC
LIMK2-3'UTR-23bmut	S-CAGGGACCACATCAATGACTGAGGAAGCCTCCACCTC AS-GAGGTGGAGGCTTCCTCAGTCATTGATGTGGTCCCTG
PIK3R3-3'UTR-23bmut	S-CACAAGAAGTGATTTTGTGAATGACTAGTGGAGAGGCCGAGCAG AS-CTGCTCGGCCTCTCCACTAGTCATTCACAAAATCACTTCTTGTG
CHFR-3'UTR-26adel	S-GCTAGCTTTGCCATGTCATCTGGAATAATTTTGATTTTTGGAAAAAAAAGTTTTTTA AS-TAAAAAACTTTTTTTTCCAAAAATCAAAATTATTCCAGATGACATGGCAAAGCTAGC
MCL1-3'UTR-26adel	S-ACTTTATTAGCCTAGTTTATCACCAATAACGGAAGGCTCAGTAA AS-TTACTGAGCCTTCCGTTATTGGTGATAAACTAGGCTAATAAAGT
1LARP1-3'UTR-26amut	S-ACATCTTCACTTTCTGAAGACACTACTATTTAGGACCGATGTATCTGTGAC AS-GTCACAGATACATCGGTCCTAAATAGTAGTGTCTTCAGAAAGTGAAGATGT
2LARP1-3'UTR-26adel	S-ATGTGCTAGGATATCATATTTAAAAGGACAAAAAAATGTAAAATGAGCTTGTATTATAACATTAA AS-TTAATGTTATAATACAAGCTCATTTTACATTTTTTTGTCCTTTTAAATATGATATCCTAGCACAT
3LARP1-3'UTR-26amut	S-ACAAAAAAATGTATAAAAATAAACACTACTAAAGGCAATCGAGGGCCGGCCG AS-CGGCCGGCCCTCGATTGCCTTTAGTAGTGTTTATTTTTATACATTTTTTTGT
YWHAE-3'UTR-26amut	S-GCTCGCTCAACCTCTTTTGTTCAGTATGTGTAACTACTAGCTAATTTGTACTACTG AS-CAGTAGTACAAATTAGCTAGTAGTTACACATACTGAACAAAAGAGGTTGAGCGAGC

Table 8. ChIP primer sequences

Gene	Primer sequence (5' to 3')
IL6 promoter	forward -CGTGCATGACTTCAGCTTTAC reverse TGCAGCTTAGGTCGTCATTG
miR-23b(1) promoter	forward GGAATACTAGGGTACCAGGGCA reverse GCAGCTTGGCTGGCTAGG
miR-23b(2) promoter	forward ACCATCTGCCTGCTCTTTCT reverse GGGACAGCAGCTTACATT
miR-23b(3) promoter	forward GCTCCTCGTTGAGTCATCAG reverse GAAGCCCGTTTTGAACACCA
miR-nc promoter	forward GAGGCTGTGCTTGGAGTAGG reverse CGTTTCCCCTGTGAAAGGTA

Table 9. RT-PCR primer sequences

Gene	Primer sequence (5' to 3')	Gene	Primer sequence (5' to 3')
ABL2	forward GCTCAGCAGTCTAATCAATGG reverse CACATACACCTTGCCATCTG	***PAK2***	forward GCATGGATGAAGCACAGA reverse AACCAAAGTCAGTGAGCTTA
ANXA2	forward CCTGAACCTGGTTCAGTGC reverse CCCTTCATGGAGTCATACAGC	***PIK3R3***	forward ATCCTCCAGCTCTTCCACC reverse GGCATATCCCGCAATTTGTC
ARHGEF6	forward ATTTCAACAGACACTCTGCCA reverse GTTCCAACTCATCACTGTGCT	***PLAU***	forward GGGAGATGAAGTTTGAGGTGG reverse TTCAGCAAGGCAATGTCGT
CFL2	forward AGGGCACTATGGCTTCTGG reverse ACCAAGATCTGCTTTGCTTCC	***PPP1R12A***	forward AAGATCAACACAGGGAGTGAC reverse TTTCTTGTTCTCTGGTTCGGG
c-JUN	forward CTCCAAGTGCCGAAAAAGGAAG reverse CACCTGTTCCCTGAGCATGTTG	***pri-miR-23a***	forward TCTCATATGCAGGAGCCACCA reverse GCAAGTTGCTGTAGCCTCCTTG
CHFR	forward CTCCAAGTGCCGAAAAAGGAAG reverse CACCTGTTCCCTGAGCATGTTG	***pri-miR-23b***	forward GTGTGTGCAGACAGCACG reverse AATCTGCAGTGAGCGCGA
ENAH	forward GCTACACAGACCTTCCACC reverse ATGTTGGCCCTGTTTCCTG	***pri-miR-26a-1***	forward GCCCAATGGCATAGCAAGA reverse GGCCAGTCATGCTTACAGTGAC
FN1	forward TCAGATAAATCAACAGTGGGAG reverse AGTCTCTTCAGCTTCAGGT	***pri-miR-26a-2***	forward AGGCATCCCTGTGATGAAGGT reverse TTGAGAGCTCCTTGCTGCTGT
GSK3B	forward ACGCTCCCTGTGATTTATGTC reverse GCTTTGCACTTCCAAAGTCAC	***RAP1A***	forward CGTTGGGAAGTCTGCTCTG reverse TTCCGTGTCCTTAACCCGT
ITGA1	forward CTTCTGGTCCCGAGATGTG reverse GCATACTGTTTCCTTTCCCTC	***RAP1B***	forward TCGTTCTTGGCTCAGGAGG reverse TGCTGTAAATTGCTCCGTTCC
LARP1	forward AGTTTGAACCTGAGTATTCCCA reverse CATCCGTAGGAACTTGCTG	***RAP2C***	forward GATTTCTACCGCAAAGAGATC reverse CTCATTGGCTTGATATCCTGAA
LIMK2	forward CCCTGAGATGCTGAACGGA reverse CCTGCCCAATGATCTCACAG	***SSH2***	forward GTTCCTGGGCTCAGAATGG reverse TAAGTGTCATTCCAGTACGCC

Gene	Primer sequence (5' to 3')	Gene	Primer sequence (5' to 3')
MACF1	forward CAGGAAGAACTCAATTCCCGA reverse CCAGCACTCCCATCATCAG	***STX2***	forward CGGAGTACAATGAGGCACAG reverse GGTGGTTCTCCCAGTTATCTC
MCL1	forward CCTTCCAAGGCATGCTTCG reverse GTTTAGCCACAAAGGCACCA	***U6 snRNA***	forward CTCGCTTCGGCAGCACA reverse AACGCTTCACGAATTTGCGT
NRAS	forward AAGACTCGGATGATGTACCT reverse GCATCTTCAACACCCTGTC	***YWHAE***	forward ACAGTTGAAGAAAGAAACCTCC reverse AGTCTCAACCATTTGCCGA

2.1.4 Plasmid vectors

Table 10. List of plasmid vectors

Plasmid	ID	Gene	Company
pEGFP-C1 Vector	6084-1	Enhanced Green Fluorescent Protein (EGFP)	Clontech Laboratories Inc., CA, USA
miR-23b-sponge-pEGFP-C1 Vector		EGFP-hsa-miR-23b-sponge	
miR-26a-sponge-pEGFP-C1 Vector		EGFP-hsa-miR-26a-sponge	
pMIR-REPORT™ miRNA Expression Vector	AM5795	*Firefly* Luciferase (Luc)	Invitrogen, Life Technologies Ltd, Paisley, UK
PAK1-3'UTR pMIR-REPORT™		*Firefly* Luc-hsa-PAK1-3˝UTR	
PAK2-3'UTR pMIR-REPORT™		*Firefly* Luc-hsa-PAK2-3˝UTR	
PAK2-3'UTR-23b mut pMIR-REPORT™		*Firefly* Luc-hsa-PAK2-3˝UTR mutated for miR-23b-binding site	
PAK2-3'UTR-26a mut pMIR-REPORT™		*Firefly* Luc-hsa-PAK2-3˝UTR mutated for miR-26a-binding site	
pRL-TK Vector	E2241	*Renilla* Luciferase	Promega, Madison, WI, USA
ANXA2-pLightSwitch_3'UTR Go Clone vector	S804350	Synthetic *Renilla* Luc *(RenSp)*-hsa-ANXA2-3˝UTR	SwitchGear Genomics, Menlo Park, CA
ANXA2-3'UTR -23bmut pLightSwitch_Go Clone vector		*RenSp* Luc-hsa-ANXA2-3˝UTR mutated for miR-23b-binding site	
ARHGEF6-pLightSwitch_3'UTR Go Clone vector	S813665	*RenSp* Luc-hsa-ARHGEF6-3˝UTR	SwitchGear Genomics, Menlo Park, CA
ARHGEF6-3'UTR -23bmut pLightSwitch_Go Clone vector		*RenSp* Luc-hsa-ARHGEF6-3˝UTR mutated for miR-23b-binding site	
CFL2-pLightSwitch_3'UTR Go Clone vector	S812911	*RenSp* Luc-hsa-CFL2-3˝UTR	SwitchGear Genomics, Menlo Park, CA
CFL2-3'UTR -23bmut pLightSwitch_Go Clone vector		*RenSp* Luc-hsa-CFL2-3˝UTR mutated for miR-23b-binding site	
CHFR-pLightSwitch_3'UTR Go Clone vector	S812599	*RenSp* Luc-hsa-CHFR-3˝UTR	SwitchGear Genomics, Menlo Park, CA
CHFR-3'UTR-26adel pLightSwitch_Go Clone vector		*RenSp* Luc-hsa-CHFR-3˝UTR deleted for miR-26a-binding site	
LARP1-pLightSwitch_3'UTR Go Clone vector	S814042	*RenSp* Luc- hsa-LARP1-3˝UTR	SwitchGear Genomics, Menlo Park, CA
1LARP1-3'UTR-26amut pLightSwitch_Go Clone vector		*RenSp* Luc- hsa-LARP1-3˝UTR mutated for miR-26a-binding site 1	
2LARP1-3'UTR-26adel pLightSwitch_Go Clone vector		*RenSp* Luc- hsa-LARP1-3˝UTR deleted for miR-26a-binding site 2	
3LARP1-3'UTR-26amut pLightSwitch_Go Clone vector		*RenSp* Luc- hsa-LARP1-3˝UTR mutated for miR-26a-binding site 3	
LIMK2-pLightSwitch_3'UTR Go Clone vector	S810231	*RenSp* Luc- hsa-LIMK2-3˝UTR	SwitchGear Genomics, Menlo Park, CA

Plasmid	ID	Gene	Company
LIMK2-3'UTR-23bmut pLightSwitch_Go Clone vector		*RenSp* Luc- hsa-LIMK2-3˝UTR mutated for miR-23b-binding site	
MCL1-pLightSwitch_3'UTR Go Clone vector	S811815	*RenSp* Luc- hsa-MCL1-3˝UTR	SwitchGear Genomics, Menlo Park, CA
MCL1-3'UTR-26adel pLightSwitch_Go Clone vector		*RenSp* Luc- hsa-MCL1-3˝UTR deleted for miR-26a-binding site	
NRAS-pLightSwitch_3'UTR Go Clone vector	S808568	*RenSp* Luc- hsa-NRAS-3˝UTR	SwitchGear Genomics, Menlo Park, CA
PAK2-pCMV6-XL5	SC315439	Untagged, full length hsa-PAK2-coding sequence (TruClone)	OriGene Technologies, Inc., Rockville, MD
pCMV6-XL5		Cloning vector	OriGene Technologies, Inc., Rockville, MD
PIK3R3-pLightSwitch_3'UTR Go Clone vector	S814084	*RenSp* Luc- hsa-PIK3R3-3˝UTR	SwitchGear Genomics, Menlo Park, CA
PIK3R3-3'UTR-23bmut pLightSwitch_Go Clone vector		*RenSp* Luc- hsa-PIK3R3-3˝UTR mutated for miR-23b-binding site	
PLAU-pLightSwitch_3'UTR Go Clone vector	S807136	*RenSp* Luc- hsa-PLAU-3˝UTR	SwitchGear Genomics, Menlo Park, CA
TLN2-pLightSwitch_3'UTR Go Clone vector	S806580	*RenSp* Luc- hsa-TNL2-3˝UTR	SwitchGear Genomics, Menlo Park, CA
YwhAE-pLightSwitch_3'UTR Go Clone vector	S806563	*RenSp* Luc- hsa-YWHAE-3˝UTR	SwitchGear Genomics, Menlo Park, CA
YWHAE-3'UTR-26amut pLightSwitch_Go Clone vector		*RenSp* Luc-hsa-YWHAE-3˝UTR mutated for miR-26a-binding site	

2.1.5 Antibodies and probes

Table 11. Primary antibodies

Antibody	Dilution	Company	Dilution buffer
Polyclonal rabbit PAK1	1/5000	abcam® , Cambridge, UK	Blocking buffer
Polyclonal rabbit PAK2	1/1000	abcam® , Cambridge, UK	Blocking buffer
Monoclonal mouse MLC	1/2500	abcam®, Cambridge, UK	Blocking buffer
Polyclonal rabbit (Thr18/Ser19) pp-MLC2	1/1000	Cell Signalling, Danvers, USA	pp-MLC 2 antibody buffer
Monoclonal mouse β-actin	1/100000	abcam®, Cambridge, UK	Blocking buffer
Monoclonal mouse E-cadherin (HECD-1)	1/1000	Takara Bio Inc., Shiga, Japan	Blocking buffer (WB), IFF (IF)
Monoclonal mouse Vinculin (V9264)	1/400	Sigma-Aldrich, Dorset, UK	IFF
Policlonal rabbit c-JUN (H-79)	1/500	Santa Cruz, California, USA	ChIP buffer/blocking buffer
Policlonal rabbit c-FOS	1/1000	abcam®, Cambridge, UK	Blockin buffer
Monoclonal rabbit CD31	1/75	Millipore, Walford, UK	1% BSA in TBST

Table 12. Secondary antibodies

Antibody	Dilution	Company	Dilution buffer
Polyclonal goat anti-rabbit IgG/HRP	1/2500	Dako, Cambridge, UK	Blocking buffer
Polyclonal goat anti-mouse IgG/HRP	1/2500	Dako, Cambridge, UK	Blocking buffer
Alexa Fluor® 555 goat anti-mouse IgG	1/1000	Invitrogen, Life Technologies Ltd, Paisley, UK	IFF
Biotinylated goat anti-rabbit IgG	1/250	abcam®, Cambridge, UK	1% BSA in TBST

Table 13. Probes

Probe	Dilution	Company	Dilution buffer
Phalloidin-Alexa Fluor® 488	1/500	Invitrogen, Life Technologies Ltd, Paisley, UK	IFF/PBS
TO-PRO-3	1/1000	Invitrogen, Life Technologies Ltd, Paisley, UK	PBS
Streptavidin-HRP complex	1/500	Amersham Pharmacia Biotech, Bucks, UK	PBS
Cole's haematoxylin		Pioneer Research Chemicals, Colchester, UK	

2.1.6 Patient samples

Table 14: Patient characteristics data

Patient characteristics	Number of patients (%)
Age	
<35 Yr	2 (3%)
35-49 Yr	13 (19.7%)
50-59 Yr	18 (27.3%)
>60 Yr	33 (50%)
Median age, years [403]	59.5 (33-84)
Nodal Status	
1-3	44 (66.7%)
≥ 4	22 (33.3%)
Tumour Size	
0-20 mm	31 (46.9%)
>20-50 mm	27 (40.9%)
>50 mm	8 (9.2%)
Tumour Grade	
Grade I	9 (13.6%)
Grade II	44 (66.7%)
Grade III	13 (19.7%)
ER Status	
ER positive	56 (84.8%)
ER negative	10 (15.2%)
HER2 Status	
Positive	9 (13.7%)
Negative	57 (86.3%)
Histological Type	
Invasive Ductal Carcinoma	59 (89.4%)
Invasive lobular Carcinoma	7 (10.6%)

2.2 Methods

2.2.1 Mammalian cell culture

2.2.1.1 Growing and passaging cells

Cells were cultured in 150 cm^2 flask or 100 mm dishes or 6-well plates unless otherwise specified and maintained at 37°C in a humidified 5% CO_2 incubator. Cells were routinely passaged when a confluence of ~90% was reached, depending on the growth curve of each cell line. To passage cells, medium was aspirated, cells were washed once with PBS and then trypsinised with EDTA-trypsin at 37°C for 3 to 10 minutes to allow them to detach. FCS was added to inactivate the trypsin (1:1 ratio) and cell clumps were disrupted through gentle pipetting. Suspension of cells was pipetted out of flask, and transferred in 15 mL sterile centrifuge tube. The cell suspension was centrifuged for 4 min at 1300 rpm. After centrifugation, the supernatant was aspirated and cell pellet was resuspended in the appropriate volume of medium. The resulting suspension was split to the desired dilution into new flasks and fresh media was added. Cells were used between passages 4 and 20 in all experiments.

2.2.1.2 Transient cell transfections

For miRNAs overexpression, indicated cell lines were plated in 6-well tissue culture plates at 50% of confluence suspended in 1.5 ml of medium. Cells were allowed to adhere and grow at 37°C with 5% CO_2. After 24 h, the proper amount of each miRNA precursor (5nM) or siRNA (40nM) oligonucleotides was added to 0.5 ml of medium without additives. 12µl/well of Hiperfect Transfection Reagent (Qiagen) were added to each solution and gently mixed. The oligonucleotides suspensions were then incubated for 9 minutes at RT to allow the formation of transfection complexes. After incubation, the complexes were added drop-wise onto the cells, and the plates were gently swirled to ensure uniform distribution of the transfection complexes in each well. The cells with the transfection complexes were then incubated under normal growth conditions for 48 h. The transfection of each oligonucleotide was performed in triplicate for both protein and RNA extractions and each assay.

For prolonged overexpression of miRNA precursors, cell were plated in 6-well plates at 30% confluence, and transfected with the miRNA precurors as described above; after 72h, cells were split and re-transfected with additional miRNA oligonucleotides; this protocol was repeated every 3 days for up to 9 days. The transfection for 9 days with each miRNA precursor was performed in triplicate.

For 3‟UTR reporter assays, HCT116 cells were plated in 24-well tissue culture plates at a density of 5 x 10^4 cells/well in 0.5ml of medium without antibiotics. Cells were allowed to adhere and grown at 37°C with 5% CO_2 for 24h. Transfection complexes were prepared as follows: 200ng of pMIR-REPORT *firefly* luciferase vectors (Applied Biosystems, Life Technologies Ltd, Paisley, UK), including miRNA-sensor, PAK2, PAK1 or their relative mutant 3‟UTRs (**Table 7**), 100ng of *Renilla* luciferase vector (pRL-TK) and the indicated miRNA precursors (100nM) or the miRNA-sponge-EGFP vectors (100ng), were added in 50µl Opti-MEM® I Medium, gently mixed and incubated for 5 minutes at RT. After incubation, the oligonucleotide solutions were combined with the appropriate volume (0.5µl/well) of Lipofectamine® 2000, gently mixed and incubated for 20 minutes at RT to allow complex formation to occur. The complexes were then added drop-wise to each well containing cells and medium, and then incubated under normal growth conditions for 48 h. Each transfection was performed in triplicate in three independent experiments. MCF-7 cells were plated in 24-well tissue culture plates at a density of 1.5 x 10^5 cells/well in 0.5ml of medium without antibiotics. Cells were allowed to adhere and grow under normal cell growth conditions for 24 h. Transfection complexes were prepared by mixing 50ng of pLightSwitch_3UTR GoClone vectors (**Table 7**) with 100nM of the indicated miRNA precursors or 150ng of miRNA-sponge-EGFP vectors or the parental plasmid and processed as previously described. The cells with the transfection complexes were then incubate under normal growth conditions for 24h. Each transfection was performed in triplicate in three independent experiments.

2.2.1.3 Cell treatments

For EGF treatment, MDA-MB-468 cells were plated in 100 mm dishes at a 50% confluence and incubated under normal growth condition to adhere. EGF (Invitrogen, Life Technologies Ltd, Paisley, UK) or its vehicle DMSO (for the time point 0) was added at a final concentration of 25ng/ml for the indicated time points in three independent biological

replicates. After each treatment time point, dishes were placed on ice and medium was aspirated. Cells were washed twice with cold PBS, scraped and centrifuged for 5 minutes at 1300rpm. The supernatant was removed and the cell pellet was processed for RNA extraction. For nocodazole treatment, MCF-7 and MDA-MB-231 cells after 9d of transfection with the indicated miRNA precursors were exposed to 200ng/ml of nocodazole (solubilised in absolute DMSO) for 12h and then processed for chromosome metaphase spread assay.

2.2.1.4 Generation and maintenance of plasmid-stable-transfected cell lines

MDA-MB-231 cells were used to generate cell lines stably expressing the pEGFP-C1 vector and its derivatives, the miR-23b-sponge-EGFP and the miR-26a-sponge-EGFP plasmid vectors (**Table 10**). The parental pEGFP-C1 plasmid carries along with the gene encoding for an enhanced variant of the wild-type green fluorescent protein (EGFP), a neomycin resistance cassette which allows stably transfected eukaryotic cells to be selected using the antibiotic G-418 solution. The first step was to determine the working concentration of G-418 so as to ensure selection and maintenance of the neomycin-resistant cells by eliminating untrasfected cells. A titration experiment was performed by exposing untrasfected MDA-MB-231 cells seeded at different densities to different doses of G-418 (0.0, 0.1, 0.3, 0.5, 0.8, 1mg/ml) for 10d, and 0.5mg/ml showed to be the minimum amount of G-418 which induced cell death of 99% at all densities. Secondly, 2 x 10^6 cells were seeded in 100mm dishes in medium without antibiotics and allowed to adhere at 37°C with 5% CO_2 ON; 10µl of Lipofectamine® 2000 Reagent were incubated with 0.5ml of Opti-MEM® I Serum Reduced Medium for 5min at RT and then mixed with 2µg of each plasmid or ddH_2O (for the negative control) previously diluted in 0.5ml of the same transfection medium; the mixture was incubated for 20min at RT and then added drop-wise onto the cells. After 48h of transfection, stably transfected cells were selected with normal growth media supplemented with 0.5mg/ml of G-418. Untrasfected cells died within 7-10d from the addiction of the antibiotic. Stably transfected cells were seeded at a low density so as that each single cell formed a monoclonal colony in presence of G-418. When colonigenic foci were visible to the naked eye, 24 colonies for each transfection condition were transferred into 24-well plates: cloning discs were immersed in trypsin-EDTA for 2-3min, then dropped on top of a single cell colony and incubated for 5min at 37 ºC to allow cells to detach. Each cloning disc carrying monoclonal cells was then transferred to

each well of a 24-well plate in presence of G-418-cointaining medium. Cells derived from monoclonal colonies were maintained by refreshing medium twice a week, and expanded to high confluence before to be transferred to 6-well plates. After cells were passaged for 2-3 times in 100mm dishes, they were assessed for EGFP expression by fluorescence activated cell sorter (FACS) analysis. Only the clones that showed an EGFP-expressing cell population higher than 80% were selected for further analysis. RT-PCR, western blotting, luciferase and proliferation assays indicated that clone n.10, n.2 and n.22 were the best representatives for miR-23b-sponge-EGFP, miR-26a-sponge-EGFP and pEGFP-C1 expression, respectively.

2.2.2 3'UTR-Luciferase reporter assays

Forty hours after transfection, cells were lysed with 50µl/well of the Cell Culture Passive Lysis Buffer (5x) (Promega, Madison, WI, USA) fivefold diluted in dH_2O and placed on agitator at constant speed for 30 minutes. For HCT116 cells, luciferase assays were performed by using the Dual-Glo Luciferase assay system (Promega, Madison, WI, USA). The lysates were transferred in an Opti-plate 96-well and mixed with 50µl/well of Dual-Glo™ Luciferase Reagent. After 10 minutes, the 96-well plate was sealed and the *firefly* luciferase activity was measured by using a luminometer. The measure of *renilla* luciferase luminescence was carried out by adding 50µl/well of Dual-Glo™ Stop & Glo® Reagent, prepared according to the manufacturer's instructions. After 10 minutes, the reading of *Renilla* luminescence was taken by a luminometer. The ratio between *firefly* and *renilla* luminescence measurements was then calculated, and averages of triplicates were determined. For MCF-7 cells, the LightSwitch Luciferase Assay System (Switchgear Genomics Menlo Park CA, USA) was used: lysates were transferred in an Opti-plate 96-well, mixed with 50µl/well of Assay Solution and incubated for 30 min out of the light. Luminescence signals were read by a luminometer and averages of triplicates were calculated.

2.2.3 Plasmid constructions

MiR-23b- or miR-26a-sponge-EGFP vectors were constructed by annealing, purifying and cloning oligonucleotides (**Table 7**) containing six adjacent bulged binding motifs for the relevant human miRNA into the HindIII and BamHI sites of the multiple cloning site (MCS) of the pEGFP-C1 plasmid. Sensor constructs for miR-26a and miR-23b were produced using a similar strategy but they were cloned as 3'UTRs into the SpeI and

HindIII sites of the MCS of p-MIR REPORT *Firefly* Luciferase vector. Amplification of PAK1 and PAK2 3‟UTRs from genomic DNA was performed by PCR by using the GoTaq Flexi DNA Polymerase kit (Promega Madison, WI, USA) and a specific primer set (**Table 7**). To check if the amplification reaction was succeed the PCR products were tested on electrophoresis running agarose gel. The amplicons were then purified by using the QIAquick PCR Purification Kit (Qiagen, West Sussex, UK) according to the manufacturer‟s instructions. Double digestion of the blunt-ends of the amplicons was performed by using *SpeI* and *MluI* restriction enzymes (New England BioLabs, Beverly, MA, USA) at 37°C ON. All the primers used for the amplification of 3‟UTRs were designed by adding a SpeI-specific restriction site on the 5‟end, and a *MluI*-specific restriction site on the 3‟end, so as to allow amplicons to be cloned in the MCS of the pMIR-REPORT *firefly* luciferase vector. The ligation reaction was carried out by incubating each amplicon with the linearized pMIR-REPORT *firefly* luciferase vector (ratio 3:1) and 1µl of T4 DNA Ligase (New England BioLabs, Beverly, MA, USA) at 16°C ON. Site-directed mutagenesis of the miRNA-binding motif within the 3‟UTR of the analysed genes was performed by using the QuikChange Site-Directed Mutagenesis II or XL Kit (Stratagene, La Jolla, CA, USA) according to the manufacturer‟s instructions, and the specific primer sets (**Table 7**). All the plasmids were confirmed by sequencing.

2.2.4 Quantitative real-time Reverse Transcription-PCR

2.2.4.1 RNA preparation

Cells were lysed with 1ml of Trizol reagent (Invitrogen, Life Technologies Ltd, Paisley, UK) through vigorous pipetting and lysates collected in Eppendorf tubes. By working under hood, 200µl of chloroform per 1ml of Trizol reagent were added to the lysates. The samples were vortexed vigorously for 15 seconds, incubated at RT for 2 to 3 minutes, and then centrifuged at 12,000 x *g* for 15 minutes at 2 to 8°C. Following centrifugation, each mixture separates into a lower phenol-red, chloroform phase, an interphase, and a colorless upper aqueous phase. RNA remains exclusively in the aqueous phase. Each aqueous phase

was transferred carefully into fresh Eppendorf tubes. The total RNA was precipitated from the aqueous phases by mixing with 500µl of isopropyl alcohol and incubating for 10 minutes at RT. The mixtures were then incubated ON at -80°C to enhance small RNA precipitation. After incubation, the RNA precipitates were centrifuged at 12,000 x *g* for 10 minutes at 2 to 4°C to form a pellet on the side-bottom of the tube. The supernatants were removed, and the RNA pellets were washed by adding 1ml of 75% ethanol and mixing by vortexing. The samples were centrifuged at 7,500 x *g* for 5 minutes at 2 to 8°C. The supernatants were removed and any residues of ethanol were air-dried. Finally the RNA pellets were resuspended in an appropriate volume of RNAse-free water. Subsequently, RNA concentration was measured at 260nm and 280nm wavelengths, using a NanoDrop ND-100-Spectrophotometer (Labtech international, East Sussex, UK). The RNA quality was determined on non-denaturing agarose electrophoresis gel: for each RNA sample isolated, two intensive bands at approximately 4.5 and 1.9 kb were observed at the transilluminator. These bands represent 28S and 18S rRNA and indicate successful RNA preparation. RNA extraction from 5 to 8 10µm FFPE sections of each tumour tissue sample was performed using the RNeasy FFPE kit (Qiagen, West Sussex, UK), in accordance to manufacturer‟s instructions.

2.2.4.2 cDNA synthesis

The reverse transcription of mature miRNAs was performed using the TaqMan MicroRNA Reverse Trascription Kit (Applied Biosystems, Life Technologies Ltd, Paisley, UK). 10ng of total RNA were mixed with 7µl of master mix and 3µl of miRNA-specific RT TaqMan Probes (Applied Biosystems) in a 48-well PCR plate (Thermo Schientific, Abgene®, Leicestershire, UK) according to manufacturer‟s instructions. The samples were incubated in a 7900Ht Thermal Cycler (Applied Biosystems) at 16°C for 30 min to allow primers annealing, following by 30 minutes at 42°C for the elongation step, and 5 minutes at 85°C to inactivate the reverse transcriptase. For gene expression, cDNA was synthetised by using the Superscript III First Strand cDNA synthesis system (Invitrogen, Life Technologies Ltd, Paisley, UK): 1 µg of purified Dnase-treated RNA was mixed with 50nM of the reverse primer of each primer set (**Table 9**) and incubated in a 7900Ht Thermal Cycler at 70°C for 10 min to allow RNA denaturation, and then place on ice to allow primer annealing. The proper amount of reverse transcriptase and dNTPs were then added to the RNA and incubated at 50ºC for 50 min, and at 85ºC for 10 min in a 7900Ht Thermal Cycler. After RT cycles, the cDNAs samples were placed on ice and then prepared for quantitative real-time PCR.

2.2.4.3 Quantitative real-time PCR

To amplify mature miRNAs, for a single reaction, 1 ng of relative cDNA template was distributed in a Fast Optical 96-well reaction plate (Applied Biosystems, Life Technologies Ltd, Paisley, UK), followed by the appropriate volume of TaqMan® Universal PCR Master Mix, No Amperase® UNG (Applied Biosystems) and the relative 20x Real Time TaqMan probe (Applied Biosystems). Each reaction was done in triplicate. The plate was then sealed using the Optical Adhesive Cover Starter Kit (Applied Biosystems) and centrifuged (2,000 x *g*) for 30 seconds at 4°C. Quantitative real-time PCR (qPCR) was performed with an ABI Prism 7900HT sequence detection system (Applied Biosystems) with a thermal cycling program as follow: a first stage of 10 min at 95°C was followed by a step of 15 sec at 95°C for 40 cycles and one last step of 1 min at 60°C. For both gene-specific expression and ChIP enrichment, 10 ng of cDNA per reaction were amplified using the Power SYBR green PCR master mix (Applied Biosystems) and the specific gene primer set. Quantitative real-time PCR (qPCR) was performed with an ABI Prism 7900HT sequence detection system) with a thermal cycling program as follow: a first stage of 10 min at 95°C was followed by 40 cycles 20 sec at 60°C and 20 sec at 72ºC. Finally, data were analysed using qBasePlus software (biogazelle). All the used primer set sequences in the qRT real-time PCR are reported in the **table 9**.

2.2.5 SDS-polyacrylamide gel electrophoresis and western blot

2.2.5.1 Protein extraction

Cell pellets were lysed in 30 to 60 µl of NP-40 lysis buffer + protease inhibitors cocktail solution (Roche, Diagnostic Ltd, West Sussex, UK). Eppendorf tubes containing cell lysates were placed on a rotator for 15 minutes at 4°C. A microcentrifugation of the lysates at maximum speed (13,000 rpm) for 15 minutes at 4°C allowed the separation of protein from insoluble elements. The supernatants containing proteins were transferred in new Eppendorf tubes and subsequently subjected to protein quantification.

To preserve protein phosphorylation, cells were washed twice with cold PBS and lysed directly in the well of the 6-well plate by adding 50 µl of Laemmli‟s buffer (**Table 3**) . Each

lysate, forming a viscous gel-like solution, was gently scraped with an end-cut tip, transferred in an Eppendorf tube, and immediately incubated at 95 °C in a pre-heated water-bath for 5 minutes to allow protein denaturation to occur. In order to reduce the viscosity, an index of the chromatin presence in the solutions, the lysates were sonicated twice for 2 seconds at constant power, and then frozen in an ethanol-dry ice bath (-80 to -70°C) to avoid the formation of crystal particles. The protein concentration in these lysate samples was not determined due to their composition.

2.2.5.2 Protein quantification

Protein concentration was determined using the Bradford Reagent Kit (Bio-Rad, Berkeley, CA, USA). Absorbance readings were measured at 595 nm using a Beckman DU® 530 Life Science UV/Visible spectrophotometer (Harlow Scientific, Arlington, MA). Upon collection of the data, the concentration of the unknown samples was determined based on standard absorbance value. The protein samples were then prepared for the SDS-polyacrilamide gel electrophoresis: 3µg/µl of protein samples were mixed with SDS Loading Buffer (5x) and boiled at 95°C for 5 minutes.

2.2.5.3 SDS-polyacrylamide gel electrophoresis

Both acrilamide (8-20%) resolving and 4% stacking gels were prepared manually as required. Once rainbow marker (Fermentas, Thermo Scientific, Leicestershire, UK)) and the protein samples (10µl) were loaded, electrophoresis was carried out for 2 to 3 h at 80V. Proteins were separated by SDS-polyacrilamide gel electrophoresis (SDS-PAGE) and run in 1x SDS-PAGE running buffer.

2.2.5.4 Western blots

The proteins were transferred to a Hybond C super nitrocellulose membrane (GE Healthcare, UK) for 1 h at 100V in transfer buffer using a Mini-PROTEAN® Tetra Cell (Bio-

Rad, Berkeley, CA, USA). The membrane was stained with Ponceau S solution (Fluka, Sigma-Alderich, Dorset, UK) to check if the transfer was successful. The membrane was washed once for 10 minutes with blocking buffer in order to remove the staining and then blocked with blocking buffer at RT for 1 hour. The membrane was then transferred in the primary antibody solution and left at 4°C ON (**Table 11**). TBST was used to wash the membrane for three times, 15 minutes each. An IgG/HRP secondary antibody (**Table 12**) diluited in blocking solution was then added, and the membrane was incubated at RT for 1 hour. The membrane was washed 3 times with TBST and Enhanced Chemiluminescence (ECL) detection system (GE Healthcare) was used for visualisation. The emitted fluorescence was detected using Hyperfilm ECL (GE Healthcare) on SRX-101A x-ray developer.

2.2.5 Chromatin Immunoprecipitation (ChIP)

MDA-MB-231 cells were seeded in 150 cm^2 dishes at a density of 9 x 10^6 cells and allowed to adhere ON. Cross-linking of proteins to DNA was performed by adding 0.75% formaldehyde drop-wise directly to the media for 10 min at RT. 125 mM glycine was added for 5 min at RT in order to stop the cross-linking reaction. Cells were then rinsed twice with cold PBS containing protease inhibitors (Roche, Diagnostic Ltd, West Sussex, UK), scraped and collected into 50 ml tube. After centrifugation at 2,000 rpm for 10 min, the resulted cell pellet was resuspended in solution 1 to lyse plasma membranes and incubate in rotation for 10 min at 4 °C. After centrifugation, lysates were washed with solution 2 in rotation for 10 min at 4 °C and then centrifuged to separate the nuclei from cytoplasmic lysates. Nuclei were then lysed in 1 ml of Sonication buffer (Millipore, Walford, UK) and processed to sonication four times for 20 seconds each. The sonicated DNA-sample was splitted in 3 equal aliquots (for mock, IgG and anti c-JUN antibody incubation) that were then incubated with salmon sperm DNA-Protein A agarose (Millipore, Walford, UK) and centrifuged at the highest speed for 10 min. The three supernatants obtained were then diluited in ChIP buffer, centrifuged to pellet the agarose away, and incubated in rotation with 1 µg of c-JUN antibody at 4 °C ON (**Table 11**). The day after c-JUN antibody/histone complex were collected by adding agarose beads to the samples for 1h. After several washes in law/high salt washing buffer, agarose beads were removed from samples by adding elution buffer (Millipore, Walford, UK) and histone-DNA crosslinking reversion was carried out by incubating the samples with 5M NaCl ON at 65 °C. On the third day, 0.25 µl of RNase (100 mg/ml, Qiagen, West Sussex, UK) were added to the samples to degrade RNA for 30 min at 37 °C. Finally, DNA was purified in chloroform

(50%)-phenol (49%)-isoamyl alcohol (1%) mix washed in 100% ethanol, and then resuspended in 100 µl of TE buffer (Qiagen).

2.2.6 Cell adhesion assay

The day before running the assay, 24-well plates were coated with 250 µl/well of 50 µM type I collagen (BD Biosciences, Oxford, UK) in sterile PBS and incubated ON at 4 °C. As control, a number of wells were coated with 5% heat-denaturated BSA. The day of the assay, pre-coated wells were washed once with PBS and blocked with 1% heat-denaturated BSA for 1 hour at 37 °C. MDA-MB-231 cells transfected for 48 h with the indicated oligonucleotides were then seeded in serum-free medium on pre-coated wells (n=3 per transfection) at a density of 1 x 10^5 cells per well and allowed to adhere for 30 minutes. Cells were then labelled with 1M Calcein/AM (Invitrogen, Life Technologies Ltd, Paisley, UK) for 15 minutes at 37 °C and carefully washed three times with PBS containing 1mM $CaCl_2$ and 1mM $MgCl_2$. The fluorescence signal was measured by using an Infinite™ 200 quad-4 spectrophotometer (Tecan UK Ltd, Reading, UK at an excitation wavelength of 485 nm and an emission wavelength of 520 nm. The differences in fluorescence measurements from three independent experiments were depicted as percentages of adherent cells.

2.2.7 Cell spreading assay

The collagen-coating procedure was performed as described for adhesion assay after inserting a rounded cover slip in each well. In this case 0.55 x 10^5 MDA-MB-231 cells were plated in triplicate on pre-coated cover slips 48 h after transfection. After 30, 60 or 90 min of incubation at 37 °C, culture medium was removed from wells and cells were fixed with pre-warm 4% (w/v) paraformaldehyde (PFA) in PBS for 10 min at RT. Cells were then gently washed twice with PBS and incubated with 0.5 M glycine in PBS for 20 min at RT in order to quench aldehyde-induced autofluorescence. Two washes with PBS were performed before to permeabilize the cells with 0.3% v/v Triton-X-100 for 10 min and block them for 30 min with IFF + 5% goat serum. Incubation of the cells with anti-vinculin primary antibody for 1 h at RT was followed by two washes with IFF. By this point all the next steps were carried out under dark conditions. Cells were incubated for 2 h with Alxa Fluor® 555 goat anti-mouse secondary antibody and phalloidin-Alexa Fluor® 488, then washed twice with IFF and nuclei staining was performed adding TO-PRO-3 in PBS for 5 min. After a last wash with PBS,

cover slips carrying the stained cells were mounted on microscopy glass slides and then processed for confocal microscopy.

2.2.8 Cell-cell junction, focal adhesion and lamellipodia visualisation

To highlight cell-cell junction formation, MCF-7 and MDA-MB-231 cells transfected with the indicated miRNA precursors for 9 days were plated at high density in 24-well plates (2 wells per condition) on top of a rounded cover slip and allowed to adhere ON at normal cell growth conditions. Cells were then fixed and processed for immunofluorescent staining as described for the spreading assay, but in this case an anti-E-cadherin primary antibody was used in order to visualise cell-cell junctions.

For focal adhesion visualisation, 0.55 x 10^5 MDA-MB-231 cells were plated in 24-well plate (in triplicate) on collagen-coated cover slips 48 h after transfection (coating was performed as described for adhesion assays). After 1h of incubation at 37 °C, culture medium was removed from wells and cells were fixed and processed for immunostaining as already described, but in this case cells were stained only with anti-vinculin primary antibody for 1 h at RT to visualise focal adhesion areas.

To detect lamellipodial structures, 0.5 x 10^5 MDA-MB-231 cells were plated on a rounded cover slip in 24-well plates 48 h after transfection. Cells were allowed to adhere ON under normal cell growth conditions and then fixed and processed for actin cytoskeleton staining as already described. For each assay, three independent experiments were performed.

2.2.9 Annexin V-apoptotic assay

To assay the apoptotic properties of miR-26a and miR-23b, MDA-MB-231 were transfected with the indicated microRNA precursor mimics and the cell death control siRNA (20nM) (Qiagen, West Sussex, UK) that was used as positive control. After 48 h, detached cells were combined with adherent cells after lifting with trypsin-EDTA, stained with Annexin V/PE apoptosis detection kit (BD Biosciences, Oxford, UK) according to manufacturer‟s protocol and analysed using a FACSCanto II flow citometer (BD Biosciences, Oxford, UK). Apoptotic cells were represented by high PE-Annexin V fluorescence signals. The assay was performed in three independent replicates.

2.2.10 Cell growth assay

Cell growth was analysed by performing a sulfoRHOdamine B colorimetric (SRB) assay. MCF-7 and MDA-MB-231 cells were seeded at a density of 0.3 x 10^4 cells/ well in 96-well plates and transfected for 48 h with the indicated molecules in quintuplicates. To assess the effect of miRNA inhibition on cell growth, the indicated miR-23b-, miR-26a-sponge-EGFP-MDA-MB-231 clones along with the pEGFP-MDA-MB-231 and normal MDA-MB-231 cells were seeded at a density of 0.3 x 10^4 cells/ well in 96-well plates in quintuplicates and allowed to adhere ON under normal cell growth condition. SRB assay was performed by processing the plates on a timeline of 7 days (one plate every two days) as follow: cells were fixed by adding 100 µl/well of ice-cold trichloroacetic acid (TCA) to each culture for 1h at 4 °C. Cells were then washed five times in running tap water and stained with 100 µl/well of 0.4% (w/v) of SRB buffer (Sigma-Aldrich, Dorset, UK) in 1% acetic acid for 30 min. After five washes with 1% acetic acid, plates were allowed to air dry ON. On the day of plate reading, SRB stain was solubilised by adding 100 µl/well of 10mM Tris-base to each well. Plates were placed on rotating platform for 10 min and absorbance was read with an Infinite™ 200 quad-4 spectrophotometer (Tecan UK Ltd, Reading, UK) at a wavelength of 492 nm.

2.2.11 Cell migration assays

2.2.11.1 Transwell migration assay

MDA-MB-231 cells transfected with the indicated oligonucleotides for 48 h or stably expressing the miR-23b-sponge-EGFP construct or the parental control, were seeded (5 x 10^4 cells/insert) in triplicate in Tranwell® Polycarbonate Membrane inserts 24-well plates atop uncoated membranes with 8.0 µm pores (BD Biosciences, Oxford, UK). Cells were plated in serum free-medium and allowed to migrate from the upper chamber of the transwell insert toward a complete growth medium in the lower chamber. After for 9 h of migration, culture medium was removed from both the chambers, and insert membranes were fixed with 4% (w/v) PFA for 30 min at 37 °C. Cells attached on both sides of the membrane were then stained with 0.2% crystal violet in 20% methanol for 30 min at 37 °C and washed five times in PBS. Further, non-migrated cells were removed by scraping the upper side of the porous membranes with a cotton swab. Membranes carrying migrated cells (bottom side) were cut

out from the insert with a scalpel and sealed on microscope glass slides for microscope imaging.

2.2.11.2 Cell tracking assay

MDA-MB-231 cells were seeded in 24-well tissue culture plates at a final density of 1 x 10^4. After 48 h of transfection, time-lapse sequences were digitally recorded at intervals of 20 minutes for 24 h using ImageXpress Micro® microscope (Molecular Devices, Sunnyvale, CA, USA) fitted with a humidified 37 °C incubation chamber and 10x objective. Cell trajectories were determined by following the centroid of the nuclei using the NHI ImageJ plugin "MTrackJ" (http://www.imagescience.org/meijering/software/mtrackj/) and speed of cell body movement was calculated for mean cell migratory speed. A 50-100 cells per each condition were analysed and three independent experiments were performed.

2.2.12 Type I collagen 3-dimensional invasion assay

MDA-MB-231 cells transfected for 48 h with the indicated miRNA precursors or stably expressing the indicated vectors were plated in black-walled 96-well plates at a final density of 7 x 10^4 and allowed to adhere ON under normal cell growth conditions. Type I collagen mixture was prepared by working on ice as follow: 20% 5x serum-free cell culture medium, 2% 1M Hepes pH 7.5 and type 1 collagen (BD Biosciences, Oxford, UK) at a final concentration of 2.3 mg/ml. Type I collagen mixture (100 µl/well) was laid over the cells and allow to polymerize for 1 hour at 37 °C and 5% CO_2. 100 µl of cell culture medium supplemented with 10% FCS as chemoattractant were added on top of the polymerized matrices and cells were allowed to invade upward through them for 16 h under normal cell growth conditions. The plates were then fixed in 100 µl of 4% (w/v) PFA for 30 min, washed twice with PBS and permeabilized with 0.2% v/v Triton-X-100 for 30 min After washing each plate well with PBS twice, staining of the actin cytoskeleton and the nuclei was achieved by incubating for 2 h the matrix-invading cells with phalloidin-Alexa Fluor® 488 and TO-PRO-3 in PBS, respectively. Plates were washed again twice with PBS and then processed for confocal microscopy. Three independent experiments per conditions were performed.

2.2.14 Metaphase chromosome spread preparations

After nocodazole treatment, MCF-7 and MDA-MB-231 cells transfected for 9 d with the indicated precursors were processed for metaphase chromosome spreads as follow: cell culture media and PBS used for rinsing cells were collected in 15 ml centrifuge tubes and spun down at 1000 rpm for 7 min in order not to lose dislodged, mitotic cells. Adherent cells were harvested by trypsinisation, collected with normal cell growth medium, added to the previously pelletted cells and spun down at 1000 rpm for 7 min. Supernatant was aspirated, leaving a small volume of medium (~300 µl) in which cells were resuspended by gently pipetting bubbles. Cells were induced to swell by adding 10 ml of hypotonic solution and incubating for 15 min at 37°C. Then few drops of fixative solution were added and cells were collected by centrifugation at 800 rpm for 8 min. After aspirating the supernatant, cells were resuspended thoroughly by gently flicking the tube. One ml of fixative solution was added drop-wise in constant agitation and cells were incubated for 1 h on ice. Cells were then spun down at 500 rpm for 5 min, the supernatant was removed and 1 ml of fixative solution was added. After repeating the last three steps three times, 20 µl of fixed swollen cells were slowly dropped onto a glass microscope slide, which was immediately run through the flame of a burner (bottom side of the slide toward the flame) in order to cause the rupture of the cell membranes and release of the chromosomes. The microscope slides were then incubated at 37°C for 1 h and then processed for chromosome staining: slides were stained with 5 ml of Giemsa stain (Sigma-Aldrich, Dorset UK) diluted 1:20 in dH_20 for 15 min, then rinsed in Gurr"s buffer for 5 min and in dH_20 for few seconds. After air-drying, few drops of Permount oil were added to the slide surface and covered with a cover slip. After drying at 37°C ON, slides were processed for microscope imaging. Tree independent experiments were performed.

2.2.13 Soft agar colony formation assay

Stocks of 3% low melting point agarose (Invitrogen, Life Technologies Ltd, Paisley, UK) in PBS (20 ml aliquots) were prepared, autoclaved and stored at 4°C before use. On the day of the assay, one 3% agarose aliquot was melted and maintained in liquid phase in a water bath at 85°C. A 6-well plate was coated with 2 ml/well of a 0.6% agarose mixture (3% agarose diluited with warm normal cell growth medium) and allowed to polymerize for 5-10 min at RT. MCF-7 cells transfected with the indicated oligonucleotides for 9 d were harvested

by trypsinisation, spun down and resuspended in warm medium at a final concentration of 1.5 x 10^4 cells/100 µl. A 0.3% agarose mixture was prepared by diluting the 3% agarose with warm medium and mixed with the transfected cell suspension (1.5 x 10^4 cells in 2 ml of 0.3% agarose). 2 ml of cell/agarose mixture was added in each well on top of the 0.6% agarose layer in triplicate per condition. The plate was then incubated under normal cell growth conditions for 3-4 weeks, to allow anchorage-independent cell growth. When formation of colonies more than 75 nm in diameter was observed, they were imaged by light microscopy. Colonies were then stained with 0.5 mg/ml of 3-(4,5-dimethylthiazol-2-yl)-2,5-diphenyltetrazolium bromide (MTT, Invitrogen, Life Technologies Ltd, Paisley, UK) in ddH_2O after incubation at normal cell growth conditions ON. Each well was then photographed to visualise MTT-stained colony formation. The assay was performed in triplicate per condition in two independent experiments.

2.2.14 Confocal microscopy and cell imaging

2.2.14.1 Confocal microscopy

For spreading assay and visualisation of cell-cell junctions, focal adhesions and lamellipodial structures, images were captured with a Plan-Apochromat 63x/1.40 oil objective using a Zeiss LSM 510 META confocal microscope fitted with an LSM 510 META scanhead and driven by Zeiss LSM 510 confocal software. 20-50 images were taken for each condition in each assay. For invasion assays, serial 5 µm-*z* sections of collagen gels containing invading cells were taken using the same confocal microscope. 5 fields per well were imaged and analysed using the Zeiss LSM 5 Image Browser (Carl Zeiss MicroImaging, Inc., Cambridge, UK). Invasion indexes were calculated as the number of cells at 40 µm divided by the number of cells at 0 µm.

2.2.14.2 Cell imaging

To determine cell-cell junction linearity, images taken by confocal microscopy were false-coloured in a black-and-white fashion and processed using the Zeiss LSM 5 Image Browser: junction lengths and distances between vertices were manually traced and their

measurements were used to calculate a linearity index. 150-250 junctions per condition in two independent experiments were counted.

To highlight the area of FAs, the images taken by confocal microscopy were false-coloured in a black-and-white fashion and 50-80 cells per condition were analysed using NHI ImageJ software. Quantification of FA area is represented as the average of FA area per cell.

Cells imaged in the time-lapse tracking assays were analysed for lamellipodial formation. Lamellipodial structures were manually counted in a blind fashion and 100 cells per each condition in the three independent experiments were considered.

For transwell migration assays, porous membranes carrying the migrated cells were imaged with 10x objective lens with an ACIS ChromaVision microscope (ChromaVision Medical Systems Inc. CA, USA). Images of five fields per triplicate per each experiment were taken. Quantification of number of migrated cells was determined by manually counting total cells per each field and transwell cell migration is expressed as percentage of the mean of the averages of three independent experiments.

Metaphase chromosome spreads were examined by 100x oil immersion lens with a Zeiss Axiovert 100 (deconvolution) microscope. About 100 chromosome spreads per condition per experiment were imaged and the percentage of chromosome spreads was determined as average of number of chromosomes per spread.

To visualise soft agar colony formation, colonies were photographed and subsequently counted by using Image, number of colonies is expressed as mean of the averages of two independent experiments performed in triplicated per condition. To analyse colony size, colonies were imaged using an ImageXpress Micro® microscope (Molecular Devices, CA, USA) fitted with humidified 37 °C incubation chamber and a 20x objective; colony size was measured by using NHI ImageJ software and percentages to control derived from mean of the average size in two independent experiments performed in triplicate per condition.

Paraffin-embedded sections from mammary gland primary tumours, lymph nodes and lungs were imaged with a 10x lens with a Zeiss Axiovert 100 microscope. Microvessels were counted per 5 high power fields per section in three different primary tumours per treatment.

Metastatic areas within the lymph nodes (n=7 per treatment) and necrotic areas within the primary tumours (n=3 per treatment) were measured using the NHI ImageJ software. Quantification of metastatic areas and normal tissue was expressed as percentage of tissue type in the lymph nodes, whereas percentage of necrotic areas within the primary tumours was measured to quantify necrosis.

2.2.15 *In vivo* studies

All procedures involving animals were performed in accordance with the UK Home Office Project licence PPL70/7256. Mir-23b-sponge-EGFP-MDA-MB-231 or pEGFP-MDA-MB-231 cells were harvested by trypsinisation, spun down at 1300 rpm for 5 min and resuspended in warm normal growth medium supplemented with 0.5 mg/ml of G-418 solution at a final concentration of $1x10^6$ cells/25 µl. Working quickly on ice, cell suspension was mixed with matrigel (BD Biosciences, Oxford, UK) with a ratio 1:1. Cell/matrigel suspensions were kept on ice during preparation of animals for cell implantation. BALB/c nude female mice (n=7 per treatment) were anaesthetised with 4% isofluorane and their body temperature was maintained by laying them on a thermal pad. Forceps were used to test rear foot reflexes in order to ensure that mice were deeply asleep before to proceed. By using surgical scissors, a small incision was made to reveal the mammary gland of the left caudal-most inguinal nipple. Cell/matrigel suspension was loaded into a 1 ml syringe fitted with a 27-gauge hypodermic needle and $1x10^6$ cells/50 µl were injected into the fat pad of the exposed mammary gland. The incision was then closed with a single suture and mice were recovered from anesthesia in a 37°C warm chamber. After recovery, a dose of 0.1 mg of the analgesic Rimadyl (Pfizer, New York, NY) was administered to the mice orally (diluted in drinking water) every day until wound healing was completed. Mice were kept under continuous sterile conditions (individually-vented cages) and had constant food and water access throughout the whole experiment period. Once orthotopic tumour formation in the injected mammary gland was observed, tumours were monitored and measured once a week. After about 2 months, when the maximal tumour volume of 300 mm^2 was reached, mice were sacrificed. Primary tumours, the left inguinal lymph nodes and lungs were removed and fixed with 10% neutral formalin for paraffin-embedded sections and immunohystochemistry staining.

2.2.14 Immunohistochemistry for histopathological analysis

Immunohistochemistry was performed using the streptavin-biotin complex indirect immunoperoxidase method. Sections of 4 µm thickness from paraffin-embedded mammary gland primary tumours, lymph nodes and lungs were dewaxed, rehydrated and incubated with 0.3% hydrogen peroxide for 30 min to block endogenous peroxidase activity. Antigen retrieval was performed by microwaving the sections for 20 minutes in 0.01 M citrate buffer (pH 6.0) at 750W. The sections were incubated with the primary antibody to cluster of

differentiation 31 (CD31, Millipore, Walford, UK) for 3 hour at RT. After washing with PBS, the sections were then incubated with a biotinylated IgG secondary antibody (Abcam, Cambridge, UK) for 30 minutes, washed with PBS, then incubated with streptavidin-peroxidase complex (1:500, Amersham Pharmacia Biotech, Bucks, UK) for 30 minutes. The sections were developed with activated 3,3-diaminobenzidine-tetrahydrochloride solution (Sigma-Aldrich, Dorset, UK) and 0.1% H_2O_2 and counterstained with Cole‟s hematoxylin. Sections were then dehydrated, mounted on glass microscopy slides using Pertex mountant (CellPath, Hemel Hempstead, UK) and processed by microscopy.

2.2.15 Illumina RNA-seq and analysis

Total RNA from MCF-7 cells transfected with miR-23b, miR-26a or miR-n.c. precursors for 9 d and from miR-23b-, miR-26a-sponge-EGFP-MDA-MB-231 and pEGFP-MDA-MB-231 cells was isolated as described in the RNA preparation section. Two micrograms of total RNA from each sample was used to produce cDNA libraries from polyA enriched RNA using the True-seq RNA preparation kit (Illumina, San Diego, USA) according to the manufacturer‟s instructions. Paired-end sequences (reads) of 100 nt in length were then generated using a HiSeq 2000 instrument (Illumina). Fastq files containing the sequenced reads, obtained at the end of the sequencing, were mapped to the University of California at Santa Cruz (UCSC) human genome (hg19 assembly) with TopHat version 1.4.1 (http://tophat.cbcb.umd.edu), using default settings. A total of 29,437,797, 26,630,458, 29,106,929, 29,977,877, 25,385,055 and 32,764,706 mapped reads for miR-23b-overexpressing MCF-7, miR-26a-overexpressing MCF-7, miR-n.c-overexpressing MCF-7, miR-23b-sponge-EGFP-MDA-MB-231, miR-26a-sponge-EGFP-MDA-MB-231 and pEGFP-MDA-MB-231 cells, were attained, respectively. The mapped bam files obtained at the end of the runs were loaded on the Partek Genomic Suite (Partek Incorporated, USA) for RNA quantification and analysis. This software is able to transform mapped bam files in kilobases per million of mapped reads (RPKM) as output for any gene, that represent the gold standard for RNA-seq normalisation. RPKMs represent the computed values. Significant change in gene expression was selected applying a Chi-square test.

2.2.16 Clinico-pathological characteristics of the patients

MiRNA expression profiling was performed on primary breast cancers and corresponding lymph node metastases from 66 patients with lymph node positive breast cancer, eligible for chemotherapy at Imperial College Healthcare NHS Trust, London, UK. All one-hundred and thirty-two samples were formalin-fixed and paraffin-embedded and prepared for miRNA processing. The clinico-pathologic characteristics are listed in **table 14**. Prospective written consent was obtained in accordance with ethical guidelines.

2.2.17 Statistical analysis

Data are presented as mean ± SEM calculated using Graph Prism software. Student‟s *t*-test and Chi-Square test were used for comparison, with $P < 0.05$ considered significant.
Sequence data were submitted to Gene Expression Omnibus database, accession number GSE37918.

CHAPTER 3

RESULTS

3.1 MiR-23b regulates cytoskeletal dynamics, migration, invasion and metastasis in BC cells

After establishment of the primary tumour, the acquisition of aggressive traits allows cancer cells to detach from their origin site through migratory and invasive events that mark the first step of the metastatic process[30]. This generally requires the disruption of existing cell-cell contacts, the establishment of cell-matrix adhesions, the degradation or rearrangement of the ECM, and finally the movement of the tumour cell. The actin cytoskeleton constitutes the structural support to cell morphology, polarity, adhesion and migration. Primary regulators of cytoskeletal dynamics are three members of the Rho family of small GTPases, RHO, RAC and cell cycle division 42 (CDC42), that, in response to external stimuli, coordinate actin-based structures via a plethora of cytoplasmic effector proteins[404]. Nevertheless, aberrant activity of Rho small GTPases results in deregulation of cytoskeletal modulators and consequent mis-organisation of the actin cytoskeleton, leading to increased migration and invasiveness[37]. Owing to their ability in regulating gene expression post-transcriptionally, microRNAs (miRNAs) are able to affect cellular pathways relevant to cell adhesion, cytoskeletal remodelling, migration and invasion thus contributing to regulation of the metastatic process[372]. In this respect, we wished to identify interesting candidate miRNAs with potential roles in metastatic progression, with particular focus on BC. We adopted a bioinformatic approach based on an extensive literature review and use of web-based resources for the prediction of miRNA putative targets and the analysis of their biological functions. Firstly, our literature research pinpointed miR-23b as a suitable candidate to fulfill the main purposes of our project. At that time, in fact, only one published research linked miR-23b function with the regulation of metastatic phenotypes, as it was found to reduce hepatocellular carcinoma cell motility through regulation of uPA and c-MET[405]. However, the role of miR-23b in BC and its relative regulatory pathways remained largely unknown.

3.1.1 Bioinformatic analysis indicates a potential role for miR-23b in cytoskeletal remodelling and cell adhesion

To gain a preliminary understanding of the biological functions of miR-23b, we obtained a list of the 938 genes predicted as putative targets for miR-23b by TargetScan web-

based tool[272, 351]. We then analysed this gene list using DAVID online database for gene ontology (GO) annotation and pathway enrichment analysis[328, 329]. In parallel, we performed an identical analysis of a list composed by 938 randomly chosen genes used as negative control. Notably, this analysis specifically implicated mir-23b in the regulation of pathways involved, cytoskeleton organisation, cell-cell junctions and actin filament-based process (**Figure 19A**). These cellular pathways were not predicted for the same number of control genes analysed (**Figure 19B**).

A Enriched pathways for miR-23b potential targets

Term	*P* Value
Regulation of transcription	3.30E-13
Protein amino acid phosphorylation	2.70E-07
Phosphorylation	1.10E-06
Protein kinase cascade	2.50E-05
Embryonic morphogenesis	2.20E-04
Regulation of JUN kinase activity	1.80E-03
Response to hormone stimulus	3.70E-03
Cell proliferation	4.50E-03
Chromatin organization	5.80E-03
Immune system development	8.40E-03
Intracellular protein transport	1.60E-02
Protein localization	1.60E-02
Protein transport	1.90E-02
Hemopoiesis	2.20E-02
Angiogenesis	2.80E-02
Cell morphogenesis involved in differentiation	3.00E-02
Cell projection organization	3.60E-02
Cell morphogenesis	4.20E-02
Nuclear transport	4.50E-02
Actin filament-based process	4.70E-02
Negative regulation of cytoskeleton organization	5.00E-02
Regulation of programmed cell death	5.00E-02
Cell junction organization	5.80E-02
Regulation of cell migration	6.90E-02
Cell division	8.40E-02
Regulation of locomotion	8.50E-02
Cell-cell junction organization	8.80E-02

B Enriched pathways for a random group of genes

Term	*P* Value
Response to organic substance	5.70E-08
Negative regulation of nitrogen compound metabolic process	3.90E-06
Response to oxygen levels	1.20E-05
Synaptic transmission	7.90E-05
Intracellular transport	1.70E-04
Immune response	1.90E-04
Secretion	4.50E-04
Response to light stimulus	8.00E-04
Vesicle-mediated transport	8.10E-04
Dna repair	8.60E-04
Regulation of cytokine production	1.20E-03
Membrane invagination	5.30E-03
Endocytosis	5.30E-03
Striated muscle cell differentiation	5.80E-03
Regulation of binding	6.00E-03
Muscle organ development	6.90E-03
Inflammatory response	1.10E-02
Cell division	1.10E-02
Defense response	2.00E-02
Cellular ion homeostasis	2.00E-02
Glucose metabolic process	2.80E-02
Muscle system process	2.90E-02
Visual perception	3.30E-02
Sensory perception of light stimulus	3.30E-02
Calcium ion homeostasis	3.60E-02
Golgi vesicle transport	4.00E-02
Chromosome organization	4.60E-02
Generation of precursor metabolites and energy	5.90E-02
Chordate embryonic development	6.20E-02
Hemopoiesis	6.60E-02
Chromatin modification	7.90E-02
Heart development	9.50E-02

Figure 19: A bioinformatic approach reveals potential roles of miR-23b in cytoskeletal dynamics and cancer-related pathways. A-B, List of pathways (Terms) retrieved using DAVID functional annotation database for the 938 potential miR-23b gene targets predicted by TargetScan software (**A**) and 938 randomly chosen genes (**B**). Each annotated Term is associated with a specific *P* value. Significant pathways enriched of miR-23b potential targets are highlighted in green.

As miRNAs typically target multiple genes within a specific regulatory pathway[406], we considered those implicated in an interaction network as high confidence candidates for mir-23b targeting, and evaluated which putative target genes were part of specific interaction networks using Cytoscape software[407]. Cytoscape is a free program developed for the analysis, integration and visualisation of molecular and genetic interaction networks. It processes large amounts of data derived from gene expression profiling, and other functional genomics and proteomics analysis, and integrates them on the base of an interaction network retrieved for the analysed genes. Data are then visualised in a network graph where biological entities, such as genes or proteins, are represented by nodes, connected with links or edges, which define intermolecular interactions. As shown in **figure 20A** we found that 176 (18%) out of 938 putative miR-23b target genes were components of such networks. Next, we analysed this smaller gene portion using DAVID and overlapped the enriched pathways retrieved for network-interacting genes with those of the original analysis (**Figure 19A**). Accordingly, we observed that the shared pathways were those involved in cytoskeletal remodelling, cellular junctions, cell adhesion and cancer (**Figure 20B**). Moreover, a total of 60% of the putative miR-23b target genes implicated in cytoskeletal remodelling by our DAVID analysis were implicated in the interaction network identified by Cytoscape (**Figure 20C**). This cross-validated bioinformatic analysis suggested a preliminary role for miR-23b in regulating cytoskeletal dynamics.

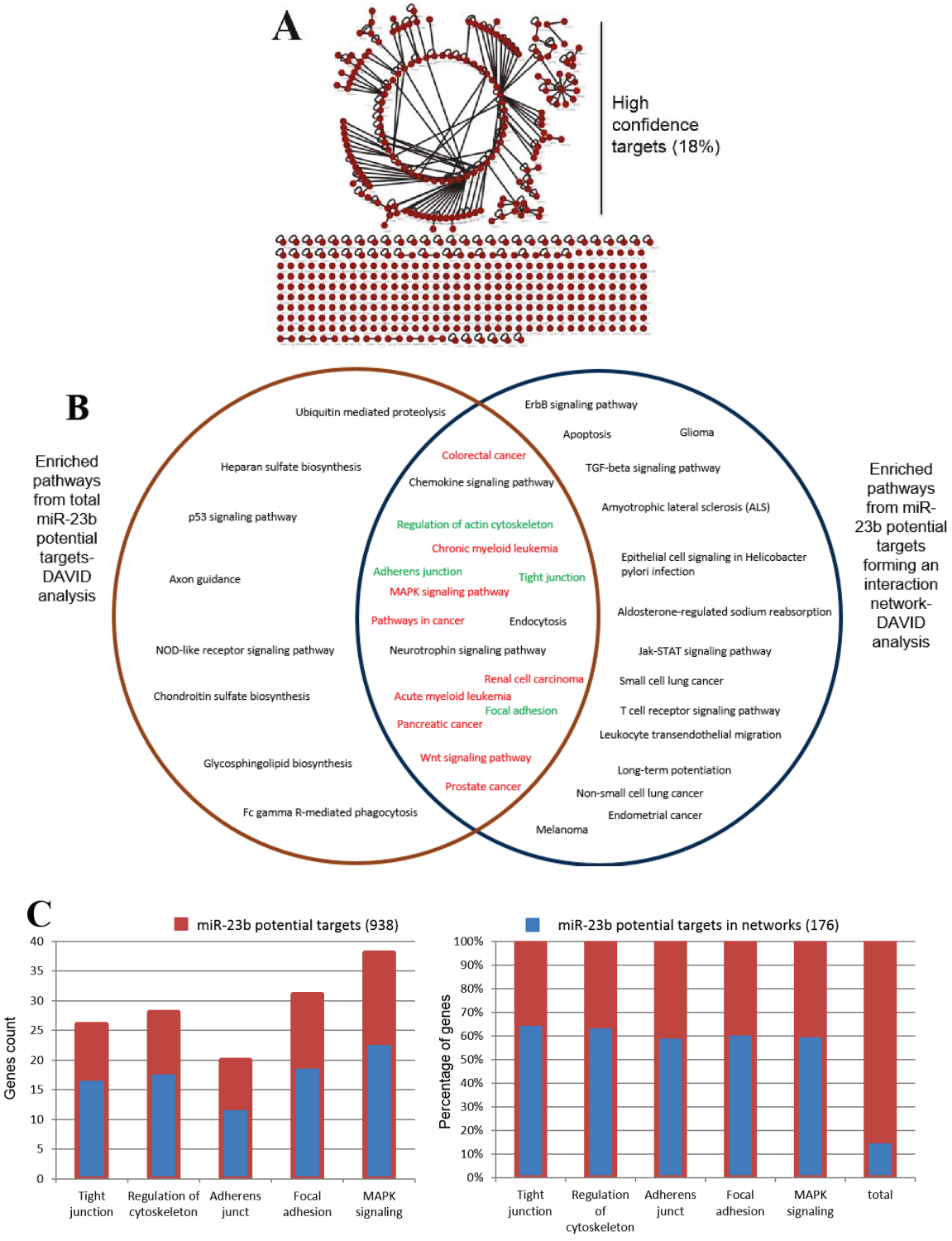

Figure 20: Bioinformatic analysis implicates a miR-23b function in cytoskeletal remodelling pathways. A, Cytoscape analysis indicates that a group (18%) of miR-23b potential gene targets (red nodes) forms interaction networks (edges) and therefore could be considered as high confidence targets. **B**, Venn diagrams show signalling pathways derived from the DAVID analysis of 938 potential miR-23b gene targets showed in fig. 20, and the same analysis on miR-23b putative targets that form an interaction network (showed in A). **C**, Gene count (left graph) and gene percentage (right graph) of both miR-23b predicted targets and miR-23b high confidence targets involved in the indicated signalling pathways.

3.1.2 *In vitro* experimental evaluation of miR-23b function in cytoskeletal remodelling pathways

3.1.2.1 Transient miR-23b overexpression enhances epithelial phenotypes of BC cells

We firstly adopted a gain-of-function approach to investigate the role of miR-23b in the regulation of cytoskeletal dynamics predicted by our bioinformatic study. We induced overexpression of miR-23b by transfecting both epithelial and mesenchymal-like BC cell lines, MCF-7 and MDA-MB-231 cells, respectively, with a synthetic miR-23b precursor (pre-miR) mimic, a negative control mimic (miR-n.c.) and miR-26a pre-miR mimic used as a further negative control (**Figure 21**). After transfection, using light microscopy visualisation, we investigated the effect of miR-23b up-regulation on in vitro 2D cultures. We observed that ectopic expression of miR-23b only increased epithelial characteristics of MCF-7 cells, demonstrated by tighter colony morphology with marked cell-cell junctions (**Figure 22A**). This effect indicated that miR-23b may regulate cell-cell adhesion pathways *in vitro*, as predicted by our bioinformatic data. Next, we found that this effect was independent from the expression levels of the cell-cell adhesion glycoprotein E-cadherin which did not change upon overexpression of the mimics (**Figure 22B**). However, we detected no changes towards an epithelial phenotype in mesenchymal-like MDA-MB-231 cells upon overexpression of the indicated pre-miRs (**Figure 22C**). This suggests that miR-23b-induced effect is unlikely to be the result of re-expression of adhesion molecules lost during the EMT process, but rather derives from a miR-23b function in enhancing existing cell-cell adhesions.

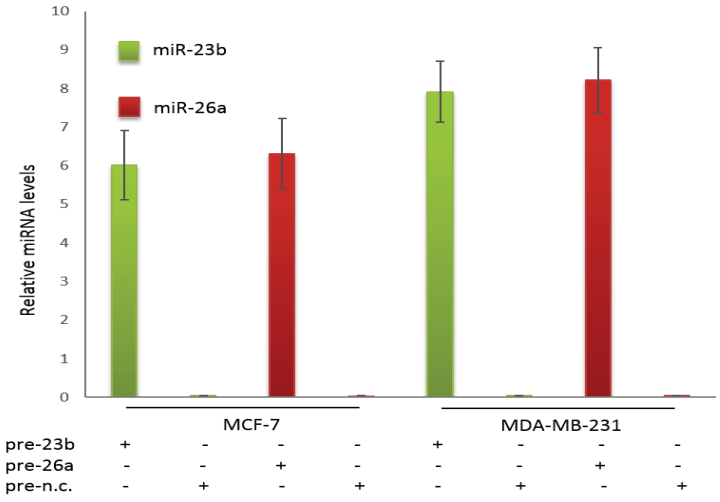

Figure 21: Overexpression of miR-23b and miR-26a in BC cells. RT-PCR assays detect mir-23b and miR-26a intracellular levels after overexpression of the indicated miRNA precursor mimics (5nM) for 48h in BC MCF-7 and MDA-MB-231 cells. MiRNAs levels were normalised to endogenous U6 snRNA levels.

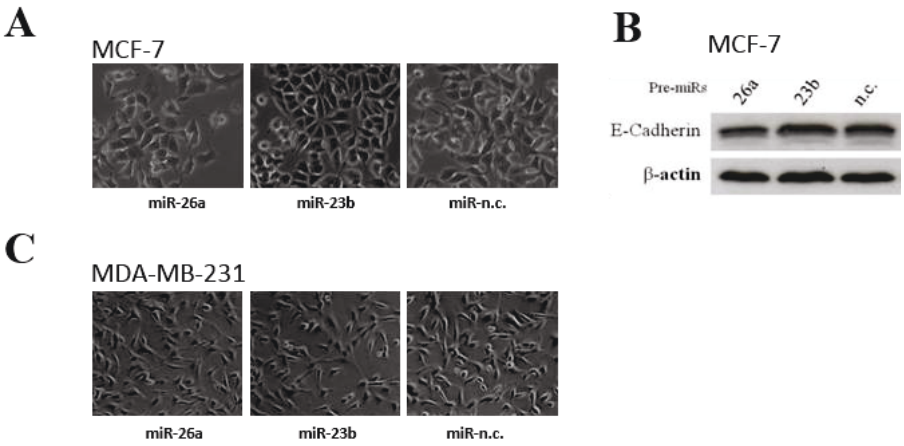

Figure 22: MiR-23b overexpression enhances epithelial phenotypes of BC cells. A, Phase-contrast images of MCF-7 cells upon transfection with miR-26a, miR-23b and miR-n.c. precursors (5nM) for 48h. **B,** Western blot showing E-cadherin and β-actin expression in MCF-7 cells transfected with miR-26a, miR-23b and miR-n.c. precursors (5nM) for 48 hours. β-actin was used as a loading control. **C,** Phase contrast images of MDA-MB-231 cells upon transfection with miR-26a, miR-23b and miR-n.c. precursors (5nM) for 48h.

3.1.2.1.1 Prolonged miR-23b overexpression in BC cells enhances cell-cell adhesion in vitro

Based on these preliminary observations, we next investigated a possible induction of the mesenchymal-to-epithelial transition (MET) by overexpressing miR-23b for a prolonged period of time (9 days). To this end we used immunofluorescence techniques to examine E-Cadherin levels and cell-cell junction formation[326]. We observed that maintained overexpression of miR-23b failed to induce MET in mesenchymal-like MDA-MB-231 cells (**Figure 23A**), but lead to a stronger epithelial phenotype in MCF-7 cell cultures, as seen upon transient miR-23b overexpression. In **figure 23B** we can appreciate that miR-23b-overexpressing MCF-7 cells formed more orderly and stable adherens junctions compare with controls, indicating that miR-23b acts by enhancing tension between existing cell-cell junctions. We then quantified this effect expressed as a linearity index, defined by the ratio of junction length to the distance between the two vertices marking each junction (**Figure 23C**). The obtained linearity index indicated that miR-23b prolonged overexpression significantly enhanced the straightness of cell-cell junctions ($P = 0.0001$, **Figure 23C**).

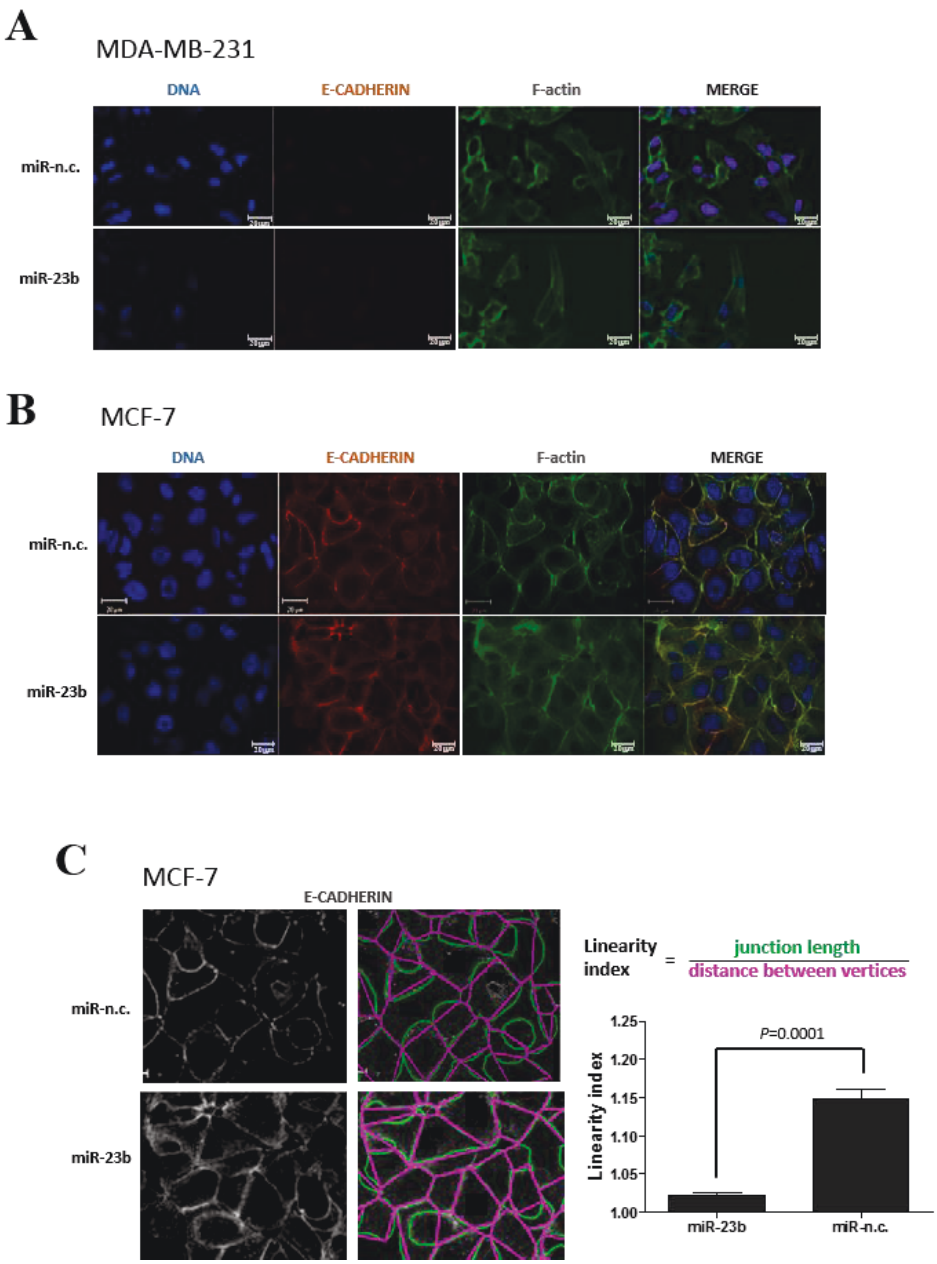

Figure 23: MiR-23b overexpression enhances cell-cell adhesion *in vitro*. A, From left to right: *TO-PRO-3* staining of DNA, immunofluorescence staining of E-cadherin (1:1000), Alexa Fluor 488 phalloidin (1:500) staining of F-actin and overlay of the three images of MDA-MB-231 cells transfected with miR-23b and miR-n.c. precursors (5nM) for 9 days. Scale bar = 20 µm. **B,** From right to left: *TO-PRO-3* staining of nuclei, immunofluorescence staining of E-cadherin (1:1000), Alexa Fluor 488 phalloidin (1:500) staining of F-actin and overlay of the three images of MCF-7 cells transfected with miR-23b and miR-n.c. precursors (5nM) for 9 days. Scale bar = 20 µm. **C,** Quantification of junction linearity. Junction length (green) and distance between vertices (pink) were measured and a linearity index was calculated by dividing the two measures (right). This index decreases in miR-23b-overexpressing MCF-7 cells. Scale bar = 20 µm. 150-250 junctions per condition in two independent experiments were counted. Data are mean ± s.e.m. (P = 0.0001, Student‟s t test).

3.1.2.3 Both miR-23b and miR-26a regulate BC cells adhesion on ECM

As our bioinformatics analysis implicated a potential regulation by miR-23b on cell adhesion and focal adhesion formation, we assessed the ability of MDA-MB-231 cells to adhere on the ECM upon miRNA overexpression. Firstly, we stained MDA-MB-231 cells for the focal adhesion (FA) marker Vinculin[408] upon transient transfection with the indicated pre-miRs and cell seeding on collagen I films. Interestingly, FAs resulted significantly enlarged in cells overexpressing miR-23b or miR-26a precursors comparing with miR-n.c.-transfected cells ($P = 0.04$, **Figure 24A**).

Secondly, we assessed the effects of these miRNAs on cell spreading capacity, by seeding MDA-MB-231 cells transiently transfected with the indicated pre-miRs on collagen I matrices for 30, 60 and 120 minutes (**Figure 24B**). MiR-23b and miR-26a-overexpressing cells spread more than controls, and after 30 minutes contained lamellar protrusions, stress fibre-like actin bundles and punctate peripheral FAs, whilst the controls remained rounded with no appearance of FAs or F-actin bundles (**Figure 24B**). Whereas this effect appeared transient upon miR-23b overexpression, it was reproducibly most pronounced in miR-26a over-expressing MDA-MB-231 cells, which after 120 minutes on Collagen I matrix, exhibited a remarkable expanded morphology with reinforced Vinculin-stained focal adhesion sites throughout the cell body and at the periphery of lamellipodia (**Figure 24B**, bottom panels).

Furthermore, the increase of intracellular miR-26a levels significantly promote ability of MDA-MB-231 cells to adhere on Collagen I matrices compared to miR-23b and miR-n.c. ($P = 0.01$, **Figure 24C**).

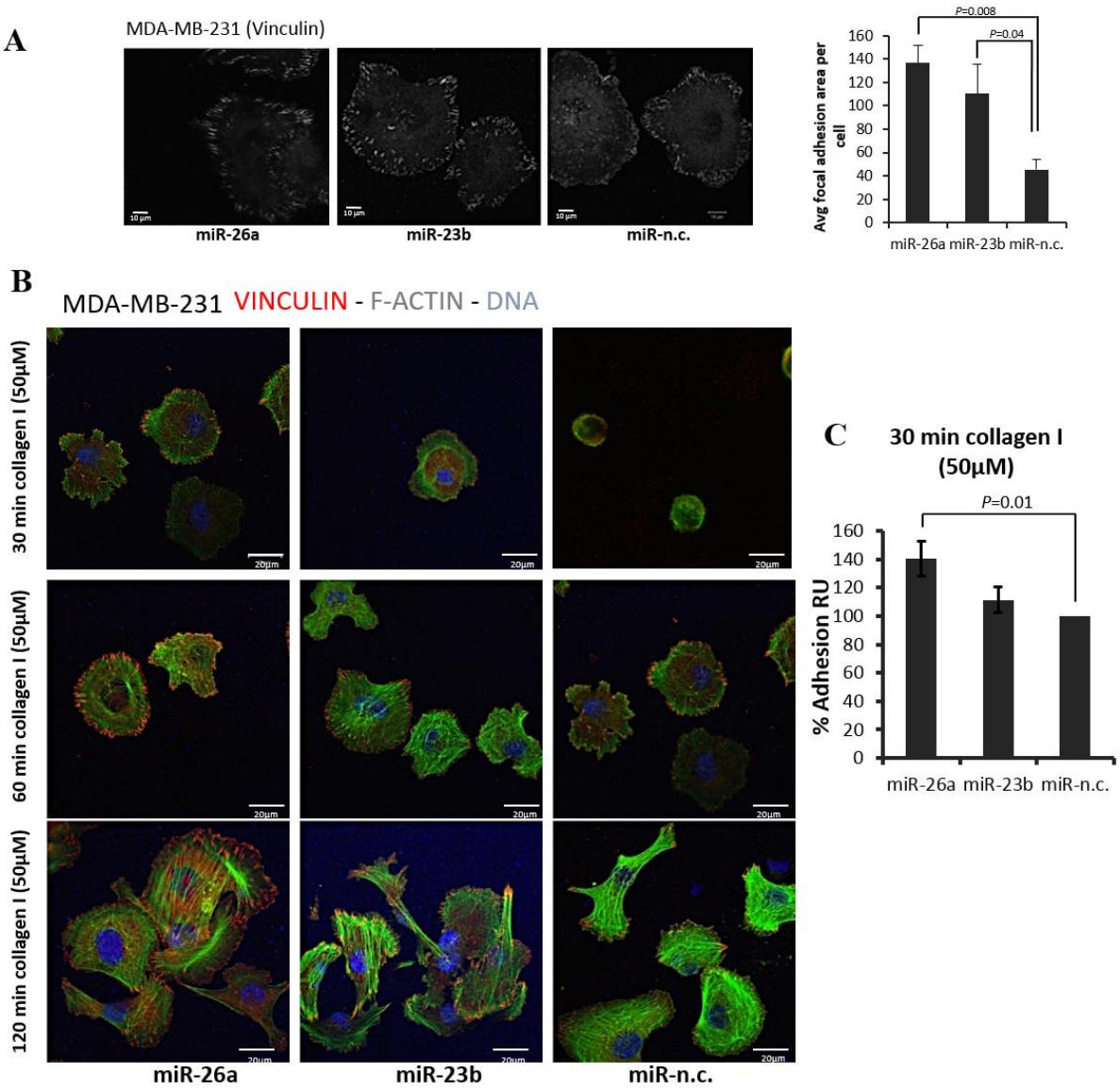

Figure 24: MiR-23b and miR-26a affects cell adhesion on ECM. A, Immunofluorescence staining of MDA-MB-231 cells using Vinculin antibody (1:400); images were false coloured in a black-and-white fashion to highlight focal adhesions (FAs). After transfection with miR-26a, miR-23b and miR-n.c. precursors (5nM) for 48 hours the cells were left to adhere on coverslips coated with 50uM of collagen I for 1 hour before staining. Scale bar = 10 µm. The graph on the right shows the FA size per treated cell. Quantification of FA size is represented as the average of FA area per cell. Data are shown as mean values ± standard error of the mean (s.e.m.) from three independent experiments (P = 0.04, Student‟s t test).**B,** For spreading assays, MDA-MB-231 cells were transfected with the indicated precursors (5nM) for 48h and seeded on collagen I (50µM) matrices for 30, 60 and 120 minutes. Cells were than fixed and stained for anti-Vinculin and phalloidin to visualise FAs and F-actin, respectively. Nuclei are visualised with TO-PRO-3 stain (blue); scale bar = 20 µm. **C,** For adhesion assays, MDA-MB-231 were transfected with the indicated precursors (5nM) and seeded on 50µM of collagen I and cell adhesion was quantified by dye retention 30 min after plating. Data are mean of three independent experiments ± s.e.m. (P = 0.01, Student‟s t-test).

3.1.2.4 The miR-23b overexpression affects formation of lamellipodia protrusion

During our transfection assays with miRNA precursors, a detailed observation of BC cell morphology revealed that miR-23b-induced overexpression was affecting the formation of lamellipodia in MDA-MB-231 cells cultured under normal cell growth conditions, and at most these formed only small, narrow protrusions (**Figure 25A**). We quantified this effect by counting the number of formed lamellipodia, the result of which was significantly diminished in miR-23b-transfected MDA-MB-231 cells (P = 0.0003, **Figure 25A**, box plot). In **figure 25B**, we can appreciate the ability of miR-23b in impairing lamellipodia formation in MDA-MB-231 cells stained for F-actin.

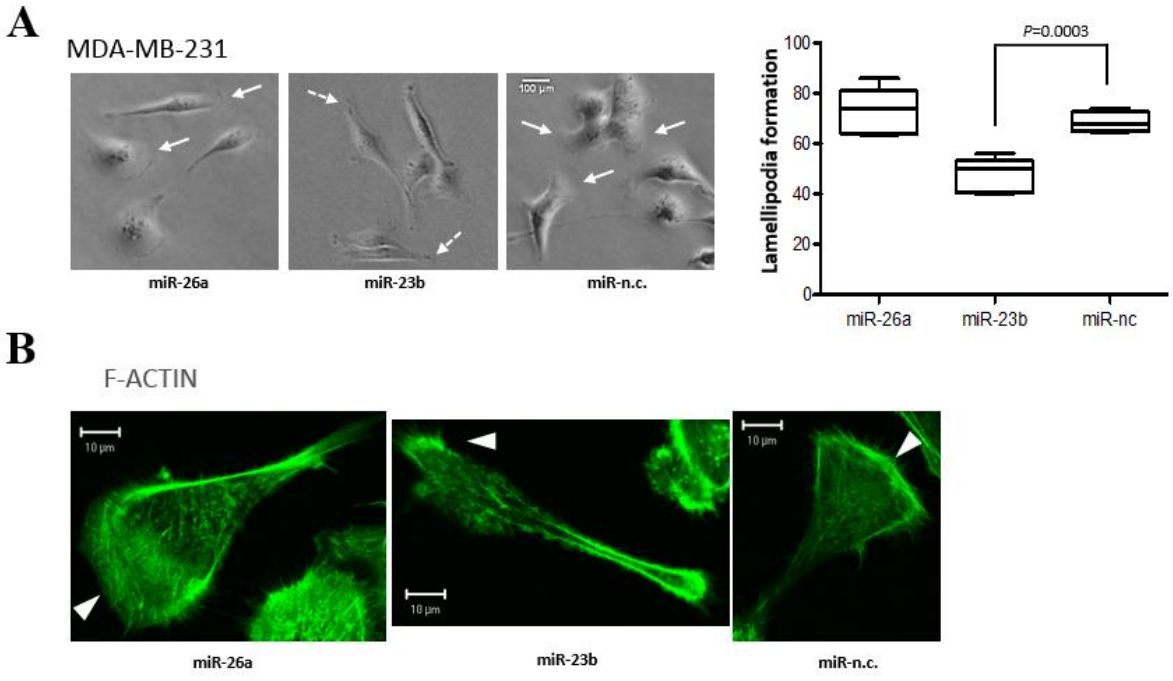

Figure 25: MiR-23b overexpression impairs lamellipodia formation. A, Phase-contrast images of MDA-MB-231 cells transfected with the indicated miRNA precursors (5nM) for 48h. Lamellipodial structures are indicated by continuous arrows; lack of lamellipodia is indicated by discontinuous arrows. Scale bar = 100µm. The box plot on the right indicates quantification of the number of lamellipodia formed after treating the cells with the indicated precursors. 50–150 cells per condition in three independent experiments were counted. Data are mean ± s.e.m. (P = 0.0003, Student‟s t test). **B,** Immunofluorescence images shows lamellipodia in MDA-MB-231 cells transfected with the indicated precursors (5nM) for 48h and stained for F-actin with Alexa Fluor 488 phalloidin.

3.1.3 Loss-of-function strategy: experimental repression of miRNA function

In order to confirm that the observed effects mediated by miRNAs were results of their intrinsic intracellular function and not of eventual indirect effect mechanisms induced by ectopic expression of synthetic molecules, we wished to investigate whether the inhibition of miR-23b was able to reverse these effects. Therefore, we adopted a loss-of-function approach based on the use of miRNA-sponge vectors, in-house made plasmid constructs that, when expressed in cellular systems, encode for transcripts containing multiple, tandem miRNA-binding sites in their 3'UTR; these sequester intracellular mature miRNA from interaction with its target mRNAs thus inhibiting miRNA activity[325]. We constructed sponge oligonucleotides carrying 6 tandem, bulged binding sites specific for miR-23b or miR-26a (**Figure 26A** and **B,** respectively), and cloned either of them into the 3'UTR of the pEGFP-C1 plasmid vector, which encodes for an enhanced form of green fluorescent protein (EGFP). We verified the functionality of our miRNA-sponge constructs by using a miRNA-sensor vector that expresses a luciferase reporter gene, carrying a sequence of 6 tandem miR-23b or miR-26a-specific binding sites in its 3'UTR (see 2.2.3) (**Figure 27A** and **B,** respectively). As expected, co-expression of the sponge vector and the relative sensor vector increases luciferase activity compared to empty vector control, thus confirming the ability of our sponge constructs in inhibiting intrinsic activity of miR-23b and miR-26a (**Figure 28A** and **B**, respectively). We then used these constructs to establish MDA-MB-231 cell lines, that stably express either of the two miRNA-sponge vectors (we called them Sp-23b-MDA and Sp-26a-MDA), or the relative parental plasmid control cells (we called them pEGFP-C1). We observed that miR-23b and miR-26a endogenous levels were reduced in different single clone-derived MDA-MB-231 cells stably expressing the miR-23b- and miR-26a-sponge vector, respectively, compared to the parental control cells (**Figure 28C** and **D**). In particular, among the different clonal Sp-23b-MDA and Sp-26a-MDA cells, the clone number 10 and the clone number 3 show the highest reduction efficiency, decreasing the levels of miR-23b and miR-26a by up to 70% and 50%, respectively (**Figure 28C** and **D**, respectively).

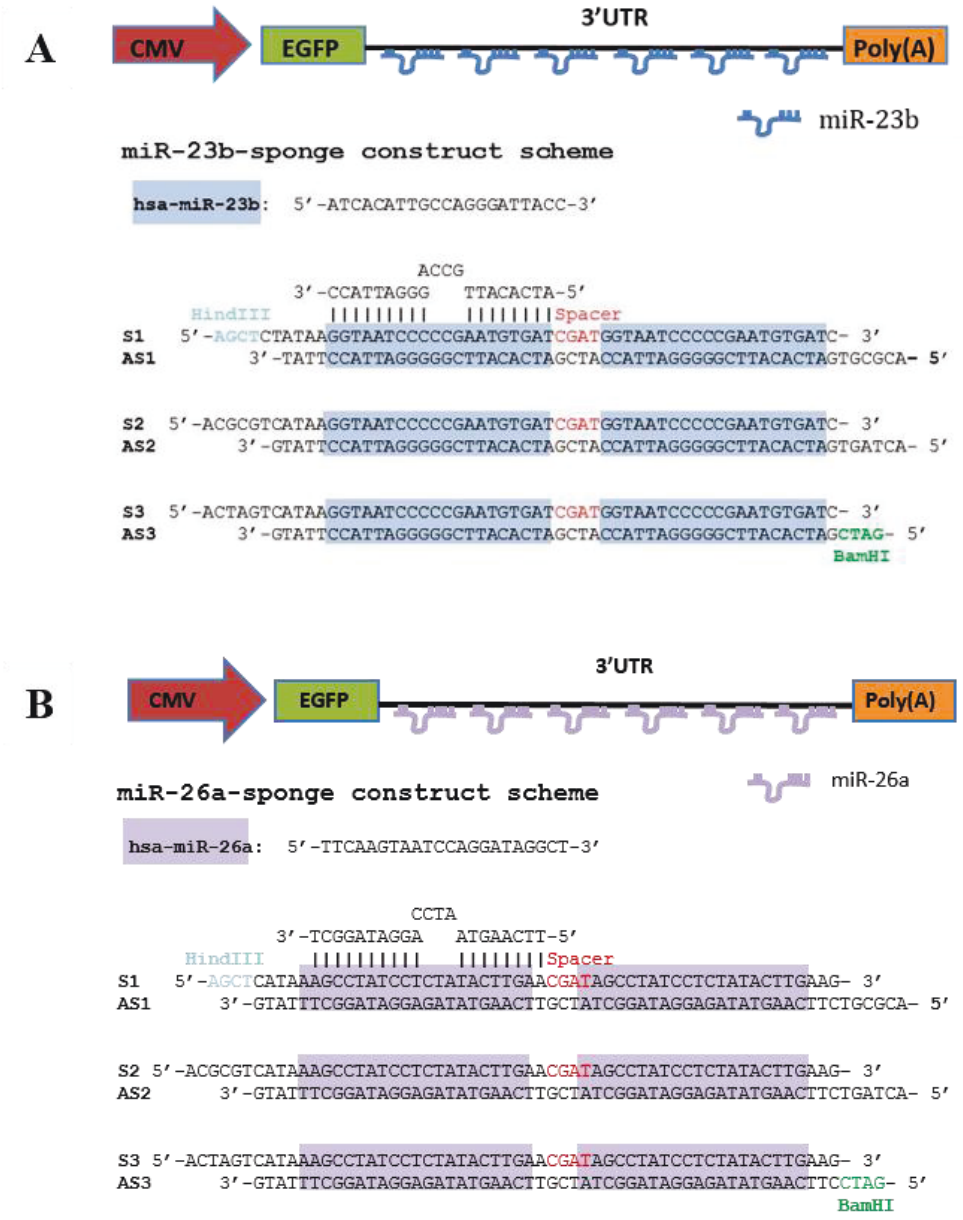

Figure 26. MiRNA-sponge construct vectors for miR-23b and miR-26a. A-B, Schematic representation of miR-23b-sponge (**A**) and miR-26a-sponge (**B**) oligonucleotides, containing 6 adjacent binding sites for the relevant human miRNA, cloned in the MCS (between the HindIII and the BamHI restriction sites) of the pEGFP-C1 plasmid vector as 3'ŮTR of the EGFP gene. The spacer is a 4nt sequence that separates the miRNA binding sites.

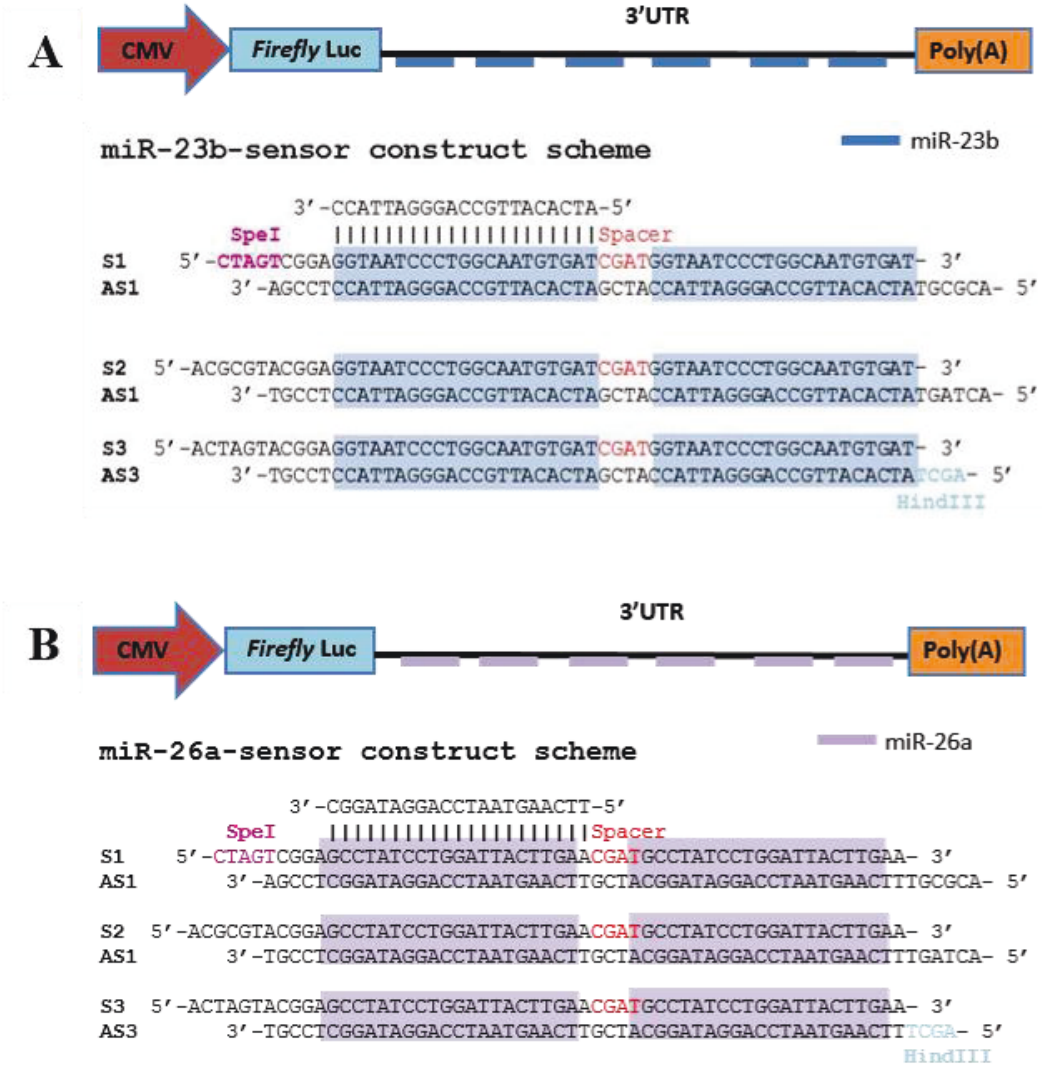

Figure 27. MiRNA-sensor construct vectors for miR-23b and miR-26a. A-B, Schematic representation of miR-23b-sensor (**A**) and miR-26a-sensor (**B**) oligonucleotides, containing 6 adjacent binding sites for the relevant human miRNA, cloned in the MCS (between the SpeI and the HindIII restriction sites) of the pMIR-REPORT plasmid vector as 3'UTR of the *Firefly* luciferase gene. The spacer is a 4nt sequence that separates the miRNA binding sites.

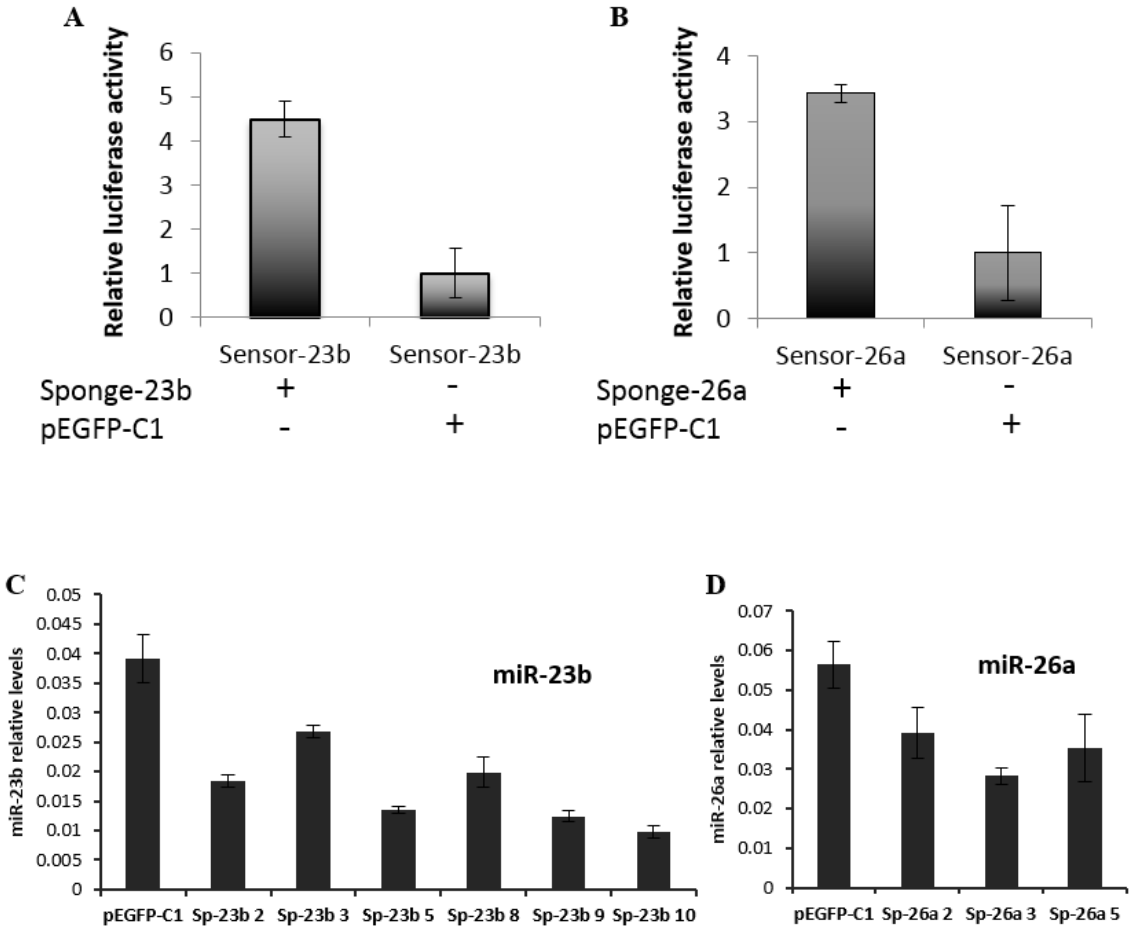

Figure 28: MiRNA-sponges reduce endogenous miRNA levels and activity *in vitro*. A-B, Relative luciferase activity levels were measured after 48h from transfection of HCT116 cells with the miR-23b-sensor (**A**) or the miR-26a-sensor construct (**B**) and the indicated plasmids (100ng). Data are mean of triplicate samples in three independent experiments ± s.e.m. **C-D,** RT-qPCR analysis quantifies endogenous levels of miR-23b (**C**) and miR-26a (**D**) expressed in different MDA-MB-231 cell clones stably expressing the correspondent miRNA-sponge vector or the parental control (MDA-MB-231 cells stably expressing pEGFP-C1 plasmid) and normalised to U6 snRNA levels. Data are mean of triplicate samples in three independent experiments ± s.e.m.

3.1.4 MiR-26a but not miR-23b regulates cell proliferation and apoptosis of BC cells

We next evaluated the ability of miR-23b and miR-26a in regulating phenotypes relevant for tumour proliferation and survival. Therefore, we performed cell growth and apoptosis assays upon ectopic overexpression of these miRNA precursor mimics in BC cells (**Figure 29**). We found that expression of miR-23b does not affect proliferation rates of cultured MDA-MB-231 and/or MCF-7 cells (**Figure 29A** and **B**) or promote apoptosis of MDA-MB-231 cells (**Figure 29C**), whereas augmented miR-26a levels slightly reduce MCF-7 cell proliferation (**Figure 29B**) and induce apoptosis in MDA-MB-231 cells (**Figure 29**C).

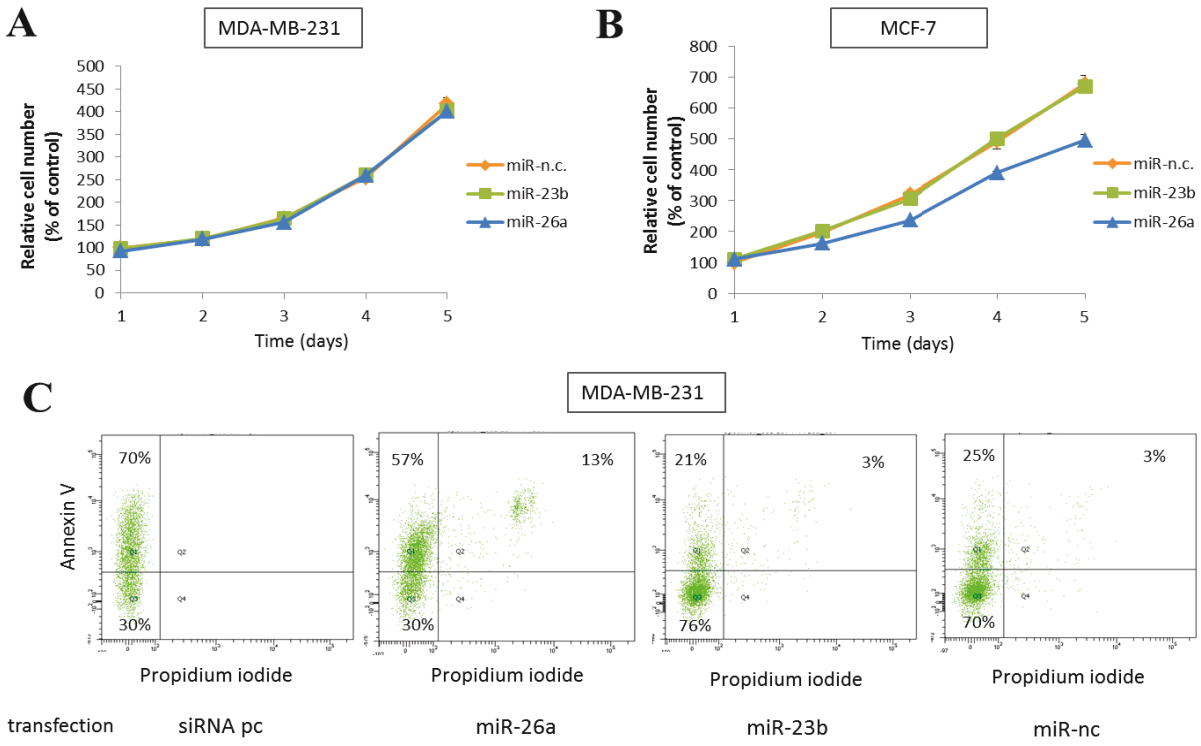

Figure 29: MiR-26a, but not miR-23b overexpression affects BC cell proliferation and apoptosis. A-B, Growth curves of MDA-MB-231 (**A**) and MCF-7 (**B**) cells transfected with miR-26a, miR-23b and miR-n.c. pre-miRs were determined performing SRB assays for the indicated time, 48 h after transfection (time day: 1). Relative cell numbers are presented as percent over controls (miR-n.c.) Data are calculated as means of two experiments performed in quintuplicates ± s.e.m. **C**, Dot plot profiles for propidium iodide (*x* axis) and annexin V (*y* axis) staining show apoptotic rate of each pre-miR-expressing MDA-MB-231 cells compared to cells transfected with 20nM of cell death control siRNAs. The percentage of positive cells in the individual quadrants is shown (*lower left panel*, viable cells, *upper left*, mid-stage to late apoptosis; *upper right*, late-stage apoptosis, *lower right*, necrotic cells).

We examined the proliferation rates of different clonal MDA-MB-231 cells stably expressing miR-23b- or miR-26a-sponge constructs, in order to investigate the effect of prolonged miRNA inhibition on tumour cell proliferation *in vitro*. As showed in the graph of **figure 30**, silencing of either miR-23b or miR-26a did not affect the proliferative phenotype of MDA-MB-231 cells, compared to parental controls, a finding that is consistent with the invariable proliferation rates of these cells observed upon overexpression of the two miRNAs (**Figure 29A**).

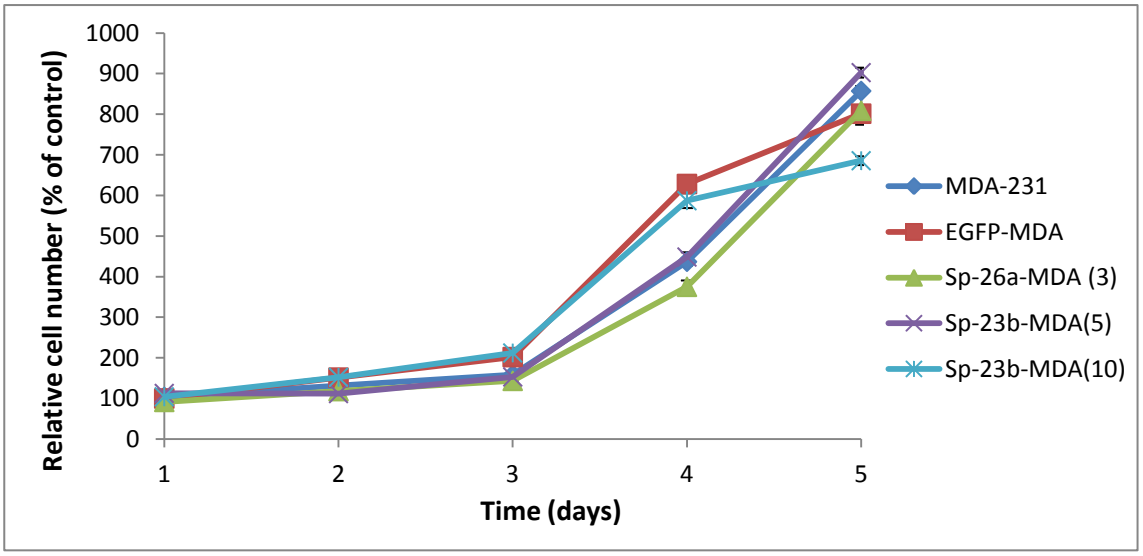

Figure 30: MiR-23b or miR-26a inhibition does not affect BC cell proliferation. Growth curves of MDA-MB-231 sponge clones and empty vector controls determined performing SRB assays for the indicated time. Relative cell numbers are presented as percent over controls (EGFP-MDA). Data are calculated as means of two independent experiments performed in quintuplicates ± s.e.m.

3.1.5 *In vitro* investigation of miR-23b function in BC cell motility and invasion

3.1.5.1 MiR-23b overexpression reduces BC cell motility

Cytoskeletal remodelling, cell adhesion and extension of membrane protrusions are crucial for the processes of cell migration and invasion[325]. As we observed alterations of these phenotypes upon overexpression of the two examined miRNAs, we hypothesised that miR-23b and miR-26a may be implicated in the regulation of motile and invasive phenotypes. To assess this, we performed Transwell migration assay and cell tracking analysis that investigated *in vitro* chemotaxis-driven cell motility and non-directional cell migration, respectively. In these assays we utilised a precursor mimic of miR-31, a miRNA previously found to strongly inhibit MDA-MB-231 cell motility and metastasis[376] as positive control. Transient overexpression of miR-23b markedly reduced chemotaxis of the highly motile MDA-MB-231 cells ($P = 0.004$) compared to miR-26a and miR-n.c, to the same extent of reduction showed by miR-31-overexpressing positive controls ($P = 0.001$, **Figure 31A**). Accordingly, miR-23b and miR-31, but not miR-26a, reduced cell migratory speed ($P < 0.0001$, **Figure 31B**) and shortened migration trajectory lines (**Figure 31C** and **D**) in migratory cell tracking assays.

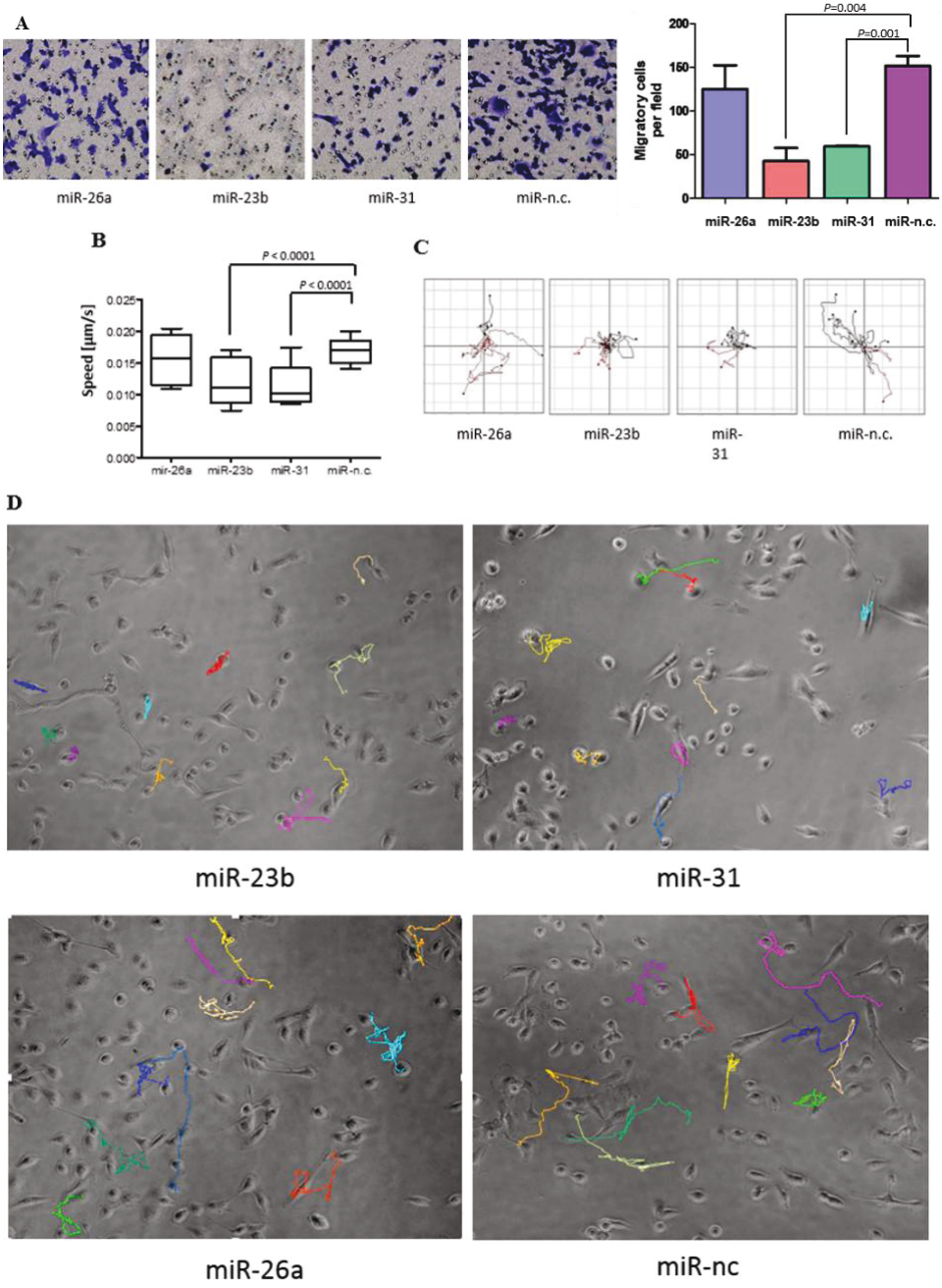

Figure 31: MiR-23b overexpression reduces BC cell motility. A, Transwell migration assays were performed for 9h after transfecting MDA-MB-231 cells with the indicated precursors (5nM) for 48h. The graph on the right indicates cell migration expressed as a percentage of the average of migratory cells per field (n=5 fields per transfection). Data are mean of three experiments ± s.e.m. performed in triplicates (P = 0.004, P = 0.001, Student‟s *t*-test). **B**, Motility of MDA-MB-231 cells expressing the indicated precursors was examined for 24h by phase-contrast, time-lapse microscopy. Cell speed of 50-100 cells per condition was quantified and speed averages are presented as mean of three experiments ± s.e.m. (P = 0.0001, Student‟s *t*-test). **C,** Plots show overlays of representative trajectories described by pre-miR-expressing MDA-MB-231 cells during time-lapse motility assays. **D,** Representative stills from time-lapse cell tracking assays showing single-cell trajectories of cultured MDA-MB-231 cells transfected for 48h with the indicated precursors.

3.1.5.2 MiR-23b loss-of-function promotes BC cell motility

To assess the effect of miR-23b inhibition on cell migration, we used MDA-MB-231 cells, stably expressing the miR23b- or miR-26a-sponge constructs (clones 10 and 3, respectively) or the parental vector to perform Transwell migration assays. In contrast to cells overexpressing miR-23b (**Figure 31**), miR-23b silencing in MDA-MB-231 cells significantly increased motility compared to cells that stably silenced miR-26a or expressed the pEGFP-C1 control ($P < 0.0001$, **Figure 32A**). Notably, the number of lamellipodia significantly increased in cells stably expressing sponge vector able to inhibit miR-23b levels ($P < 0.0001$, **Figure 32B**), which was consistent with the effect of miR-23b overexpression on lamellipodia formation (**Figure 25**).

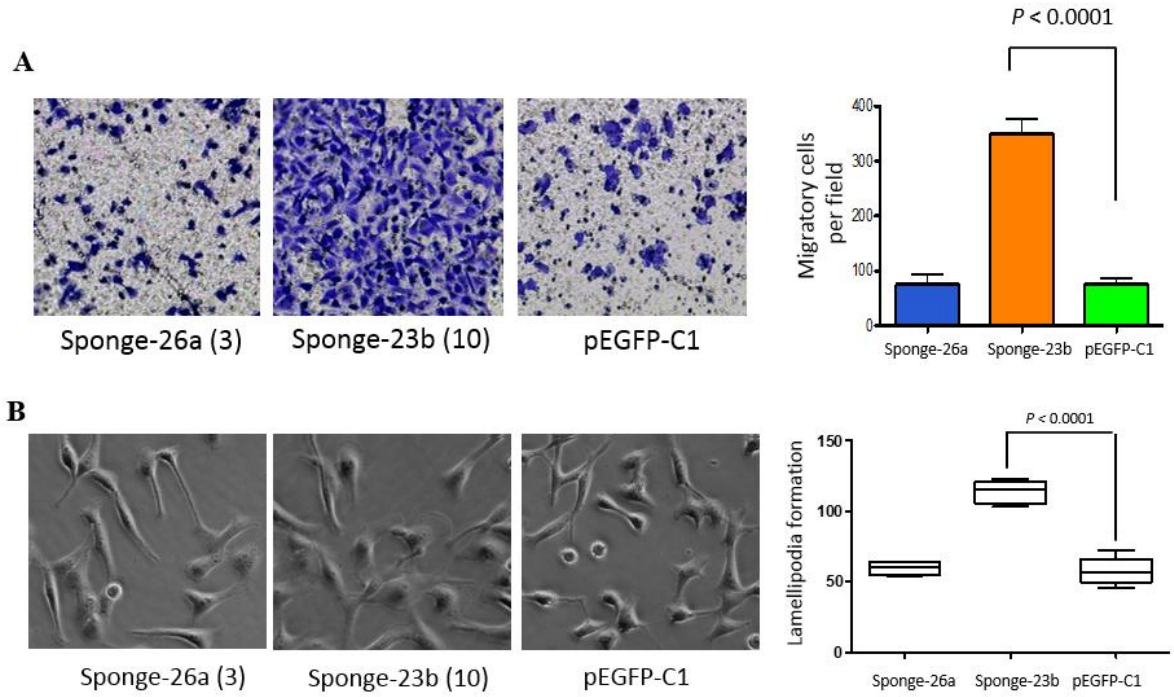

Figure 32: MiR-23b inhibition promotes BC cell migration and lamellipodia formation. A, Transwell migration assays of MDA-MB-231 cells stably expressing the indicated construct vectors were performed for 9h. The graph on the right indicates cell migration expressed as a percentage of the average of migratory cells per field (n=5 fields per transfection). Data are mean of three experiments ± s.e.m. performed in triplicates ($P < 0.0001$ Student‟s *t*-test). **B**, MDA-MB-231 cells stably expressing the indicated constructs grown in 2D cultures were imaged by phase-contrast microscopy to show lamellipodia structures. 50–150 cells per condition in three independent experiments were counted. Data are mean ± s.e.m. ($P < 0.0001$, Student‟s *t* test).

3.1.5.3 MiR-23b regulates BC cell invasion *in vitro*

Next, we wished to evaluate the role of miR-23b in the regulation of invasive phenotypes. Therefore, we tested MDA-MB-231 cell migration in 3D- collagen I matrices upon experimental induction or inhibition of miR-23b expression. Overexpression of miR-23b significantly reduces cell invasion of MDA-MB-231 cells (P = 0.001, **Figure 33A**), whilst silencing of miR-23b sponge construct activity markedly elicits invasive capabilities of MDA-MB-231 cells (P = 0.04, **Figure 33B**).

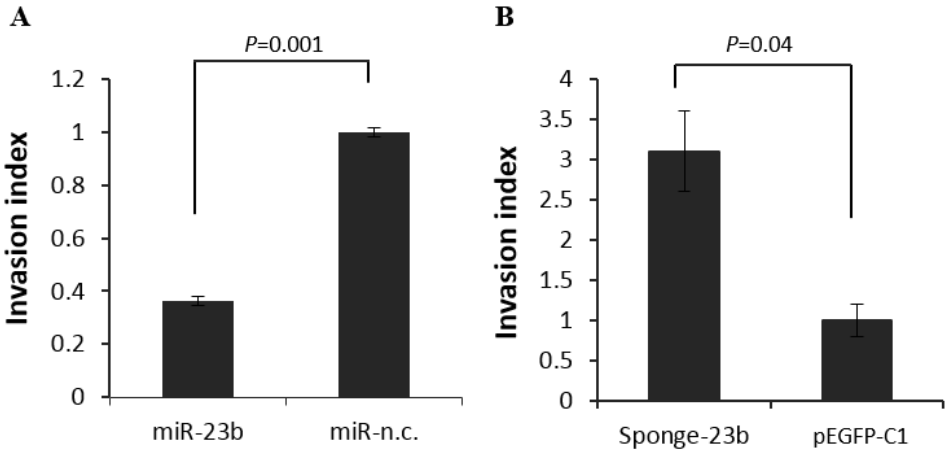

Figure 33: MiR-23b regulates BC cell invasion *in vitro*. A, Invasion of MDA-MB-231 cells transfected with miR-23b and miR-n.c. precursors (5nM) for 48h was assessed in 3D-collagen-I matrices (2.3mg/ml) for 16h. Confocal *z* sections were collected from each well at 0µm (bottom of the well) and 40µm and invasion indexes were calculated as the number of cells at 40µm divided by those at 0µm. Invasion indexes are mean of three experiments ± s.e.m. performed in quintuplicates (P = 0.001 Student‟s *t*-test). **B,** Invasion assays using MDA-MB-231 cells stably expressing the miR-23b-sponge construct or the parental control pEGFP-C1 plasmid vector were performed as in **A**. Invasion indexes are mean of three experiments ± s.e.m. performed in quintuplicates (P = 0.04, Student‟s *t*-test).

3.1.6 Identification and validation of miRNA gene targets

3.1.6.1 MiR-23b and miR-26a target PAK2 kinase and leads to induction of MLC II phosphorylation

Thus far our results implicated both miR-23b and miR-26a in regulation of cytoskeletal dynamics, and we chose the PAK2 kinase as a candidate target since both miRNAs were identified by Targetscan as potential *PAK2* regulators in highly conserved sites of its 3′UTR (**Figure 34A** and **B**). Furthermore, PAK2 is interesting in this context as its

knockdown by small RNA interference (siRNA) in T47D BC cell lines reduces cell motility and invasion, increases the size of FAs, and promotes phosphorylation of the myosin light chain II (MLC II)[129]. We first demonstrated that PAK2 silencing is also able to reduce motility and increase MLC II phosphorylation in MDA-MB-231 cells (P = 0.003, **Figure 34C** and **D**).

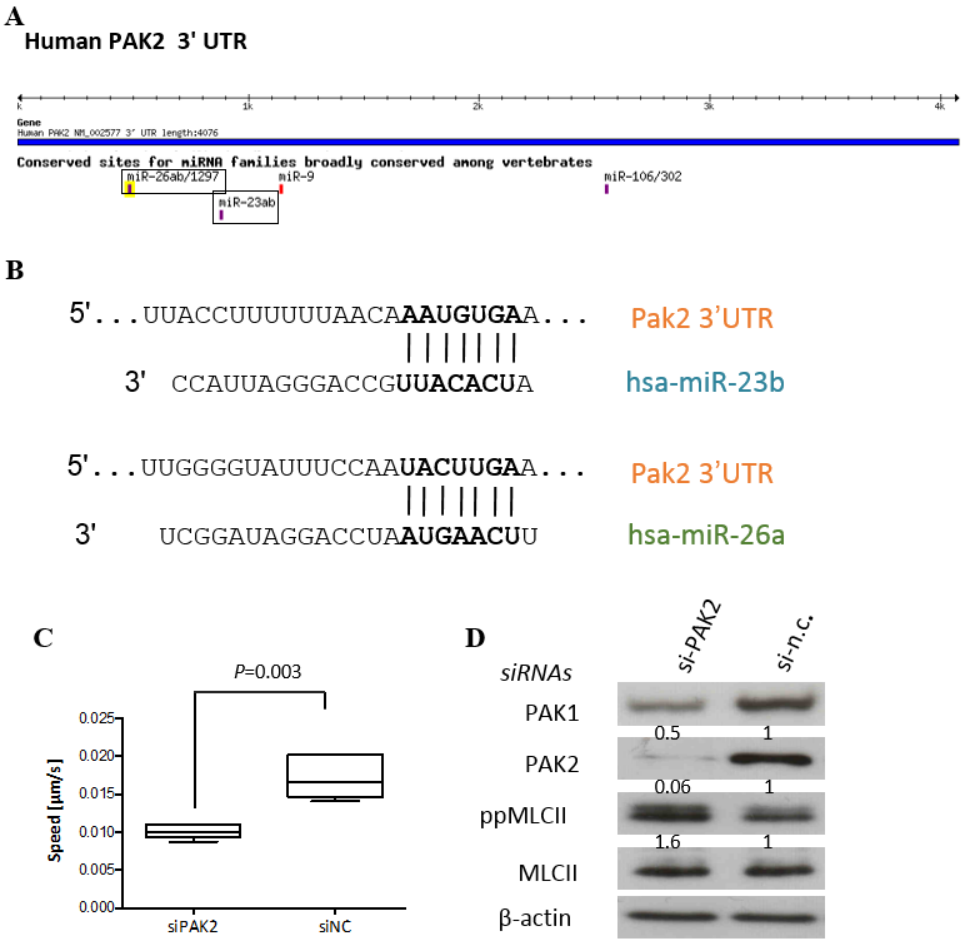

Figure 34: PAK2, a predicted target for miR-23b and miR-26a, regulates cell motility and MLC II phosphorylation in BC cells. A, Representation of human PAK2 3′UTR presenting conserved sites for the indicated putative miRNA families; miR-23b and miR-26a families are highlighted by a rectangular box (adapted from TargetScan). **B,** Predicted duplex formation between human PAK2 3′UTR and hsa-miR-23b (top) or hsa-miR-26a (bottom). **C,** MDA-MB-231 cells were transfected with the indicated siRNAs (5nM) for 48h and then cell migration was examined by phase-contrast, time-lapse microscopy for 24h. Cell speed of 50 cells per condition was quantified and is presented as mean of the averages of three experiments ± s.e.m. (P = 0.003, Student's t-test). **D,** Western blots show PAK1, PAK2, (Thr18/Ser19)-ppMLC II and MLC II levels in MDA-MB-231 cells after transfection with the indicated siRNAs (5nM). β-actin was used as a loading control. Fold changes in protein expression levels normalised for β-actin using ImageJ software are shown underneath each relative protein plot.

Mammals express six isoforms of PAK (1–6), subdivided into two groups: Group I consists of PAK1, PAK2, and PAK3 and Group II includes PAK4, PAK5 and PAK6[126]. Only group I members are directly activated by CDC42 or RAC[125]. We then measured group I PAKs upon miRNA overexpression in three epithelial cancer cell lines (**Figure 35A**). We could not detect PAK3 expression in any of the three cell lines by either western blotting or RT-qPCR, a finding consistent with the known restricted tissue expression pattern for this enzyme [409]. However, we showed that miR-23b and miR-26a specifically reduced PAK2 levels in all of the cell lines tested (**Figure 35A**). Expression levels of PAK1, although not predicted to be a target of miR-23b or miR-26a (**Figure 35B**), is slightly reduced probably due to a concurrent decrease in PAK2 (**Figure 35A**), as PAK1 levels are seen to decline upon PAK2 silencing (**Figure 34D**). Consequently, the phosphorylation of the cytoskeletal remodelling regulator MLC II, an indicator of active contractility, was up-regulated by both miRNAs (**Figure 35C**).

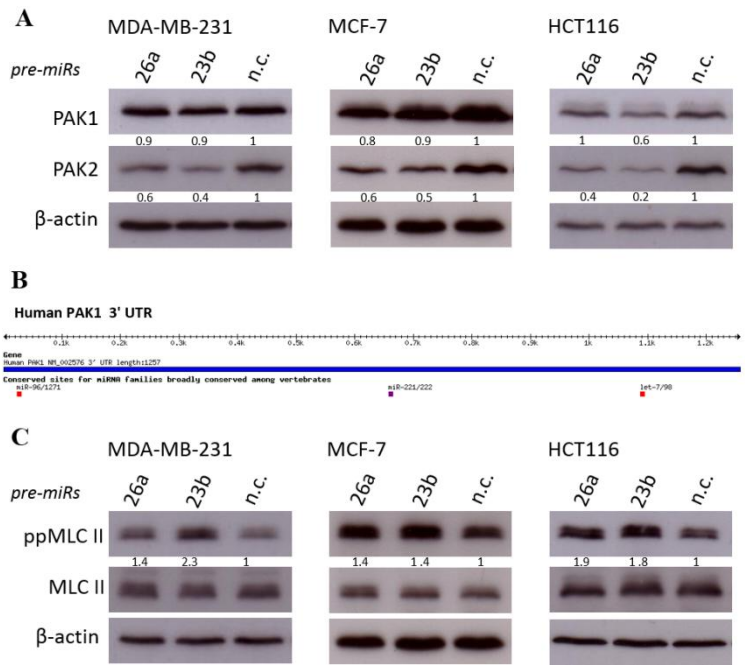

Figure 35: Overexpression of mir-23b and miR-26a results in PAK2 repression and increase of MLC II phosphorylation. A, Western blots showing PAK1 and PAK2 levels after transfection for 48h of the indicated miRNA precursors (5nM) in BC MDA-MB-231 and MCF-7 cells and colon cancer HCT116 cells. **B,** Representation of human PAK1 3'UTR presenting conserved sites for the indicated putative miRNA families (adapted from TargetScan). **C,** Western blots showing MLC II levels and phosphorylation of MLC II at Thr18/Ser19 position, after transfection for 48h of miR-23b and miR-n.c. precursors (5nM) in the same cancer cell lines described in **A**. Fold changes in protein expression levels normalised for β-actin using ImageJ software are shown underneath each relative protein plot.

3.1.6.2 Inhibition of miR-23b and miR-26a releases PAK2 expression from miRNA-mediated silencing

In order to exclude eventual off-target effects on the repression of PAK2 expression upon miR-23b and miR-26a overexpression, we wished to confirm that PAK2 is a physiological target of both these miRNAs under loss-of-function conditions. Therefore, we transiently transfected miR-26a- and miR-23b-sponge constructs in MCF-7 cells, and confirmed that inhibition of both miRNAs was able to release PAK2 expression by miR-23b and miR-26a-mediated silencing (**Figure 36A**). Furthermore, we measured PAK2 levels in different clones of MDA-MB-231 cells stably expressing miRNA-sponge constructs; we found that where maximal miRNA silencing was achieved by an efficient miRNA-sponge activity (clone 10 and 3 for miR-23b and miR-26a, respectively, **Figure 28C and D**), PAK2 expression levels increased compared to parental control cells (**Figure 36B**).

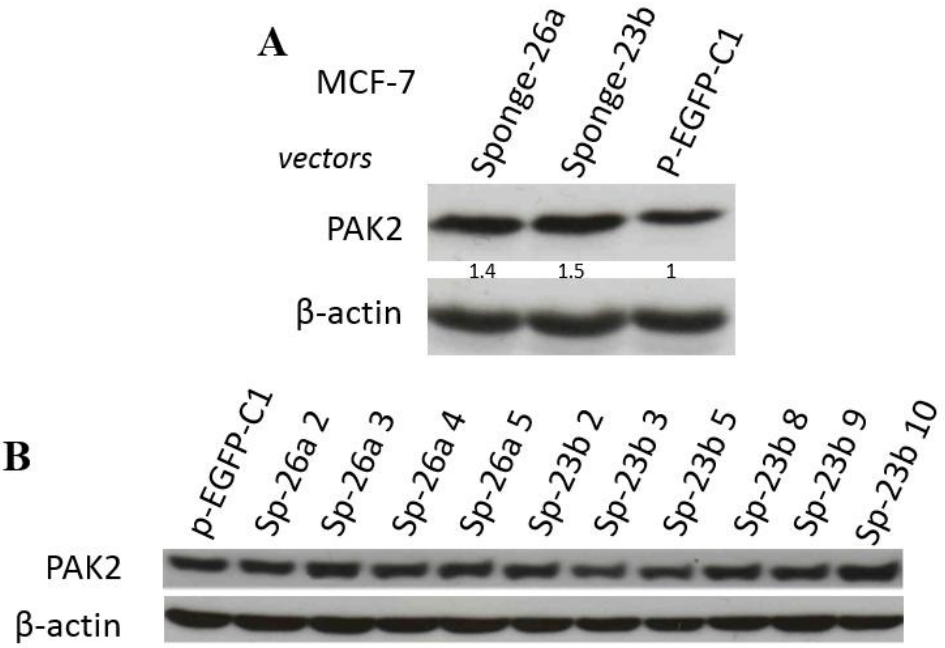

Figure 36: Inhibition of mir-23b and miR-26a releases PAK2 expression from miRNA-mediated silencing. A, Western blots showing PAK2 levels after transient transfection for 48h of MCF-7 cells with the indicated miRNA-sponge constructs or the pEGFP-C1 parental control (2μg). β-actin was used as a loading control. Fold changes in protein expression levels normalised for β-actin using ImageJ software are shown underneath each relative protein plot. **B,** Western blot showing PAK2 expression levels in different clonal MDA-MB-231 cells stably expressing the indicated plasmid constructs. β-actin was used as a loading control.

3.1.6.3 PAK2 is a direct target of miR-23b and miR-26a

Next, we wished to confirm that miR-23b and miR-26a repress *PAK2* translation by direct interaction with their relative miRNA-binding sites contained in *PAK2* 3'UTR and predicted by TargetScan (**Figure 34A** and **B**). For this purpose, we cloned *PAK2* 3'UTR in a luciferase reporter vector (pMIR-REPORT) (**Figure 37A**); additionally, we produced two variants of the *PAK2*-3'UTR-pMIR REPORT construct, each carrying mutations in the miRNA-binding site predicted for miR-23b or miR-26a (*PAK2* 3'UTR-23b mut and *PAK2* 3'UTR-26a mut), which cause disruption of heteroduplex formation between each miRNA and its relative binding site in *PAK2* 3'UTR (**Figure 37B**). By performing luciferase reporter assays, we showed that miR-23b and miR-26a regulate *PAK2* by interacting directly with its 3'UTR, since co-expression of the two miRNAs with *PAK2* 3'UTR pMIR-REPORT, reduced luciferase levels when the binding sites did not contain mutations (**Figure 37C**). This reduction was not observed when the miRNAs were co-expressed with a pMIR-REPORT construct containing *PAK1* 3'UTR which do not contain any predicted site of interaction for these two miRNAs in its 3'UTR (**Figure 37A** and **D,** and **35B**).

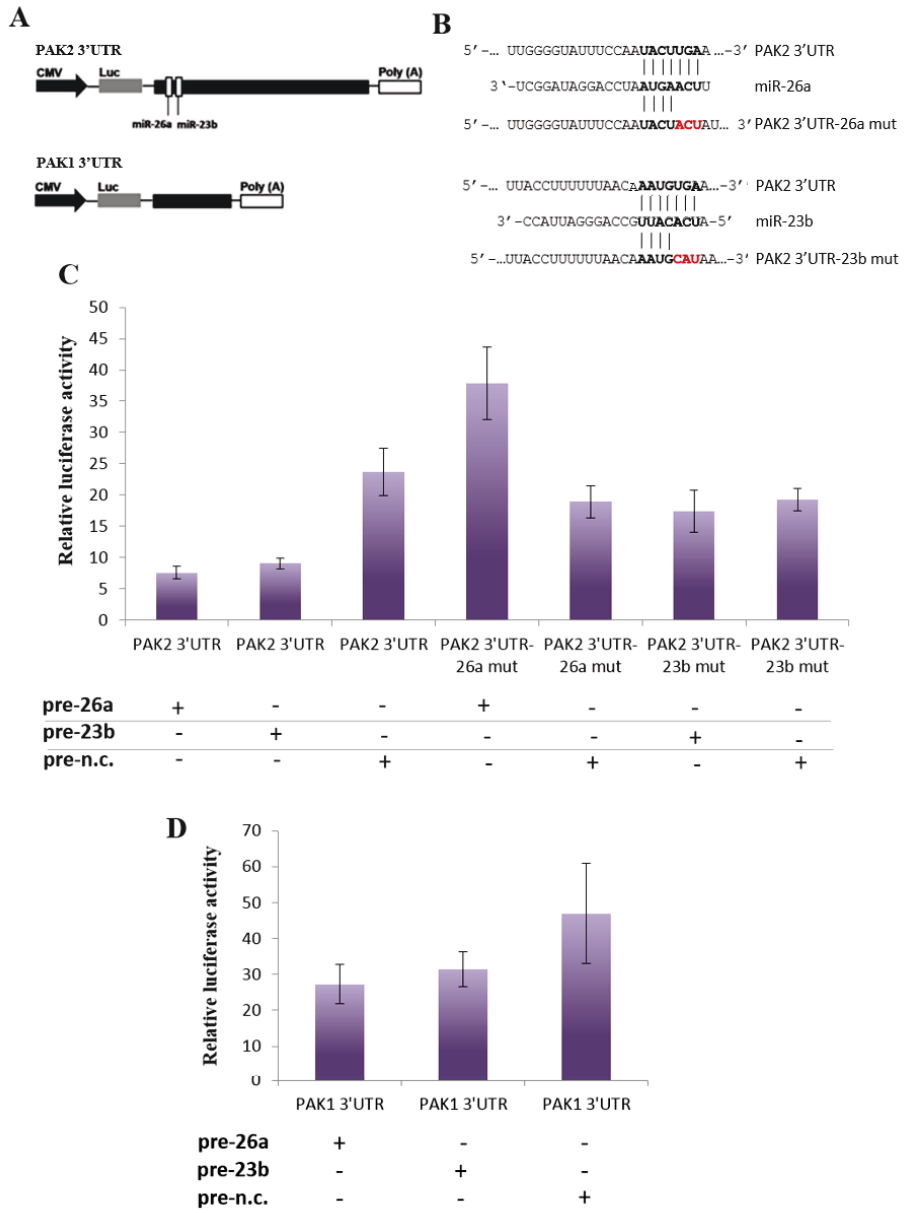

Figure 37: ***PAK2*** **is a direct target of both miR-23b and miR-26a. A,** Schematic representation of the 3′UTR of either *PAK2* or *PAK1* cloned in the pMIR REPORT *Firefly* luciferase vector. **B**, Representation of the heteroduplex between miR-26a or miR-23b and *PAK2* 3′UTR: base-pairing between the miR-26a- or miR-23b-binding site and the relative miRNA is lost when the miRNA-binding sites are mutated (in red). **C-D,** Relative luciferase activity levels were measured after 48h from co-transfection of HCT116 cells with *PAK2* 3′UTR-pMIR construct (wild-type or mutated in the interaction site for miR-26a or miR-23b) (**C**) or *PAK1* 3′UTR-pMIR construct (**D**) and the indicated miRNA precursors. Data are mean of three independent experiments ± s.e.m.

3.1.7 Regulation of miR-23b transcriptional expression

3.1.7.1 AP-1 transcriptionally suppresses miR-23b expression

Next, we wondered whether miR-23b expression is subject to eventual regulatory mechanisms relevant to BC. MiR-23b is encoded in the complex transcription unit (TU), *Chromosome 9 open reading frame 3* (*C9orf3*), which contains at least three transcriptional start sites (TSSs) (**Figure 38A**). The transcription factor c-MYC has been shown to suppress miR-23b expression by directly interacting with its most upstream TSS[299]. We performed *in silico* analysis of the miR-23b gene TU for transcription factors that may regulate expression of this miRNA gene; it revealed the presence of conserved and less conserved TPA-responsive elements (TREs), which are genomic sequences specifically recognised by the transcription factor activator protein 1 (AP-1) (**Figure 38A**). Functional AP-1 is formed upon heterodimerisation of c-JUN and c-FOS and plays major roles in transcriptional regulatory processes relevant to BC. It is in fact activated through EGFR and HER-2 signalling pathways and subsequently recognises TREs in promoter and enhancer regions of target genes involved in cell motility, invasion and growth[194].

In order to determine whether AP-1 regulates miR-23b expression at the transcriptional level, we silenced *c-FOS* and *c-JUN* in MDA-MB-231 cells (**Figure 38B**). We observed that individual gene silencing had little effect on miR-23b expression, whereas co-silencing of both genes significantly increased primary miR-23b (pri-miR-23b) but not pri-mir-26a-1 and pri-mir-26a-2 that do not present conserved TRE's along their TUs ($P = 0.0008$, **Figure 38C**). Furthermore, endogenous mature miR-23b levels were increased after simultaneous knockdown of *c-JUN* and *c-FOS*, whereas mature miR-26a levels remained unchanged (**Figure 38D** and **E**). These data implicate AP-1 in the negative regulation of miR-23b expression. We then hypothesised that AP-1-mediated regulation of miR-23b levels may result in a perturbation of downstream events that are controlled by miR-23b. Indeed, we found that *c-JUN-c-FOS* co-silencing reduced PAK2 levels and greatly increased MLC II phosphorylation (**Figure 38F**).

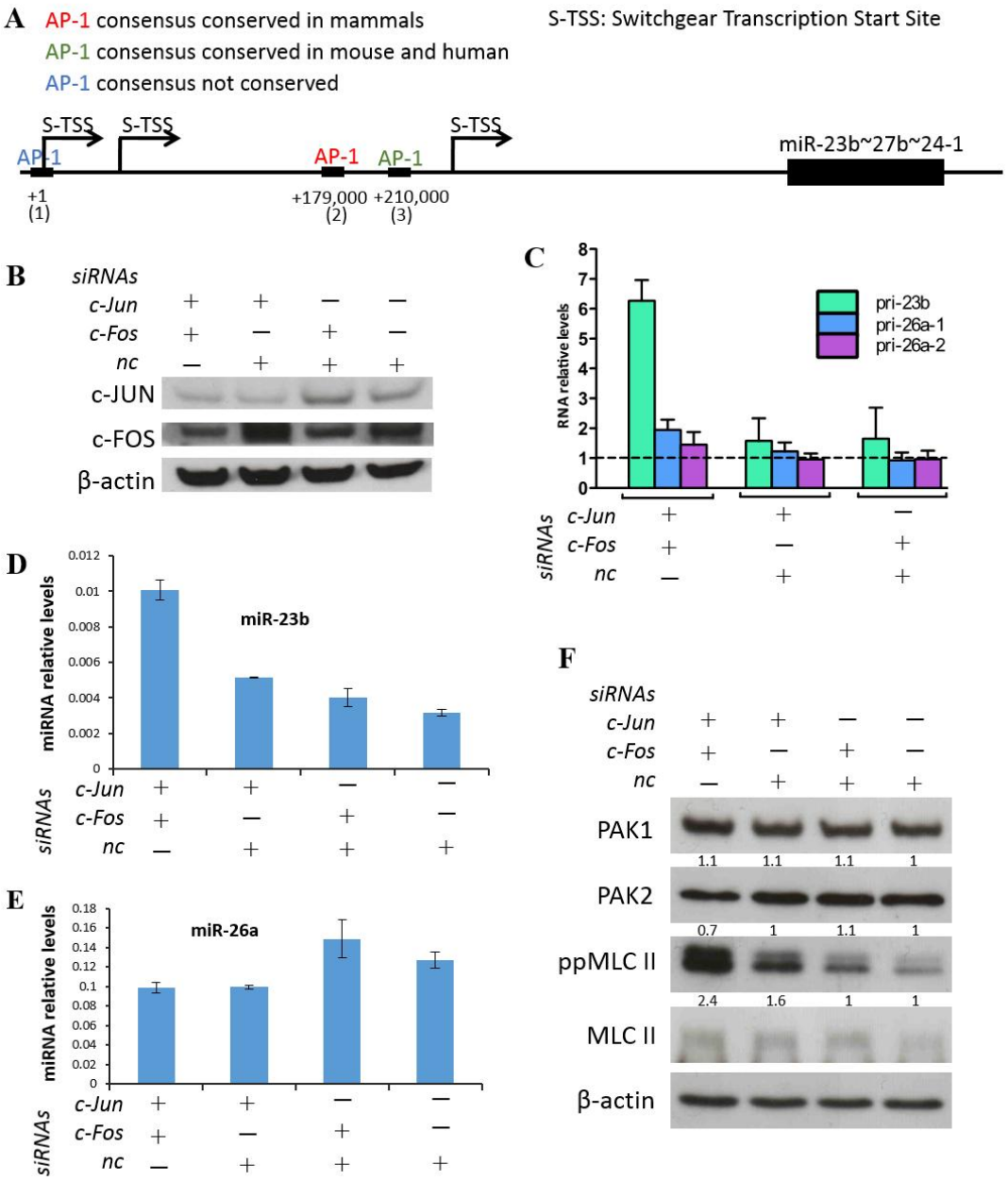

Figure 38: AP-1 transcriptionally suppresses miR-23b expression. A, Schematic representation of transcription unit (TU) of miR-23b~27b~24-1 cluster showing conserved, less conserved and non-conserved AP-1-specific TREs. Switchgear TSS: transcription start site experimentally validated by Switchgear Genomics **B**. Western blot showing c-JUN and c-FOS levels in MDA-MB-231 cells after transfection with the indicated siRNAs for 48h. β-actin was used as a loading control. **C**, Relative levels of pri-miR-23b, pri-miR-26a-1 and pri-miR-26a-2 were measured by RT-qPCR and normalised to U6 snRNA levels after co-silencing of *c-JUN* and *c-FOS*, or single silencing of the two genes by using siRNAs (20nM) in MDA-MB-231 cells for 48h. Data are presented relative to the siRNA n.c. (40nM) single transfection (dotted line). Data are mean of three experiments ± s.e.m. (P = 0.0008, Student"s t-test). **D-E**, RT-qPCR of miR-23b (**D**) and miR-26a (**E**) relative levels normalised to U6 snRNA levels after transfection with the indicated siRNAs (20nM) of MDA-MB-231 cells for 96h. Data are mean of three independent experiments ± s.e.m. **F**, Western blot showing PAK1, PAK2, (Thr18/Ser19)-ppMLC II and MLC II levels in MDA-MB-231 cells after transfection with the indicated siRNAs. β-actin was used as a loading control. Fold changes in protein expression levels normalised for β-actin using ImageJ software are shown underneath each relative protein plot.

3.1.7.2 AP-1 directly interacts with miR-23b promoter

We then wished to investigate whether AP-1 suppresses miR-23b expression by directly binding to the TREs present in the TU of miR-23b. Thus, we performed chromatin immunoprecipitation (ChIP) for c-JUN interaction with genomic regions in MDA-MB-231 cells. Our ChIP analysis revealed that AP-1 could be directly involved in the transcriptional inhibition of miR-23b, as c-JUN directly bound to at least two evolutionarily conserved TREs in the TU of *C9orf3* (**Figure 39** and **38A**). As expected, c-JUN also bound to the IL-6 gene promoter, used as positive control[410], but not a genomic DNA region that lacks the presence of TREs and was used as negative control (**Figure 39**).

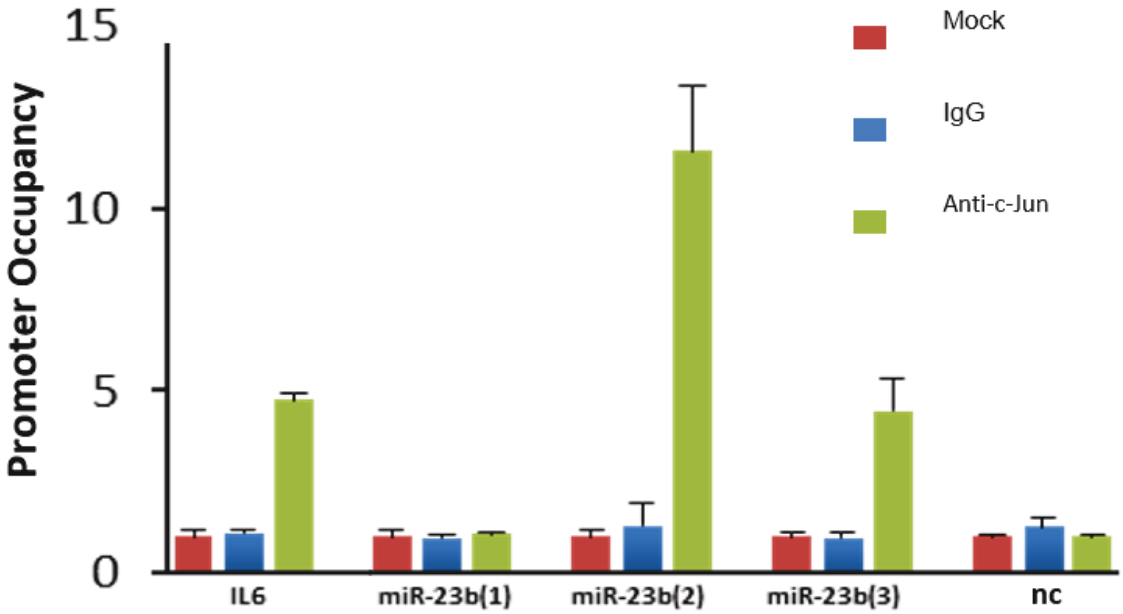

Figure 39: c-JUN directly interacts with miR-23b promoter. MDA-MB-231 cells were processed for ChIP assays and RT-qPCR was performed. The c-JUN-interaction site genomic regions are presented, expressed as promoter occupancy. MiR-23b (1), (2), (3) represent each AP-1-specific TREs present in the TU of miR-23b promoter, respectively. IL6: interleuchin-6 promoter region; n.c.: a genomic region that does not contain AP-1-specific TREs. Data are mean of two independent experiments ± s.e.m.

3.1.7.3 EGF stimulation inhibits miR-23b expression

We next wished to investigate whether activation of AP-1 by upstream signalling pathways is able to regulate miR-23b expression. AP-1 is a well-described oncogenic transcription factor activated downstream of EGFR/HER2 signalling, triggered by receptor stimulation with extracellular ligands, such as EGF[186]. It is known that EGF stimulation induces transcriptional expression of the AP-1-component *c-JUN* via downstream activation of AP-1 itself[199]. In order to evaluate whether miR-23b is inhibited by the same treatment, we treated EGFR positive BC MDA-MB-468 cell lines with EGF. As shown, levels of c-JUN mRNA increased within 20 min to 2 hours upon EGF stimulation confirming the validity of our methods (**Figure 40A**)[199]. We demonstrated that miR-23b levels decreased when *c-JUN* levels increased (**Figure 40B**), indicating that EGF reduces miR-23b expression through the c-JUN transcription factor.

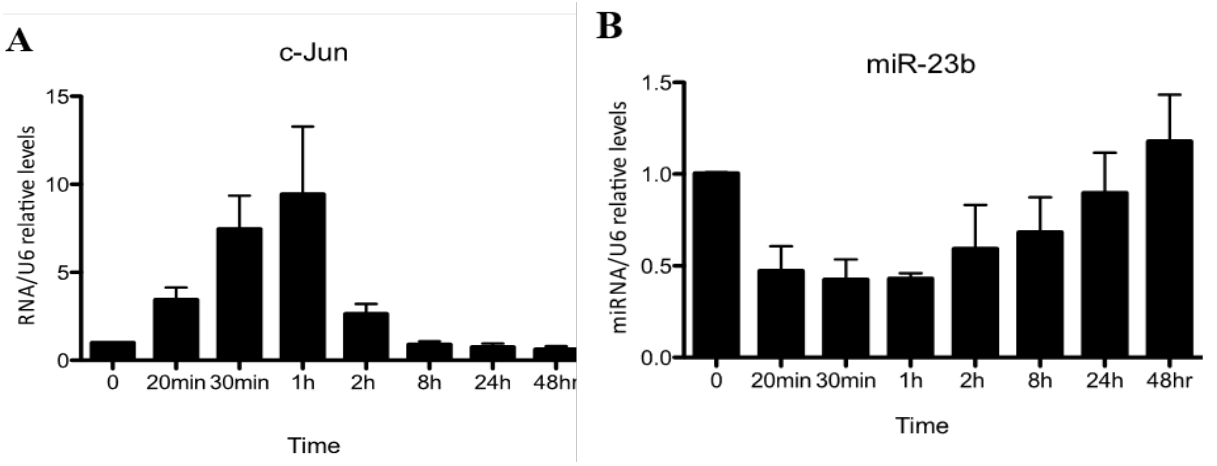

Figure 40: EGF stimulation inhibits miR-23b expression. A-B, RT-qPCR detected levels of c-JUN mRNA (**A**) and miR-23b (**B**) after EGF treatment (25 ng/ml) in MDA-MB-468 cells over the time course shown. C-JUN and miR-23b levels were normalised to U6 snRNA. Data are mean of three independent experiments ± s.e.m.

.

3.1.8 MiR-23b plays a role in BC metastasis

3.1.8.1 MiR-23b expression is inversely correlated with BC metastasis

Due to its crucial role in cytoskeletal remodelling, migration and invasion in BC, we hypothesised that loss of miR-23b may be involved in BC metastatic spread. Therefore, we examined miR-23b levels in MDA-MB-231 cells isolated from primary tumours or metastatic loci in different distal organs, formed after inoculation of a parental population of MDA-MB-231 cells into the mammary fat pads of nude mice[411]. Levels of miR-23b, but not miR-26a (measured as control), were higher in cells that formed the primary tumour at the inoculated site (TMD-231), compared to the cells that metastasised to the adrenal gland (ADMD-231), bone (BMD-231) or lung (LMD-231) (**Figure 41A** and **B**). Subsequently**,** we measured miR-23b and miR-26a levels in a small number of paired primary tumour and lymph-node metastasis specimens isolated from BC patients. Accordingly, miR-23b levels were higher in primary tumours, compared to their corresponding lymph-node metastases, whereas miR-26a expression did not change (**Figure 41C**). To increase the statistical significance of this finding, we next examined the expression of both miRNAs in a larger cohort of BC patients (n=132; 66 primary tumours and matching lymph-node metastases; **Table 12**). In accordance with our previous observations the mean expression of miR-23b, but not miR-26a, was significantly higher in the primary tumours than in the matching lymph node metastases (P = 0.004; **Figure 41D**)

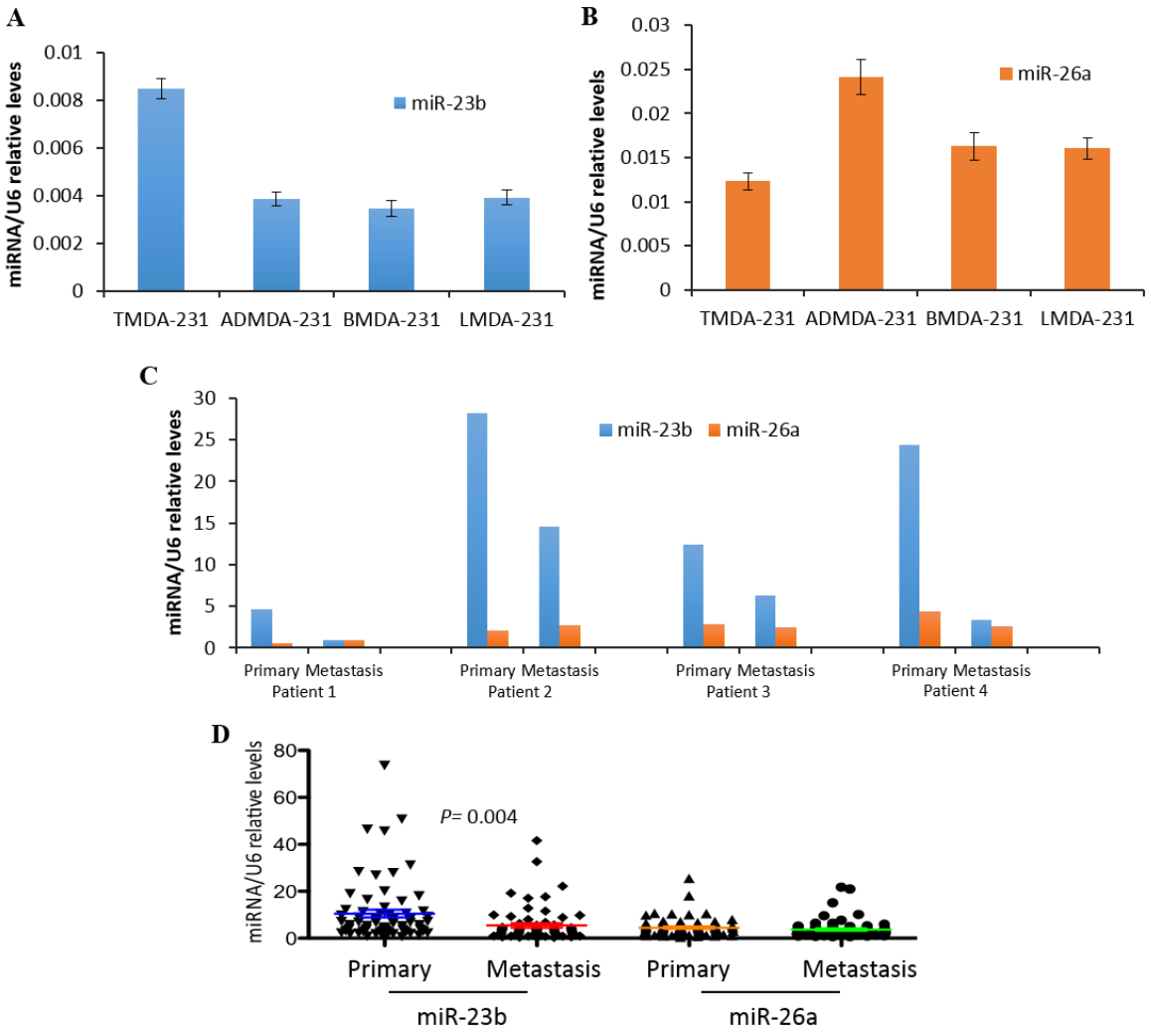

Figure 41: MiR-23b expression levels inversely correlate with BC metastasis. A-B, RT-qPCR shows relative expression levels of miR-23b (**A**) and miR-26a (**B**) in MDA-MD-231 BC cell lines isolated from primary tumour at the inoculation site (TMD-231) and metastatic loci in the adrenal gland (AMD-231), bone (BMD-231) and lung (LMD-231) formed after inoculation of a parental cell line in the mammary fat pads of nude mice. Data are mean of triplicate samples in one experiment ± s.e.m. **C**, MiR-23b and miR-26a relative levels in 4 pairs of human primary BC samples and their matched lymph-node metastases. Data are mean of triplicate samples in one experiment. **D**, Scatter plot shows the mean of miR-23b and miR-26a expression levels in 66 primary breast tumours and their corresponding metastatic specimens (P = 0.004, Student"s t-test). MiRNAs levels were normalised to endogenous U6 snRNA levels.

3.1.8.2 MiR-23b inhibition increases *in vivo* experimental metastasis and tumour growth

Based on our observations that miR-23b expression levels are markedly reduced in BC metastases, and that miR-23b inhibition promotes BC cell motility and invasion *in vitro*, we wished to further investigate these findings *in vivo*. MDA-MB-231 cell lines stably transfected with miR-23b-sponge or pEGFP-C1 vector control constructs were injected into the mammary fat pad of BALB/c Nude mice and primary tumours were allowed to grow until the volume reached about 300 mm^2 (n=7 per treatment). Histopathological analysis of the isolated primary tumours showed that local tumour invasion into the surrounding fat was dramatically increased by long-term miR-23b inhibition (**Figure 42A**), which was consistent with our *in vitro* findings (**Figure 33B**). In addition, immunohistochemistry of draining lymph nodes revealed the presence of extensive metastatic deposits only in the mice injected with stably transfected miR-23b sponge cells, indicating an enhanced ability of these cells with reduced miR-23b activity, to form spontaneous metastases ($P < 0.0001$; **Figure 42B**).

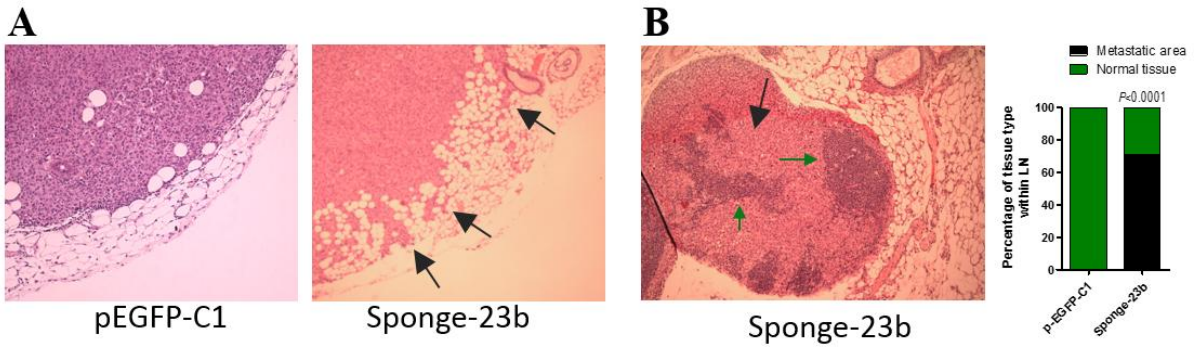

Figure 42: MiR-23b inhibition elicits BC cell invasion and metastasis *in vivo*. A, Hematoxillin and eosin (H&E) stain of primary tumours formed by miR-23b-sponge expressing- or pEGFP-C1 expressing-MDA-MB-231 cells 2 months after their orthotopic injection in mammary gland fat pads of BALB/c nude mice. Black arrows indicate regions of invasion into the surrounding fat. **B**, Representation of a lymph node isolated from an experimental metastatic animal study after injection of miR-23b-sponge expressing-MDA-MB-231 cells and stained by H&E. The black arrow indicates metastatic areas whereas green arrows indicate residual normal tissue characterised by the presence of smaller nuclei (n=7 per treatment). A quantification of the tissue type within the lymph nodes is shown in the graph on the right ($P < 0.0001$, Chi-Square test).

Surprisingly, we observed that inhibition of miR-23b elicited tumour growth *in vivo* (**Figure 43A**), which was inconsistent with our *in vitro* findings, where neither overexpression (**Figure 29A**), nor inhibition of miR-23b (**Figure 30**) significantly altered proliferation of MDA-MB-231 cells. Normally xenografts derived by injection of human breast MDA-MB-

231 cells into the mammary fat pad of immunocompromised mice have an extensive central necrotic area [412]. Notably, we found that down-regulation of miR-23b by the sponge construct, dramatically reduced tumour necrosis (P = 0.002; **Figure 43B**). This could explain the differential effect on cell growth exerted by miR-23b inhibition, *in vivo* and *in vitro.* Conversely, the tumours derived from miR-23b-sponge-expressing cells did not show any significant difference in the number of tumour microvessels compared to primary tumours formed by parental control cells (**Figure 43C**), suggesting that miR-23b is not implicated in the regulation of neoangiogenesis.

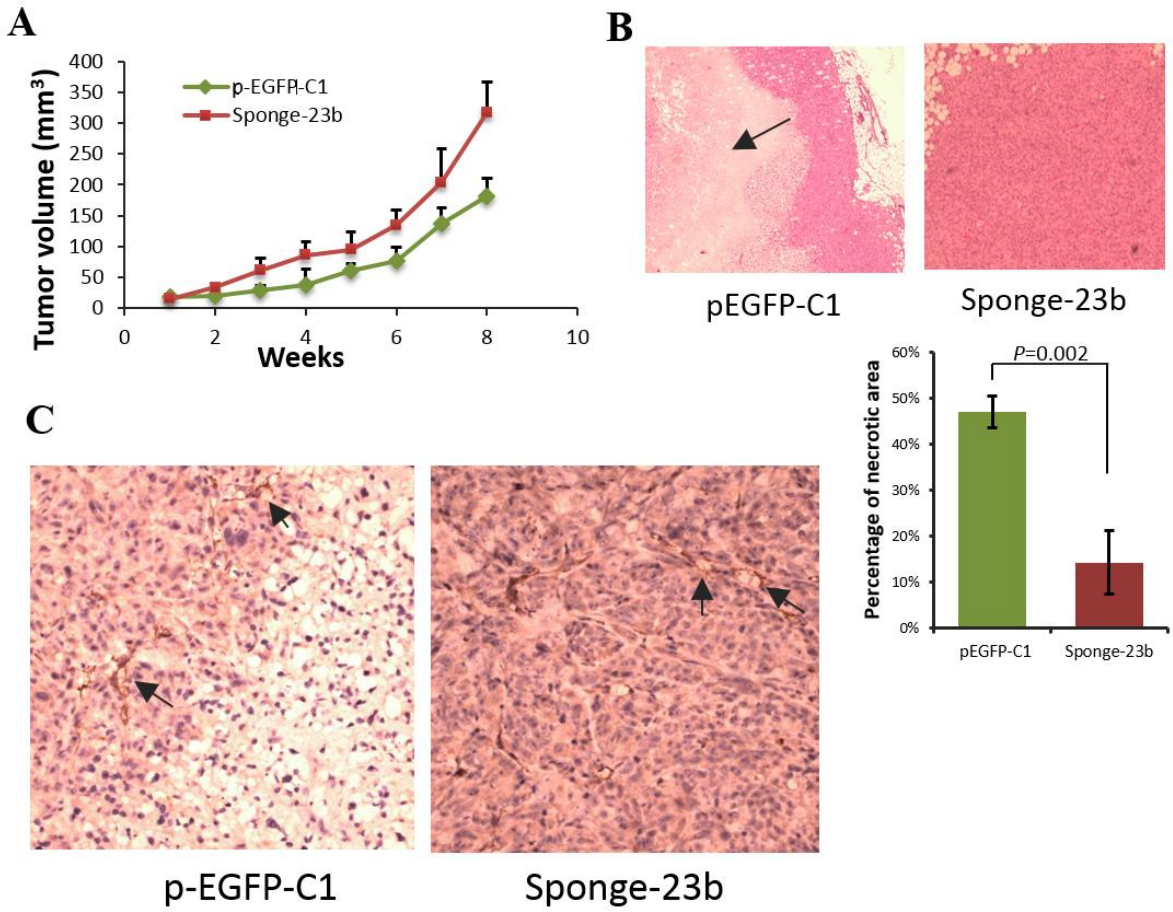

Figure 43: MiR-23b inhibition elicits tumour growth and reduces tumour-related necrosis *in vivo*. A, Line chart showing changes in tumour volume (mm^3) over time (weeks) after injection of 1 x 10^6 miR-23b-sponge expressing- or pEGFP-C1 expressing-MDA-MB-231 cells into the mammary fat pad of BALB/c nude mice (n=7 per treatment). **B,** H&E stain of representative MDA-MB-231 cell primary tumours formed 2 months after orthotopic injection of the same cells as in **A**. Arrow indicates region of necrosis. The graph below shows quantification of necrosis expressed as percentage of necrotic areas formed within the primary tumours (n=7 per treatment; P = 0.002, Student's t-test). **C**, CD31 stain of representative primary tumours formed as explained in **A** and **B** (n=7 per treatment). Arrows indicate microvessels formation. Average of intratumoural vessels counts per five high power fields, per section (n=4 sections) in three different tumours per treatment was performed.

3.2 MiR-26a plays a role in cytokinesis, aneuploidy and anchorage-independent cell growth in BC

3.2.1 Prolonged miR-26a overexpression leads to formation of giant binucleated cells *in vitro*

So far, our data suggest an unpredicted role for miR-26a in regulation of cytoskeletal dynamics. We demonstrated that ectopic overexpression of miR-26a promotes cell spreading and adhesion on ECM and leads to formation of enlarged focal adhesion sites in BC cell lines; furthermore miR-26a directly targets PAK2 and promotes phosphorylation of the MLC II.
Owing to its role in cytoskeletal remodelling, we wished to further investigate the effect that prolonged miR-26a overexpression may have in BC cell lines, using a similar approach to that used to assess miR-23b function.
We performed long-term (9 days) transfections of both MCF-7 and MDA-MB-231 cells with a miR-26a precursor or a pre-miR-n.c. mimic. Unexpectedly we observed that, compared to controls, both miR-26a-overexpressing cell lines grown in 2D-cultures exhibit a heterogeneous cell population, comprising cells of normal morphology, and giant cells displaying enlarged nuclei or two nuclei within their expanded cytoplasm. This effect suggests that events of impaired cytokinesis may be occurring upon miR-26a prolonged overexpression (**Figure 44A and B**). We quantified this effect by counting the number of multinucleated cells presenting in MCF-7 cell cultures after long-term-transfections with miRNA precursors. We found that a significant fraction (20%) of the miR-26a-overexpressing cell population was multinucleated compared to 3% of multinucleated cells present in MCF-7 cell cultures transfected with either miR-n.c. or miR-23b precursor ($P = 0.0002$; **Figure 44C**), which exhibit overall normal sized nuclei and cytoplasm (**Figure 44A and 23B**). This phenotype indicates that miR-26a activity may lead to impaired cytokinesis, implying the occurrence of aneuploidy. Moreover, the population of mononucleated cells overexpressing miR-26a appeared to have nuclei almost double in size compared with miR-n.c. or miR-23b transfected cells, indicating that nuclear division[413] could also be affected by this miRNA. After long-term transfection of miR-26a precursor, MCF-7 cells appeared to undergo a redistribution of F-actin in cortical microspikes, whilst E-cadherin levels and cell-cell junction were almost completely absent (**Figure 44A**).

Consistent with the effect of miR-26a on apoptosis and cell proliferation (**Figure 29**), we noticed that over the 9 days transfection treatment, MCF-7 cell cultures overexpressing miR-26a were progressively slowing their proliferation rates and displayed reduced working cell densities, compared to control cells. We recorded MCF-7 cells after completion of the 9 days transfection with miR-26a or miR-n.c precursor mimics in light microscopy-based videos for a time-lapse of 3 days. MiR-26a-overexpressing giant cells (bi- or mononucleated) showed slower proliferation rates over the time compared to control cells; nevertheless, they were able to complete mitosis forming two viable daughter cells (data not shown). Taken together, these observations indicate that miR-26a is involved in both cell cycle progression and cytoskeletal remodelling, but that interestingly its regulation of the cytoskeleton re-organisation may be different to that of miR-23b.

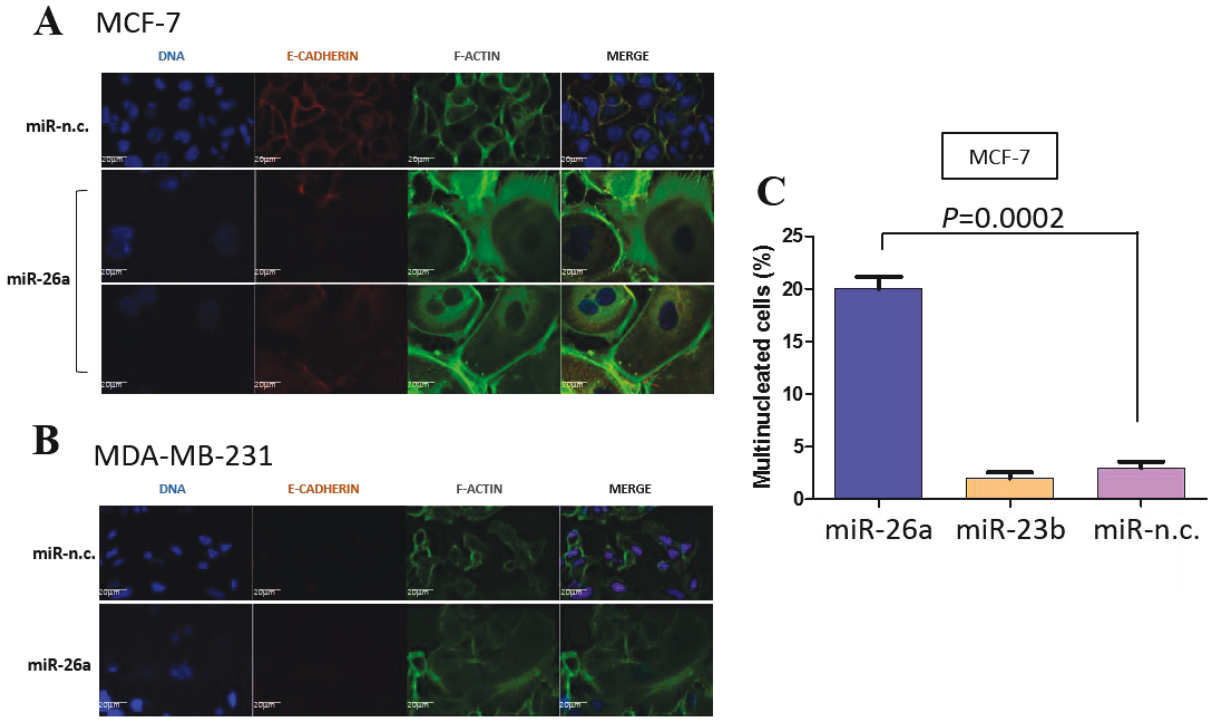

Figure 44: Prolonged miR-26a overexpression results in formation of giant bi/mononucleated cells. A-B, From left to right: *TO-PRO-3* staining of DNA, immunofluorescence staining of E-cadherin (1:1000), Alexa Fluor 488 phalloidin (1:500) staining of F-actin and overlay of the three images of MCF-7 (**A**) or MDA-MB-231 cells (**B**) transfected with miR-26a and miR-n.c. precursors (5nM) for 9 days. Scale bar = 20 µm **C,** The graph shows the percentages of multinucleated cells observed in MCF-7 cell cultures after long term-transfection with the indicated miRNA precursors. 50-100 cells were counted per condition in two independent experiments were counted. Data are mean ± s.e.m. (P = 0.0002, Student‟s t test).

3.2.2 Prolonged miR-26a overexpression leads to aneuploidy

Next, we wished to examine whether the delay in cytokinesis process induced by miR-26a affects chromosome stability leading to establishment of aneuploidy. Therefore, we prepared metaphase chromosome spreads from MCF-7 and MDA-MB-231 cells transfected for 9 days with miR-26a or miR-n.c. precursor mimic. We observed that both miR-26a- and miR-n.c.-expressing cells displayed a high percentage of aneuploidy, which is not surprising as tumour cells derive from multiple events of chromosome instability and are generally aneuploid[[414] (**Figure 45A** and **B**). Nevertheless, we found that prolonged overexpression of miR-26a led to a significant increase of aneuploidy (>80 chromosomes per spread) in ~10% of the total chromosome spreads analysed derived from MCF-7 and MDA-MB-231 cells, respectively ($P = 0.04$ and $P = 0.02$, respectively; **Figure 45**).

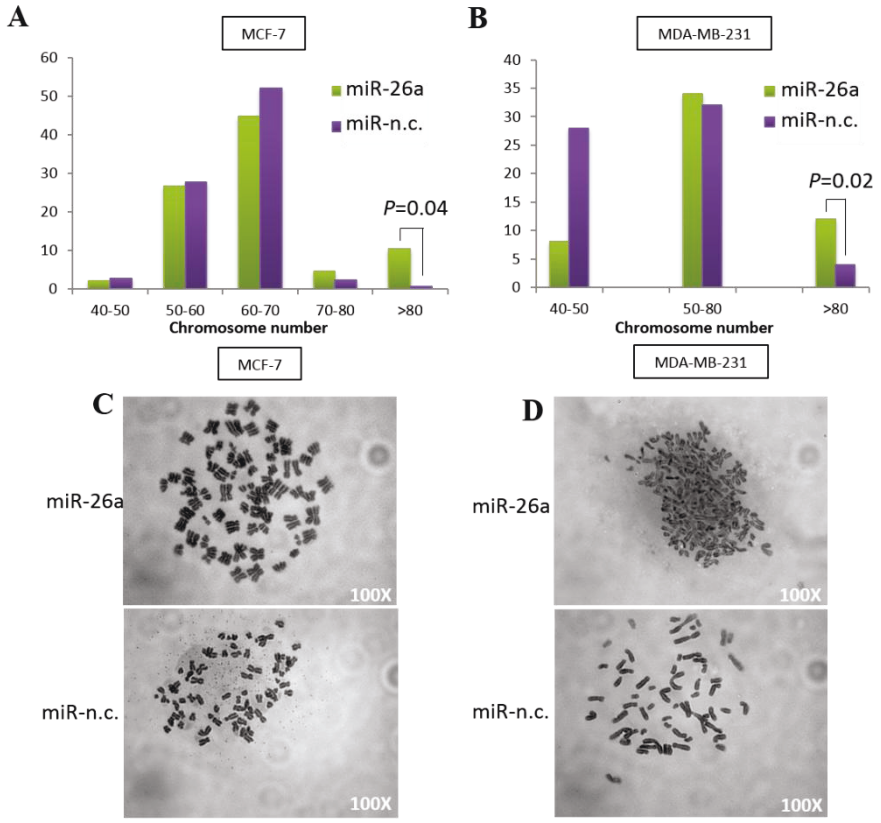

Figure 45: Prolonged miR-26a overexpression increases aneuploidy in BC cells. A-B, Percentages of metaphase chromosome spreads containing a number of chromosomes within the indicated ranges. The chromosome number of 50-100 methaphase spreads from MCF-7 (**A**) or MDA-MB-231 (**B**) cells transfected for 9 days with the indicated miRNA precursors were counted. Data are mean of two independent experiments ($P = 0.04$ and $P = 0.02$, Student‟s t test). **C-D,** Representative metaphase chromosome spreads from MCF-7 (**C**) or MDA-MB-231 (**D**) cells transfected for 9 days with the indicated miRNA precursors. Magnification 100X.

3.2.3 Prolonged miR-26a overexpression promotes tumourigenic potential of BC cells

Since aneuploidy is frequently associated with tumourigenic and transforming phenotypes[216], we investigated the impact that maintained miR-26a levels may have on the tumourigenic abilities of BC MCF-7 cells. Therefore, we performed anchorage-independent cell growth assays by seeding MCF-7 cells transfected for 9 days with either miR-26a or miR-n.c. precursor mimic on soft agar substrates, thus impeding cell adhesion[92] and allowed them to form spontaneous colonies. We found that MCF-7 cells expressing high levels of miR-26a exhibit increased transformation potential by forming a significantly greater number of colonies compared to control cells ($P < 0.0001$; **Figure 46A**). Moreover, the size of colonies produced by miR-26a-expressing MCF-7 cells was markedly larger than the one of control colonies ($P < 0.0001$; **Figure 46B**).

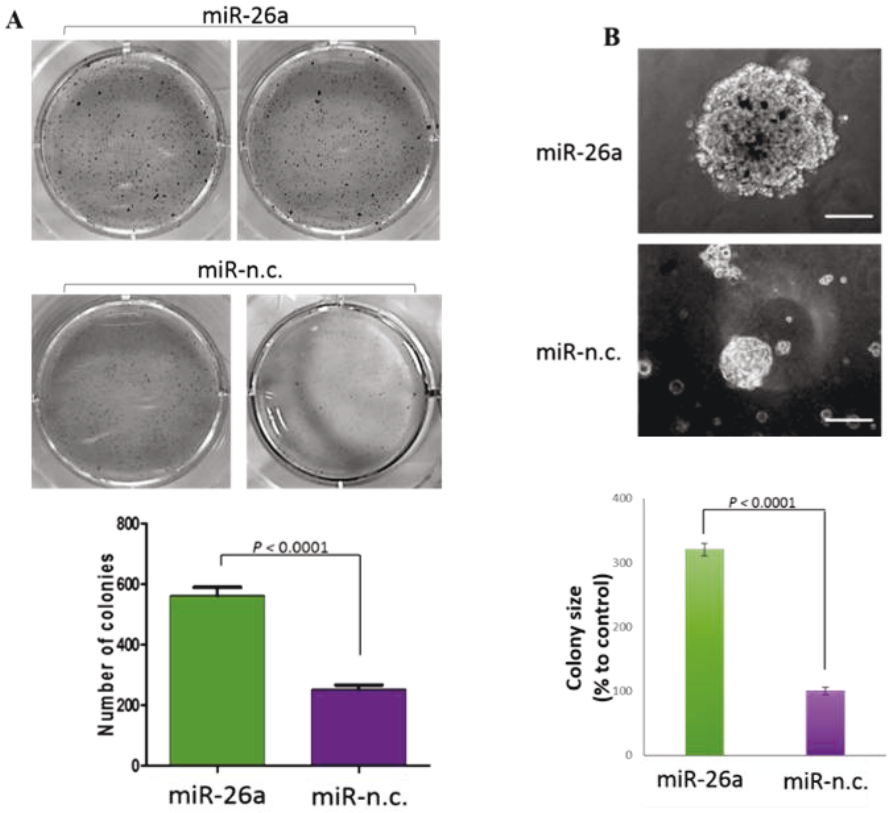

Figure 46: Prolonged miR-26a overexpression promotes tumourigenic potential of BC cells. A, Spontaneous colony formation by MCF-7 cells transfected for 9 days with the indicated miRNA precursors and plated on soft agar substrates in 6-well plates. After 3-4 weeks cells were fixed and stained with MTT. Number of colonies was quantified by using ImageJ software (right graph). Triplicates per conditions were assessed in two independent experiments. Data are mean ± s.e.m. ($P < 0.0001$, Student‟s *t* test). **B,** Size of colonies formed as described in (**A)** was visualised by light microscopy before colony staining with MTT and quantified by using ImageJ tool (right graph). The size bar shows equivalent magnification (20X) of both images. Data are mean of two independent experiments ($P < 0.001$, Student‟s t test).

3.3 Mir-23b and miR-26a exhibit distinct gene targeting relevant to cellular phenotypes regulated by each single miRNA

3.3.1 RNA-seq and bioinformatic analysis reveal regulation of distinct gene patterns by miR-23b and miR-26a

By performing experimental phenotypic analysis we found that miR-23b and miR-26a have both overlapping and distinct functions, despite regulating at least one common gene, *PAK2*, at the post-transcriptional level (**Figure 35**, **36** and **37**). This suggests that although both miRNAs modulate cytoskeletal dynamics partially by targeting *PAK2*, their general function is determined by coordinated regulation of distinct gene sets which is expected since miRNAs can target hundreds of different genes within the same tissue or cell[414]. In order to characterise the specific gene pattern controlled by each of these miRNAs and gain insight into the molecular mechanisms responsible for the observed phenotypes, we adopted a large-scale experimental approach based on high-throughput RNA sequencing (RNA-seq) analysis. Next generation RNA-seq represents a potent and accurate tool to assess transcript level changes for the identification of potential miRNA targets, by providing digital data of absolute transcript abundance[414]. Therefore, we performed global RNA-seq to analyse transcriptome changes mediated by ectopic manipulation of both miR-23b and miR-26a in BC cells. Particularly, we induced long-term (9 days) overexpression of each miRNA in epithelial MCF-7 cells and used MDA-MB-231 cells stably expressing a miRNA-sponge construct that silences each miRNA (**Figure 28C** and **D**) along with their relative controls.

3.3.1.1 RNA-seq and bioinformatic analysis confirm a role of miR-23b in cytoskeletal dynamics

Considering a significant cut off of 1.5 fold, analysis of our RNA-seq data relative to miR-23b manipulation revealed that prolonged overexpression of this miRNA in MCF-7 cells affected (down-regulated or up-regulated) levels of 7.4% of transcripts, whereas in MDA-MB-231 cells stably inhibiting miR-23b, gene expression changes were detected in 22.9% of total transcripts.

To understand the biological relevance of the genes regulated by miR-23b, we performed pathway enrichment analysis of the detected up-regulated and down-regulated transcripts using web-based DAVID tool[414].

Consistent with the phenotypes that we observed in MCF-7 cells overexpressing miR-23b, (**Figure 22** and **23**), we appreciated an enrichment of genes involved in adherens junction formation; particularly, we found up-regulated a set of genes, such as CTNNB1, PVRL1 and 2 (Poliovirus-receptor-like 1 and 2), TJP1 (Tight junction protein 1) and LMO7 (LIM domain 7), which encode for the cell adhesion molecules Catenin β-1, Nectin1 and 2, TJP1 and LMO7, respectively (**Table 15**).

On the other hand, reduced miR-23b activity in MDA-MB-231 cells was associated with enriched genes implicated in the regulation of actin cytoskeleton. These cells showed up-regulation of genes that promote lamellipodia and filopodia formation, such as *LIMK1*, *LIMK2* and *CFL2 and ARHGEF6*, encoding for LIM kinase 1 and 2, Cofilin 2 and the RAC/CDC42 guanine exchange factor 6, respectively, as well as central modulators of cytoskeletal dynamics that promote migratory phenotypes, such as myosin light chain 9 (MYL9), the non-muscle, myosin heavy chain 9 (MYH9) and p21-activated kinase 2 (PAK2), the latter shown to be direct miR-23b target, once again confirming our *in vitro* findings (**Table 16**).

Adherens junctions-related genes regulated by miR-23b in MCF-7 cells

Gene Name	ov_mirR-23b (RPKM)	ov_miR-nc (RPKM)	Fold ov_miR-23b vs ov_nc
CTNNB1	20.88	11.15	1.87
SMAD3	10.49	5.62	1.87
BAIAP2	1.58	0.87	1.81
TJP1	9.13	5.22	1.75
PVRL2	32.08	18.76	1.71
LMO7	3.17	1.99	1.59
PVRL1	16.98	10.73	1.58
CSNK2A1	5.37	3.42	1.57
EGFR	1.72	1.14	1.51
SRC	2.41	4.02	-1.66
MAP3K7	1.08	1.96	-1.81
TGFBR2	0.77	2.57	-3.32

Table 15: Genes differentially regulated in MCF-7 cells upon prolonged overexpression of miR-23b (ov_miR-23b) or miR-n.c. (ov_miR-nc) and relevant to adherens junction pathways. RPKM: Reads per kilobase per million. Change fold of gene expression between ov_miR-23b and ov-miR-nc indicates genes that are up-regulated or down-regulated (-).

Cytoskeleton-associated genes regulated by miR-23b in MDA-MB-231 cells

Gene Name	Sp-23b (RPKM)	pEGFP (RPKM)	Fold Sp-23b vs pEGFP	Gene Name	Sp-23b (RPKM)	pEGFP (RPKM)	Fold Sp-23b vs pEGFP
PIK3R3	3.14	0.41	7.63	ARPC5	102.32	63.42	1.61
ITGB8	1.27	0.17	7.31	ACTN4	244.50	151.73	1.61
MYL9	114.01	18.56	6.14	ITGAE	3.81	2.41	1.58
PDGFRB	1.20	0.29	4.15	MAPK3	13.09	8.42	1.55
ARHGEF6	1.25	0.32	3.85	TMSB4X	500.82	323.73	1.55
PAK4	2.49	0.69	3.60	LIMK1	10.31	6.73	1.53
DIAPH3	6.52	1.89	3.45	TIAM1	2.75	1.79	1.53
MYL6	154.80	46.53	3.33	VCL	32.93	21.73	1.52
FGF5	3.78	1.20	3.16	PIK3C3	13.13	19.89	-1.52
IQGAP3	37.42	12.09	3.10	SOS2	15.53	23.68	-1.52
PFN2	11.68	3.97	2.94	PIP4K2A	16.58	26.17	-1.58
MYH10	22.92	8.16	2.81	RRAS	22.83	36.35	-1.59
ACTB	1470.61	570.23	2.58	SSH3	2.17	3.53	-1.63
MSN	292.48	120.94	2.42	ITGA6	58.71	97.58	-1.66
FGD1	5.71	2.43	2.34	BRAF	2.23	3.72	-1.67
GNG12	119.18	53.65	2.22	PIK3C2B	1.32	2.47	-1.87
MAPK1	5.61	2.74	2.05	ITGB4	3.70	8.33	-2.25
ACTG1	691.17	343.81	2.01	ARHGEF4	1.19	2.83	-2.38
PAK2	44.54	22.21	2.01	ITGA1	5.28	12.64	-2.39
ENAH	2.62	1.33	1.97	PIK3CD	3.15	7.56	-2.40
FN1	25.44	13.49	1.89	ITGB2	4.93	13.14	-2.67
ACTN1	204.18	108.46	1.88	BAIAP2	1.89	5.20	-2.75
DIAPH2	1.67	0.89	1.86	MRAS	0.25	0.73	-2.92
CFL2	501.99	271.25	1.85	ITGA2	31.08	106.00	-3.41
LIMK2	1.37	0.77	1.78	ITGA10	1.60	6.04	-3.78
ABI2	13.83	8.16	1.69	PIP5K1B	0.01	1.03	-103.22
MYH9	243.58	145.53	1.67				

Table 16: Genes differentially regulated in MDA-MB-231 cells stably expressing the miR-23b sponge construct (Sp-23b) or the pEGFP-C1 parental control (pEGFP) and relevant to cytoskeleton pathways. RPKM: Reads per kilobase per million. Change fold of gene expression between Sp-23b and pEGFP indicates genes that are up-regulated or down-regulated (-)

3.3.1.2 RNA-seq and bioinformatic analysis confirm a role of miR-26a in cytoskeletal dynamics, cell adhesion and cell cycle

Manipulation of miR-26a affected the expression of 16.2% and 22.9% of total transcripts upon prolonged miR-26a overexpression in MCF-7 cells and stable miR-26a inhibition in MDA-MB-231 cells, respectively, considering a significant cut off of 1.5 fold.

Pathway enrichment analysis of the genes differentially regulated by miR-26a overexpression in MCF-7 cells showed significant changes in expression of cytoskeletal remodelling-related genes (**Table 17**) such as *MYLK* and *PAK2*, (that we validated as miR-26a direct target and considered this gene as a positive control of our methods), genes relative to focal adhesion pathways, including *Vinculin* (*VCL*) or to matrix-cell adhesion interactions, such as Fibronectin (*FN1*) and a cohort of integrin subunits (*ITGAM*, *ITGB8*, *ITGA1*, *ITGB6*, *ITGAV*, *ITGB7*). Interestingly, cell-adhesion related genes were found conversely down-regulated in MDA-MB-231 cell stably inhibiting miR-26a activity (**Table 18**). Up-regulation of this gene set may explain the phenotypic effects induced by miR-26a overexpression on focal adhesion, cell spreading and adhesion on the ECM (**Figure 24** and **45**). Additionally, among the genes enriched in adherens junction pathways upon miR-26a overexpression in MCF-7 cells, we found up-regulation of genes that belong to the TGFβ signalling pathway known to induce disruption of cell-cell adhesions, such as *TGFβ receptor 1* and 2 (*TGFRB1* and *2), SMAD family member 3* (*SMAD3*) and *SNAIL homolog 2* (*SNAI2*)[50, 51] (**Table 19**).

Cytoskeleton-associated genes regulated by miR-26a in MCF-7 cells

Gene Name	ov_miR-26a (RPKM)	ov_nc (RPKM)	Fold ov_miR-26a vs ov_nc	Gene Name	ov_miR-26a (RPKM)	ov_nc (RPKM)	Fold ov_miR-26a vs ov_nc
VIL1	0.66	0.05	13.13	PIK3C2B	15.42	9.41	1.64
ITGAM	0.47	0.04	12.91	FGD1	1.78	1.13	1.58
ITGB8	2.97	0.29	10.23	GNG12	32.73	21.16	1.55
ARHGEF6	0.24	0.03	9.30	ITGB1	56.24	37.05	1.52
FN1	24.83	2.75	9.03	DOCK1	8.43	5.58	1.51
ITGA1	0.46	0.06	7.93	ITGB1	41.64	27.64	1.51
MYLK	5.23	0.70	7.50	MAP2K1	18.61	12.36	1.51
FN1	31.16	4.28	7.28	RRAS2	4.00	2.66	1.50
FN1	23.59	3.62	6.52	GRLF1	28.41	42.71	-1.50
FN1	19.58	3.09	6.34	PIK3CB	15.25	24.43	-1.60
FN1	16.39	2.67	6.15	ITGB4	3.06	5.13	-1.68
MYLK	4.21	0.71	5.90	KRAS	4.98	8.37	-1.68
F2R	1.07	0.23	4.54	MAPK6	39.50	67.14	-1.70
ITGB6	15.29	3.67	4.16	ITGB4	10.38	17.65	-1.70
BDKRB2	6.10	1.61	3.80	PIK3R3	8.97	15.54	-1.73
FGFR2	0.71	0.20	3.64	MYH10	6.26	10.85	-1.73
ARPC4	1.92	0.59	3.25	PAK4	3.45	6.19	-1.79
ITGAV	17.95	6.70	2.68	ITGB4	7.89	14.26	-1.81
VAV1	1.51	0.60	2.54	PAK2	2.97	5.49	-1.85
EGFR	2.80	1.14	2.45	PIK3R1	20.12	37.21	-1.85
ITGB7	1.11	0.47	2.36	MAPK3	14.24	27.42	-1.92
ITGA6	3.47	1.48	2.35	ARPC3	42.58	84.76	-1.99
MYLK	0.41	0.18	2.28	PDGFB	1.22	2.57	-2.11
FGD3	6.62	3.07	2.16	CSK	1.84	4.07	-2.21
VCL	13.12	6.48	2.03	WASF1	0.91	2.15	-2.36
LIMK2	4.15	2.07	2.01	ARHGEF1	0.70	1.68	-2.41
SSH1	9.32	5.07	1.84	FGFR4	0.59	1.46	-2.46
CFL2	3.50	2.00	1.75	DIAPH2	0.90	2.24	-2.50
ENAH	12.91	7.75	1.67	WASF1	0.74	1.91	-2.57
RDX	68.60	41.20	1.66	FGF12	0.36	1.13	-3.12
GNA13	34.60	20.88	1.66	FGFR4	0.44	1.50	-3.37
ACTN1	73.52	44.66	1.65	LIMK2	1.66	6.79	-4.10
VCL	25.74	15.67	1.64				

Table 17: Genes differentially regulated in MCF-7 cells upon prolonged overexpression of miR-26a (ov_miR-26a) or miR-n.c. (ov_miR-nc) and relevant to cytoskeletal remodelling. RPKM: Reads per kilobase per million. Change fold of gene expression between ov_miR-26a and ov-miR-nc indicates genes that are up-regulated or down-regulated (-).

Cytoskeleton-associated genes regulated by miR-26a in MDA-MB-231 cells

Gene Name	Sp-26a (RPKM)	pEGFP (RPKM)	Fold Sp-26a vs pEGFP	Gene Name	Sp-26a (RPKM)	pEGFP (RPKM)	Fold Sp-26a vs pEGFP
PIK3CG	1.64	0.01	144.97	BRAF	2.39	3.72	-1.56
PIK3R3	1.90	0.41	4.62	ROCK2	15.76	24.58	-1.56
ITGB8	0.73	0.17	4.22	RRAS	22.68	36.35	-1.60
IQGAP3	35.20	12.09	2.91	PIK3CB	8.99	14.44	-1.61
MSN	335.16	120.94	2.77	SOS1	7.94	13.31	-1.68
ACTB	1552.12	570.00	2.72	FN1	6.53	10.99	-1.68
FGF5	8.43	3.15	2.67	GSN	6.78	11.91	-1.76
ARPC5L	77.04	32.31	2.38	PFN2	15.99	28.58	-1.79
HRAS	47.98	20.70	2.32	GRLF1	20.94	37.78	-1.80
CDC42	106.85	47.32	2.26	ITGA5	16.39	31.22	-1.90
ARPC2	132.84	59.53	2.23	WASF1	1.73	3.60	-2.08
GNG12	119.71	53.65	2.23	EGFR	42.68	88.86	-2.08
ITGAE	5.33	2.41	2.21	PIK3CD	3.59	7.56	-2.11
ARPC5	134.71	63.42	2.12	FGFR1	1.86	4.04	-2.18
PFN1	1158.13	546.73	2.12	CYFIP2	0.40	0.87	-2.19
CFL1	561.85	271.25	2.07	IQGAP2	0.34	0.74	-2.20
PFN2	8.11	3.97	2.04	SSH3	1.59	3.53	-2.23
MYH10	16.19	8.16	1.98	ITGB2	5.79	13.14	-2.27
ACTG1	666.85	343.81	1.94	BAIAP2	2.08	5.20	-2.50
PAK4	2.37	1.32	1.80	SOS2	9.11	23.68	-2.60
NRAS	39.17	23.23	1.69	ITGA1	4.73	12.64	-2.67
DIAPH1	28.85	17.23	1.67	ITGA2	36.69	106.00	-2.89
KRAS	5.05	3.02	1.67	ARHGEF4	0.74	2.83	-3.84
RHOA	324.36	194.57	1.67	ITGB4	6.72	26.36	-3.92
RAC1	56.57	36.71	1.54	ITGB3	0.21	1.09	-5.32
ROCK1	35.03	23.29	1.50	ITGA10	1.11	6.04	-5.45
MYLK	2.66	4.06	-1.53	PIK3C2B	0.33	2.47	-7.57

Table 18: Genes differentially regulated in MDA-MB-231 cells stably expressing the miR-26a sponge construct (Sp-26a) or the pEGFP-C1 parental control (pEGFP) and relevant to cytoskeleton pathways. RPKM: Reads per kilobase per million. Change fold of gene expression between Sp-26a and pEGFP indicates genes that are up-regulated or down-regulated (-)

Adherens junctions-related genes regulated my miR-26a in MCF-7 cells

Name	ov_miR-26a (RPKM)	ov_miR-nc (RPKM)	Fold ov_miR-26a vs ov_miR-nc
PTPRB	0.60	0.02	30.63
FYN	2.35	0.21	11.29
FYN	4.71	1.24	3.81
FYN	2.44	0.65	3.77
TGFBR2	4.57	1.50	3.05
EGFR	2.80	1.14	2.45
PTPRM	0.51	0.22	2.35
TGFBR1	11.63	5.17	2.25
SMAD3	12.05	5.62	2.14
CTNNB1	40.89	19.11	2.14
VCL	13.12	6.48	2.03
SNAI2	12.74	6.36	2.00
ACTN1	73.52	44.66	1.65
VCL	25.74	15.67	1.64
LMO7	3.13	1.99	1.57
SRC	6.04	3.99	1.51
ACP1	4.10	6.32	-1.54
PTPN6	1.82	2.99	-1.64
MAPK6	39.50	67.14	-1.70
FER	1.25	2.26	-1.81
MAPK3	14.24	27.42	-1.92
WASF1	0.91	2.15	-2.36
WASF1	0.74	1.91	-2.57

Table 19: Genes differentially regulated in MCF-7 cells upon prolonged overexpression of miR-26a (ov_miR-26a) or miR-n.c. (ov_miR-nc) and relevant to adherens junction pathways. RPKM: Reads per kilobase per million. Change fold of gene expression between ov_miR-26a and ov-miR-nc indicates genes that are up-regulated or down-regulated (-).

In addition to cytoskeletal remodelling pathways, our DAVID analysis confirmed ours and others published findings[325], that miR-26a is implicated in the regulation of the cell cycle process, as a large panel of genes relevant to cell cycle progression were found widely dysregulated after miR-26a manipulation. These include: (1) numerous cyclins, such as CCNE1, a previously validated miR-26a target[325], was found down-regulated in MCF-7 cells overexpressing miR-26a (**Table 20**) and up-regulated in MDA-MB-231 cells stably inhibiting this miRNA, and CCNB1, CCNB2, CCND3 and CCNE2 (the latter validated as miR-26a target[325]), all up-regulated when miR-26a was silenced (**Table 21**); (2) the cyclin-dependent kinase 6 (CDK6), another confirmed miR-26a target[325], was down-regulated by miR-26a overexpression; (3) several cyclin-dependent kinase (CDK) inhibitors, namely CDKN2B, CDKN1A, CDKN2C and CDKN2D, were up-regulated after miR-26a overexpression in

MCF-7 cells (**Table 20**); (4) modulators of mitosis entry and progression, such as RB1, and two components of the anaphase-promoting complex/cyclosome (APC/C), the anaphase-promoting complex subunit 10 (ANAPC10) and cell division cycle 20 (CDC20), were increased in MDA-MB-231 cell stably inhibiting miR-26a (**Table 21**). Interestingly, related serine/threonine kinases of the mitotic spindle checkpoint, budding uninhibited by benzimidazoles 1 (BUB1), budding uninhibited by benzimidazoles 1 homolog beta (BUB1B), and budding uninhibited by benzimidazoles 3 (BUB3) were also up-regulated upon miR-26a inhibition (**Table 21**).

Cell cycle-related genes regulated by miR-26a in MCF-7 cells

Gene Name	ov_miR-26a (RPKM)	ov_miR-nc (RPKM)	Fold ov_miR-26a vs ov_miR-nc	Gene Name	ov_miR-26a (RPKM)	ov_miR-nc (RPKM	Fold ov_miR-26a vs ov_miR-nc
TGFB2	3.66	0.45	8.23	ORC3	4.44	6.94	-1.56
CDC25C	2.24	0.3	7.42	CDC25B	8.57	13.42	-1.57
SMC1B	0.3	0.06	4.65	SKP2	2.86	4.64	-1.62
CDKN2B	3.96	1.18	3.37	E2F6	3.04	5.03	-1.66
CDKN2B	6.83	2.58	2.64	GADD45B	12.04	20.92	-1.74
CDC14B	1.2	0.49	2.45	PKMYT1	1.91	3.42	-1.79
HDAC4	1.12	0.46	2.43	CDC25B	7.47	13.5	-1.81
CDC25A	4.39	1.97	2.23	HDAC5	0.47	0.95	-2.02
SMAD3	12.05	5.62	2.14	HDAC5	0.46	0.94	-2.02
ANAPC11	5.34	2.60	2.05	CDK6	1.33	2.82	-2.13
CDKN1A	35.14	17.85	1.97	CDC25A	0.63	1.48	-2.34
E2F3	13.27	6.92	1.92	CCNE1	0.88	2.07	-2.35
CDKN2C	4.01	2.19	1.83	CDC25B	5.13	13.71	-2.67
HDAC7	5.47	3.13	1.75	HDAC8	1.29	3.88	-3.01
YWHAG	81.38	48.15	1.69	ANAPC11	1.16	3.90	-3.35
ABL1	4.31	2.75	1.57	CHEK2	0.53	2.34	-4.39
PKMYT1	7.04	10.85	-1.54	CDC25C	0.74	4.09	-5.55

Table 20: Genes differentially regulated in MCF-7 cells upon prolonged overexpression of miR-26a (ov_miR-26a) or miR-n.c. (ov_miR-nc) and relevant to cell cycle signalling. RPKM: Reads per kilobase per million. Change fold of gene expression between ov_miR-26a and ov-miR-nc indicates genes that are up-regulated or down-regulated (-).

Cell cycle-related genes regulated by miR-26a in MDA-MB-231 cells

Gene Name	Sp-26a (RPKM)	pEGFP (RPKM)	Fold Sp-26a vs pEGFP	Name	Sp-26a (RPKM)	pEGFP (RPKM)	Fold Sp-26a vs pEGFP
CDC20	88.23	7.93	11.13	CDC6	57.46	29.55	1.94
PLK1	44.86	4.32	10.38	CCNH	29.54	15.39	1.92
CCNB1	168.27	16.54	10.18	ORC1	3.55	1.90	1.87
CCNA2	82.90	10.94	7.57	PCNA	73.81	39.85	1.85
CHEK1	2.53	0.37	6.75	HDAC2	18.07	9.94	1.82
PTTG1	197.70	30.86	6.41	HDAC3	51.66	28.64	1.80
CCNB2	45.79	8.13	5.63	TFDP1	24.34	13.55	1.80
CDK1	92.20	16.75	5.50	CDC14B	1.15	0.64	1.79
CDC25C	11.52	2.15	5.37	CDC25B	12.09	6.98	1.73
BUB1	73.08	16.30	4.48	MCM4	30.75	17.79	1.73
MAD2L1	47.28	10.68	4.43	ANAPC7	6.72	3.90	1.72
BUB1B	31.19	7.68	4.06	E2F2	1.19	0.72	1.67
CCND3	37.77	9.46	3.99	WEE1	10.91	6.54	1.67
DBF4	8.16	2.12	3.84	MCM3	105.16	63.30	1.66
CDKN2C	24.23	6.51	3.72	ORC5	10.59	6.50	1.63
CDC25A	8.60	2.43	3.55	PRKDC	26.35	16.31	1.62
SKP2	13.49	4.00	3.37	MDM2	13.30	8.29	1.60
ESPL1	5.91	1.80	3.28	ORC3	3.42	2.15	1.59
CDK2	33.93	10.96	3.10	E2F3	23.71	14.95	1.59
BUB3	136.78	45.24	3.02	RB1	16.79	10.98	1.53
CDKN2D	26.58	10.35	2.57	ANAPC11	10.95	7.17	1.53
FZR1	2.88	1.24	2.32	ABL1	4.94	7.65	-1.55
CCNE1	2.85	1.25	2.28	MAD1L1	3.10	4.92	-1.59
ORC4	1.99	0.89	2.24	EP300	9.56	16.81	-1.76
CCNE2	16.98	7.64	2.22	HDAC6	7.99	14.46	-1.81
CHEK1	30.84	14.59	2.11	MCM7	7.91	14.62	-1.85
E2F4	35.94	17.13	2.10	CDC14A	1.31	2.43	-1.86
CDC45	12.07	5.84	2.07	CCNB3	0.44	0.84	-1.90
HDAC8	6.03	2.98	2.02	SMAD3	6.73	13.90	-2.07
ANAPC10	10.88	5.49	1.98	HDAC5	1.63	3.55	-2.18
ORC6	11.39	5.76	1.98	CCND2	0.36	7.16	-20.10
PKMYT1	5.55	2.82	1.97				

Table 21: Genes differentially regulated in MDA-MB-231 cells stably expressing the miR-26a sponge construct (Sp-26a) or the pEGFP-C1 parental control (pEGFP) and relevant to cell cycle signalling. RPKM: Reads per kilobase per million. Change fold of gene expression between Sp-26a and pEGFP indicates genes that are up-regulated or down-regulated (-)

Finally, perturbation of miR-26a intracellular levels implied an enrichment of genes implicated in the SNARE vesicular transport. Strikingly, two central players of this pathway, Syntaxin 2 (STX2) and Endobrevin (VAMP8) are required for cytokinesis[231]. Their down-regulation by RNAi impedes the completion of cytokinesis, thus leading to the formation of binucleated cells[231]. These genes are down-regulated and up-regulated upon miR-26a

overexpression and inhibition, respectively, indicating a possible explanation for why miR-26a overexpressing cells tend to contain two nuclei (**Table 22** and **23**).

SNARE vesicle transport-related genes regulated by miR-26a in MCF-7 cells

Gene Name	ov_miR-26a (RPKM)	ov_miR-nc (RPKM)	Fold ov_miR-26a vs ov_miR-nc
VAMP1	0.95	0.18	5.41
STX11	0.85	0.34	2.51
STX1A	4.99	2.83	1.77
GOSR1	1.19	1.81	-1.52
STX16	5.10	8.24	-1.62
STX16	2.51	4.08	-1.63
VAMP2	6.85	12.10	-1.77
GOSR1	0.55	1.00	-1.82
VAMP7	2.70	5.33	-1.98
STX8	5.37	11.23	-2.09
SNAP23	5.43	11.58	-2.13
STX1B	0.28	0.64	-2.26
STX2	1.41	3.79	-2.69
VAMP8	0.20	0.78	-3.97

Table 22: Genes differentially regulated in MCF-7 cells upon prolonged overexpression of miR-26a (ov_miR-26a) or miR-n.c. (ov_miR-nc) and relevant to SNARE vesicular transport pathway. RPKM: Reads per kilobase per million. Change fold of gene expression between ov_miR-26a and ov-miR-nc indicates genes that are up-regulated or down-regulated (-).

SNARE vesicle transport-related genes regulated by miR-26a in MDA-MB-231 cells

Gene Name	Sp-26a (RPKM)	pEGFP (RPKM)	Fold Sp-26a vs pEGFP
SNAP23	2.15	0.60	3.58
VAMP7	7.05	2.86	2.46
GOSR2	8.83	4.36	2.02
VAMP8	97.57	56.72	1.72
SEC22B	60.37	35.87	1.68
VAMP3	64.95	42.96	1.51
STX2	8.09	5.39	1.50
VAMP2	14.98	25.79	-1.72
STX1A	6.93	12.29	-1.77
GOSR1	1.14	2.11	-1.86

Table 23: Genes differentially regulated in MDA-MB-231 cells stably expressing the miR-26a sponge construct (Sp-26a) or the pEGFP-C1 parental control (pEGFP) and relevant to SNARE vesicular transport pathway. RPKM: Reads per kilobase per million. Change fold of gene expression between Sp-26a and pEGFP indicates genes that are up-regulated or down-regulated (-).

3.3.1.3 Bioinformatic analysis of miR-23b and miR-26a targetomes

In order to gain insight into the molecular mechanisms that may explain the observed phenotypes induced by the two miRNAs, we performed RNA-seq-based targetome analysis to evaluate the direct effect of these miRNAs on gene expression in BC cells. Since miRNAs repress gene expression[276], we selected all the genes found to be down-regulated in MCF-7 cells overexpressing either of the two miRNAs, and the genes up-regulated in MDA-MB-231 cells where activity of each miRNA was inhibited by the miRNA sponge vectors. Firstly, we performed GO term enrichment analysis on these particular genes to gain insight into their biological function. Consistent with the phenotypes observed in our *in vitro* findings and our pathway analysis, we found genes associated with functions relevant to cytoskeleton organisation in both cell lines after miR-23b manipulation (**Figure 47A** and **B**). On the other hand GO term analysis of the transcripts modulated by miR-26a produced significant

enrichments of genes involved in cell cycle, p53 signalling, pathways in cancer, and also cytoskeletal remodelling, focal adhesion and ECM receptor interaction (**Figure 47C** and **D**). This output is consistent with our findings of a miR-26a role in cell adhesion and cell cycle progression, and also with documented evidences that miR-26a regulates cell cycle, apoptosis and that its expression is modulated by p53[302, 361, 364-366, 368, 370, 415].

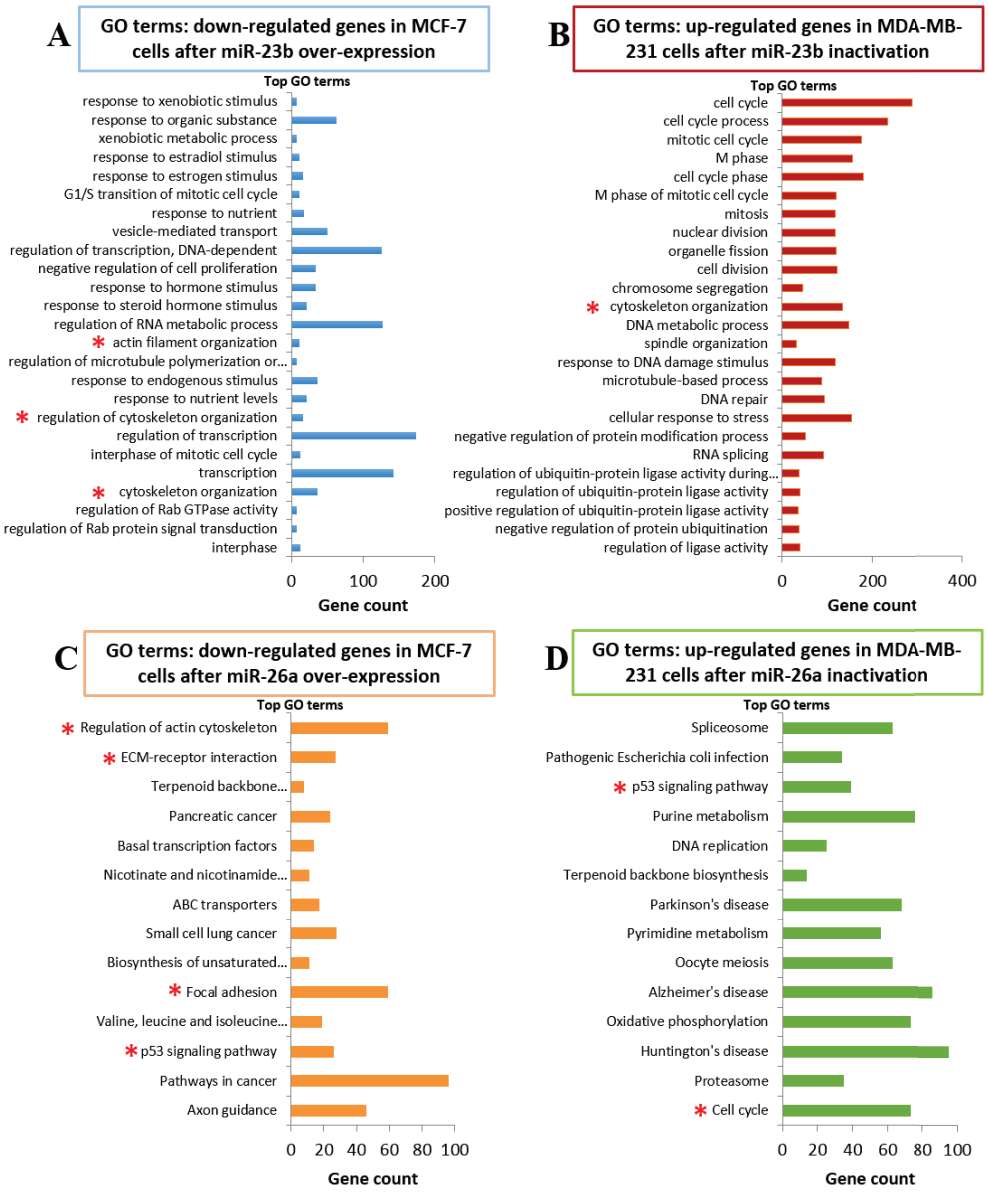

Figure 47: GO term analyses of miR-23b and miR-26a-regulated genes retrieved after RNA-seq confirm the functional phenotypes affected by each miRNA. A-B, The two charts show the top 25 significantly enriched GO terms found with DAVID bioinformatic tool. Genes down-regulated after miR-23b overexpression in MCF-7 cells (**A**) or up-regulated after miR-23b inactivation in MDA-MB-231 cells (**B**) were used. Red asterisks indicate GO terms related to cytoskeletal remodelling organisation. **C-D,** Charts show the top 25 significantly enriched GO terms retrieved as described in A-B relative to genes down-regulated after miR-26a overexpression in MCF-7 cells (**C**) or up-regulated after miR-26a inactivation in MDA-MB-231 cells (**D**). Red asterisks indicate GO terms related to cytoskeletal organisation, focal adhesion, ECM receptor interaction, p53 signalling and cell cycle.

Next, to uncover direct target candidates of miR-23b and miR-26a, we intersected all the down-regulated genes in MCF-7 cells overexpressing either of the two miRNAs with the up-regulated genes in MDA-MB-231 cells that stably silence the relative miRNA, we then combined the resulting intersection lists with the gene targets predicted for each miRNA by TargetScan. With this analytic approach we obtained an overlap of 103 and 119 gene transcripts for miR-23b and miR-26a, respectively (**Figure 48A** and **B**, **Table 24** and **25**). We reasoned that the intersection would contain a highly enriched list of direct targets, and considered a cut-off expression change of 1.2 fold sufficient, given that miRNAs regulate transcripts by promoting destabilisation through deadenylation[284], although mediating a stronger effect on protein translation[416]. Higher fold changes may result in omitting many relevant targets. Furthermore, the impact of miRNAs on gene targets is variable and usually mild[323]. To validate our findings, we performed a thorough literature search and used the miRTarBase database[417] to identify and analyse experimentally confirmed targets of both miRNAs. 70% and 81% of previously described miR-23b and miR-26a gene targets, respectively, were among the intersection representing those genes down-regulated in MCF-7 and/or up-regulated in MDA-MB-231 cells, and those in the TargetScan prediction list, indicating the reliability of our methods (**Table 24** and **25**). Particularly, within the 103 overlapping genes regulated by miR-23b, we detected *CELF1*, *MAP3K1*, *FZD7*, *TGFBR2*, *PLAU* (encoding for uPA), PAK2 ans GLS (**Table 24**)[353, 418]. On the other hand, previously validated targets of miR-26a retrieved in our analysis included *CCNE2*, *CCNE1, RB1, EZH2*, *PTEN*, *GSK3B* and *MCL1*[362, 364, 366, 368, 369, 419] (**Table 25**). Moreover, we observed that *PAK2* is present in the same intersections for both miR-23b and miR-26a regulation (**Table 24** and **25**), supporting our findings.

In order to cross-validate both our RNA-seq output and our initial bioinformatic analysis on the potential function of miR-23b (**Figure 19A**), we performed GO term analysis of the gene list reported in **Table 24**, which resulted from the intersection between the down-regulated genes in MCF-7 cells overexpressing miR-23b, the up-regulated ones in MDA-MB-231 cells upon miR-23b inactivation and the miR-23b potential gene targets predicted by TargetScan. Notably, this further analisys retrieved numerous pathways that have been pointed out by our first DAVID analysis (**Figure 19A**); among these, regulation of cytoskeletal and cell-cell junction organisation are of particular interest, as they confirm our *in vitro* findings of a crucial role of miR-23b in controlling cytoskeleton remodelling and cell-cell interactions (**Figure 49**).

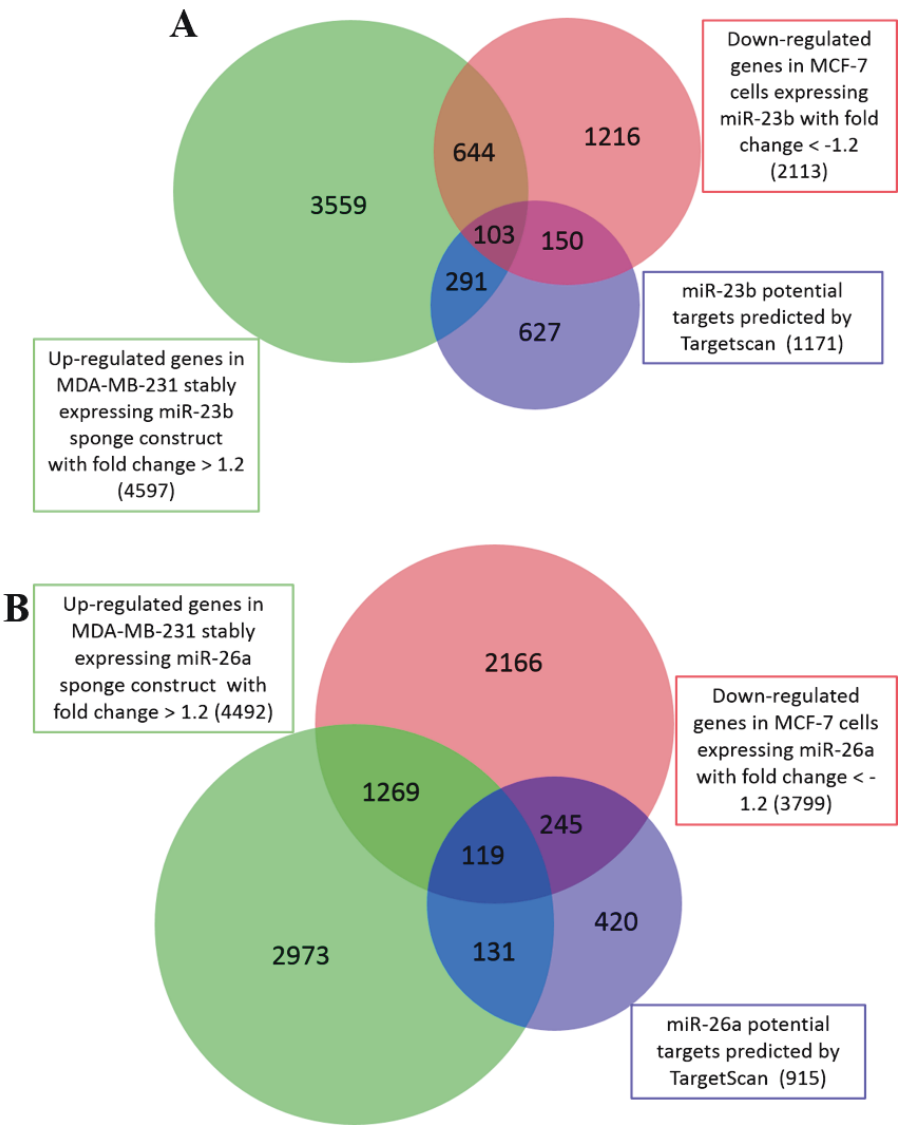

Figure 48: Intersection of genes differentially regulated by miR-23b and miR-26a after RNA-seq analysis with TargetScan prediction gene targets for each miRNA. A, The Venn diagram shows groups of overlapping genes after cross-intersections of genes down-regulated in miR-23b-overexpressing MCF-7 cells with those up-regulated in MDA-MB-231 cells stably expressing a miR-23b-sponge construct, and with gene targets predicted for this miRNA by TargetScan algorithm. **B,** The Venn diagram shows groups of overlapping genes found as described in (**A)** but relative to miR-26a-regulated genes.

Intersection of TargetScan prediction gene list and down-regulated genes in MCF-7 over-expressing miR-23b			Intersection of TargetScan prediction gene list and up-regulated in MDA-MB-231 stably expressing miR-23b-sponge construct						Intersection of up-regulated genes in MDA-MB-231 expressing sponge-23b, down-regulated genes in MCF-7 over-expressing miR-23b and TargetScan prediction gene list		
CXCL12	TET3	NEU1	PLAU	ARL6IP1	ASXL1	HNRNPU	SOCS6	RNF219	CELF1	HSPA12A	DYRK1A
FZD7	DCP2	MAP4	GLS	SLC22A23	CTSC	BCLAF1	CCND1	ICMT	MAP3K1	WHSC1	NPR3
TGFBR2	POM121C	GOLPH3L	TRIOBP	GPSM1	REEP1	SMAD5	ZNF286A	AFF3	PAK2	ZNF117	CLK3
GPBP1	MEF2A	FBXO11	ZNF655	MEF2C	ZNF676	DHRS11	CS	TMEM135	HMGN2	DTNA	
BBX	ATXN1	JAK1	NRK	DDAH1	NCBP1	KIAA1462	WTAP	MCM3AP	TOP1	RPIA	
PNRC1	GSK3B	DLX1	LSAMP	C13orf34	WNK3	WWC2	PRDM10	ANKRD17	PPM1A	UBL3	
APPBP2	CCNG1	RBL2	PLCXD3	THAP2	HAS2	MAP3K3	TMEM109	FLNB	FAM43b	ZNF721	
TAOK1	ATRN	PAX9	GREM2	COL4A1	EGLN2	KBTBD8	CDC23	C3orf63	MTMR9	ASF1A	
EPS15	TNKS2	FUT4	QKI	FAS	MDFIC	PDXDC1	ANKRD57	LYPLA1	TIPRL	LONRF2	
ARHGAP5	ATXN7L3	PNRC2	APOLD1	AMMECR1	SGK1	GDAP2	NACC1	CPOX	ANKRD52	PIGX	
MLL2	DIP2C	SLC13b6	SLC4A4	HMGB2	MBOAT7	FUNDC2	CDC6	NUDT21	ADRBK1	ZNF708	
TMEM194A	KIAA1737	PGR	NRXN3	DAPK1	TMEM48	UBA6	NUCKS1	MAML1	PPP2R3A	NEK7	
CLASP2	KLHL5	CPEB2	ITGB8	SEC14L1	ENAH	ODZ1	TPST1	PTPN14	PKP4	PRDX3	
HIVEP2	TRAPPC6B	MAF	SHROOM2	ARNT2	OTUB1	IRF1	AEBP2	CSNK2A1	PRMT6	PARD6B	
PRKRIR	SLC38A1	MSL2	TRPC3	CPM	CHST7	CMIP	SLC12A2	TNRC6A	C5orf42	SC4MOL	
LPGAT1	FAM134A	AGPAT9	NAP1L5	C1orf96	PPIF	SNX5	IPO8	SPRY2	G3BP2	MACF1	
OSBPL8	C3orf64	ZNF253	MPP2	FAM199X	MTHFS	ZFHX4	RCOR1	PRRC2B	GXYLT1	CHST15	
HS6ST3	CTNNBIP1	TMEM120B	DEPDC1	TJP2	ZNF626	ZNF81	NDUFA3	DTL	PURB	C2orf69	
CSNK1G1	TXNDC15	ZNF680	C8orf58	MYCT1	SLC5A3	VCP	ARPP19	IRS2	LANCL1	STRN4	
MYO6	ZNF793	VRK3	GJA1	GPR155	TAB3	KHSRP	IPPK	SSH2	PIGS	PTGER4	
STK4	KIAA0922	HOOK2	SMS	SAFB	TXLNG	ALG6	NDFIP2	WASF2	ZAK	ZNF138	
PBRM1	MCFD2	FAM46C	MYCBP	KLHL15	DYRK2	MTM1	NUP50	SIK2	CHUK	CALCR	
RUFY2	SLC38A2	EIF4E3	SLC1A3	SYNJ1	ZNRF3	CCNT2	ISCA2	UTP23	ETNK1	ATP2B4	
GLYR1	SETD1B	TXNRD1	PDE4B	FLJ36031	KIAA1804	PNMA2	MAT2A	LPHN2	DENND1B	PMAIP1	
CSRNP2	WBP2	CNOT2	SLC6A14	C18orf54	XIAP	RBM12B	ALDH1A2	SET	(SEPT11)	CFL2	
TMEM170B	C3orf57	MADD	ZC4H2	NRGN	LPAR1	GBAS	DUSP5	EPN2	USP5	APAF1	
LRIG1	ZNF254	ADCY1	PHF19	RAD51AP1	SMC5	RAP1A	NLK	EPN1	LPP	E2F6	
ADNP	MFSD8	ZDBF2	PRRG1	CELF2	SNRPC	SMN1	KDM6A	TJP1	PPP1R12A	TMOD2	
FAM107B	TUSC2	SMN2	SLC16A2	SIX2	ARID3B	CRLF3	TRRAP	HELZ	MYL12B	TBC1D9	
ATP11B	TMEM150C	LRCH1	AKAP12	SPOCK1	BICD2	UBE2D3	RBM12	RCHY1	TLN2	CASP7	
ZNRF2	N4BP1	STX12	CASK	ZNF238	ST7L	ABL2	USP24	FOPNL	ZNF107	AHI1	
TGIF1	SESN2	CLCN3	IL11	TPM3	MAK16	NFIA	KPNA3	DDX5	ATP6V1E1	KITLG	
MAP4K4	PRKCE	ERBB4	NEGR1	NKX3-2	FANCI	ERBB2IP	PROSC	TMEM2	FNBP1L	CPSF4	
MAP3K9	C6orf204	B3GNT1	CRISPLD1	RAB35	S100PBP	B3GNT5	ASAP1	PGRMC2	LBR	TMPO	
USP30	MTF1	NEDD4	TOP2A	ZNF280C	PNMAL1	TANC2	YWHAG	CBX5	ULK2	PIK3R3	
LAMP1	TMEM101	RASSF8	RUNX1	MEIS1	NDST1	MAP7D1	ZNF761	PIP4K2B	DMXL1	PPM1K	
CDC40	TRERF1	IL6R	NDRG4	FAM123B	MAPRE1	MARCKS	SEH1L	FKBP5	POM121	C1orf9	
NCOA1	ANKRD50	KIAA1467	ARHGEF6	JAZF1	SIX1	KPNA4	RAI14	EXOC5	UHMK1	NEDD4L	
SERINC1	CPEB4	FUT9	MEIS2	DHX15	BRWD1	RAP1B	ARSB	STARD3NL	USP46	TTC7B	
JMJD1C	TBC1D15	CTAGE5	SLC1A1	ZNF100	C3orf52	DLD	ZYG11B	CDS2	SETD8	CREBZF	
WDR37	WBP1	ELOVL2	DNM3	ATP11C	CDKN2AIPNL	PKNOX1	CHST3	PIK3C2A	STAT5B	ZNF493	
TCEB3	MDM4	ZNF506	PBX1	ADAMTS6	NAA15	PHACTR2	MAST4		ATXN7L3B	PPP3CA	
UVRAG	SH2B3	SH3BGR	VGLL3	NUAK1	TGFB2	CAPRIN1	ZNF91		BLCAP	DNAJC6	
ELF2	CHST10	ZIC4	TSPYL4	HNRNPA2B1	FBN1	LASP1	WNK1		ANXA2	LIMK2	
RSBN1	ZNF765	CARD8	TBC1D12	SLC39A10	WDR33	YIPF6	ZBTB34		ENC1	DACH1	
ATXN7	ZNF287	COL11A2	MITF	NFIB	TMEM64	TNPO1	DCUN1D5		PREB	ZNF30	
RAPGEF2	MARCKSL1	TMEM136	ZHX1	MPP5	CDK17	EML4	SRPK1		C12orf23	VEPH1	
SRGAP1	RAD17	PRDM1	ELF4	ADAM19	SEC24A	NAA50	HIAT1		STK35	BCL2	
ORMDL1	TET2	MKX	MAGOHB	QSER1	RBM25	UACA	YOD1		CNN2	VCAN	
SYS1	KDM4A	PCDHA3	FMR1	CCM2	TEAD1	DOCK7	RAD23B		EIF4EBP2	RNF43	

Table 24: Cross-intersection of genes differentially regulated by miR-23b after RNA-seq analysis with TargetScan prediction gene targets for this miRNA. Gene previously validated as miR-23b targets are highlighted in green.

Intersection of TargetScan prediction gene list and down-regulated genes in MCF-7 over-expressing miR-26a					Intersection of TargetScan prediction gene list and up-regulated in MDA-MB-231 stably expressing miR-26a-sponge construct			Intersection of up-regulated genes in MDA-MB-231 expressing sponge-26a, down-regulated genes in MCF-7 over-expressing miR-26a and TargetScan prediction gene list		
CPEB4	HOMER1	HIAT1	TP53INP1	ULK2	CTGF	RP2	ETNK1	RB1	NAA15	ADAM9
GSK3B	CARM1	ZNF192	UBN2	TBC1D15	CCNE2	SFPQ	TP53INP2	SERBP1	CTNNBIP1	MAEA
PTEN	NIPBL	NHSL1	KLHDC5	FRAT2	COL11A1	CDK2AP1	GRSF1	EZH2	HSPA8	SRP19
HMGA1	ANKRD11	PTPN13	RTF1	FGFR1OP2	CDH2	G2E3	DCAF7	PAK2	ARPP19	FAM98B
MAP3K2	CHD1	BBX	STRBP	C2CD2L	PRELP	NSF	LPP	CDC6	KPNA2	GPSM1
CDK8	WWP2	ATAD2B	KIAA1737	SH3D19	PITPNC1	NUP50	PHF20	MCL1	LARP1	KALRN
CPEB2	DMXL1	CPSF2	CREBL2	CEP68	SRSF3	PI4K2B	PGRMC2	CCNE1	ANKRD52	CHORDC1
SMAD1	EPC2	WIPF2	RHOQ	PAPD4	ZNF655	SLC7A6	PLOD2	PPP4R1	LUZP6	CDR2L
STRADB	SLC35A3	REPS2	PPP1R3D	FANCF	RGS4	GDF11	C18orf25	RBM12B	MTPN	ALS2
MTDH	ATP9A	JARID2	KIAA0528	TNRC6B	DEPDC1	PCNA	TMEM64	TNPO1	GMFB	MTERFD2
ESR1	DNAJC21	NIPA1	OSBPL2	RDH14	PRR5L	KIAA1383	CHST3	WAPAL	RAB11A	PDIK1L
CDK6	PJA2	YTHDF3	TMEM189	AMOT	CKS2	ZNF238	ADAM19	SFXN1	ACSL3	YAF2
CSNK1G1	LTBP1	FUT9	REST	CBLL1	DEPDC1B	TTC39C	AGPS	COPS6	EIF2S1	FPGT
KLF4	ZDHHC20	RANBP9	ANKRD50	RUFY3	RNF138	UMPS	IPPK	TGIF2-C20ORF24	MREG	ARMCX2
HSDL2	PRKCD	SLC38A1	SLC16A6	FAM55C	C7orf58	DBR1	LASP1	EIF4G2	RAB18	NCEH1
MYO5B	EP300	GREB1	FAM8A1	LIMS1	NAP1L5	KLHL15	ROD1	TMEM194A	RAP2C	(SEPT10)
TMTC3	COPS7B	SLC38A2	OSBPL11	MXI1	EPHA5	PSD3	NAV1	FAM136A	EAF1	ARL6IP6
ZFHX3	CREBZF	TRPS1	BAZ2B	PCDH9	TSPYL4	FAM118B	CMTM4	DDX17	OTUD4	TTC13
C12orf51	TANK	RAB31	ABR	TTC28	LEF1	PURA	KCMF1	YWHAE	MYH10	(MARCH1)
TMEM33	TNKS1BP1	TET2	SLC35E2	CCNJ	MKRN3	PTP4A1	UBE2K	UBE2G1	PRDX3	UBR3
BOD1	HUWE1	MLEC	TBC1D13	C5orf41	ITGB8	C16orf70	ADNP2	USP15	RAB21	
CAMSAP1	SRCAP	TOB1	HSPA13	KIAA1539	PCDH18	ADAMTS6	FAM49B	PPP3CB	TAF9B	
TAOK1	XPR1	MAPK6	FBXO28	BAG4	ACSL4	E2F2	RCOR1	RCN2	SC4MOL	
E2F7	NAB1	DLG5	CTNND2	MMP16	SLC25A20	UCK2	ATXN7	CHAF1A	HNRNPUL1	
ARHGEF12	MAP9	TFAP2C	MKNK2	STAG3L4	MITF	TFAM	BRWD3	RNF6	EHD1	
NT5DC1	TMCC1	CTDSP2	ALDH5A1	CCDC28A	MAP2	TMEM200B	DAB2	UBE3A	LETM1	
ADRBK1	ZNF516	MEGF9	ZDHHC6	C2CD2	TBC1D4	BAK1	LARP4B	PPP2R3A	ZFC3H1	
SLC25A36	CCDC6	SERP1	BLOC1S2	FAM160A1	KAZN	ARHGAP29	PIM1	PDCD10	FAM98A	
BFAR	EYA3	GOLGA3	LNX2	FA2H	ENC1	VSIG10	G3BP2	GNPNAT1	WDR33	
RPRD2	NLK	SSFA2	STYX	C17orf103	MTMR1	ZFX	SLC12A2	DDX52	SAR1B	
GTF3C2	WNK1	TET3	KCNK1	PPP1R9A	ATP10A	SGMS2	TIAL1	PIK3R3	PPP2R5A	
EPG5	SULF1	CELSR1	EPHA7	NOVA1	HAS2	MAT2A		PHAX	ATPAF1	
CLASP2	POM121	ULK1	TSC22D4	SLC1A1	TBC1D12	LLPH		COPS2	ARHGEF26	
ERMP1	SENP5	PGR	ST8SIA4	PALM3	VMA21	LSM11		AMMECR1	C20orf24	
REEP3	NR1D2	FBXW2	FAM46C	ZNF44	POLR3G	METAP2		DYRK1A	FKTN	
MFSD6	KIAA0240	PFDN4	CASZ1	GGA3	ERLIN1	COX5A		CAPZB	ARHGAP17	
CCDC50	CEBPG	KPNA6	VGLL4	PRKAG2	FAM199X	SH3RF1		ABL2	BCL7B	
TTPAL	SLC22A23	NUS1	DCDC2	HTR2C	MICAL3	MFAP3		RAP1A	PHF6	
EP400	RAB3IP	KIAA1598	LRRC16A	KIAA2022	PGM2	MATR3		BICD2	ATP11C	
DIDO1	SLC33A1	KIAA0947	ATF2	INTU	MEF2C	WDR20		NRAS	MTX2	
TAB3	SLC19A2	BCR	SNN	MYPOP	CELF2	C10orf12		CELF1	ACBD5	
PLEKHH1	RNF141	EPS15	FBXL19	MUM1L1	ABHD5	KPNA3		UBTD2	PMAIP1	
MAP7	TBC1D30	PHF3	SAMD8	GRB10	ADAT1	NCOA4		SACS	CCDC90A	
POM121C	TNKS2	ZNF410	KIAA2013	RPS6KA2	CORO1C	C10orf137		LSM12	REEP4	
CTTNBP2NL	THRAP3	SLC9A2	CHIC1	MAP1A	DAPK1	RFX7		SETD8	RBM24	
C12orf35	TMEM106B	SLC35E2B	PHF21A	TXNRD3	PTER	JAG1		CHFR	COMMD8	
HOOK1	SRGAP1	HS6ST1	HECTD3		WHSC1	NUP153		PDHX	KLHL18	
ZNF275	GMDS	NCAM2	UBE2E2		KBTBD8	AP1S3		UBTF	TFAP2A	
ZFP106	TLK2	ZBTB38	TMEM184B		UBE2D1	TWF1		C9orf40	PLCB1	
	FBXO11	UBE4B	ACVR2B		DNA2	RHOU		MTM1	MYCBP	

Table 25: Cross-intersection of genes differentially regulated by miR-26a after RNA-seq analysis with TargetScan prediction gene targets for this miRNA. Gene previously validated as miR-26a targets are highlighted in green.

GO: cross-intersections of genes down-regulated in miR-23b-overexpressing MCF-7 cells with those up-regulated in MDA-MB-231 cells after miR-23b inactivation, and with TargetScan-predicted targets for miR-23b

Term	*P* Value
Phosphorylation	2.20E-04
Peptidyl-serine modification	1.60E-03
Protein amino acid autophosphorylation	1.60E-03
Hemopoiesis	1.30E-02
cAMP-mediated signaling	1.90E-02
Immune system development	2.40E-02
Cell junction assembly	2.40E-02
Axonogenesis	2.70E-02
Osteoclast differentiation	3.50E-02
Neuron projection morphogenesis	3.70E-02
Negative regulation of cytoskeleton organization	4.20E-02
Leukocyte differentiation	4.30E-02
Response to hydrogen peroxide	4.30E-02
Cell junction organization	4.50E-02
Cell morphogenesis involved in differentiation	5.60E-02
Cell death	6.20E-02
Response to organic substance	6.20E-02
Response to peptide hormone stimulus	6.30E-02
Programmed cell death	6.90E-02
Response to reactive oxygen species	7.30E-02
Regulation of gene expression, epigenetic	7.60E-02
Regulation of transcription	7.60E-02
Tissue morphogenesis	9.10E-02

Figure 49: GO term analysis of miR-23b potential gene targtes retrieved after RNA-seq confirms the initial bioinformatic DAVID analysis on the miR-23b targets predicted by TargetScan and the functional phenotypes affected by miR-23b *in vitro*. List of enriched GO terms found using DAVID functional annotation database for the gene list resulted from the intersection of the 938 potential miR-23b gene targets predicted by TargetScan software, the genes down-regulated after miR-23b overexpression in MCF-7 cells, and the ones up-regulated after miR-23b inactivation in MDA-MB-231 cells. Each annotated Term is associated with a specific *P* value. Significant pathways enriched for these intersected genes and retrieved in the initial DAVID analysis are highlighted in blue. Significant pathways enriched for these intersected genes which are retrieved in the initial DAVID analysis and confirmed by our experimental investigation are highlighted in red.

3.3.1.3.1 RT-qPCR validation of a set of transcripts from the RNA-seq experiments

Considering that the intersection lists of genes reported in **tables 22** and **23** probably contain several direct targets of these miRNAs, we wished to experimentally validate our RNA-seq analysis by performing RT-qPCR assays on selected transcript belonging to this intersection. Our selection and the function of potential direct targets of miR-23b or miR-26a are reported in **table 24** and **25**, respectively.

Gene	Function	Ref.
ANXA2 (Annexin 2)	Phospholipid-binding protein involved in plasminogen activation, interaction with the ECM, cell invasion, neoangiogenesis and metastasis	[68, 70, 73, 74]
ARHGEF6 (RAC/CDC42 guanine nucleotide exchange factor)	Guanine nucleotide exchange factor (GEF) specific for RAC and CDC42 small GTPases, induces lamellipodia and filopodia formation, localises PAK at focal adhesion sites	[156, 173, 174, 176]
CFL2 (Cofilin 2)	Actin filament depolymerisation factor, controls lamellipodia formation, its depletion reduced migration and invasion of BC MDA-MB-231 cells	[420-422]
ENAH (Enabled Homolog [Drosphila])	Actin-associated protein, involved in cytoskeletal dynamics, lamellipodia and filopodia formation, cell spreading	[423]
GSK3B (Glycogen synthase kinase 3 beta)	Serine-threonine kinase mainly involved in glycogen metabolism, contributes to cytoskeletal dynamics, cell-matrix interactions, lamellipodia formation and cell migration by activating Rho small GTPases	[424]
LIMK2 (LIM domain kinase 2)	Regulates cytoskeletal dynamics by phosphorylating and inactiving cofilin, leading to inhibition of cofilin-mediated actin nucleation severing; its depletion reduced migration and invasion of BC MDA-MB-231 cells	[124, 425, 426]
MACF7 (Microtubule-actin cross linking factor 1)	F-actin-binding protein, mediates interaction of actin cytoskeleton with microtubules, necessary for HER2-induced chemotaxis and microtubule capture at the leading edge of migrating cells	[427]
PIK3R3 (Phosphoinositide-3-kinase, regulatory subunit 3)	Encodes for the p55γ subunit of the phosphoinositide-3-kinase (PI3K) wich mediates recruitment and activation of PI3K by membrane receptor-triggered signalling cascades that regulates cytoskeletal dynamics and migration in response to external stimuli	[428]
PLAU (Plasminogen activator, urokinase)	Serine protease involved in plasminogen activator, degradation of the ECM and cancer cell invasion; inhibition of its activity abolishes BC invasion and metastasis *in vivo*	[66, 429]
PPP1R12A1(Protein phosphatase 1, regulatory subunit 12A)	Also known as MLC phosphatase targeting subunit 1 (MYPT1) allows myosin phosphatase to dephosphorylate MLC, resulting in its inactivation; its depletion causes inhibition of MLC dephosphorylation, cell migration and adhesion	[430]
RAP1A and RAP1B (Ras-related protein Krev-1 A and B)	Two isoforms of the RAP1 member of the Ras GTPases family, orchestrate signalling pathways that regulate cell-cell and cell-matrix adhesions and ECM degradation, leading to cell proliferation migration and invasion	[431]
SSH2 (Slingshot homolog 2 [Drosophila])	Protein phosphatase, that dephosphorylates cofilin thus leading to its activation, promotes lamellipodia formation, cell migration and invasion	[432]
TLN2 (Talin 2)	Cytoskeletal protein involved in focal adhesion formation by linking integrins to vinculin and actin; its depletion inhibits BC cell migration and invasion	[433]

Table 26: Description and functions of genes differentially regulated by miR-23b after RNA-seq analysis and predicted as putative miR-23b targets (TargetScan analysis).

Gene	Function	Ref.
ABL2 (Abelson Tyrosine kinase-protein 2)	Non-receptor tyrosine protein kinase and F-actin-binding protein, regulates cytoskeletal dynamics involved in cell adhesion	[434]
CHFR (Checkpoint with forkhead and ring finger doamins)	E3 ubiquitin-protein ligase and early mitotic checkpoint that delays transition to metaphase in response to mitotic stress. Its expression is lost in BC leading to aneuploidy and increased tumourigenicity	[213, 220]
LARP1 (La ribonucleoprotein domain family member 1)	RNA-binding protein involved in translational initiation; its knockdown results in cell cycle arrest in G2/M due to defective chromosome segregation and cytokinesis, apoptosis, inhibition of cell migration and ipaired distribution of actin isoforms	[435]
MCL1 (Myeloic cell leukemia sequence 1)	Member of the Bcl2 family, with pro-survival and anti-apoptotic functions; reduction of its expression sensitizes cells to apoptosis and tumourigenicity in BC	[436] [437]
NRAS2 (Neuroblastoma RAS viral oncogene homolog)	GTPase member of the Ras oncogene family, functions in signal transduction pathways to control cell proliferation, differentiation and survival; regulates cytoskeletal dynamics relevant to cell adhesion	[438]
RAP2C (Ras-related protein Rap-2c)	GTPase member of the Ras-related protein subfamily of the Ras oncogene superfamily, mainly involved in regulation of cytoskeletal re-organisation and cell spreading on ECM	[439]
STX2 (Syntaxin 2)	Member of the SNARE protein superfamily implicated in the exocytosis of transport vescicles; its knockdown in mammalian cells results in failure of late stages of the cytokinesis process leading to formation of binucleated cells	[231]
YWHAE (Tyrosine 3-Monooxygenase/Tryptophan 5-Monooxygenase Activation Protein,Epsilon Polypeptide)	Member Epsilon of the 14-3-3 family of phospho-serine/phospho-threonine-binding proteins implicated in a wide variety of biological processes including cell adhesion, apoptosis, anchorage-independent growth and cytokinesis; their down-regulation induces cytokinesis defects, resulting in enlarged multinucleated cells	[224, 230, 440]

Table 26: Description and functions of genes differentially regulated by miR-26a after RNA-seq analysis and predicted as putative miR-26a targets (TargetScan analysis).

Our RT-qPCR experiments confirmed the down-regulation of these genes in MCF-7 cells overexpressing either miR-23b or miR-26a, and their up-regulation in MDA-MB-231 cells where miR-23b or miR-26a activity was inhibited by the miRNA sponge constructs, thus confirming the reliability of our methods (**Figure 50** and **51**).

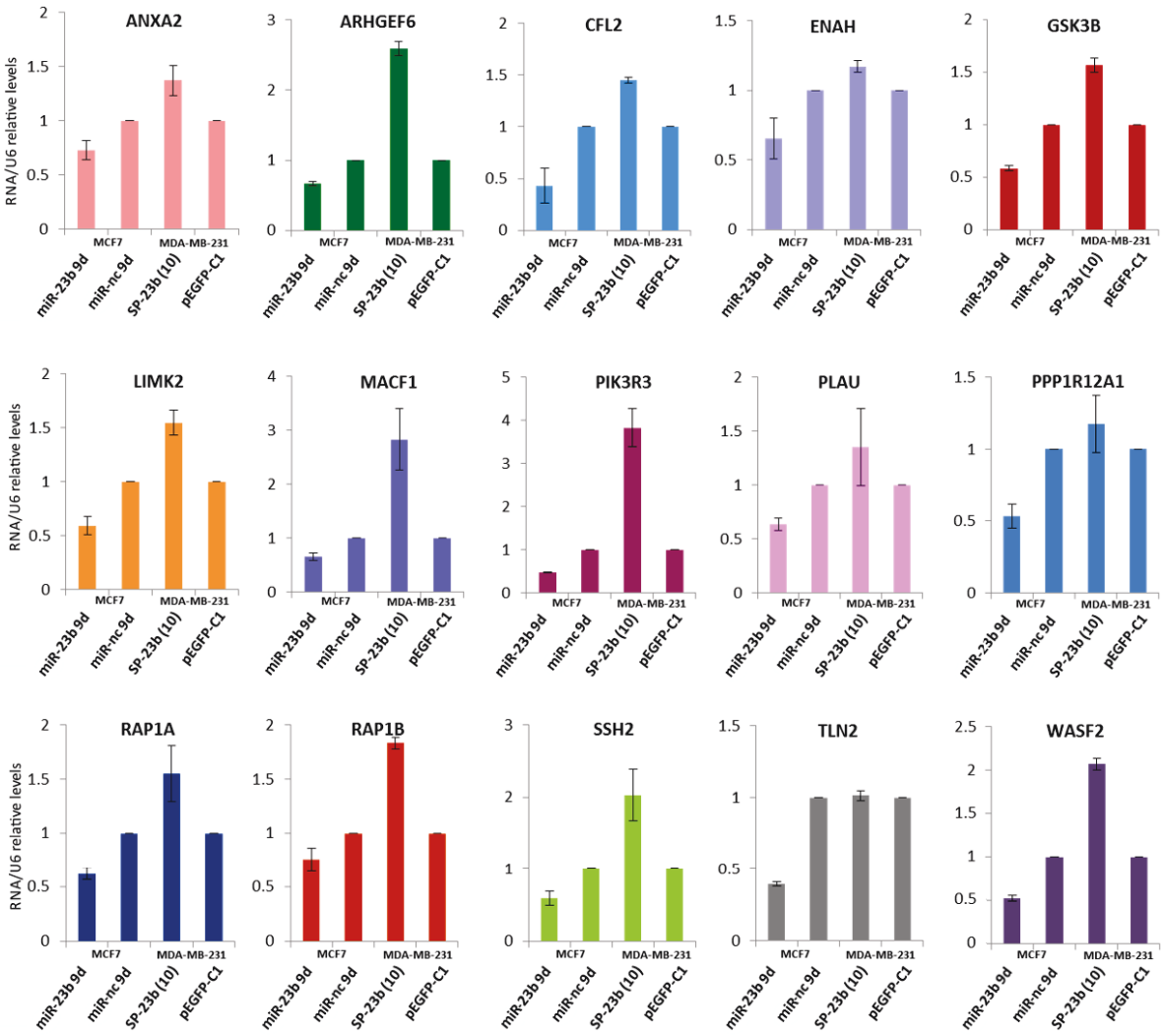

Figure 50: Validation of RNA-seq results relative to genes differentially regulated by miR-23b. RT-qPCR assays of the indicated mRNAs in MCF-7 cells transfected with miR-23b or miR-n.c. precursors (5nM) for 9 days and in MDA-MB-231 cells stably expressing the miR-23b-sponge construct or the pEGFP-C1 parental control vector. Data are mean of three independent experiments ± s.e.m.

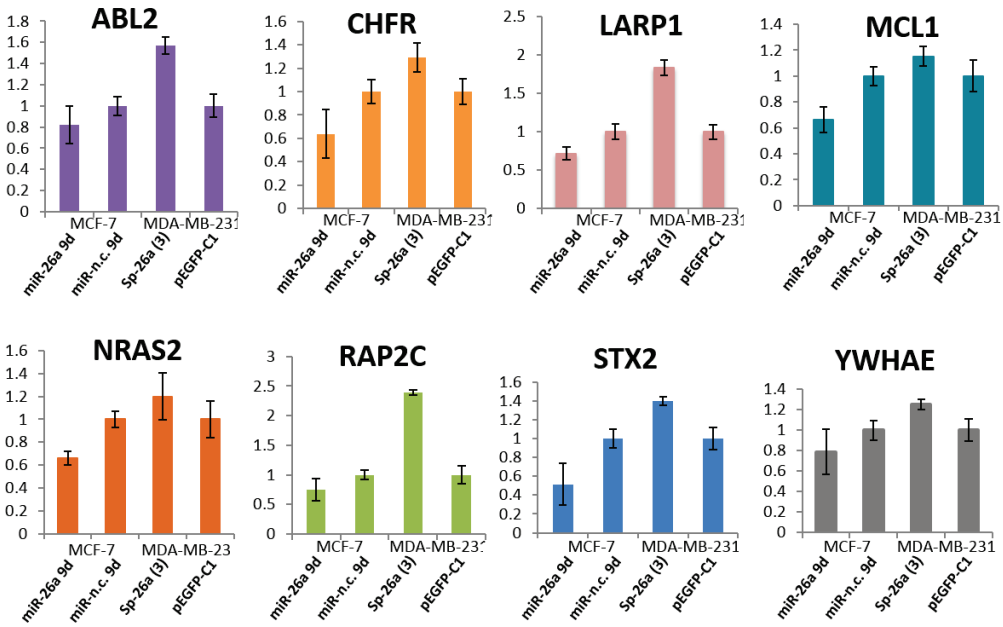

Figure 51: Validation of RNA-seq results relative to genes differentially regulated by miR-26a. RT-qPCR assays of the indicated mRNAs in MCF-7 cells transfected with miR-26a or miR-n.c. precursors (5nM) for 9 days and in MDA-MB-231 cells stably expressing the miR-26a-sponge construct or the pEGFP-C1 parental control vector. Data are mean of three independent experiments ± s.e.m.

3.3.1.3.2 Validation of miR-23b and miR-26a specific gene targets

3.3.1.3.2.1 MiR-23b directly targets a set of genes relevant to cytoskeletal remodelling, migration and invasion in BC

In order to validate these genes as direct targets of the miR23b, we further selected 7 of those genes (*LIMK2*, *ARHGEF6*, *CFL2*, *PIK3R3*, *PLAU*, *ANXA2*, *TLN2*) that are well described as regulators of cytoskeleton organisation, cell migration, invasion and metastasis (**Table 26**) and performed 3'UTR luciferase reporter assays (**Figure 52B** and **C**). Under conditions of both gain- and loss-of-function for miR-23b, we could demonstrate the direct regulation by mir-23b of 6 out of 7 of these genes (**Figure 52B** and **C**). In fact, overexpression of miR-23b in MCF-7 cells resulted in a significant reduction of the luciferase activity of reporter constructs containing the 3'UTR of each *ANXA2, ARHGEF6, CFL2, LIMK2*, *PIK3R3* and *PLAU* (**Figure 52A** and **B**). Contrarily, inhibition of miR-23b activity by transfection of MCF-7 cells with the miR-23b-sponge vector was able to release the luciferase activity of the same 3'UTR reporter constructs from the suppressive activity of endogenous miR-23b (**Figure 52C**). In addition, we performed site-directed mutagenesis of the miR-23b-binding sites present in the 3'UTR of these genes (excluding PLAU as it is a previously

validated miR-23b target) followed by further 3‘UTR luciferase reporter assays upon miR-23b overexpression (**Figure 52A** and **B**). As shown in **Figure 52B**, miR-23b was unable to repress the luciferase activity of the mutated 3‘UTRs constructs compared to correspondent wild type variant and negative control. Therefore, we were able to precisely define the interaction site used by miR-23b to directly repress these gene targets.

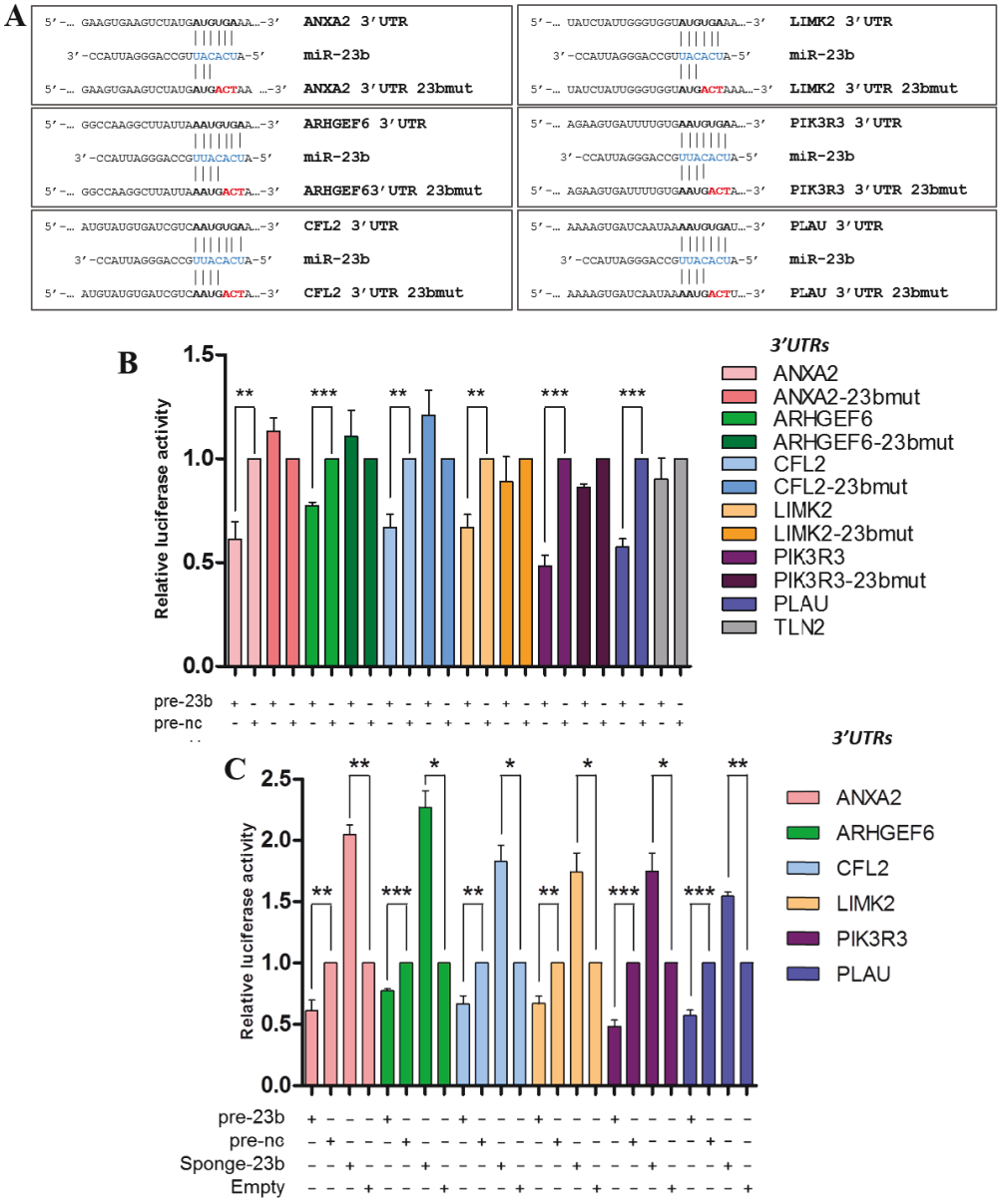

Figure 52: MiR-23b targets *ANXA2*, *ARHGEF6*, *CFL2*, *LIMK2*, *PIK3R3* and *PLAU* mRNAs by directly interacting with their relative 3’UTRs. A, Representation of the miR-23b and the indicated target mRNA 3‘UTR heteroduplexes: base pairing between the miR-23b-binding site (in bold) and the miR-23b “*seed*“ region (in blue) is disrupted when the miR-23b-binding site are mutated (in red). **B-C,** Relative luciferase activity levels were measured after 24h from co-transfection of MCF-7 cells with the indicated 3‘UTR-luciferase reporter constructs either with miR-23b or miR-n.c. precursors (100nM) or with mi-23b-sponge construct or pEGFP-C1 parental control (150ng). Data are mean of three independent experiments (each of them performed in triplicate) ± s.e.m (*P < 0.05, **P ≤ 0.006,***P ≤ 0.0005).

3.3.1.3.2.2 MiR-26a directly targets a set of genes relevant to cytokinesis and apoptosis

We then validated additional targets of miR-26a using the same experimental approach undertaken for miR-23b. In this case, we selected 5 genes (*CHFR*, *LARP1*, *NRAS*, *MCL1*, and *YWHAE*) with important functions in cytoskeletal remodelling, cytokinesis and apoptosis (**Table 26**). As shown in **figure 53A** all the chosen genes present one miR-26a-binding site in their 3'UTR, except *LARP1* which contains three miR-26a interaction sites that are found highly conserved (1LARP1 and 2LARP1) or poorly conserved (3LARP1) across vertebrates. By performing 3'UTR luciferase reporter assays, we demonstrated that miR-26a overexpression in MCF-7 cells significantly suppresses the luciferase activity of reporter constructs containing the 3'UTR of *CHFR*, *LARP1*, *MCL1* and *YWHAE* (**Figure 53B**), which was conversely increased upon inhibition of the miRNA by co-transfecting these cells with the miR-26a-sponge vector, compared to relative controls (**Figure 53C**). NRAS 3'UTR-relative luciferase activity did not change upon miR-26a overexpression suggesting that NRAS is not a direct target of this miRNA (**Figure 53B**).

We then wished to describe the precise 3'UTR-embedded interaction sites by which miR-26a regulate expression of these reporter constructs. Therefore, we mutated or deleted all the predicted miR-26a-binding sites included in the 3'UTR of the genes that are regulated by miR-26a; in the case of LARP1 3'UTR, we also created reporter construct variants in which any of the three miR-26a interaction sites were mutated or deleted (**Figure 53A**). In **figure 53B**, it is observed that miR-26a-mediated repression of *CHFR*, *MCL1* and *YWHAE* is impaired when they carry mutated or deleted binding-sites for the interaction of this miRNA. Concerning *LARP1* regulation, we observed that miR-26a suppresses luciferase activity of the reporter containing the wild type 3'UTR by binding to the second (2LARP1) and the third interaction site (3LARP1), the latter seemingly less functional for miR-26a-mediated LARP1 repression (**Figure 53B**), but not to the first one (1LARP1). Indeed, deletion of 2LARP1 site completely abrogates repression of LARP1 3'UTR luciferase activity by miR-26a, whereas mutated 3LARP1 only partially affects miR-26a activity in targeting this gene. Mutations in the first interaction site (1LARP1) instead fail to impair miR-26a-mediated repression of LARP1 3'UTR (**Figure 53B**).

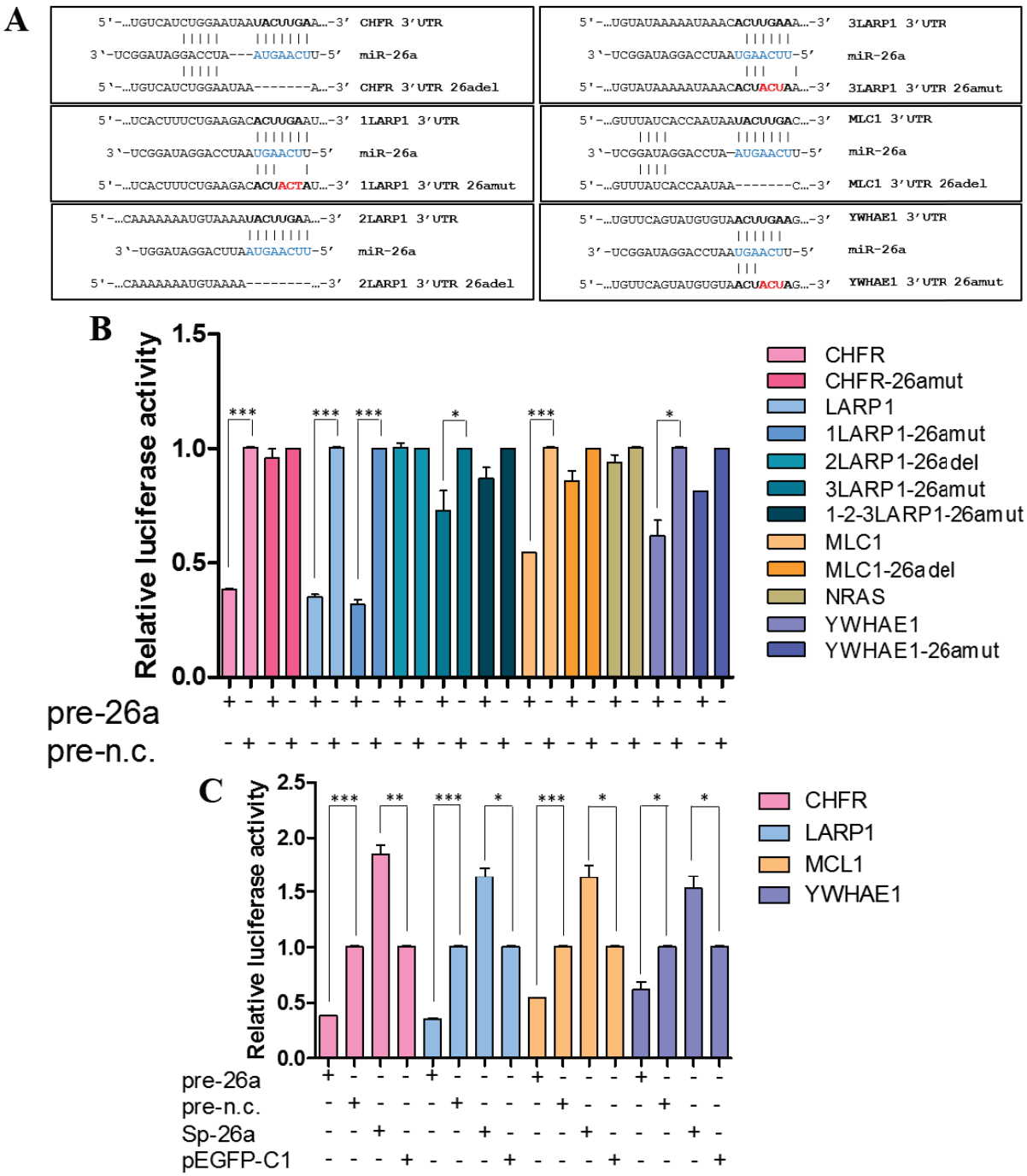

Figure 53: MiR-26a targets *CHFR*, *LARP1*, *MCL1* and *YWHAE* by directly interacting with their relative 3'UTRs. A, Representation of the miR-26a and the indicated target mRNA 3'UTR heteroduplexes: base pairing between the miR-23b-binding site (in bold) and the miR-23b "*seed*" region (in blue) is disrupted when the miR-23b-binding site are mutated (in red). **B-C,** Relative luciferase activity levels were measured after 24h from co-transfection of MCF-7 cells with the indicated 3'UTR-luciferase reporter constructs either with miR-26a or miR-n.c. precurors (100nM) or with mi-26a-sponge construct or pEGFP-C1 parental control (150ng). Data are mean of three independent experiments (each of them performed in triplicate) ± s.e.m (*P < 0.05,**P ≤ 0.006,***P ≤ 0.0005).

CHAPTER 4

DISCUSSION

4.1 Roles of miR-23b and miR-26a in BC

The role of microRNAs (miRNAs) in regulation of molecular pathways relevant to tumourigenesis and cancer progression has been largely investigated[247, 406]. In the course of this thesis, we have described two miRNAs, miR-23b and miR-26a, as crucial regulators of BC pathogenesis. By using a strategic approach based on both bioinformatic and experimental evaluation, we show that miR-23b and miR-26a participate in multiple processes during BC development, by performing both similar and distinct functions.

Initially we focused on miR-23b, as its involvement in hepatocellular carcinoma was known[405], but its global function in BC was poorly understood. Using a bioinformatic approach based on pathway enrichment analyses, we proposed a role for miR-23b in cytoskeletal remodelling, subsequently demonstrating this experimentally and validating *PAK2*, a key modulator of cytoskeletal dynamics, as its direct target. Interestingly, we demonstrated that miR-26a also targets *PAK2* at a different site on its 3΄΄UTR, thus implicating this miRNA in regulation of cytoskeletal remodelling. We demonstrated that experimental expression of miR-23b and miR-26a in BC cells promotes focal adhesion and cell spreading on the ECM, phenotypes that are partly ascribed to miRNA-mediated regulation of PAK2. Nevertheless, the phenotypic changes observed following manipulation of either miRNA did not entirely overlap. In fact, we observed that miR-23b alone controls cell-cell adhesion and lamellipodia formation, whereas miR-26a enhances BC cells capabilities to adhere to the ECM. Further investigation pinpointed a striking ability of miR-23b in the control of BC progression, as it affects cell migration, invasion and metastasis both *in vitro* and *in vivo*. On the other hand, miR-26a seems to affect cytokinesis and to enhance aneuploidy occurrence and tumourigenicity *in vitro*.

The observation that miR-23b and miR-26a mediate different cellular phenotypes, despite regulating a common gene target (*PAK2*) is expected, as it is well-known that a single miRNA is able to control multiple genes [272]. In order to evaluate the entire gene set regulated by either miRNA, we performed high throughput RNA-sequencing (RNA-seq) analysis upon engineered manipulation of the intracellular levels of either miRNA. Notably, we experimentally induced long-term (9 days) overexpression or stable inhibition of miR-23b or miR-26a in two BC cell lines, MCF-7 and MDA-MB-231 cells, respectively, as maximal effect of miRNA activity on gene expression is achieved under conditions of prolonged miRNA-specific deregulation[326]. It is well established that miRNAs mediate destabilisation of target mRNAs by inducing their deadenylation and degradation[284-286]. With this in mind,

we reasoned that, among the transcripts found to be down- or up-regulated upon miRNA overexpression or inhibition, respectively, those that contain predicted sites for the specific interaction with miR-23b or miR-26a are to be considered as high confident targets of either miRNA. By performing 3'UTR-luciferase reporter assays, we validated a specific subset of genes as direct targets of miR-23b or miR-26a; the physiological roles of these genes is relevant to distinct molecular pathways implicated in the cellular phenotypes observed following targeted miRNA manipulation. Coordinated repression of these targets along with specific miRNA-mediated perturbation of the transcriptome state of BC cells enabled our understanding of the molecular mechanism(s) that underlies the cellular functions of miR-23b and miR-26a.

4.1.1 Roles of miR-23b and miR-26a in cytoskeletal dynamics

4.1.1.1 MiR-23b regulates cell-cell adhesion in epithelial BC cells

Firstly, we outlined a role of miR-23b in the regulation of cell-cell interactions. Under transient transfection conditions, we observed that ectopic overexpression of miR-23b, but not miR-26a, enhanced epithelial characteristics of BC MCF-7 cells (**Figure 22A**), without affecting protein expression levels of the epithelial molecular marker E-cadherin (**Figure 22B**). Under the same conditions, miR-23b failed to induce an epithelial phenotype in MDA-MB-231 cell line (**Figure 22C**), a mesenchymal model of BC cells in which E-cadherin is normally not expressed, probably because miR-23b was unable to promote E-cadherin expression or form new adherens junctions (AJs). E-cadherin is, in fact, a key component of AJs, adhesive structures that mediate interaction of two adjacent cells by anchoring their actin cytoskeleton at the intracellular level via α- and β-catenin[139]. During the course of our study, several groups have reported the ability of miR-23b in promoting epithelial characteristics of colon and prostate cancer metastatic cell models, by inducing up-regulation of E-cadherin and repression of mesenchymal markers, such as Vimentin and Snail[353, 355, 356]. On this basis, we hypothesised that miR-23b may have a role in inhibiting epithelial-to-mesenchymal transition (EMT) during BC progression and that its potential regulation of E-cadherin expression may depend on a temporal factor. Therefore we performed long-term (9 days) overexpression of miR-23b in both MCF-7 and MDA-MB-231 cells, in order to potentially revert EMT and release E-cadherin from its mesenchymal marker-mediated repression in the latter cell line[326, 375]. However, we observed that prolonged miR-23b overexpression failed to revert EMT in

mesenchymal-like MDA-MB-231 cells (**Figure 23A**) and to induce E-cadherin up-regulation in both MDA-MB-231 and MCF-7 cells, neither at the protein nor at the mRNA level (**Figure 23A** and **B)**. On the other hand, maintained miR-23b levels improved the overall architecture of epithelia formed by 2-D cultures of MCF-7 cells, which exhibited more orderly and stable AJs compared to control-treated cells (**Figure 23B** and **C**). Taken together, these data suggest that in the context of BC, miR-23b reinforces epithelial characteristics by different mechanisms that do not imply E-cadherin up-regulation and *de novo* formation of AJs, but that rather confer enhanced tension between existing E-cadherin-mediated cell-cell adhesions. Nevertheless, analysis of our RNA-seq data revealed that prolonged overexpression of miR-23b in MCF-7 cells induced transcriptional up-regulation of *Nectin 1* (*PVRL1*) and *Nectin 2* (*PVRL2*), *β-catenin* (*CTNNB1*) and *LMO7*, encoding for cell adhesion molecules highly involved in cell-cell junction formation[136, 137, 143, 441] (**Table 15**). Particularly, Nectin1 and 2 are members of the Nectin family of transmembrane receptors that are involved in early establishment of cell-cell contacts, known as tight and adherens junctions[136]. These findings suggest that miR-23b may actually induce *de novo* formation of both tight and AJs through a mechanism that requires Nectin1 and Nectin2 overexpression and is independent of E-cadherin; in order to address this point, experimental analysis of protein levels and sub-cellular localisation of both Nectin 1 and Nectin 2 isoforms upon prolonged miR-23b over-expression in MCF-7 cells should be further investigated. Alongside the potential establishment of new cell-cell contacts, miR-23b may be involved in cell-cell contacts development, by stabilising existing and newly formed AJs via up-regulation of β-catenin and LMO7, adaptor molecules that mediate aggregation of E-cadherin- and Nectin-based adhesive clusters and strengthen the adhesive capabilities of E-cadherin[143, 441]. Moreover, mir-23b likely contributes to enhance the junctional tension during assembly of the epithelia, by indirectly promoting local myosin II activity, which is required to produce the contractile force that mediates aggregation of E-cadherin clusters and maintains the tension during AJs maturation. Indeed, we detected increased myosin light chain II (MLCII) phosphorylation, indicative of myosin II activity, upon miR-23b overexpression in different cell lines, including MCF-7 cells.

4.1.1.2 MiR-23b and miR-26a share limited overlapping functions

4.1.1.2.1 MiR-23b and miR-26a target PAK2 and induce MLCII phosphorylation

We identified PAK2 as a candidate target of both miR-23b and miR-26a, as its 3′UTR contains a specific binding site for the interaction with either miRNA (**Figure 34A**). By combining different experimental techniques, we demonstrated that both miR-23b and miR-26a directly target PAK2, inducing its repression both at the protein and the mRNA level. Western blot analysis showed that miR-23b overexpression reduces PAK2 protein levels up to 60% and 50% in BC MDA-MB-231 and MCF-7 cells, respectively, and up to 80% in HCT116 colon cancer cell line (**Figure 35A**), consistently with the observation by Zhang *et al.*[353]. Although at a minor extent compared to miR-23b activity, ectopic expression of miR-26a was also able to decrease PAK2 protein levels in all three of the cell lines analysed (40%, 40% and 60%, respectively) (**Figure 35A**), indicating for the first time PAK2 as a target of miR-26a. Moreover, miRNA loss-of-function investigation using miRNA-sponge constructs, confirmed that inhibition of the endogenous activity of either miRNA enabled the release of PAK2 expression from miRNA-mediated repression in both MCF-7 and MDA-MB-231 cells (**Figure 36**). Our RNA-seq data showed that PAK2 mRNA levels were greatly down-regulated in MCF-7 cells upon prolonged overexpression of miR-23b or miR-26a and up-regulated in MDA-MB-231 cells that stably express a sponge construct that mediates specific inhibition of miR-23b or miR-26a (**Table 24** and **25**). These data confirmed not only the experimental validity of our RNA-seq analysis, but also that miR-23b and miR-26a are implicated in the repression of PAK2. In addition, by performing 3′UTR-luciferase reporter assays, we confirmed that miR-23b or miR-26a mediates PAK2 repression by interacting directly with its own predicted binding site embedded in the PAK2 3′UTR, as site-direct mutations that disrupt this interaction impede each miRNA to repress PAK2 3′UTR-relative luciferase activity (**Figure 37B** and **C**). However, our miRNA-sponge constructs failed to induce an increase of luciferase activity of PAK2 3′UTR (data not shown). This suggests that the regulation exerted by miR-23b and miR-26a on PAK2, by binding to the analysed site, makes a minor contribution to the repression of PAK2, indicating that other mechanisms indirectly mediated by either of the miRNA may be involved. Our 3′UTR-luciferase reporter analysis also showed that neither miRNA mediates post-transcriptional regulation of PAK1 (**Figure 37D**), an expected finding as it is not a predicted target for miR-23b or miR-26a (**Figure 35B**). However, we observed that overexpression of miR-23b or miR-26a in three

cell lines, where PAK2 is greatly down-regulated, slightly reduced PAK1 protein levels (**Figure 35A**). This effect is consistent with our observation that PAK2 knockdown by siRNA in MDA-MB-231 cells is accompanied by a marked reduction of PAK1 (**Figure 34D**). Although an off-side effect in the specificity of PAK2 siRNA is not to be excluded, it is plausible that a decrease of intracellular PAK2 levels leads to a consequent reduction of PAK1 protein levels. Accordingly, it has been demonstrated that PAK1 and PAK2 *trans*-interact to form heterodimers in order to inhibit each other activity and stabilise their cytoplasmic forms. In addition, altered expression of either isoforms disrupts heterodimerisation, thus enhancing their sensitivity to degradation[442, 443].

Additionally, we found that miR-23b and miR-26a overexpression greatly promoted phosphorylation of the MLCII in MDA-MB-231, MCF-7 and HCT116 cells (**Figure 35B**). Since we observed that siRNA-mediated PAK2 depletion in MDA-MB-231 cells was accompanied by a marked increase of MLCII phosphorylated levels (**Figure 34D**), which was consistent with the effect observed upon PAK2 silencing in BC T47D cells[129], it seems that miR-23b/miR-26a promote MLCII phosphorylation through down-regulation of PAK2. Moreover, our RNA-seq analysis showed a dramatic increase of the MLCK transcript levels in MCF-7 cells overexpressing miR-26a, suggesting that increased MLCII phosphorylation by miR-26a occurs also through MLCK up-regulation (**Table 17**).

4.1.1.2.2 MiR-23b and miR-26a promote focal adhesion maturation and cell spreading on the ECM

Our results suggest that both miR-23b and miR-26a modulate maturation of FAs and increase the properties of cells to spread on the ECM (**Figure 24**). We observed that MDA-MB-231 cells spreading on collagen I matrixes and stained for the FA marker Vinculin exhibit larger FA sites upon transient transfection of either miR-23b or miR-26a mimic compared to control-treated cells (**Figure 24A**). The average of FA areas was shown to be significantly increased in cells overexpressing either miRNA, and this increase was slightly more pronounced in miR-26a-transfected cells (**Figure 24A,** graph). FAs are adhesive complexes that connect the actin cytoskeleton to elements of the ECM in order to support cell morphology and movement along the ECM[153, 408]. Multiple cytoplasmic proteins are implicated in the formation and maturation of FAs, including integrins, Vinculin and PAKs. Larger FA sites manifest upon excessive maturation of newly formed FAs, a process that

requires local activity of myosin II[162, 408]. At FA sites, myosin II activity is tightly regulated by the PAKs. PAKs control the activation state of myosin II either by directly phosphorylating MLCII or by inhibiting the activity of MLCK, which results in reduced myosin II phosphorylation[126, 442]. PAK2 seems to have a major role in FA maturation, by limiting the size of FA sites. Indeed, it has been shown that PAK2 depletion in T47D BC cells resulted in larger FA sizes, increased MLCII phosphorylation and reduced migratory capabilities of these cells[129]. Accordingly, we demonstrated that PAK2 silencing is able to increase phosphorylated MLCII levels and reduce cell migration in MDA-MB-231 cells (**Figure 34C** and **D**). These data along with our findings that miR-23b or miR-26a overexpression in MDA-MB-231 cells led to repression of PAK2 and enhanced MLCII phosphorylation (**Figure 35**) indicate that these two miRNAs contribute to FA maturation partly via repression of PAK2 and stimulation of myosin II activity.

Moreover, miR-23b may also enhance FA development by limiting PAK2 localisation and activity at the FA sites through repression of ARHGEF6, which we found to be a miR-23b direct target (**Figure 52**). ARHGEF6, also known as PAK-interacting exchange factor alpha (αPIX) or Cloned out of library 2 (COOL2) is a well-described activator of RAC and CDC42 small GTPases; it directly interacts with PAKs and mediate their localisation at FA sites where it induces PAK activation through local stimulation of RAC and CDC42.

Additionally, since fully developed FAs are associated with slower migration rates[32], miR-23b-mediated negative regulation of PAK2 expression and effect on FA maturation can partly contribute to miR-23b ability in inhibiting migratory capabilities of MDA-MB-231 cells (**Figure 31A**). However, our findings that miR-26a did not affect cell migration, but yet shared with miR-23b overlapping functions in the regulation of FA, PAK2 expression and myosin II activity imply that miR-23b exert a negative control of migratory phenotypes by regulating other specific genes.

Moreover, it is well-known that maturation of FAs promote cell spreading on the ECM[444], which is in accordance with increased spreading abilities on ECM exhibited by MDA-MB-231 cells overexpressing miR-23b or miR-26a (**Figure 34B**). Although both miRNAs enhanced the ability of MDA-MB-231 cells to spread on Collagen I substrates after only 30 minutes, miR-26a was more effective in inducing this effect, as cells expressing this miRNA exhibited a markedly expanded morphology with increased number and area of Vinculin-stain FA sites under prolonged cell spreading conditions compared to miR-23b- or miR-n.c.-treated cells. Thus, it seems that miR-26a mediates a more robust activity compared to miR-23b in the formation and development of FAs and in cell spreading. Analysis of our RNA-seq data

pinpointed that Vinculin transcript (*VLC*) is among the genes up-regulated in miR-26a-overexpressing MCF-7 cells (**Table 17**). Moreover, these cells showed a conspicuous up-regulation of genes encoding for ECM receptors crucial for cell adhesion and FA formation, including several integrin subunits, which were conversely down-regulated in MDA-MB-231 cells stably inhibiting miR-26a (**Table 18**). Taken together, these data suggest that miR-26a may contribute to cell spreading, maturation and *de novo* formation of FA sites at later stages by indirectly inducing up-regulation of key components of FAs. The regulation of these genes by miR-26a may also underlie the molecular mechanism by which miR-26a promotes cell adhesion on the ECM in MDA-MB-231 cells (**Figure 34C**).

4.1.1.3 MiR-23b impairs lamellipodia formation

Beside the regulation of cellular pathways implicated in cell-cell interactions, focal adhesion and cell spreading on ECM, miR-23b exerts a broader effect in modulation of cytoskeletal remodelling with a robust impact on the formation of lamellipodia protrusions. We found that miR-23b-overexpressing MDA-MB-231 cells exhibited a significantly impaired formation of lamellipodia protrusions at their leading edge and, in contrast, MDA-MB-231 cells stably inhibiting miR-23b activity extended larger lamellipodia (**Figure 25** and **32B**). Analysis of our RNA-seq data show that several genes involved in cytoskeletal dynamics that induce lamellipodia and filopodia formation at the cell leading edge were differently modulated upon overexpression or inhibition of miR-23b. Among these genes, we confirmed that *ARHGEF6*, *LIMK2* and *CFL2* were down-regulated in miR-23b-expressing MCF-7 cells and up-regulated in MDA-MB-231 cells in which miR-23b was stably silenced (**Figure 50**). In addition, we validated each of these genes as direct targets of miR-23b by both experimental miRNA gain- and loss-of function approaches (**Figure 52**). ARHGEF6, LIMK2 and CFL2 are well-known modulators of cytoskeletal dynamics with major involvement in the formation of plasma membrane protrusion at the leading edge of motile cells. Indeed, it has been shown that ARHGEF6 overexpression dramatically promotes formation of lamellipodia and filipodia protrusions, likely as result of ARHGEF6-mediated activation of RAC and CDC42[176]; this is consistent with our observation that ARHGEF6 is overexpressed in MDA-MB-231 cells that stably inhibit miR-23b and exhibit pronounced lamellipodia protrusions. Moreover, LIMK2 and Cofilin 2 are key cytoplasmic effectors of the RAC/CDC42-activated PAK1/LIMK/cofilin pathway, which orchestrates actin

polymerisation and appropriate formation of lamellipodia at the cell leading edge[425]. Indeed, through activation of LIMK, which results in the phosphorylation and inhibition of cofilin, PAK1 ensures correct lamellipodia formation by limiting their expansion extents, that are under the control of cofilin activity[425]. Owning to its ability in inducing severing of actin filaments (F-actin), cofilin, in fact, promotes lamellipodia assembly by enhancing F-actin turnover that produces free barbed end for the polymerisation of new actin filaments[421]. Nevertheless, uncontrolled cofilin activity leads to accelerated F-actin turnover resulting in widening of the lamellipodium[425]. In light of this, it is reasonable to infer that the coordinated repression of ARHGEF6, LIMK2 and CFL2 by miR-23b disrupts crucial steps of the molecular pathway that supervises correct lamellipodia extension. Nevertheless, to confirm a direct involvement of these proteins in the miR-23b-regulation of lamellipodia formation, further investigation is required; this would focus on analysis of ARHGEF6, LIMK2 and CFL2 protein levels upon miR-23b manipulation, as well as evaluation of lamellipodia formation upon either silencing of each of these genes or their simultaneous expression with miR-23b in MDA-MB-231 cells.

Notably, miR-23b-induced corruption of lamellipodia formation likely encompasses the suppressive effect of miR-23b on MDA-MB-231 cell migration, as protrusion of lamellipodia at the leading edge is essential for cells to migrate[102].

4.1.2 Roles of miR-23b in BC cell migration, invasion and metastasis

4.1.2.1 Roles of miR-23b in BC cell migration

The ability of miR-23b and miR-26a of regulating similar and distinct aspects of cytoskeletal remodelling suggested a potential role for these miRNAs in the control of migratory phenotypes. By performing two different experimental techniques of cell migration analysis, we observed that overexpression of miR-23b, but not miR-26a, greatly inhibited both chemotaxis and random migration of highly motile MDA-MB-231 cells (**Figure 31**). Notably, reduction of migratory phenotypes induced by miR-23b was equivalent to that observed upon overexpression of miR-31 (**Figure 31**), a tumour suppressor miRNA that was previously shown to abolish MDA-MB-231 cell migration, invasion and metastasis both *in vitro* and *in vivo*[376]. In contrast, we found that stable inhibition of miR-23b activity via expression of a miR-23b-sponge construct was able to improve migratory capabilities of

MDA-MB-231 cells; accordingly, experimental suppression of miR-23b function is associated with increased migratory abilities of BC MCF-7 cells, as reported by Zhang *et al.*[353]. Moreover, we demonstrated that miR-23b-mediated alteration of cell migration was independent of eventual ongoing effects on cell proliferation or apoptosis, as neither overexpression nor inhibition of miR-23b affected proliferative and apoptotic phenotypes of MDA-MB-231 cells (**Figure 29A-C** and **30**).

To understand the molecular mechanism(s) that lies behind the robust ability of miR-23b in regulating cell migration, it is essential to uncover the physiological significance of genes differentially modulated by miR-23b in the contest of BC. Down-regulation of PAK2 by miR-23b could partially explain the inhibition of cell motility as its role in cytoskeletal remodelling and cell migration in BC is well established[129]; additionally, we confirmed a reduction in MDA-MB-231 cell motility upon silencing of PAK2 using small RNA interference (**Figure 34C**). Nevertheless, PAK2 down-regulation by miR-23b cannot completely explain the effect of miR-23b on cell migration, since miR-23b induces a stronger inhibition of MDA-MB-231 cell motility compared to the effect mediated by PAK2 depletion in the same cells (notably our PAK2 siRNA treatment was more effective in reducing PAK2 levels compared to miR-23b over-expression) (**Figure 31B** and **34C**). This suggested that miR-23b suppresses BC cell migration by regulating other genes with functions relevant to this cellular phenotype. We validated as miR-23b direct targets, two crucial cytoskeletal modulators, LIMK2 and CFL2 (**Figure 50**), of which down-regulation has been previously reported to abolish migration and invasion of MDA-MB-231 cells[124, 422]. Notably, none of these genes other than PAK2 are modulated by miR-26a inhibition and/or over-expression, for which we did not see any effect on cell motility.

4.1.2.2 Role of miR-23b in BC cell invasion

Additionally, we reported that overexpression of miR-23b greatly reduced invasion of MDA-MB-231 cells in 3-D collagen I matrixes; whereas inhibition of miR-23b activity strongly enhanced the invasive properties of these cells both *in vitro* and *in vivo* (**Figure 33 and 43A**). This effect was consistent with several pieces of evidence that support a role of miR-23b in suppressing cell invasion in different types of cancer[353, 355, 356].

Along with the ability of the newly discovered miR-23b cytoskeletal targets, such as PAK2, LIMK2 and CFL2 in affecting BC cell invasion[124, 129, 422], miR-23b could be implicated in the regulation of invasive processes, owing to its ability for directly repressing expression of

uPA (PLAU) and Annexin 2 (ANXA2) (**Figure 50** and **52**), two main components of the cellular invasive machinery. Indeed, uPA and Annexin 2 play crucial roles in the extracellular cascade that converts plasminogen in plasmin, a serine protease largely implicated in invasion, neoangiogenesis and metastasis[68, 70, 73, 429, 445]. Regulation of uPA by miR-23b has already been described in different tumour types[353, 354, 405] and we demonstrate that miR-23b is able to repress uPA expression also in BC (**Table 24**, **Figure 50** and **52**). Moreover, it has been shown that inhibition of uPA activity abolishes BC invasion and metastasis *in vivo*[66], which is consistent with our data showing that miR-23b suppression promotes invasion and metastasis in animal BC models (**Figure 42**). On the other hand, overexpression of Annexin 2 is found in many tumours, including highly aggressive BCs where it correlates with increased invasiveness, neoangiogenesis and metastasis[74]; conversely, silencing of Annexin2 reduced migration of MDA-MB-231 cells[73]. These observations suggest that miR-23b may further inhibit the invasive and metastatic potential of BC cells through repression of Annexin 2.

4.1.2.3 EGF controls transcriptional expression of miR-23b via AP-1

By combining small interference RNA (siRNA) techniques and ChIP analysis, we showed that miR-23b is a miRNA transcriptionally suppressed by the transcription factor AP-1 in BC MDA-MB-231 cells (**Figure 38** and **39**). Indeed, we demonstrated that the AP-1 component c-JUN directly interacts with TPA response elements (TREs) present in the promoter region of miR-23b (**Figure 39**), and that depletion of the AP-1 components c-JUN and c-FOS resulted in specific up-regulation of the expression levels of both precursor (pre-miR-23b) and mature miR-23b, whereas miR-26a expression remained unaltered (**Figure 38C-E**). Importantly, miR-23b is part of a cluster composed of miR-23b, miR-27b and miR-24-2 that are transcribed as a unique primary transcript[350]. This may indicate that AP-1 mediates its effect by regulating all the miRNA components of this cluster, but this hypothesis requires further investigation.

Notably, disruption of AP-1-mediated repression of miR-23b expression establishes important features observed upon miR-23b-overexpression, such as reduction of PAK2 levels and increase of MLCII phosphorylation (**Figure 38F** and **35**). The discrepancy in PAK2 repression levels observed in the two analyses (**Figure 35A** and **38F**) may depend on the different intracellular abundance of mature miR-23b achieved upon experimental miR-23b overexpression (**Figure 21**) and AP-1 depletion (**Figure 38D**). Mature miR-23b up-regulation after AP-1 knockdown can only partially explain the massive increase of MLCII

phosphorylation (**Figure 38F**), thus indicating that other mechanisms, likely dependent on AP-1 reduced activity, contribute to promote the phosphorylation state of MLCII.

Additionally, we observed that EGF stimulation induces an early inhibition of miR-23b levels in MDA-MB-468 cells (**Figure 40**). EGF is an extracellular ligand that specifically activates EGFR, a member of the ERBB family of receptor tyrosine kinases. Activated EGFR dimerises with its preferred partner HER2 and triggers multiple signalling cascades leading to survival and metastatic outcomes, through activation of several cytoplasmic effectors and transcription factors, including AP-1[184, 194]. Importantly, EGFR-induced AP-1 activity is mediated by PAK2 itself, which, once activated by EGFR promotes AP-1 nuclear activity via stimulation of the JNK pathway[191-194, 198, 446]. EGFR-mediated activation of PAK2 occurs through different intracellular pathways: (1) via recruitment by EGFR of the adaptor NCK which directly activates PAK2[192, 193], (2) through RAC and CDC42 stimulation by EGFR-mediated activation of their specific activator, the nucleotide exchange factor ARGHEF6/αPIX/COOL2[190], which we demonstrate to be a direct target of miR-23b (**Figure 52**), and (3) via recruitment and activation of regulatory subunits of PI3K, which, in turn, activates RAC and CDC42, leading to PAK2 activation[186, 188]. Notably, it has been shown that siRNA molecules directed against the *PI3K regulatory subunit gamma* or *3* (*PIK3R3*) gene, which is directly targeted by miR-23b as shown by our data (**Figure 52**), completely abrogate the AP-1 activation following growth factor stimulation[446]. Moreover, PI3K3 has been directly associated with acquisition of oncogenic phenotypes, as its repression by miR-7 leads to inhibition of tumour growth, invasion and metastatic potential[447]. Although further investigation of the direct effect of miR-23b-mediated repression of PAK2, ARHGEF6, and PIK3R3 on downstream AP-1 activation is required, it is reasonable to delineate a positive feedback loop mechanism that regulates miR-23b expression: signal transduction cascades involving cytoplasmic effectors, such as PAK2, ARHGEF6 and PIK3R3, activate AP-1, which in turn, suppresses miR-23b expression, thus releasing these three factors from miR-23b-mediated post-transcriptional regulation and facilitating AP-1 action (**Figure 54**). It is likely that, in the contest of BC, where amplification or hyperactivation of EGFR and HER2 is frequently observed[178, 179], the miR-23b regulatory mechanism is impaired, thus resulting in excessive inhibition of miR-23b expression and consequent release of pro-invasive targets, such as PAK2, LIMK2, CFL2, uPA and ANXA2, from their post-transcriptional repression.

Recently published data have suggested a different regulation of mir-23b expression by EGFR-associated activity. Lin *et al*. observed that EGF stimulation in BT-474 BC cells induces expression of miR-23b and its paralogue miR-27b; moreover they observed that

overexpression of HER2 in MCF10A induces miR-23b/27b up-regulation through activation of the PI3K/AKT/NF-κB pathway[357]. In contrast, miR-23b and miR-27b expression levels were found to be markedly down-regulated in HER2-trasformed MCF10A mammary epithelial cells[358], an observation that supports our findings. The use of BC cell models that exhibit distinctive molecular and phenotypical features might explain the discrepancy between these and our data relative to the molecular mechanisms that control miR-23b expression. Moreover, it is possible that EGFR/HER2 signalling differentially regulates miR-23b expression depending on the molecular state of AKT/NF-κB or AP-1, which may vary between distinct BC cells.

4.1.2.3 Role of miR-23b in BC initiation and progression

Our evidence of the robust effect of miR-23b on cytoskeletal remodelling, cell migration and invasion in BC cell lines has suggested that miR-23b is potentially involved in the regulation of the metastatic process associated with BC. Establishment of mammary xenograft tumours in nude mice after implantation of MDA-MB-231-cells stably expressing the miR-23b sponge construct or the parental control vector allowed us to investigate the effect of miR-23b inhibition on BC growth and metastasis *in vivo*. By monitoring tumour volume rates over the time required for the formation of mammary xenografts, we observed that inhibition of miR-23b activity resulted in increased tumour growth (**Figure 43A**). This was consistent with previous evidence that miR-23b inhibited tumour proliferation of prostate and colon cancer cells *in vivo*[353, 355]. The effect of miR-23b in regulating tumour growth was unexpected, since our *in vitro* analysis showed that neither overexpression nor inhibition of miR-23b altered proliferation of MDA-MB-231 cells (**Figure 29A** and **30**). Contrarily, a miR-23b effect on cell growth has been appreciated in other tumour types, such as prostate cancer and B-cell lymphoma, where c-MYC-induced inhibition of miR-23b results in increased cell proliferation, due to release from miR-23b-mediated repression of the mitochondrial glutaminase (GLS)[299]. Our characterisation of xenograft tumours by H&E staining showed a dramatic reduction of necrosis when miR-23b was inhibited (**Figure 43B**), suggesting that reduced miR-23b function may enhance the metabolic activity of these tumours, thus promoting *in vivo* tumour growth. Accordingly, our RNA-seq analysis shows that GLS is up-regulated in MDA-MB-231 cells in which miR-23b was stably inhibited (**Table 24**).

Importantly, we observed that suppression of miR-23b induced spontaneous lymph-node metastases, which were not detected in the control mice (**Figure 42B**). This finding suggests

that reduction of miR-23b expression is required for BC cells to metastasise *in vivo*. Notably, we found that the expression of miR-23b, but not of miR-26a, is inversely correlated with BC metastasis. MiR-23b is selectively down-regulated in BC cell lines that metastasised to different distal organs compared to cells derived from mammary primary tumours after inoculation in the mammary fat pads of nude mice (**Figure 41A**). Accordingly, we detect that miR-23b is greatly reduced in a large cohort of lymph-node metastatic samples in comparison with their matched primary tumours derived from BC patients (**Figure 41C** and **D**). Since we observed that miR-23b expression is negatively regulated by EGF stimulation and consequently by AP-1, this could contribute to the metastatic impact of AP-1 in BC cells[186, 194, 195, 198]. AP-1 mediated suppression of miR-23b expression may then promote release of pro-invasive miR-23b gene targets from their post-transcriptional repression, thus eliciting BC invasion and metastasis (**Figure 54**). Taken together, these data suggests that loss of miR-23b expression and consequently disruption of its regulatory network, are crucial events in the initiation of BC progression. Thus, replacing miR-23b in BC patients may represent a novel therapeutic strategy to prevent tumour progression and metastatic spread.

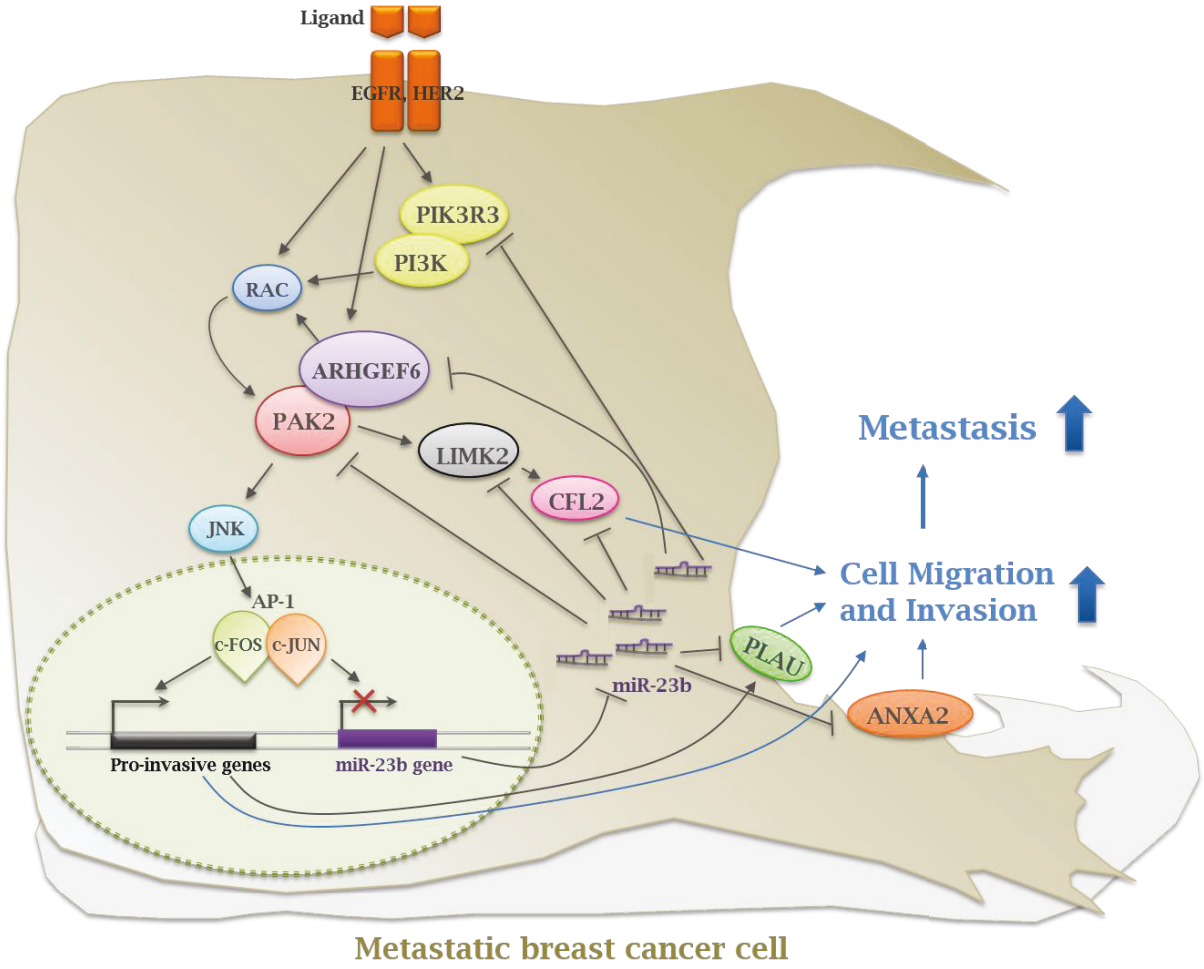

Figure 54: Model of mode of action of miR-23b regulatory network in suppressing BC metastasis. Mature miR-23b block the expression of a set of cytoskeletal and pro-metastatic genes to suppress BC cell migration, invasion and metastasis. Upon activation of stimulated EGFR/HER2 signalling, the transcription factor AP-1 (Activator protein 1) inhibits miR-23b transcriptional expression and up-regulates several pro-invasive genes, and ultimately promotes metastasis. Among miR-23b targets, PIK3R3, ARHGEF6 and PAK2 participate to AP-1 activation. Therefore, through a positive feed back loop mechanism, activated AP-1 suppresses expression of miR-23b, resulting in the release from miR-23b-mediated repression of PAK2, PIK3R3 and ARHGEF6, which in turn, cooperate to enhance AP-1 activation and consequently miR-23b suppression. EGFR: epidermal growth factor receptor; HER2: human epidermal growth factor receptor 2; PIK3R3: phosphatidylinositol-3 kinase regulatory subunit 3 or gamma; PI3K: phosphatidylinositol-3 kinase; ARHGEF6: RAC/CDC42 guanine nucleotide exchange factor 6; PAK2: p21-activated kinase 2; JNK: c-JUN N-terminal kinase; LIMK2: LIM-domain kinase 2; CFL2: cofilin 2; PLAU: urokinase-like plasminogen activator; ANXA2: annexin 2.

4.1.2.3.1 Evidences show conflicting roles of miR-23b in BC

A recently published research article by Lin *et al.*[357] showed conflicting functions of miR-23b and its family member miR-27b in BC initiation and progressioncomparing to our findings. They demonstrated that miR-23b/27b function as oncogenic miRNAs in BC by promoting proliferation, anchorage-independent cell growth, migration and invasion *in vitro*. By performing a number of experimental assays, they observed that independent gain- and loss-of-function of the two miRNAs increases and inhibits both migratory and invasive capabilities of BC cell lines, respectively. These findings are in contrast with our *in vitro* data where miR-23b overexpression and inhibition abolishes and enhances migration and invasion of our BC cells, respectively. The use of different BC cell lines (ZR35/MDA-MB-231-4135 versus MCF-7 and MDA-MB-231 cells) and technical approaches could rely behind this discrepancy. Beside these experimental variances, it is noteworthy to highlight that Lin *et al.* did not discriminate between the pro-proliferative and pro-migratory/invasive effects of miR-23b in BC cells, which is of fundamental importance when investigating phenotypes such as cell motility and invasion[353, 355, 375]. By performing independent assays (scratch wound healing and transwell assays), they found that mir-23b/27b modulation deregulates the migratory and invasive capabilities of BC cell lines; nevertheless, these assays were performed by incubating the cells for times longer than their doubling times (24-48h). As they observed that both miRNAs affect also cell proliferation, the possibility that increased/decreased proliferative rates of cells expressing miR-23b or miR-27b could contaminate the enhanced/reduced effect on their migration and invasion remains really high. Our choice to investigate the effect of miR-23b modulation on BC cell migration and invasion by performing different experimental techniques comparing to those used by Lin and colleagues (time-lapse tracking and type I-collagen 3D invasion assays) has allowed us to visualise single cells in their migrating/invasive cycles, thus analysing them independently from their proliferating state. Differently to the investigative approach adopted by Lin *et al.*, we performed the migration assays by using cells overexpressing, alongside with miR-23b, also miR-31 (a pleiotropic suppressor of BC cell migration and invasion[375]), by which motility was reduced at the same extent as for miR-23b-overexpressing cells, and miR-26a, which did not affect cell migration, thus functioning as a reliable, further negative control.
Furthermore, we demonstrated that miR-23b suppresses migration and invasion independently of cell proliferation by highlighting its effect on distinct features of cytoskeletal organisation (cell-cell junctions, lamellipodia and FA formation), on cell spreading on the ECM, and on

MLC phosphorylation state. Whereby, Lin and colleagues have appointed the effect of miR-23b on deregulated proliferation/migration to the physiological function of Nischarin, a miR-23b target identified in their study. They had previously shown that Nischarin knockdown increases both proliferation and migration/invasion in the same BC cell lines[448]; thus they confirmed that rescuing Nischarin expression in miR-23b-overexpressing cells partly reverts the miR-23b-mediated advantages on cell proliferation and motility. In order to validate their findings, they analysed the endogenous protein levels of other 6 predicted miR-23b targets, including PAK2, upon miR-23b inhibition and they observed that none of these genes were real targets of miR-23b, except for *Nischarin*.

These findings are highly inconsistent with evidences showed in our and Zhang *et al.*'[353] studies, that PAK2 is effectively a physiological target of miR-23b in breast (**Figure 35**, **36** and **37**) and colon cancer. We demonstrated that PAK2 is a real target of miR-23b by using a number of assays (**Figure 35A**, **36** and **37**). Notably, we also found *PAK2* to be up-regulated by the miR-23b-sponge construct and down-regulated by miR-23b overexpression in our RNA-seq data (**Table 24**). Moreover, we proved that miR-23b directly targets uPA in BC (**Figure 52**), thus confirming several reports of a direct control of miR-23b on the regulation of this crucial metastatic gene[353, 418]; additionally, we observe that 70% of previously validated miR-23b targets are found to be deregulated by miR-23b manipulation in BC cells, as shown by our RNA-seq data, many of which are pro-metastatic genes (**Table 26**). Noteworthy, no differential expression of *Nischarin* was detected upon miR-23b modulation in our RNA seq analysis, indicating that miR-23b is not able to regulate these two putative targets in our BC cell models, at least at the mRNA level. Our cross-validating approach proves not only the reliability of our experimental methods, but also that the physiological function of miR-23b in BC relies on the coordinated down-regulation of a broader set of genes. Consistently, we demonstrated that miR-23b coordinates the repression of a cohort of gene targets (**Figure 50** and **52**, **Table 24**), crucial for cytoskeletal dynamics, cell migration, invasion and metastatic dissemination that likely encompass its pleiotropic activity in negatively regulating these cellular phenotypes.

In accordance with the effect of miR-23b/27b manipulation on BC cell proliferation and migration seen *in vitro*, Lin and colleagues observed that inhibition of these two miRNAs reduces both tumour growth and metastasis *in vivo*. After injection of BC cells into the mammary fay pad of immunocompromised mice, they found that miR-23b/27b silencing reduces tumour volume of the formed BC xenografts; this is in contrast with the tumour suppressor activity of miR-23b in BC *in vivo* models (as shown in our study, **Figure 42** and

43), and other animal models of different tumour types (human colon and prostate cancer)[353, 355]. Moreover, by performing a long-term lung colonisation assay upon tail vein injection, Lin *et al.* showed that miR-23b/27b inhibition represses the metastatic potential of human BC cells. This experimental approach of *in vivo* metastasis does not allow to reproduce with high fidelity the pathological multi-step process which cancer cells undertake in order to metastasise (local migration and invasion, intravasation, extravasation and organ colonisation). In fact, under these conditions, cancer cells enter directly the hematogenous stream, bypassing the invasion and intravasation steps. We used BC mammary gland xenograft models to investigate the impact of miR-23b inhibition on both tumour growth and metastasis *in vivo*. This method replicated our *in vitro* findings that miR-23b silencing elicits the ability of BC cell to invade the ECM (**Figure 33B**). Moreover, inhibition of miR-23b increased the extravasation and the metastatic spread of BC cells from the primary tumours to the lymph nodes (**Figure 42B**). Unfortunately, we did not detect metastatic dissemination to any bodily organ in our BC animal models, probably due to the limited time given to BC cells to systemically spread, as primary tumours had to be harvested early during the experiment course in accordance with licence restrictions.

Finally, Lin and colleagues investigated the clinical relevance of miR-23b and miR-27b by measuring their endogenous levels in BC patients. Since they pinpointed a role of miR-23b and 27b as oncomiRs and metastatic miRNAs in their *in vitro* and *in vivo* findings, they compared their expression between primary breast tumour samples and normal tissues. They found that expression of both miRNAs is higher in BC patients and inversely correlates with Nischarin levels; moreover, they could be used as markers for BC prognosis and metastasis as their endogenous abundance correlates with poor overall survival and with the invasiveness of BC cell lines. On the other hand, we showed that miR-23b is expressed at lower levels in metastatic BC cell lines compared to primary tumour cells (**Figure 41A**), which was consistent with the data reported by Patel *et al.*[411], where they profiled miRNAs expression in the same BC cell lines which have been isolated from BC primary tumours and different metastatic loci after orthotopic injection in immunocompromised mice. Additionally, we report that miR-23b expression is significantly decreased in lymph node metastases compared to matched primary BC samples (**Figure 41C-D**), indicating that reduction of miR-23b levels is a physiological event during BC progression. Although our clinical data provide a more realistic picture of the relevance of miR-23b expression during BC cancer metastatic development comparing to Lin *et al.*‟ findings, a more accurate analysis of miR-23b and its paralogs abundance in metastatic tissues of BC origin would require further investigation.

4.1.3 Roles of miR-26a in BC tumourigenesis

4.1.3.1 Roles of miR-26a in BC cell proliferation and apoptosis

Beside the activity of miR-26a in modulating cytoskeletal dynamics to promote focal adhesion maturation, cell spreading and adhesion on ECM, we also pinpointed a role for this miRNA in the regulation of BC cell proliferation and apoptosis.

In hepatocellular carcinoma, miR-26a shows robust activity in inhibition of cell proliferation and cell cycle progression, owing to its ability in directly repressing cell cycle key modulators, such as the cyclins CCND1, CCNE1 and CCNE2, the cyclin-dependent kinase CDK6 and RB1[361, 362]. We also showed that overexpression of this miRNA in MCF-7 cells reduces proliferation rates (**Figure 29B**), as well as expression of CDK6, CCNE1, and RB1 (**Table 20** and **25**). Additionally, inhibition of miR-26a activity in MDA-MB-231 cells is associated with increase of RB1, CCNB1 and 2, CCNE1 and 2, and CCND3 (**Table 21**); this indicates that miR-26a may impair proliferative properties also through down-regulation of a wider cohort of cyclins.

In confirmation of the ability of miR-26a in slowing cell proliferation rates, we observed that its overexpression induces MDA-MB-231 cells to undergo apoptosis (**Figure 29C**). Notably, we identified and validated as a miR-26a direct target, the myeloid leukemia cell differentiation protein 1 (MCL1), a key member of the BCL2 family with antiapoptotic and pro-survival functions (**Figure 53** and **Table 26**). In keeping with our findings, miR-26a has recently been implicated in BC as a negative regulator of cell proliferation by promoting cell cycle arrest and apoptosis, via down-regulation of EZH2 and MCL1[367-369]. Interestingly, we retrieve EZH2 in our miR-26a targetome list of genes down-regulated or up-regulated after miR-26a overexpression or inhibition, respectively (**Table 26**). Moreover, siRNA-mediated knockdown of the RNA-binding protein LARP1, a novel miR-26a direct target validated in our study (**Figure 53**), has been shown to induce apoptosis of mammalian cells[435]. Taken together, these data strongly suggest that miR-26a controls apoptosis and proliferation pathways through coordinated repression of MCL1, EZH2 and LARP1 in our experimental BC cell models.

Detailed analysis of our RNA-seq data revealed that the number of genes involved in cell cycle progression which are dysregulated by miR-26a manipulation is actually much larger than previously appreciated. Importantly, cyclin-dependent kinase (CDK) inhibitors,

including CDKN1A, CDKN2B, CDKN2C and CDKN2D were highly up-regulated in MCF-7 cells after overexpressing this miRNA (**Table 20**). This indicates that concomitant reduction of cell cycle-promoting genes and up-regulation of cell cycle-inhibiting genes may represent a broader line of action adopted by miR-26a in inhibiting BC cell proliferation.

Transcriptome analysis of MDA-MD-231 cells upon miR-26a manipulation shows instead a balance between cell cycle-promoting genes and cell cycle-inhibiting genes, as distinct cyclins and CDK inhibitors are both up-regulated or down-regulated (**Table 21**). This observation may explain why miR-26a inhibition or overexpression did not alter proliferation of MDA-MB-231 cells (**Figure 29A** and **30**). However, the discrepancy in finding that MDA-MB-231 cells displayed increased apoptosis, but exhibited the same proliferation rates as the control cells, upon miR-26a transient transfection (**Figure 29C** and **B**), remains unsolved and would require further investigation.

Our pathway enrichment analysis of the miR-26a targetome revealed that several miR-26a predicted targets are implicated in the p53 signalling pathways. MiR-26a has been shown to be transcriptionally up-regulated by p53 and p53 activation is known to induce cell cycle arrest through down-regulation of cell cycle-promoting genes and up-regulation of the CDK inhibitor CDKN1A[449]. This suggests that miR-26a increases CDK inhibitor levels through p53 stabilisation and/or activation, because in miR-26a-overexpressing MDA-MB-231 cells, which express mutated p53, CDK inhibitors are not regulated and cell cycle progression does not seem to be affected (**Figure 29A**). Interestingly, the F-box protein 11 (FBXO11), known to inhibit p53 transcriptional activity by promoting its neddylation[450], is a predicted target of miR-26a and it also appears to be down-regulated upon miR-26a overexpression of in MCF-7 cells (**Table 25**). Finally, miR-26a over-expression increases two members of the TGFβ (Transforming growth factor beta) receptor family, TGFBR1 and TGFBR2, and also their effector SMAD3 (**Table 19**), which is known to directly increase the expression of CDKN2B[451], indicating that miR-26a may also inhibit cell cycle progression by promoting the TGFβ signalling pathway.

4.1.3.2 Mir-26a implication in cytokinesis, aneuploidy and BC tumourigenesis

Prolonged administration of a miR-26a precursor mimic induced dramatic morphological changes in MCF-7 and MDA-MB-231 2-D cell cultures, leading to formation

of giant, expanded cells frequently containing two nuclei or a single enlarged nucleus (**Figure 45**). This characteristic phenotype implies a robust involvement of miR-26a in cytoskeletal rearrangements and also in late stages of the cell cycle progression (mitosis), such as cytokinesis and karyokinesis.

Maintenance of the intracellular miR-26a abundance at high levels may enhance the ability of this miRNA in promoting focal adhesion development, as well as cell spreading and adhesion on the substratum, thus contributing to the expanded, flat morphology displayed by MCF-7 and MDA-MB-231 cells (**Figure 44**). The biological functions of specific transcripts found differentially modulated in our RNA-seq analysis after manipulation of miR-26a in BC cells support this hypothesis. Indeed, as previously discussed, miR-26a overexpression in MCF-7 cells greatly up-regulates a cohort of genes involved in cell-matrix adhesion pathways, such as Vinculin (VLC) and several integrin subunits (**Table 17**), which were consistently down-regulated in MDA-MB-231 cells stably inhibiting miR-26a activity (**Table 18**). Additionally, in epithelial contests (MCF-7 cells), prolonged miR-26a overexpression appears to affect cell-cell interactions, as these giant cells display disrupted adherens junctions with scanty E-cadherin accumulation at cell-cell adhesion sites (**Figure 44A**). Nevertheless, expression levels of the E-cadherin (CDH1) transcript were not affected in MCF-7 cells overexpressing miR-26a or MDA-MB-231 cells stably inhibiting this miRNA (RNA-seq data not shown); this suggests that miR-26a may cause aberrant E-cadherin expression at the post-transcriptional level, a hypothesis that is a matter of future investigation.

Manifestation of giant mononucleated or binucleated cells is a characteristic consequence of impaired nuclear division and/or cytokinesis, respectively, as well as a striking cause of aneuploidy/polyploidy occurrence and increased chromosome instability (CIN)[222, 413]. Here we show for the first time that prolonged overexpression of miR-26a significantly enhances the aneuploid state of both MCF-7 and MDA-MB-231 cells, which exhibited a larger percentage of cells with near-tetraploid (or higher than tetraploid) karyotypes compared to relative controls (**Figure 46**). This phenotype implies that these cells encounter difficulties in the completion of nuclear division and/or cytokinesis, with consequent acquisition of a polyploid karyotype. Although further investigation is required to demonstrate the direct involvement of miR-26a in affecting karyokinesis or cytokinesis events, our RNA-seq data and experimental validation of novel miR-26a gene targets strongly suggest that this miRNA may actually impair these cellular pathways.

In support of a possible karyokinesis failure, we observed that several genes involved in crucial steps of chromosome segregation during mitosis are dysregulated after miR-26a

perturbation. Indeed, different members of the mitotic spindle assembly checkpoint (SAC), BUB1, BUB1B, BUB3 and the mitotic arrest deficient, yeast, homolog-like 1 (MAD2L1) are greatly up-regulated in MDA-MB-231 cells that stably inhibit miR-26a activity (**Table 21**). Similarly, increased transcript levels of two crucial promoters of sister chromatids detachment, ANAPC10, encoding for the subunit 10 of the anaphase-promoting complex/cyclosome (APC/C) and its partner cell division cycle 20 (CDC20) were observed in the same cells (**Table 21**). This suggests that miR-26a may indirectly induce dysregulation of these crucial players, which is believed to induce karyokinesis failure and tetraploidisation due to impaired mitotic checkpoint response and/or failed chromatids separation[217]. Moreover, a potential deregulation of these proteins by miR-26a imply a high risk of aneuploidy occurrence and consequent enhancement of CIN[217].

On the other hand, failure of cytokinesis is mainly caused by defects in different steps of this process, such as central spindle formation, actinomyosin ring assembly/closure and final abscission, due to dysregulation of several cytokinetic proteins that orchestrate all these events. We depict a potential role of miR-26a in early-middle steps of the cytokinesis, by directly targeting YWHAE, the member epsilon of the 14-3-3 protein family, which is found to be down-regulated in MCF-7 cells overexpressing miR-26a and up-regulated in MDA-MB-231 cells stably inhibiting this miRNA (**Figure 51, 53** and **Table 25**). 14-3-3 members form functional heterodimers to ensure both proper formation of the central spindle in collaboration with Aurora B, and efficient closure of the actinomyosin ring by associating with PKCε; their down-regulation has been shown to imply a broad range of cytokinesis defects with consequent formation of binucleated cells[224, 225, 230, 440]. However, miR-26a activity could also participate in later phases of the cytokinesis process, by impairing furrow ingression, and consequent abscission, necessary for the separation of the two daughter cells. Indeed, prolonged miR-26a overexpression in MCF-7 cells causes down-regulation of the Ras small GTPase RAB21 (**Table 25**), which has been shown to yield binucleated cells, due to delayed furrow ingression and consequent cytokinesis failure[227]. Interestingly, RAB21 3'UTR contains a specific binding site for the mature miR-26a[351](**Table 25**), strongly suggesting that its direct interaction and repression by miR-26a can occur in physiological conditions. Moreover, we demonstrated that miR-26a overexpression in MCF-7 cells and its inhibition in MDA-MB-231 cells down-regulates and up-regulates, respectively, the expression of two members of the SNARE vesicle transport system, Endobrevin (VAMP8) and Syntaxin 2 (STX2) (**Table 22** and **23**). These proteins are required for membrane fusion events that allow efficient separation of the two daughter cells, and their depletion has been shown to severely

impair cytokinesis completion leading to binucleation[231]. Interestingly, STX2 is a predicted target of miR-26a, as shown by our targetome analysis (**Table 25**), thus implicating a direct regulation of its expression by this miRNA.

Additional direct targets of miR-26a validated in our study are the RNA-binding protein LARP1 and the early mitotic checkpoint CHFR (**Figure 53**), which are consistently found to be down-regulated and up-regulated upon miR-26a overexpression and inhibition in MCF-7 and in MDA-MB-231 cells, respectively (**Table 25**). Potential miR-26a-mediated repression of these two gene targets in physiological conditions greatly supports a role for this miRNA in affecting cytokinetic events, as depletion of both LARP1 and CHFR results in cytokinesis failure and tetraploidisation[213, 435]. In particular, LARP1 knockdown in mammalian cells causes several aberrant mitotic features, such as failure of bipolar mitotic spindle formation, aberrant centrosome migration, abnormal nuclear morphology and impaired cytokinesis[435]. Moreover, it was associated with mitotic arrest and increased apoptosis, which is consistent with our observation that miR-26a induces apoptosis, whereas it affects cell proliferation in BC cells (**Figure 29C** and **B**). On the other side, depletion of CHFR produces severe CIN, arising from centrosome amplification, spindle mis-organisation, aneuploidy and cytokinesis/karyokinesis failure, which are associated with increased tumourigenicity[213]. CHFR is, in fact, a well-established tumour suppressor, as its down-regulation or complete loss is frequently observed in a wide variety of cancers, including primary tumours of the breast[213, 220]. CHFR-deficient mice display higher tumour incidence and formation of spontaneous aneuploid and polyploid tumours[213]; moreover, CHFR knockdown results in enhanced aneuploidy and induced transforming potential of human immortalised MCF10 breast cells[220]. These data represent an example of the direct link between aneuploidy/polyploidy occurrence and malignant transformation. Indeed, it is well documented that aneuploid cells, derived from events of cytokinesis or karyokinesis failure, exhibit enhanced tumourigenic and transforming potentials due to increased CIN[200, 201, 204, 205, 222, 235]. Here, we show that prolonged miR-26a overexpression in MCF-7 cells promotes the tumourigenic potential of these cells *in vitro*. MCF-7 cells transfected for 9 days with a miR-26a precursor mimic form a significantly increased number of colonies, which were also larger in size, compared to control-treated cells in soft agar colony formation assays (**Figure 46**), a clear indication of enhanced tumourigenic and transforming capabilities[143]. This is in contrast with recently reported data where miR-26a exhibits tumour suppressor abilities in BC both *in vitro* and *in vivo*[366, 368]. Zhang *et al*. demonstrated that delivery of miR-26a using a retrovirus-based system in MCF-7 cells reduces soft agar colony formation and

tumourigenesis *in vivo*, due to miR-26a-induced apoptosis and inhibition of cell proliferation, via down-regulation of the anti-apoptotic EZH2 and MTDH[366]. A second study by Gao *et al*. reported that transient miR-26a overexpression in MCF-7 cells impairs cell proliferation and soft agar colony formation, and promoted apoptosis via repression of MCL1[368]. The difference in the temporal and technical administration systems adopted in these and our studies may lie behind the discrepant effect of miR-26a on tumourigenic abilities of MCF-7 cells. Noteworthy, we also demonstrate that miR-26a overexpression reduces MCF-7 cell proliferation and induces apoptosis of MDA-MB-231 cells (**Figure 28B** and **C**); furthermore, we also confirm MCL1 as direct target of miR-26a (**Figure 53**), and that expression of both MCL1 and EZH2 is inversely correlated with miR-26a overexpression or inhibition in our BC cell models (**Table 25**). The reproducibility of these findings supports a major role for miR-26a in negative regulation of apoptosis and cell proliferation. Despite this, we observe that prolonged miR-26a overexpression promotes the establishment of a subpopulation of bi/mononucleated, polyploid cells, likely derived from events of cytokinesis/karyokinesis failure. This finding provides, for the first time, evidence of the ability of miR-26a to control additional steps of the cell cycle (mitosis), beside its previously reported role in inducing cell cycle arrest in G1 phase in BC cells[367]. We suppose that ectopic overexpression of miR-26a may differentially affect cell cycle progression, depending on the specific cycling state that these cells are experiencing at the timing of administration of this miRNA. Cells that overpassed phase G1 of the cell cycle may be affected by the continued administration of miR-26a. Therefore, increase and maintenance of miR-26a levels in cells that are entering or proceeding through later stages of the cell cycle may impair mitosis completion, due to cytokinesis/karyokinesis failure, thus resulting in polyploidisation. Polyploid cells are able to succeed cell cycle progression by escaping cell death or cell cycle arrest, and after completing cytokinesis, produce a progeny of aneuploid cells with enhanced CIN and increased transforming potential[229, 232, 235]. The observation in time-lapse experiments that giant, bi/mononucleated MCF-7 cells overexpressing miR-26a are able to accomplish cell division, although at much slower rates compared to miR-n.c.-treated (data not shown), suggests that these cells are viable and in advanced passages they may give origin to a cell population with worsened aneuploid and CIN phenotypes and increased tumourigenic abilities. This may explain the effect of prolonged miR-26a overexpression in improving the *in vitro* tumourigenicity of MCF-7 cells, observed in our study (**Figure 46**). Nevertheless, this hypothesis requires further investigation, to better characterise the proliferative and transforming properties of these cells.

A major consequence of polyploidisation is the acquisition of an aberrant number of centrosomes (centrosome duplication), which dramatically elicits CIN and aneuploidy occurrence following successful mitosis of tetraploid cells. About 80% of invasive breast carcinomas manifest abnormal number and/or structure of centrosomes, indicating that the risk to develop CIN and aneuploidy increase with tumour progression[233]. Although miR-26a has been found to be down-regulated in patients with primary breast carcinomas compared to control normal specimens[366, 368], it would be interesting to investigate miR-26a expression profile in advanced stages of BC progression associated with an aneuploid/polyploid state.

4.1.4 Future directions

In light of the results presented in this thesis, several aspects of the overall function of miR-23b and miR-26a remain to be addressed.

Concerning the miR-23b role in BC progression, we demonstrate that this miRNA regulates cytoskeletal dynamics, migration and invasion of BC cells.

We show that miR-23b overexpression enhances the epithelial architecture of MCF-7 cells, probably by inducing up-regulation of cell-cell adhesion molecules, including Nectin 1 and Nectin 2 at the transcriptional level, as suggested by our RNA-seq analysis. To address this hypothesis, it would be necessary to assess:

- the endogenous protein levels of these cell-cell adhesion mediators after miR-23b manipulation in BC cells;
- whether their potential deregulation by miR-23b affects their localisation and functionality at cell-cell adhesions sites;
- the mechanism(s) used by miR-23b to eventually regulate their expression. Although the ability of miRNAs to induce transcriptional expression of specific genes at their promoter levels has been demonstrated[290], they mainly function in repressing gene target expression at the post-transcriptional level[248]. Therefore, miR-23b could down-regulate potential transcriptional suppressors of these cell-cell adhesion molecules, thus increasing their expression. However, eventual indirect effects induced by miR-23b overexpression could also determine the up-regulation of these adhesion genes.

We further demonstrate that miR-23b inhibits lamellipodia formation, cell migration and invasion in BC cells and we validate a subset of genes with crucial functions in these cellular processes as miR-23b direct targets. Experimental down-regulation of most of these genes in

the same BC cell model has been shown to induce similar effects to the overexpression of miR-23b. Nevertheless, to investigate how repression of each single miR-23b target contributes to the phenotypic effect induced by miR-23b, it would be necessary to overexpress each miR-23b target in order to restore its intracellular levels upon overexpression of miR-23b.

We also show that the transcription factor AP-1 transcriptionally represses miR-23b expression; the AP-1 component c-JUN directly interacts with the miR-23b promoter region and silencing of both C-JUN and c-FOS results in increased levels of both precursor and mature miR-23b. Since miR-23b is part of a miRNA cluster, along with its paralogs miR-27b and miR-24-1[350], it is likely that AP-1 also controls the expression of these two miRNAs. Therefore, investigation of miR-27b and miR-24-2 levels after AP-1 silencing would be required. Additionally, we show that mature miR-23b levels are reduced after stimulation of BC cells with EGF, which is known to induce AP-1 activation through EGF receptor signal transduction[194]. In order to confirm that EGF represses miR-23b expression via AP-1 activity, disruption of the EGFR signalling pathway by silencing or inhibiting crucial effectors, would be required.

On the other hand, we show that miR-26a impairs cell proliferation and induces apoptosis in BC cells and regulates cytoskeletal dynamics, inducing several phenotypes, some of which are shared by miR-23b activity.

MiR-26a overexpression in BC cells promotes cell adhesion on the ECM, probably due to up-regulation of several ECM-cell adhesion genes. Analysis of protein levels of these genes and investigation of the mechanism(s) that trigger their up-regulation would be required.

We show that long-term overexpression of miR-26a determines the establishment of characteristic sub-populations of cells, displaying a dramatic enlargement of their cell body, often containing two nuclei or one oversized nucleus. In epithelial contests (MCF-7 cell cultures), these effects are also accompanied by an apparent disruption of E-cadherin-mediated cell-cell adhesions. Since we observe no changes in E-cadherin transcript levels in our RNA-seq data, it is possible that post-transcriptional deregulation of E-cadherin indirectly induced by miR-26a could explain this phenotype. Therefore, further investigation, such as Western blot analysis of *E-cadherin* protein levels upon miR-26a overexpression and/or eventual mechanisms that might control this gene post-transcriptionally, is required to uncover this hypothesis.

The formation of giant, bi/mononucleated cells observed upon miR-26a long-term transfection indicates that defects in cytokinesis/karyokinesis events may occur in these cells.

In support of this point, we find that (1) overexpression of miR-26a increases the number of cells with a polyploid karyotype; (2) miR-26a directly targets genes, such as YWHAE, CHFR and LARP1, relevant to cytokinesis and/or nuclear division pathways; (3) miR-26a manipulation procures changes in the expression of genes crucial for the proper execution of these processes. In order to unravel whether and how failure of cytokinesis/karyokinesis occurs upon miR-26a overexpression, and to unravel the molecular mechanism(s) responsible for these phenotypes, we aim to perform:

- analysis of the ploid content of cells by flow cytometry, in order to confirm the increased observed aneuploidy;
- systematic investigation of mitotic features, such as mitotic spindle formation, chromosome segregation, nuclear division and cytokinetic progression aspects, by using light/fluorescence, time-lapse microscopy and cellular markers, such as fluorescent dyes for the staining of nuclei (DAPI), microtubules, and plasma membranes;
- RNA interference (RNAi) of miR-26a gene targets in our BC cell models, and their overexpression in cells overexpressing miR-26a followed by investigation of eventual effects on cell division;

Additionally, the observation that giant, bi/mononucleated MCF-7 cells overexpressing miR-26a are able to complete mitosis is a manifestation of cell viability. Nevertheless, further investigation is necessary to confirm this hypothesis and a variety of experimental assays can be performed to assess cell cycle progression, apoptosis, cell proliferation, cell death, or senescence upon prolonged overexpression of miR-26a.

Finally, we aim to confirm the tumourigenic potential of miR-26a in BC, because of the clinical relevance that this may imply. Since miR-26a-overexpressing cells display increased polyploidy, it is likely that miR-26a confer tumourigenic and transforming abilities, by promoting aneuploidy and CIN. In this respect, we aim to investigate:

- the ability of miR-26a in inducing *in vitro* transformation of immortalised, normal breast cells, such as MCF-10 breast cell line, under conditions of long-term (9 days) transfection;
- how miR-26a impacts tumourigenicity of MCF-7/MDA-MB-231 cells *in vivo*, by inducing xenograft tumours formation following ectopic implantation of these cells in immunocompromised mice, either after *in vitro* long-term miR-26a transfection, or by

performing a series of intratumoural injections of miR-26a mimics and relative controls;

- the euploidy state of xenograft tumours after completion of the *in vivo* analysis;
- miR-26a expression in BC specimens manifesting aneuploidy/polyploidy characteristics.

4.1.5 Conclusions

This work has enabled us to characterise the specific roles of miR-23b and miR-26a in BC pathogenesis.

In particular, we have pinpointed miR-23b as a potent suppressor of BC progression, by affecting motile and invasive abilities necessary for cancer cells to metastasise. By picturing the overall action that miR-23b takes in the contest of BC, we extrapolated a complex regulatory network that miR-23b orchestrates to impede acquisition of aggressive traits. This network employs mechanisms of post-transcriptional repression, transcriptomic changes and intracellular dynamics affecting multiple genes that differentially promote or inhibit BC progression. We demonstrate the clinical importance of miR-23b down-regulation in BC metastasis and we propose that loss of miR-23b expression and consequent disruption of its regulatory network are crucial events in the initiation of BC progression. Therefore, it is conceivable that replacing miR-23b in patients affected by BC may represent a novel therapeutic strategy to prevent tumour progression and metastatic spread.

On the other hand, we confirm a major role for miR-26a in inhibiting BC cell proliferation, and inducing apoptosis and cell cycle arrest, as previously demonstrated. Moreover, we describe novel additional functions of miR-26a in BC cells. It is involved in cytoskeletal remodelling pathways, leading to enhanced cell adhesion, and in later steps of cell cycle progression by promoting binucleation and polyploidy occurrence. Finally, we demonstrate the ability of miR-26a to elicit tumourigenicity of BC cells, likely due to increased aneuploidy and CIN.

Since miR-26a exhibits tumour suppressor activity by inducing cell cycle arrest and apoptosis, it has been proposed as a potential therapeutic candidate of both breast and hepatocellular carcinoma. However, we believe that caution should be taken when considering miR-26a as an anti-cancer therapeutic agent; indeed, its persistent administration could elicit delayed manifestation of mechanisms, such as aneuploidy and CIN, that could be a prelude to tumourigenesis.

REFERENCES

1. *The Global Burden of Disease 2004 Update Introduction.* Global Burden of Disease: 2004 Update, 2008.

2. Bray, F., et al., *Global cancer transitions according to the Human Development Index (2008-2030): a population-based study.* Lancet Oncol, 2012. **13**(8): p. 790-801.

3. Cameron, D., et al., *Research-intensive cancer care in the NHS in the UK.* Annals of Oncology, 2011. **22**: p. 29-35.

4. Mistry, M., et al., *Cancer incidence in the United Kingdom: projections to the year 2030.* British Journal of Cancer, 2011. **105**(11): p. 1795-1803.

5. UK, C.R., *Cancer Research UK (2013). Cancer Statistics Report: Cancer Mortality in the UK in 2010*. 2013.

6. UK, C.R., *http://www.cancerresearchuk.org/cancer-info/cancerstats/mortality/mortality-projections/.*

7. UK, C.R., *http://www.cancerresearchuk.org/cancer-info/cancerstats/incidence/all-cancers-combined/#source1.*

8. Siegel, R., D. Naishadham, and A. Jemal, *Cancer statistics, 2012.* CA Cancer J Clin, 2012. **62**(1): p. 10-29.

9. UK, C.R., *http://www.cancerresearchuk.org/cancer-info/cancerstats/types/breast/.* 2013.

10. Weigelt, B., J.L. Peterse, and L.J. van 't Veer, *Breast cancer metastasis: markers and models.* Nat Rev Cancer, 2005. **5**(8): p. 591-602.

11. Hajdu, S.I., *Greco-roman thought about cancer.* Cancer, 2004. **100**(10): p. 2048-2051.

12. Lobo, N.A., et al., *The biology of cancer stem cells.* Annu Rev Cell Dev Biol, 2007. **23**: p. 675-99.

13. Chaffer, C.L. and R.A. Weinberg, *A Perspective on Cancer Cell Metastasis.* Science, 2011. **331**(6024): p. 1559-1564.

14. Husemann, Y., et al., *Systemic spread is an early step in breast cancer.* Cancer Cell, 2008. **13**(1): p. 58-68.

15. Briasoulis, E. and N. Pavlidis, *Cancer of Unknown Primary Origin.* Oncologist, 1997. **2**(3): p. 142-152.

16. L., F., *The experimental study of tumour progression: A review.* Cancer research, 1954. **14**: p. 327-39.

17. Bonnet, D. and J.E. Dick, *Human acute myeloid leukemia is organized as a hierarchy that originates from a primitive hematopoietic cell.* Nature Medicine, 1997. **3**(7): p. 730-737.

18. Nguyen, L.V., et al., *Cancer stem cells: an evolving concept.* Nat Rev Cancer, 2012. **12**(2): p. 133-43.

19. Weiss, L., *Metastatic inefficiency.* Adv Cancer Res, 1990. **54**: p. 159-211.

20. Wong, C.W., et al., *Apoptosis: an early event in metastatic inefficiency.* Cancer Res, 2001. **61**(1): p. 333-8.

21. Sahai, E., *Illuminating the metastatic process.* Nat Rev Cancer, 2007. **7**(10): p. 737-49.

22. Fidler, I.J., *The pathogenesis of cancer metastasis: the 'seed and soil' hypothesis revisited.* Nat Rev Cancer, 2003. **3**(6): p. 453-8.

23. O'Brien, L.E., M.M. Zegers, and K.E. Mostov, *Opinion: Building epithelial architecture: insights from three-dimensional culture models.* Nat Rev Mol Cell Biol, 2002. **3**(7): p. 531-7.

24. Alberts B., J.A., Lewis J., Raff M., Roberts K., Walter P. , *Molecular Biology of the Cell.* 2008.

25. Yurchenco, P.D. and J.J. O'Rear, *Basal lamina assembly.* Curr Opin Cell Biol, 1994. **6**(5): p. 674-81.

26. A., B.R., *Atlas of Microscopic Anatomy - A Functional Approach: Companion to Histology and Neuroanatomy: Second Edition.* 1999.

27. Guillot, C. and T. Lecuit, *Mechanics of epithelial tissue homeostasis and morphogenesis.* Science, 2013. **340**(6137): p. 1185-9.

28. Mantovani, A., et al., *Cancer-related inflammation.* Nature, 2008. **454**(7203): p. 436-44.

29. Ma, X.J., et al., *Gene expression profiles of human breast cancer progression.* Proc Natl Acad Sci U S A, 2003. **100**(10): p. 5974-9.

30. Ridley, A.J., et al., *Cell migration: integrating signals from front to back.* Science, 2003. **302**(5651): p. 1704-9.

31. Condeelis, J. and J.E. Segall, *Intravital imaging of cell movement in tumours.* Nature reviews. Cancer, 2003. **3**(12): p. 921-30.

32. Friedl, P. and K. Wolf, *Plasticity of cell migration: a multiscale tuning model.* J Cell Biol, 2010. **188**(1): p. 11-9.

33. Friedl, P., et al., *Migration of coordinated cell clusters in mesenchymal and epithelial cancer explants in vitro.* Cancer research, 1995. **55**(20): p. 4557-60.

34. Fackler, O.T. and R. Grosse, *Cell motility through plasma membrane blebbing.* J Cell Biol, 2008. **181**(6): p. 879-84.

35. Sanz-Moreno, V. and C.J. Marshall, *Rho-GTPase signaling drives melanoma cell plasticity.* Cell Cycle, 2009. **8**(10): p. 1484-7.

36. Friedl, P. and K. Wolf, *Tumour-cell invasion and migration: diversity and escape mechanisms.* Nature reviews. Cancer, 2003. **3**(5): p. 362-74.

37. Raftopoulou, M. and A. Hall, *Cell migration: Rho GTPases lead the way.* Developmental biology, 2004. **265**(1): p. 23-32.

38. Deisboeck, T.S. and I.D. Couzin, *Collective behavior in cancer cell populations.* BioEssays : news and reviews in molecular, cellular and developmental biology, 2009. **31**(2): p. 190-7.

39. Wolf, K., et al., *Compensation mechanism in tumor cell migration: mesenchymal-amoeboid transition after blocking of pericellular proteolysis.* The Journal of cell biology, 2003. **160**(2): p. 267-77.

40. Paulus, W., et al., *Diffuse brain invasion of glioma cells requires beta 1 integrins.* Laboratory investigation; a journal of technical methods and pathology, 1996. **75**(6): p. 819-26.

41. Thiery, J.P., *Epithelial-mesenchymal transitions in tumour progression.* Nat Rev Cancer, 2002. **2**(6): p. 442-54.

42. Ozerlat, I., *Cell migration: The benefit of being single.* Nature reviews. Molecular cell biology, 2009. **10**(12): p. 816.

43. Thiery, J.P., *Epithelial-mesenchymal transitions in tumour progression.* Nature reviews. Cancer, 2002. **2**(6): p. 442-54.

44. Batlle, E., et al., *The transcription factor snail is a repressor of E-cadherin gene expression in epithelial tumour cells.* Nature cell biology, 2000. **2**(2): p. 84-9.

45. Comijn, J., et al., *The two-handed E box binding zinc finger protein SIP1 downregulates E-cadherin and induces invasion.* Molecular cell, 2001. **7**(6): p. 1267-78.

46. Eger, A., et al., *DeltaEF1 is a transcriptional repressor of E-cadherin and regulates epithelial plasticity in breast cancer cells.* Oncogene, 2005. **24**(14): p. 2375-85.

47. Hajra, K.M., D.Y. Chen, and E.R. Fearon, *The SLUG zinc-finger protein represses E-cadherin in breast cancer.* Cancer research, 2002. **62**(6): p. 1613-8.

48. Yang, J., et al., *Twist, a master regulator of morphogenesis, plays an essential role in tumor metastasis.* Cell, 2004. **117**(7): p. 927-39.

49. Peinado, H., F. Portillo, and A. Cano, *Transcriptional regulation of cadherins during development and carcinogenesis.* The International journal of developmental biology, 2004. **48**(5-6): p. 365-75.

50. Zavadil, J. and E.P. Bottinger, *TGF-beta and epithelial-to-mesenchymal transitions.* Oncogene, 2005. **24**(37): p. 5764-74.

51. Larue, L. and A. Bellacosa, *Epithelial-mesenchymal transition in development and cancer: role of phosphatidylinositol 3' kinase/AKT pathways.* Oncogene, 2005. **24**(50): p. 7443-54.

52. Yang, J. and R.A. Weinberg, *Epithelial-mesenchymal transition: at the crossroads of development and tumor metastasis.* Developmental cell, 2008. **14**(6): p. 818-29.

53. Zeisberg, M., A.A. Shah, and R. Kalluri, *Bone morphogenic protein-7 induces mesenchymal to epithelial transition in adult renal fibroblasts and facilitates regeneration of injured kidney.* The Journal of biological chemistry, 2005. **280**(9): p. 8094-100.

54. Johnsen, M., et al., *Cancer invasion and tissue remodeling: common themes in proteolytic matrix degradation.* Current Opinion in Cell Biology, 1998. **10**(5): p. 667-671.

55. Sameni, M., K. Moin, and B.F. Sloane, *Imaging proteolysis by living human breast cancer cells.* Neoplasia, 2000. **2**(6): p. 496-504.

56. Pulyaeva, H., et al., *MT1-MMP correlates with MMP-2 activation potential seen after epithelial to mesenchymal transition in human breast carcinoma cells (vol 15, pg 117, 1997).* Clinical & Experimental Metastasis, 1997. **15**(3): p. 338-338.

57. Jeffers, M., S. Rong, and G.F. VandeWoude, *Enhanced tumorigenicity and invasion-metastasis by hepatocyte growth factor scatter factor-met signalling in human cells concomitant with induction of the urokinase proteolysis network.* Molecular and Cellular Biology, 1996. **16**(3): p. 1115-1125.

58. Nabeshima, K., et al., *Front-cell-specific expression of membrane-type 1 matrix metalloproteinase and gelatinase A during cohort migration of colon carcinoma cells induced by hepatocyte growth factor/scatter factor.* Cancer Res, 2000. **60**(13): p. 3364-9.

59. Wolf, K., et al., *Multi-step pericellular proteolysis controls the transition from individual to collective cancer cell invasion.* Nat Cell Biol, 2007. **9**(8): p. 893-904.

60. Sabeh, F., R. Shimizu-Hirota, and S.J. Weiss, *Protease-dependent versus -independent cancer cell invasion programs: three-dimensional amoeboid movement revisited.* J Cell Biol, 2009. **185**(1): p. 11-9.

61. Gaggioli, C., et al., *Fibroblast-led collective invasion of carcinoma cells with differing roles for RhoGTPases in leading and following cells.* Nat Cell Biol, 2007. **9**(12): p. 1392-400.

62. Andreasen, P.A., et al., *The urokinase-type plasminogen activator system in cancer metastasis: A review.* International Journal of Cancer, 1997. **72**(1): p. 1-22.

63. Dano, K., et al., *Plasminogen activation and cancer.* Thrombosis and Haemostasis, 2005. **93**(4): p. 676-681.

64. Andreasen, P.A., R. Egelund, and H.H. Petersen, *The plasminogen activation system in tumor growth, invasion, and metastasis.* Cellular and Molecular Life Sciences, 2000. **57**(1): p. 25-40.

65. Stephens, R.W., et al., *The urokinase plasminogen activator system as a target for prognostic studies in breast cancer.* Breast Cancer Research and Treatment, 1998. **52**(1-3): p. 99-111.

66. Rabbani, S.A. and J. Gladu, *Urokinase receptor antibody can reduce tumor volume and detect the presence of occult tumor netastases in vivo.* Cancer Research, 2002. **62**(8): p. 2390-2397.

67. Rao, J.S., *Molecular mechanisms of glioma invasiveness: The role of proteases.* Nature Reviews Cancer, 2003. **3**(7): p. 489-501.

68. Kassam, G., et al., *The role of annexin II tetramer in the activation of plasminogen.* Journal of Biological Chemistry, 1998. **273**(8): p. 4790-4799.

69. Grondahlhansen, J., F. Bach, and P. Munkholmlarsen, *Tissue-Type Plasminogen-Activator in Plasma from Breast-Cancer Patients Determined by Enzyme-Linked-Immunosorbent-Assay.* British Journal of Cancer, 1990. **61**(3): p. 412-414.

70. Mai, J.X., D.M. Waisman, and B.F. Sloane, *Cell surface complex of cathepsin B/annexin II tetramer in malignant progression.* Biochimica Et Biophysica Acta-Protein Structure and Molecular Enzymology, 2000. **1477**(1-2): p. 215-230.

71. Murphy, G., et al., *Mechanisms for pro matrix metalloproteinase activation.* Apmis, 1999. **107**(1): p. 38-44.

72. Chiquetehrismann, R., et al., *Tenascin - an Extracellular-Matrix Protein Involved in Tissue Interactions during Fetal Development and Oncogenesis.* Cell, 1986. **47**(1): p. 131-139.

73. Sharma, M., R.T. Ownbey, and M.C. Sharma, *Breast cancer cell surface annexin II induces cell migration and neoangiogenesis via tPA dependent plasmin generation.* Experimental and Molecular Pathology, 2010. **88**(2): p. 278-286.

74. Shetty, P.K., et al., *Reciprocal Regulation of Annexin A2 and EGFR with Her-2 in Her-2 Negative and Herceptin-Resistant Breast Cancer.* Plos One, 2012. **7**(9).

75. Bacac, M. and I. Stamenkovic, *Metastatic cancer cell.* Annu Rev Pathol, 2008. **3**: p. 221-47.

76. Bergers, G. and L.E. Benjamin, *Tumorigenesis and the angiogenic switch.* Nature Reviews Cancer, 2003. **3**(6): p. 401-410.

77. Alitalo, K., *Lymphangiogenesis in development and human disease.* Journal of Vascular Research, 2006. **43**: p. 24-24.

78. Valastyan, S. and R.A. Weinberg, *Tumor Metastasis: Molecular Insights and Evolving Paradigms.* Cell, 2011. **147**(2): p. 275-292.

79. Yamaguchi, H., J. Wyckoff, and J. Condeelis, *Cell migration in tumors.* Current Opinion in Cell Biology, 2005. **17**(5): p. 559-564.

80. Wyckoff, J.B., et al., *Direct visualization of macrophage-assisted tumor cell intravasation in mammary tumors.* Cancer Research, 2007. **67**(6): p. 2649-2656.

81. Davidson, B., *Malignant Effusions: From Diagnosis to Biology.* Acta Cytologica, 2010. **54**(3): p. 385-386.

82. Cailleau, R., et al., *Breast Tumor-Cell Lines from Pleural Effusions.* Journal of the National Cancer Institute, 1974. **53**(3): p. 661-674.

83. Marinho, V.F.Z., et al., *Lymph vascular invasion in invasive mammary carcinomas identified by the endothelial lymphatic marker D2-40 is associated with other indicators of poor prognosis.* Bmc Cancer, 2008. **8**.

84. Gupta, G.P. and J. Massague, *Cancer metastasis: Building a framework.* Cell, 2006. **127**(4): p. 679-695.

85. Butler, T.P. and P.M. Gullino, *Quantitation of Cell Shedding into Efferent Blood of Mammary Adenocarcinoma.* Cancer Research, 1975. **35**(3): p. 512-516.

86. Liu, M.C., et al., *Circulating Tumor Cells: A Useful Predictor of Treatment Efficacy in Metastatic Breast Cancer.* Journal of Clinical Oncology, 2009. **27**(31): p. 5153-5159.

87. Cristofanilli, M., et al., *Circulating tumor cells: A novel prognostic factor for newly diagnosed metastatic breast cancer.* Journal of Clinical Oncology, 2005. **23**(7): p. 1420-1430.

88. Guo, W. and F.G. Giancotti, *Integrin signalling during tumour progression.* Nat Rev Mol Cell Biol, 2004. **5**(10): p. 816-26.

89. Taddei, M.L., et al., *Anoikis: an emerging hallmark in health and diseases.* J Pathol, 2012. **226**(2): p. 380-93.

90. Frisch, S.M. and H. Francis, *Disruption of epithelial cell-matrix interactions induces apoptosis.* J Cell Biol, 1994. **124**(4): p. 619-26.

91. Douma, S., et al., *Suppression of anoikis and induction of metastasis by the neurotrophic receptor TrkB.* Nature, 2004. **430**(7003): p. 1034-9.

92. Klein, C.A., *The biology and analysis of single disseminated tumour cells.* Trends Cell Biol, 2000. **10**(11): p. 489-93.

93. Fernandez, Y., et al., *Inhibition of apoptosis in human breast cancer cells: role in tumor progression to the metastatic state.* Int J Cancer, 2002. **101**(4): p. 317-26.

94. Frankel, A., et al., *Induction of anoikis and suppression of human ovarian tumor growth in vivo by down-regulation of Bcl-X(L).* Cancer Res, 2001. **61**(12): p. 4837-41.

95. Taylor, I., *Liver metastases from colorectal cancer: lessons from past and present clinical studies.* Br J Surg, 1996. **83**(4): p. 456-60.

96. Al-Mehdi, A.B., et al., *Intravascular origin of metastasis from the proliferation of endothelium-attached tumor cells: a new model for metastasis.* Nat Med, 2000. **6**(1): p. 100-2.

97. Valastyan, S. and R.A. Weinberg, *Tumor metastasis: molecular insights and evolving paradigms.* Cell, 2011. **147**(2): p. 275-92.

98. Kaplan, R.N., et al., *VEGFR1-positive haematopoietic bone marrow progenitors initiate the pre-metastatic niche.* Nature, 2005. **438**(7069): p. 820-7.

99. Kang, S.Y., et al., *Prosaposin inhibits tumor metastasis via paracrine and endocrine stimulation of stromal p53 and Tsp-1.* Proceedings of the National Academy of Sciences of the United States of America, 2009. **106**(29): p. 12115-20.

100. Minn, A.J., et al., *Genes that mediate breast cancer metastasis to lung.* Nature, 2005. **436**(7050): p. 518-524.

101. Gupta, G.P., et al., *Mediators of vascular remodelling co-opted for sequential steps in lung metastasis.* Nature, 2007. **446**(7137): p. 765-U2.

102. Ridley, A.J., *Life at the leading edge.* Cell, 2011. **145**(7): p. 1012-22.

103. Ponti, A., et al., *Two distinct actin networks drive the protrusion of migrating cells.* Science, 2004. **305**(5691): p. 1782-6.

104. Machesky, L.M. and A. Li, *Fascin: Invasive filopodia promoting metastasis.* Communicative & integrative biology, 2010. **3**(3): p. 263-70.

105. Block, J., et al., *Filopodia formation induced by active mDia2/Drf3.* Journal of microscopy, 2008. **231**(3): p. 506-17.

106. Fackler, O.T. and R. Grosse, *Cell motility through plasma membrane blebbing.* Journal of Cell Biology, 2008. **181**(6): p. 879-884.

107. Buccione, R., J.D. Orth, and M.A. McNiven, *Foot and mouth: Podosomes, invadopodia and circular dorsal ruffles.* Nature Reviews Molecular Cell Biology, 2004. **5**(8): p. 647-657.

108. Poincloux, R., F. Lizarraga, and P. Chavrier, *Matrix invasion by tumour cells: a focus on MT1-MMP trafficking to invadopodia.* Journal of cell science, 2009. **122**(17): p. 3015-3024.

109. Gligorijevic, B., et al., *N-WASP-mediated invadopodium formation is involved in intravasation and lung metastasis of mammary tumors.* Journal of cell science, 2012. **125**(3): p. 724-734.

110. Hall, A., *Rho GTPases and the actin cytoskeleton.* Science, 1998. **279**(5350): p. 509-14.

111. Myat, M.M., et al., *MARCKS regulates membrane ruffling and cell spreading.* Curr Biol, 1997. **7**(8): p. 611-4.

112. Nakahara, H., et al., *Transmembrane/cytoplasmic domain-mediated membrane type 1-matrix metalloprotease docking to invadopodia is required for cell invasion.* Proc Natl Acad Sci U S A, 1997. **94**(15): p. 7959-64.

113. Nurnberg, A., T. Kitzing, and R. Grosse, *Nucleating actin for invasion.* Nat Rev Cancer, 2011. **11**(3): p. 177-87.

114. Nobes, C.D. and A. Hall, *Rho, rac and cdc42 GTPases: regulators of actin structures, cell adhesion and motility.* Biochem Soc Trans, 1995. **23**(3): p. 456-9.

115. Rohatgi, R., et al., *The interaction between N-WASP and the Arp2/3 complex links Cdc42-dependent signals to actin assembly.* Cell, 1999. **97**(2): p. 221-31.

116. Nobes, C.D. and A. Hall, *Rho, rac, and cdc42 GTPases regulate the assembly of multimolecular focal complexes associated with actin stress fibers, lamellipodia, and filopodia.* Cell, 1995. **81**(1): p. 53-62.

117. Buccione, R., G. Caldieri, and I. Ayala, *Invadopodia: specialized tumor cell structures for the focal degradation of the extracellular matrix.* Cancer metastasis reviews, 2009. **28**(1-2): p. 137-49.

118. Ridley, A.J., *Life at the Leading Edge.* Cell, 2011. **145**(7): p. 1012-1022.

119. Wang, W., et al., *Identification and testing of a gene expression signature of invasive carcinoma cells within primary mammary tumors.* Cancer Res, 2004. **64**(23): p. 8585-94.

120. Campellone, K.G. and M.D. Welch, *A nucleator arms race: cellular control of actin assembly.* Nat Rev Mol Cell Biol, 2010. **11**(4): p. 237-51.

121. Yamaguchi, H., et al., *Molecular mechanisms of invadopodium formation: the role of the N-WASP-Arp2/3 complex pathway and cofilin.* Journal of Cell Biology, 2005. **168**(3): p. 441-452.

122. Takenawa, T. and S. Suetsugu, *The WASP-WAVE protein network: connecting the membrane to the cytoskeleton.* Nature reviews. Molecular cell biology, 2007. **8**(1): p. 37-48.

123. Bernard, O., *Lim kinases, regulators of actin dynamics.* International Journal of Biochemistry & Cell Biology, 2007. **39**(6): p. 1071-1076.

124. Johnson, E.O., et al., *LIMK2 is a crucial regulator and effector of Aurora-A-kinase-mediated malignancy.* Journal of Cell Science, 2012. **125**(5): p. 1204-1216.

125. Sells, M.A., et al., *Human p21-activated kinase (Pak1) regulates actin organization in mammalian cells.* Current biology : CB, 1997. **7**(3): p. 202-10.

126. Kumar, R., A.E. Gururaj, and C.J. Barnes, *p21-activated kinases in cancer.* Nat Rev Cancer, 2006. **6**(6): p. 459-71.

127. van Rheenen, J., J. Condeelis, and M. Glogauer, *A common cofilin activity cycle in invasive tumor cells and inflammatory cells.* Journal of cell science, 2009. **122**(3): p. 305-311.

128. Delorme, V., et al., *Cofilin activity downstream of Pak1 regulates cell protrusion efficiency by organizing lamellipodium and lamella actin networks.* Developmental cell, 2007. **13**(5): p. 646-662.

129. Coniglio, S.J., S. Zavarella, and M.H. Symons, *Pak1 and Pak2 mediate tumor cell invasion through distinct signaling mechanisms.* Mol Cell Biol, 2008. **28**(12): p. 4162-72.

130. Sahai, E. and C.J. Marshall, *Differing modes of tumour cell invasion have distinct requirements for Rho/ROCK signalling and extracellular proteolysis.* Nat Cell Biol, 2003. **5**(8): p. 711-9.

131. Vicente-Manzanares, M., et al., *Non-muscle myosin II takes centre stage in cell adhesion and migration.* Nat Rev Mol Cell Biol, 2009. **10**(11): p. 778-90.

132. Katoh, K., et al., *Rho-kinase-mediated contraction of isolated stress fibers.* Journal of Cell Biology, 2001. **153**(3): p. 569-583.

133. Katoh, K., et al., *Rho-kinase--mediated contraction of isolated stress fibers.* J Cell Biol, 2001. **153**(3): p. 569-84.

134. Kardash, E., et al., *A role for Rho GTPases and cell-cell adhesion in single-cell motility in vivo.* Nature cell biology, 2010. **12**(1): p. 47-U112.

135. Hanna, S. and M. El-Sibai, *Signaling networks of Rho GTPases in cell motility.* Cell Signal, 2013. **25**(10): p. 1955-1961.

136. Rikitake, Y., K. Mandai, and Y. Takai, *The role of nectins in different types of cell-cell adhesion.* Journal of cell science, 2012. **125**(Pt 16): p. 3713-22.

137. Takai, Y. and H. Nakanishi, *Nectin and afadin: novel organizers of intercellular junctions.* Journal of cell science, 2003. **116**(Pt 1): p. 17-27.

138. Yonemura, S., *Cadherin-actin interactions at adherens junctions.* Current opinion in cell biology, 2011. **23**(5): p. 515-22.

139. Meng, W. and M. Takeichi, *Adherens junction: molecular architecture and regulation.* Cold Spring Harbor perspectives in biology, 2009. **1**(6): p. a002899.

140. Mandai, K., et al., *Ponsin/SH3P12: an l-afadin- and vinculin-binding protein localized at cell-cell and cell-matrix adherens junctions.* The Journal of cell biology, 1999. **144**(5): p. 1001-17.

141. Asada, M., et al., *ADIP, a novel Afadin- and alpha-actinin-binding protein localized at cell-cell adherens junctions.* The Journal of biological chemistry, 2003. **278**(6): p. 4103-11.

142. Ooshio, T., et al., *Involvement of LMO7 in the association of two cell-cell adhesion molecules, nectin and E-cadherin, through afadin and alpha-actinin in epithelial cells.* The Journal of biological chemistry, 2004. **279**(30): p. 31365-73.

143. Brieher, W.M. and A.S. Yap, *Cadherin junctions and their cytoskeleton(s).* Current Opinion in Cell Biology, 2013. **25**(1): p. 39-46.

144. Verma, S., et al., *A WAVE2-Arp2/3 actin nucleator apparatus supports junctional tension at the epithelial zonula adherens.* Molecular biology of the cell, 2012. **23**(23): p. 4601-10.

145. Smutny, M., et al., *Myosin II isoforms identify distinct functional modules that support integrity of the epithelial zonula adherens.* Nature Cell Biology, 2010. **12**(7): p. 696-U147.

146. Yonemura, S., et al., *alpha-Catenin as a tension transducer that induces adherens junction development.* Nature cell biology, 2010. **12**(6): p. 533-42.

147. Takai, Y., et al., *Nectins and nectin-like molecules: roles in contact inhibition of cell movement and proliferation.* Nature reviews. Molecular cell biology, 2008. **9**(8): p. 603-15.

148. Xiong, J.P., et al., *Crystal structure of the extracellular segment of integrin alpha Vbeta3 in complex with an Arg-Gly-Asp ligand.* Science, 2002. **296**(5565): p. 151-5.

149. Huang, R.Y., P. Guilford, and J.P. Thiery, *Early events in cell adhesion and polarity during epithelial-mesenchymal transition.* Journal of cell science, 2012. **125**(Pt 19): p. 4417-22.

150. Hynes, R.O., *Integrins: versatility, modulation, and signaling in cell adhesion.* Cell, 1992. **69**(1): p. 11-25.

151. Koivunen, E., B. Wang, and E. Ruoslahti, *Phage libraries displaying cyclic peptides with different ring sizes: ligand specificities of the RGD-directed integrins.* Bio/technology, 1995. **13**(3): p. 265-70.

152. Petit, V. and J.P. Thiery, *Focal adhesions: structure and dynamics.* Biology of the cell / under the auspices of the European Cell Biology Organization, 2000. **92**(7): p. 477-94.

153. Wehrle-Haller, B., *Structure and function of focal adhesions.* Current opinion in cell biology, 2012. **24**(1): p. 116-24.

154. Geiger, B., et al., *Transmembrane crosstalk between the extracellular matrix--cytoskeleton crosstalk.* Nature reviews. Molecular cell biology, 2001. **2**(11): p. 793-805.

155. Turner, C.E., K.A. West, and M.C. Brown, *Paxillin-ARF GAP signaling and the cytoskeleton.* Curr Opin Cell Biol, 2001. **13**(5): p. 593-9.

156. Stofega, M.R., et al., *Constitutive p21-activated kinase (PAK) activation in breast cancer cells as a result of mislocalization of PAK to focal adhesions.* Mol Biol Cell, 2004. **15**(6): p. 2965-77.

157. Bailly, M., *Ena/VASP family: new partners, bigger enigma.* Dev Cell, 2004. **7**(4): p. 462-3.

158. Yu, C.H., et al., *Early integrin binding to Arg-Gly-Asp peptide activates actin polymerization and contractile movement that stimulates outward translocation.* Proceedings of the National Academy of Sciences of the United States of America, 2011. **108**(51): p. 20585-90.

159. Hanna, S. and M. El-Sibai, *Signaling networks of Rho GTPases in cell motility.* Cellular signalling, 2013.

160. Friedl, P. and K. Wolf, *Plasticity of cell migration: a multiscale tuning model.* The Journal of cell biology, 2010. **188**(1): p. 11-9.

161. Geiger, B., et al., *Transmembrane crosstalk between the extracellular matrix--cytoskeleton crosstalk.* Nat Rev Mol Cell Biol, 2001. **2**(11): p. 793-805.

162. Chrzanowska-Wodnicka, M. and K. Burridge, *Rho-stimulated contractility drives the formation of stress fibers and focal adhesions.* J Cell Biol, 1996. **133**(6): p. 1403-15.

163. Webb, D.J., et al., *FAK-Src signalling through paxillin, ERK and MLCK regulates adhesion disassembly.* Nature cell biology, 2004. **6**(2): p. 154-+.

164. Sanders, L.C., et al., *Inhibition of myosin light chain kinase by p21-activated kinase.* Science, 1999. **283**(5410): p. 2083-5.

165. Chew, T.L., et al., *Phosphorylation of non-muscle myosin II regulatory light chain by p21-activated kinase (gamma-PAK).* J Muscle Res Cell Motil, 1998. **19**(8): p. 839-54.

166. Stockton, R.A., E. Schaefer, and M.A. Schwartz, *p21-activated kinase regulates endothelial permeability through modulation of contractility.* J Biol Chem, 2004. **279**(45): p. 46621-30.

167. Zeng, Q., et al., *Endothelial cell retraction is induced by PAK2 monophosphorylation of myosin II.* J Cell Sci, 2000. **113 (Pt 3)**: p. 471-82.

168. Schmidt, A. and A. Hall, *Guanine nucleotide exchange factors for Rho GTPases: turning on the switch.* Genes & Development, 2002. **16**(13): p. 1587-1609.

169. Buchsbaum, R.J., *Rho activation at a glance.* Journal of Cell Science, 2007. **120**(7): p. 1149-1152.

170. Schiller, M.R., *Coupling receptor tyrosine kinases to Rho GTPases - GEFs what's the link.* Cellular Signalling, 2006. **18**(11): p. 1834-1843.

171. Sah, V.P., et al., *The role of Rho in G protein-coupled receptor signal transduction.* Annual Review of Pharmacology and Toxicology, 2000. **40**: p. 459-489.

172. Yoshii, S., et al., *alpha PIX nucleotide exchange factor is activated by interaction with phosphatidylinositol 3-kinase.* Oncogene, 1999. **18**(41): p. 5680-5690.

173. Filipenko, N.R., et al., *Integrin-linked kinase activity regulates Rac- and Cdc42-mediated actin cytoskeleton reorganization via alpha-PIX.* Oncogene, 2005. **24**(38): p. 5837-5849.

174. Baird, D., Q.Y. Feng, and R.A. Cerione, *The cool-2/alpha-Pix protein mediates a Cdc42-Rac signaling cascade.* Current Biology, 2005. **15**(1): p. 1-10.

175. Feng, Q.Y., D. Baird, and R.A. Cerione, *Novel regulatory mechanisms for the Dbl family guanine nucleotide exchange factor Cool-2/alpha-Pix.* Embo Journal, 2004. **23**(17): p. 3492-3504.

176. Rosenberger, G., A. Gal, and K. Kutsche, *alpha PIX associates with calpain 4, the small subunit of calpain, and has a dual role in integrin-mediated cell spreading.* Journal of Biological Chemistry, 2005. **280**(8): p. 6879-6889.

177. Vicente-Manzanares, M., D.J. Webb, and A.R. Horwitz, *Cell migration at a glance.* Journal of Cell Science, 2005. **118**(21).

178. Hynes, N.E. and G. MacDonald, *ErbB receptors and signaling pathways in cancer.* Current Opinion in Cell Biology, 2009. **21**(2): p. 177-184.

179. Slamon, D.J., et al., *Human breast cancer: correlation of relapse and survival with amplification of the HER-2/neu oncogene.* Science, 1987. **235**(4785): p. 177-82.

180. Bazley, L.A. and W.J. Gullick, *The epidermal growth factor receptor family.* Endocr Relat Cancer, 2005. **12 Suppl 1**: p. S17-27.

181. Harris, R.C., E. Chung, and R.J. Coffey, *EGF receptor ligands.* Exp Cell Res, 2003. **284**(1): p. 2-13.

182. Riese, D.J., et al., *The Cellular-Response to Neuregulins Is Governed by Complex Interactions of the Erbb Receptor Family.* Molecular and Cellular Biology, 1995. **15**(10): p. 5770-5776.

183. Yarden, Y. and M.X. Sliwkowski, *Untangling the ErbB signalling network.* Nat Rev Mol Cell Biol, 2001. **2**(2): p. 127-37.

184. Brandt, B.H., et al., *c-erbB-2/EGFR as dominant heterodimerization partners determine a motogenic phenotype in human breast cancer cells.* FASEB J, 1999. **13**(14): p. 1939-49.

185. Guy, C.T., et al., *Expression of the neu protooncogene in the mammary epithelium of transgenic mice induces metastatic disease.* Proc Natl Acad Sci U S A, 1992. **89**(22): p. 10578-82.

186. Moghal, N. and P.W. Sternberg, *Multiple positive and negative regulators of signaling by the EGF-receptor.* Curr Opin Cell Biol, 1999. **11**(2): p. 190-6.

187. Hill, K., et al., *Specific requirement for the p85-p110alpha phosphatidylinositol 3-kinase during epidermal growth factor-stimulated actin nucleation in breast cancer cells.* J Biol Chem, 2000. **275**(6): p. 3741-4.

188. Feldner, J.C. and B.H. Brandt, *Cancer cell motility - On the road from c-erbB-2 receptor steered signaling to actin reorganization.* Experimental Cell Research, 2002. **272**(2): p. 93-108.

189. Moores, S.L., et al., *Vav family proteins couple to diverse cell surface receptors.* Mol Cell Biol, 2000. **20**(17): p. 6364-73.

190. He, H., et al., *Signal therapy for RAS-induced cancers in combination of AG 879 and PP1, specific inhibitors for ErbB2 and Src family kinases, that block PAK activation.* Cancer Journal, 2001. **7**(3): p. 191-202.

191. Eferl, R. and E.F. Wagner, *AP-1: A double-edged sword in tumorigenesis.* Nature Reviews Cancer, 2003. **3**(11): p. 859-868.

192. Lu, W.G., et al., *Activation of Pak by membrane localization mediated by an SH3 domain from the adaptor protein Nck.* Current Biology, 1997. **7**(2): p. 85-94.

193. Frost, J.A., et al., *Actions of Rho family small G proteins and p21-activated protein kinases on mitogen-activated protein kinase family members.* Molecular and Cellular Biology, 1996. **16**(7): p. 3707-3713.

194. Malliri, A., et al., *The transcription factor AP-1 is required for EGF-induced activation of rho-like GTPases, cytoskeletal rearrangements, motility, and in vitro invasion of A431 cells.* Journal of Cell Biology, 1998. **143**(4): p. 1087-1099.

195. Ozanne, B.W., et al., *Transcription factors control invasion: AP-1 the first among equals.* Oncogene, 2007. **26**(1): p. 1-10.

196. Rao, C.V., et al., *Human chorionic gonadotropin decreases proliferation and invasion of breast cancer MCF-7 cells by inhibiting NF-kappa B and AP-1 activation.* Journal of Biological Chemistry, 2004. **279**(24): p. 25503-25510.

197. Das, R., G.H. Mahabeleshwar, and G.C. Kundu, *Osteopontin induces AP-1-mediated secretion of urokinase-type plasminogen activator through c-Src-dependent epidermal growth factor receptor transactivation in breast cancer cells.* Journal of Biological Chemistry, 2004. **279**(12): p. 11051-11064.

198. Ozanne, B.W., et al., *Transcriptional regulation of cell invasion: AP-1 regulation of a multigenic invasion programme.* European Journal of Cancer, 2000. **36**(13): p. 1640-1648.

199. Schaerli, P. and R. Jaggi, *EGF-induced programmed cell death of human mammary carcinoma MDA-MB-468 cells is preceded by activation AP-1.* Cell Mol Life Sci, 1998. **54**(2): p. 129-38.

200. Siegel, J.J. and A. Amon, *New insights into the troubles of aneuploidy.* Annu Rev Cell Dev Biol, 2012. **28**: p. 189-214.

201. Pfau, S.J. and A. Amon, *Chromosomal instability and aneuploidy in cancer: from yeast to man.* EMBO Rep, 2012. **13**(6): p. 515-27.

202. Hassold, T. and P. Hunt, *To ERR (meiotically) is human: The genesis of human aneuploidy.* Nature Reviews Genetics, 2001. **2**(4): p. 280-291.

203. Vitre, B.D. and D.W. Cleveland, *Centrosomes, chromosome instability (CIN) and aneuploidy.* Current Opinion in Cell Biology, 2012. **24**(6): p. 809-815.

204. Weaver, B.A.A. and D.W. Cleveland, *Does aneuploidy cause cancer?* Current Opinion in Cell Biology, 2006. **18**(6): p. 658-667.

205. Gordon, D.J., B. Resio, and D. Pellman, *Causes and consequences of aneuploidy in cancer.* Nat Rev Genet, 2012. **13**(3): p. 189-203.

206. Nasmyth, K. and C.H. Haering, *Cohesin: its roles and mechanisms.* Annu Rev Genet, 2009. **43**: p. 525-58.

207. Musacchio, A. and E.D. Salmon, *The spindle-assembly checkpoint in space and time.* Nat Rev Mol Cell Biol, 2007. **8**(5): p. 379-93.

208. Kops, G.J., B.A. Weaver, and D.W. Cleveland, *On the road to cancer: aneuploidy and the mitotic checkpoint.* Nat Rev Cancer, 2005. **5**(10): p. 773-85.

209. Cimini, D., et al., *Merotelic kinetochore orientation is a major mechanism of aneuploidy in mitotic mammalian tissue cells.* Journal of Cell Biology, 2001. **153**(3): p. 517-527.

210. Thompson, S.L. and D.A. Compton, *Chromosome missegregation in human cells arises through specific types of kinetochore-microtubule attachment errors.* Proceedings of the National Academy of Sciences of the United States of America, 2011. **108**(44): p. 17974-17978.

211. Maddika, S., S.M.H. Sy, and J.J. Chen, *Functional Interaction between Chfr and Kif22 Controls Genomic Stability.* Journal of Biological Chemistry, 2009. **284**(19): p. 12998-13003.

212. Kang, D.M., et al., *The checkpoint protein Chfr is a ligase that ubiquitinates Plk1 and inhibits Cdc2 at the G2 to M transition.* Journal of Cell Biology, 2002. **156**(2): p. 249-259.

213. Yu, X.C., et al., *Chfr is required for tumor suppression and Aurora A regulation.* Nature Genetics, 2005. **37**(4): p. 401-406.

214. Tillement, V., et al., *Spindle assembly defects leading to the formation of a monopolar mitotic apparatus.* Biology of the Cell, 2009. **101**(1): p. 1-11.

215. Theodor, B., *Zur frage der Entsehung maligner Tumoren (The origin of malignant tumors).* 1914.

216. Rajagopalan, H. and C. Lengauer, *Aneuploidy and cancer.* Nature, 2004. **432**(7015): p. 338-341.

217. Ricke, R.M., J.H. van Ree, and J.M. van Deursen, *Whole chromosome instability and cancer: a complex relationship.* Trends Genet, 2008. **24**(9): p. 457-66.

218. Solomon, D.A., et al., *Mutational inactivation of STAG2 causes aneuploidy in human cancer.* Science, 2011. **333**(6045): p. 1039-43.

219. Zhou, H., et al., *Tumour amplified kinase STK15/BTAK induces centrosome amplification, aneuploidy and transformation.* Nat Genet, 1998. **20**(2): p. 189-93.

220. Privette, L.M., et al., *Altered expression of the early mitotic checkpoint protein, CHFR, in breast cancers: implications for tumor suppression.* Cancer Res, 2007. **67**(13): p. 6064-74.

221. Puc, J., et al., *Lack of PTEN sequesters CHK1 and initiates genetic instability.* Cancer Cell, 2005. **7**(2): p. 193-204.

222. Lacroix, B. and A.S. Maddox, *Cytokinesis, ploidy and aneuploidy.* Journal of Pathology, 2012. **226**(2): p. 338-351.

223. Glotzer, M., *The molecular requirements for cytokinesis.* Science, 2005. **307**(5716): p. 1735-1739.

224. Douglas, M.E., et al., *Aurora B and 14-3-3 coordinately regulate clustering of centralspindlin during cytokinesis.* Curr Biol, 2010. **20**(10): p. 927-33.

225. Saurin, A.T., et al., *The regulated assembly of a PKC epsilon complex controls the completion of cytokinesis.* Nature Cell Biology, 2008. **10**(8): p. 891-901.

226. Low, S.H., et al., *Syntaxin 2 and endobrevin are required for the terminal step of cytokinesis in mammalian cells.* Developmental Cell, 2003. **4**(5): p. 753-759.

227. Pellinen, T., et al., *Integrin trafficking regulated by Rab21 is necessary for cytokinesis.* Developmental Cell, 2008. **15**(3): p. 371-385.

228. Fededa, J.P. and D.W. Gerlich, *Molecular control of animal cell cytokinesis.* Nature Cell Biology, 2012. **14**(5): p. 440-447.

229. Sagona, A.P. and H. Stenmark, *Cytokinesis and cancer.* FEBS Lett, 2010. **584**(12): p. 2652-61.

230. Zhou, Q., et al., *14-3-3 coordinates microtubules, Rac, and myosin II to control cell mechanics and cytokinesis.* Curr Biol, 2010. **20**(21): p. 1881-9.

231. Low, S.H., et al., *Syntaxin 2 and endobrevin are required for the terminal step of cytokinesis in mammalian cells.* Dev Cell, 2003. **4**(5): p. 753-9.

232. Ganem, N.J., Z. Storchova, and D. Pellman, *Tetraploidy, aneuploidy and cancer.* Current Opinion in Genetics & Development, 2007. **17**(2): p. 157-162.

233. Lingle, W.L., et al., *Centrosome amplification drives chromosomal instability in breast tumor development.* Proc Natl Acad Sci U S A, 2002. **99**(4): p. 1978-83.

234. Andreassen, P.R., et al., *Tetraploid state induces p53-dependent arrest of nontransformed mammalian cells in G1.* Mol Biol Cell, 2001. **12**(5): p. 1315-28.

235. Fujiwara, T., et al., *Cytokinesis failure generating tetraploids promotes tumorigenesis in p53-null cells.* Nature, 2005. **437**(7061): p. 1043-7.

236. Nelson, D.A., et al., *Hypoxia and defective apoptosis drive genomic instability and tumorigenesis.* Genes Dev, 2004. **18**(17): p. 2095-107.

237. Lee, R.C., R.L. Feinbaum, and V. Ambros, *The C. elegans heterochronic gene lin-4 encodes small RNAs with antisense complementarity to lin-14.* Cell, 1993. **75**(5): p. 843-54.

238. Reinhart, B.J., et al., *The 21-nucleotide let-7 RNA regulates developmental timing in Caenorhabditis elegans.* Nature, 2000. **403**(6772): p. 901-906.

239. Pasquinelli, A.E., et al., *Conservation of the sequence and temporal expression of let-7 heterochronic regulatory RNA.* Nature, 2000. **408**(6808): p. 86-9.

240. Lagos-Quintana, M., et al., *Identification of novel genes coding for small expressed RNAs.* Science, 2001. **294**(5543): p. 853-8.

241. Lau, N.C., et al., *An abundant class of tiny RNAs with probable regulatory roles in Caenorhabditis elegans.* Science, 2001. **294**(5543): p. 858-62.

242. miRBase, *http://www.mirbase.org/cgi-bin/browse.pl?org=hsa*. 2013.

243. Chiang, H.R., et al., *Mammalian microRNAs: experimental evaluation of novel and previously annotated genes.* Genes Dev, 2010. **24**(10): p. 992-1009.

244. Friedman, R.C., et al., *Most mammalian mRNAs are conserved targets of microRNAs.* Genome Research, 2009. **19**(1): p. 92-105.

245. Iorio, M.V. and C.M. Croce, *MicroRNAs in cancer: small molecules with a huge impact.* J Clin Oncol, 2009. **27**(34): p. 5848-56.

246. Sotiropoulou, G., et al., *Emerging roles of microRNAs as molecular switches in the integrated circuit of the cancer cell.* RNA, 2009. **15**(8): p. 1443-61.

247. Lujambio, A. and S.W. Lowe, *The microcosmos of cancer.* Nature, 2012. **482**(7385): p. 347-355.

248. Ul Hussain, M., *Micro-RNAs (miRNAs): genomic organisation, biogenesis and mode of action.* Cell and Tissue Research, 2012. **349**(2): p. 405-413.

249. Cai, X.Z., C.H. Hagedorn, and B.R. Cullen, *Human microRNAs are processed from capped, polyadenylated transcripts that can also function as mRNAs.* Rna-a Publication of the Rna Society, 2004. **10**(12): p. 1957-1966.

250. Saini, H.K., S. Griffiths-Jones, and A.J. Enright, *Genomic analysis of human microRNA transcripts.* Proceedings of the National Academy of Sciences of the United States of America, 2007. **104**(45): p. 17719-17724.

251. Baskerville, S. and D.P. Bartel, *Microarray profiling of microRNAs reveals frequent coexpression with neighboring miRNAs and host genes.* Rna-a Publication of the Rna Society, 2005. **11**(3): p. 241-247.

252. Ota, A., et al., *Identification and characterization of a novel gene, C13orf25, as a target for 13q31-q32 amplification in malignant lymphoma.* Cancer Research, 2004. **64**(9): p. 3087-3095.

253. Ruby, J.G., C.H. Jan, and D.P. Bartel, *Intronic microRNA precursors that bypass Drosha processing.* Nature, 2007. **448**(7149): p. 83-86.

254. Rodriguez, A., et al., *Identification of mammalian microRNA host genes and transcription units.* Genome Research, 2004. **14**(10A): p. 1902-1910.

255. Borchert, G.M., W. Lanier, and B.L. Davidson, *RNA polymerase III transcribes human microRNAs.* Nature Structural & Molecular Biology, 2006. **13**(12): p. 1097-1101.

256. Zeng, Y. and B.R. Cullen, *Efficient processing of primary microRNA hairpins by drosha requires flanking nonstructured RNA sequences.* Journal of Biological Chemistry, 2005. **280**(30): p. 27595-27603.

257. Denli, A.M., et al., *Processing of primary microRNAs by the Microprocessor complex.* Nature, 2004. **432**(7014): p. 231-235.

258. Lee, Y., et al., *The nuclear RNase III Drosha initiates microRNA processing.* Nature, 2003. **425**(6956): p. 415-9.

259. Castellano, L. and J. Stebbing, *Deep sequencing of small RNAs identifies canonical and non-canonical miRNA and endogenous siRNAs in mammalian somatic tissues.* Nucleic Acids Res, 2013. **41**(5): p. 3339-51.

260. Okada, C., et al., *A high-resolution structure of the pre-microRNA nuclear export machinery.* Science, 2009. **326**(5957): p. 1275-9.

261. Yi, R., et al., *Exportin-5 mediates the nuclear export of pre-microRNAs and short hairpin RNAs.* Genes Dev, 2003. **17**(24): p. 3011-6.

262. Schmidt, F.R., *About the nature of RNA interference.* Appl Microbiol Biotechnol, 2005. **67**(4): p. 429-35.

263. Hutvagner, G., et al., *A cellular function for the RNA-interference enzyme Dicer in the maturation of the let-7 small temporal RNA.* Science, 2001. **293**(5531): p. 834-838.

264. Ketting, R.F., et al., *Dicer functions in RNA interference and in synthesis of small RNA involved in developmental timing in C. elegans.* Genes Dev, 2001. **15**(20): p. 2654-9.

265. Grishok, A., et al., *Genes and mechanisms related to RNA interference regulate expression of the small temporal RNAs that control C. elegans developmental timing.* Cell, 2001. **106**(1): p. 23-34.

266. Chendrimada, T.P., et al., *TRBP recruits the Dicer complex to Ago2 for microRNA processing and gene silencing.* Nature, 2005. **436**(7051): p. 740-4.

267. Lee, Y., et al., *The role of PACT in the RNA silencing pathway.* Embo Journal, 2006. **25**(3): p. 522-532.

268. Robb, G.B. and T.M. Rana, *RNA helicase A interacts with RISC in human cells and functions in RISC loading.* Molecular Cell, 2007. **26**(4): p. 523-537.

269. Khvorova, A., A. Reynolds, and S.D. Jayasena, *Functional siRNAs and miRNAs exhibit strand bias (vol 115, pg 209, 2003).* Cell, 2003. **115**(4): p. 505-505.

270. Jinek, M. and J.A. Doudna, *A three-dimensional view of the molecular machinery of RNA interference.* Nature, 2009. **457**(7228): p. 405-412.

271. Filipowicz, W., S.N. Bhattacharyya, and N. Sonenberg, *Mechanisms of post-transcriptional regulation by microRNAs: are the answers in sight?* Nature Reviews Genetics, 2008. **9**(2): p. 102-114.

272. Lewis, B.P., C.B. Burge, and D.P. Bartel, *Conserved seed pairing, often flanked by adenosines, indicates that thousands of human genes are microRNA targets.* Cell, 2005. **120**(1): p. 15-20.

273. Yekta, S., I.H. Shih, and D.P. Bartel, *MicroRNA-directed cleavage of HOXB8 mRNA.* Science, 2004. **304**(5670): p. 594-596.

274. Elbashir, S.M., W. Lendeckel, and T. Tuschl, *RNA interference is mediated by 21- and 22-nucleotide RNAs.* Genes Dev, 2001. **15**(2): p. 188-200.

275. Rivas, F.V., et al., *Purified Argonaute2 and an siRNA form recombinant human RISC.* Nat Struct Mol Biol, 2005. **12**(4): p. 340-9.

276. Bushati, N. and S.M. Cohen, *MicroRNA functions.* Annual Review of Cell and Developmental Biology, 2007. **23**: p. 175-205.

277. Meltzer, P.S., *Cancer genomics - Small RNAs with big impacts.* Nature, 2005. **435**(7043): p. 745-746.

278. Kiriakidou, M., et al., *An mRNA m(7)G cap binding-like motif within human Ago2 represses translation.* Cell, 2007. **129**(6): p. 1141-1151.

279. Chendrimada, T.P., et al., *MicroRNA silencing through RISC recruitment of eIF6.* Nature, 2007. **447**(7146): p. 823-U1.

280. Kim, J., et al., *Identification of many microRNAs that copurify with polyribosomes in mammalian neurons.* Proceedings of the National Academy of Sciences of the United States of America, 2004. **101**(1): p. 360-365.

281. Lanet, E., et al., *Biochemical Evidence for Translational Repression by Arabidopsis MicroRNAs.* Plant Cell, 2009. **21**(6): p. 1762-1768.

282. Petersen, C.P., et al., *Short RNAs repress translation after initiation in mammalian cells.* Mol Cell, 2006. **21**(4): p. 533-42.

283. Nottrott, S., M.J. Simard, and J.D. Richter, *Human let-7a miRNA blocks protein production on actively translating polyribosomes.* Nat Struct Mol Biol, 2006. **13**(12): p. 1108-14.

284. Wu, L., J. Fan, and J.G. Belasco, *MicroRNAs direct rapid deadenylation of mRNA.* Proc Natl Acad Sci U S A, 2006. **103**(11): p. 4034-9.

285. Braun, J.E., et al., *GW182 Proteins Directly Recruit Cytoplasmic Deadenylase Complexes to miRNA Targets.* Molecular Cell, 2011. **44**(1): p. 120-133.

286. Behm-Ansmant, I., et al., *MRNA degradation by miRNAs and GW182 requires both CCR4 : NOT deadenylase and DCP1 : DCP2 decapping complexes.* Genes & Development, 2006. **20**(14): p. 1885-1898.

287. Orban, T.I. and E. Izaurralde, *Decay of mRNAs targeted by RISC requires XRN1, the Ski complex, and the exosome.* Rna, 2005. **11**(4): p. 459-69.

288. Vasudevan, S. and J.A. Steitz, *AU-rich-element-mediated upregulation of translation by FXR1 and argonaute 2.* Cell, 2007. **128**(6): p. 1105-1118.

289. Kim, D.H., et al., *MicroRNA-directed transcriptional gene silencing in mammalian cells.* Proc Natl Acad Sci U S A, 2008. **105**(42): p. 16230-5.

290. Place, R.F., et al., *MicroRNA-373 induces expression of genes with complementary promoter sequences.* Proc Natl Acad Sci U S A, 2008. **105**(5): p. 1608-13.

291. Weinmann, L., et al., *Importin 8 Is a Gene Silencing Factor that Targets Argonaute Proteins to Distinct mRNAs.* Cell, 2009. **136**(3): p. 496-507.

292. Shi, X.B., C.G. Tepper, and R.W. deVere White, *Cancerous miRNAs and their regulation.* Cell Cycle, 2008. **7**(11): p. 1529-38.

293. Calin, G.A., et al., *Human microRNA genes are frequently located at fragile sites and genomic regions involved in cancers.* Proceedings of the National Academy of Sciences of the United States of America, 2004. **101**(9): p. 2999-3004.

294. Saito, Y., et al., *Specific activation of microRNA-127 with downregulation of the proto-oncogene BCL6 by chromatin-modifying drugs in human cancer cells.* Cancer Cell, 2006. **9**(6): p. 435-443.

295. Brueckner, B., et al., *The human let-7a-3 locus contains an epigenetically regulated microRNA gene with oncogenic function.* Cancer Research, 2007. **67**(4): p. 1419-1423.

296. Castellano, L., et al., *The estrogen receptor-alpha-induced microRNA signature regulates itself and its transcriptional response.* Proc Natl Acad Sci U S A, 2009. **106**(37): p. 15732-7.

297. O'Donnell, K.A., et al., *c-Myc-regulated microRNAs modulate E2F1 expression.* Nature, 2005. **435**(7043): p. 839-43.

298. Chang, T.C., et al., *Widespread microRNA repression by Myc contributes to tumorigenesis.* Nat Genet, 2008. **40**(1): p. 43-50.

299. Gao, P., et al., *c-Myc suppression of miR-23a/b enhances mitochondrial glutaminase expression and glutamine metabolism.* Nature, 2009. **458**(7239): p. 762-U100.

300. Suzuki, H.I., et al., *Modulation of microRNA processing by p53.* Nature, 2009. **460**(7254): p. 529-33.

301. Bommer, G.T., et al., *p53-mediated activation of miRNA34 candidate tumor-suppressor genes.* Curr Biol, 2007. **17**(15): p. 1298-307.

302. He, L., et al., *A microRNA component of the p53 tumour suppressor network.* Nature, 2007. **447**(7148): p. 1130-4.

303. Shi, X.B., et al., *An androgen-regulated miRNA suppresses Bak1 expression and induces androgen-independent growth of prostate cancer cells.* Proc Natl Acad Sci U S A, 2007. **104**(50): p. 19983-8.

304. Kluiver, J., et al., *Regulation of pri-microRNA BIC transcription and processing in Burkitt lymphoma.* Oncogene, 2007. **26**(26): p. 3769-76.

305. Feingold, E.A., et al., *The ENCODE (ENCyclopedia of DNA elements) Project.* Science, 2004. **306**(5696): p. 636-640.

306. Wang, Z.F., et al., *Transcriptional and epigenetic regulation of human microRNAs.* Cancer Letters, 2013. **331**(1): p. 1-10.

307. Gregory, R.I., et al., *The Microprocessor complex mediates the genesis of microRNAs.* Nature, 2004. **432**(7014): p. 235-40.

308. Fukuda, T., et al., *DEAD-box RNA helicase subunits of the Drosha complex are required for processing of rRNA and a subset of microRNAs.* Nat Cell Biol, 2007. **9**(5): p. 604-11.

309. Guil, S. and J.F. Caceres, *The multifunctional RNA-binding protein hnRNP A1 is required for processing of miR-18a.* Nat Struct Mol Biol, 2007. **14**(7): p. 591-6.

310. Obernosterer, G., et al., *Post-transcriptional regulation of microRNA expression.* RNA, 2006. **12**(7): p. 1161-7.

311. Viswanathan, S.R., G.Q. Daley, and R.I. Gregory, *Selective blockade of microRNA processing by Lin28.* Science, 2008. **320**(5872): p. 97-100.

312. Newman, M.A., J.M. Thomson, and S.M. Hammond, *Lin-28 interaction with the Let-7 precursor loop mediates regulated microRNA processing.* RNA, 2008. **14**(8): p. 1539-49.

313. Piskounova, E., et al., *Determinants of microRNA processing inhibition by the developmentally regulated RNA-binding protein Lin28.* J Biol Chem, 2008. **283**(31): p. 21310-4.

314. Rybak, A., et al., *A feedback loop comprising lin-28 and let-7 controls pre-let-7 maturation during neural stem-cell commitment.* Nat Cell Biol, 2008. **10**(8): p. 987-93.

315. Heo, I., et al., *Lin28 mediates the terminal uridylation of let-7 precursor MicroRNA.* Mol Cell, 2008. **32**(2): p. 276-84.

316. Trabucchi, M., et al., *The RNA-binding protein KSRP promotes the biogenesis of a subset of microRNAs.* Nature, 2009. **459**(7249): p. 1010-4.

317. Doench, J.G. and P.A. Sharp, *Specificity of microRNA target selection in translational repression.* Genes Dev, 2004. **18**(5): p. 504-11.

318. Lewis, B.P., et al., *Prediction of mammalian microRNA targets.* Cell, 2003. **115**(7): p. 787-98.

319. Krek, A., et al., *Combinatorial microRNA target predictions.* Nat Genet, 2005. **37**(5): p. 495-500.

320. Kiriakidou, M., et al., *A combined computational-experimental approach predicts human microRNA targets.* Genes Dev, 2004. **18**(10): p. 1165-78.

321. Baek, D., et al., *The impact of microRNAs on protein output.* Nature, 2008. **455**(7209): p. 64-U38.

322. Wang, X. and X. Wang, *Systematic identification of microRNA functions by combining target prediction and expression profiling.* Nucleic Acids Res, 2006. **34**(5): p. 1646-52.

323. Selbach, M., et al., *Widespread changes in protein synthesis induced by microRNAs.* Nature, 2008. **455**(7209): p. 58-63.

324. Hutvagner, G., et al., *Sequence-specific inhibition of small RNA function.* PLoS Biol, 2004. **2**(4): p. E98.

325. Ebert, M.S., J.R. Neilson, and P.A. Sharp, *MicroRNA sponges: competitive inhibitors of small RNAs in mammalian cells.* Nat Methods, 2007. **4**(9): p. 721-6.

326. Gregory, P.A., et al., *The miR-200 family and miR-205 regulate epithelial to mesenchymal transition by targeting ZEB1 and SIP1.* Nat Cell Biol, 2008. **10**(5): p. 593-601.

327. Cohen, S.M., *Use of microRNA sponges to explore tissue-specific microRNA functions in vivo.* Nature Methods, 2009. **6**(12): p. 873-874.

328. Huang, D.W., B.T. Sherman, and R.A. Lempicki, *Systematic and integrative analysis of large gene lists using DAVID bioinformatics resources.* Nature Protocols, 2009. **4**(1): p. 44-57.

329. Ashburner, M., et al., *Gene Ontology: tool for the unification of biology.* Nature Genetics, 2000. **25**(1): p. 25-29.

330. Dvinge, H., et al., *The shaping and functional consequences of the microRNA landscape in breast cancer.* Nature, 2013. **497**(7449): p. 378-382.

331. Kong, Y.W., et al., *microRNAs in cancer management.* Lancet Oncology, 2012. **13**(6): p. E249-E258.

332. Lu, J., et al., *MicroRNA expression profiles classify human cancers.* Nature, 2005. **435**(7043): p. 834-8.

333. Thomson, J.M., et al., *Extensive post-transcriptional regulation of microRNAs and its implications for cancer.* Genes & Development, 2006. **20**(16): p. 2202-2207.

334. Kumar, M.S., et al., *Impaired microRNA processing enhances cellular transformation and tumorigenesis.* Nature Genetics, 2007. **39**(5): p. 673-677.

335. Merritt, W.M., *Dicer, Drosha, and Outcomes in Patients with Ovarian Cancer (vol 359, pg 2641, 2008).* New England Journal of Medicine, 2010. **363**(19): p. 1877-1877.

336. Shi, X.B., C.G. Tepper, and R.W.D. White, *Cancerous miRNAs and their regulation.* Cell Cycle, 2008. **7**(11): p. 1529-1538.

337. Meng, F.Y., et al., *MicroRNA-21 regulates expression of the PTEN tumor suppressor gene in human hepatocellular cancer.* Gastroenterology, 2007. **133**(2): p. 647-658.

338. Zhu, S.M., et al., *MicroRNA-21 targets the tumor suppressor gene tropomyosin 1 (TPM1).* Journal of Biological Chemistry, 2007. **282**(19): p. 14328-14336.

339. Frankel, L.B., et al., *Programmed cell death 4 (PDCD4) is an important functional target of the microRNA miR-21 in breast cancer cells.* Journal of Biological Chemistry, 2008. **283**(2): p. 1026-1033.

340. Bueno, M.J. and M. Malumbres, *MicroRNAs and the cell cycle.* Biochimica Et Biophysica Acta-Molecular Basis of Disease, 2011. **1812**(5): p. 592-601.

341. He, L., et al., *microRNAs join the p53 network - another piece in the tumour-suppression puzzle.* Nature Reviews Cancer, 2007. **7**(11): p. 819-822.

342. Lodygin, D., et al., *Inactivation of miR-34a by aberrant CpG methylation in multiple types of cancer.* Cell Cycle, 2008. **7**(16): p. 2591-2600.

343. Fabbri, M., et al., *MicroRNA-29 family reverts aberrant methylation in lung cancer by targeting DNA methyltransferases 3A and 3B.* Proceedings of the National Academy of Sciences of the United States of America, 2007. **104**(40): p. 15805-15810.

344. Varambally, S., et al., *Genomic Loss of microRNA-101 Leads to Overexpression of Histone Methyltransferase EZH2 in Cancer.* Science, 2008. **322**(5908): p. 1695-1699.

345. Portela, A. and M. Esteller, *Epigenetic modifications and human disease.* Nature Biotechnology, 2010. **28**(10): p. 1057-1068.

346. Tricoli, J.V. and J.W. Jacobson, *MicroRNA: Potential for Cancer Detection, Diagnosis, and Prognosis.* Cancer Res, 2007. **67**(10): p. 4553-5.

347. Hossain, A., M.T. Kuo, and G.F. Saunders, *Mir-17-5p regulates breast cancer cell proliferation by inhibiting translation of AIB1 mRNA.* Molecular and Cellular Biology, 2006. **26**(21): p. 8191-8201.

348. Olive, V., et al., *miR-19 is a key oncogenic component of mir-17-92.* Genes & Development, 2009. **23**(24): p. 2839-2849.

349. UCSC, *http://genome.ucsc.edu/*.

350. Chhabra, R., R. Dubey, and N. Saini, *Cooperative and individualistic functions of the microRNAs in the miR-23a similar to 27a similar to 24-2 cluster and its implication in human diseases.* Molecular Cancer, 2010. **9**.

351. http://www.targetscan.org/vert_61/.

352. Salvi, A., et al., *MicroRNA-23b mediates urokinase and c-met downmodulation and a decreased migration of human hepatocellular carcinoma cells.* FEBS J, 2009. **276**(11): p. 2966-82.

353. Zhang, H.S., et al., *Genome-wide functional screening of miR-23b as a pleiotropic modulator suppressing cancer metastasis.* Nature Communications, 2011. **2**.

354. Au Yeung, C.L., et al., *Human papillomavirus type 16 E6 induces cervical cancer cell migration through the p53/microRNA-23b/urokinase-type plasminogen activator pathway.* Oncogene, 2011. **30**(21): p. 2401-10.

355. Majid, S., et al., *miR-23b Represses Proto-oncogene Src Kinase and Functions as Methylation-Silenced Tumor Suppressor with Diagnostic and Prognostic Significance in Prostate Cancer.* Cancer Research, 2012. **72**(24): p. 6435-6446.

356. Ishteiwy, R.A., et al., *The microRNA-23b/-27b Cluster Suppresses the Metastatic Phenotype of Castration-Resistant Prostate Cancer Cells.* Plos One, 2012. **7**(12).

357. Lin, L.J. and S. Alahari, *Pro-oncogenic factors miR-23b-and miR-27b are regulated by Her2/Neu, EGF, and TNF alpha in breast cancer.* Tumor Biology, 2012. **33**: p. 34-34.

358. Pincini, A., et al., *Identification of p130Cas/ErbB2-dependent invasive signatures in transformed mammary epithelial cells.* Cell Cycle, 2013. **12**(15).

359. Omnibus, G.E., *http://www.ncbi.nlm.nih.gov/gds/*.

360. Luo, X., et al., *MicroRNA-26 governs profibrillatory inward-rectifier potassium current changes in atrial fibrillation.* J Clin Invest, 2013. **123**(5): p. 1939-51.

361. Zhu, Y., et al., *MicroRNA-26a/b and their host genes cooperate to inhibit the G1/S transition by activating the pRb protein.* Nucleic Acids Res, 2012. **40**(10): p. 4615-25.

362. Kota, J., et al., *Therapeutic microRNA Delivery Suppresses Tumorigenesis in a Murine Liver Cancer Model.* Cell, 2009. **137**(6): p. 1005-1017.

363. Zhu, Y., et al., *MicroRNA-26a/b and their host genes cooperate to inhibit the G1/S transition by activating the pRb protein.* Nucleic Acids Research, 2012. **40**(10): p. 4615-4625.

364. Sander, S., et al., *MYC stimulates EZH2 expression by repression of its negative regulator miR-26a.* Blood, 2008. **112**(10): p. 4202-12.

365. Ciarapica, R., et al., *Deregulated expression of miR-26a and Ezh2 in rhabdomyosarcoma.* Cell Cycle, 2009. **8**(1): p. 172-175.

366. Zhang, B., et al., *Pathologically decreased miR-26a antagonizes apoptosis and facilitates carcinogenesis by targeting MTDH and EZH2 in breast cancer.* Carcinogenesis, 2011. **32**(1): p. 2-9.

367. Ichikawa, T., et al., *Trastuzumab Produces Therapeutic Actions by Upregulating miR-26a and miR-30b in Breast Cancer Cells.* Plos One, 2012. **7**(2).

368. Gao, J., et al., *MiR-26a Inhibits Proliferation and Migration of Breast Cancer through Repression of MCL-1.* Plos One, 2013. **8**(6).

369. Zhang, J.Q., C. Han, and T. Wu, *MicroRNA-26a Promotes Cholangiocarcinoma Growth by Activating beta-catenin.* Gastroenterology, 2012. **143**(1): p. 246-U467.

370. Huse, J., et al., *The PTEN-Regulating MicroRNA miR-26a is Amplified in High-Grade Glioma and Facilitates Gliomagenesis in vivo.* Journal of Neuropathology and Experimental Neurology, 2009. **68**(5): p. 558-558.

371. Hurst, D.R., M.D. Edmonds, and D.R. Welch, *Metastamir: The Field of Metastasis-Regulatory microRNA Is Spreading.* Cancer Research, 2009. **69**(19): p. 7495-7498.

372. Dumont, N. and T.D. Tlsty, *Reflections on miR-ing effects in metastasis.* Cancer Cell, 2009. **16**(1): p. 3-4.

373. Ma, L., et al., *miR-9, a MYC/MYCN-activated microRNA, regulates E-cadherin and cancer metastasis.* Nat Cell Biol, 2010. **12**(3): p. 247-56.

374. Gregory, P.A., et al., *MicroRNAs as regulators of epithelial-mesenchymal transition.* Cell Cycle, 2008. **7**(20): p. 3112-8.

375. Park, S.M., et al., *The miR-200 family determines the epithelial phenotype of cancer cells by targeting the E-cadherin repressors ZEB1 and ZEB2.* Genes Dev, 2008. **22**(7): p. 894-907.

376. Valastyan, S., et al., *A pleiotropically acting microRNA, miR-31, inhibits breast cancer metastasis.* Cell, 2009. **137**(6): p. 1032-46.

377. Muller, D.W. and A.K. Bosserhoff, *Integrin beta(3) expression is regulated by let-7a miRNA in malignant melanoma.* Oncogene, 2008. **27**(52): p. 6698-6706.

378. Zhu, S., et al., *Ubc9 promotes breast cell invasion and metastasis in a sumoylation-independent manner.* Oncogene, 2010. **29**(12): p. 1763-1772.

379. Ma, L., J. Teruya-Feldstein, and R.A. Weinberg, *Tumour invasion and metastasis initiated by microRNA-10b in breast cancer.* Nature, 2007. **449**(7163): p. 682-8.

380. Moriarty, C.H., B. Pursell, and A.M. Mercurio, *miR-10b targets Tiam1: implications for Rac activation and carcinoma migration.* J Biol Chem, 2010. **285**(27): p. 20541-6.

381. Ding, J., et al., *Gain of miR-151 on chromosome 8q24.3 facilitates tumour cell migration and spreading through downregulating RhoGDIA.* Nat Cell Biol, 2010. **12**(4): p. 390-9.

382. Wong, C.C., et al., *The microRNA miR-139 suppresses metastasis and progression of hepatocellular carcinoma by down-regulating Rho-kinase 2.* Gastroenterology, 2011. **140**(1): p. 322-31.

383. Reddy, S.D., et al., *MicroRNA-7, a homeobox D10 target, inhibits p21-activated kinase 1 and regulates its functions.* Cancer Res, 2008. **68**(20): p. 8195-200.

384. Sossey-Alaoui, K., K. Bialkowska, and E.F. Plow, *The miR200 family of microRNAs regulates WAVE3-dependent cancer cell invasion.* J Biol Chem, 2009. **284**(48): p. 33019-29.

385. Yan, D., et al., *MicroRNA-1/206 targets c-Met and inhibits rhabdomyosarcoma development.* J Biol Chem, 2009. **284**(43): p. 29596-604.

386. Li, N., et al., *miR-34a inhibits migration and invasion by down-regulation of c-Met expression in human hepatocellular carcinoma cells.* Cancer Lett, 2009. **275**(1): p. 44-53.

387. Lin, S.L., et al., *Loss of mir-146a function in hormone-refractory prostate cancer.* RNA, 2008. **14**(3): p. 417-24.

388. Scott, G.K., et al., *Coordinate suppression of ERBB2 and ERBB3 by enforced expression of micro-RNA miR-125a or miR-125b.* J Biol Chem, 2007. **282**(2): p. 1479-86.

389. Meng, F., et al., *MicroRNA-21 regulates expression of the PTEN tumor suppressor gene in human hepatocellular cancer.* Gastroenterology, 2007. **133**(2): p. 647-58.

390. Garofalo, M., et al., *miR-221&222 regulate TRAIL resistance and enhance tumorigenicity through PTEN and TIMP3 downregulation.* Cancer Cell, 2009. **16**(6): p. 498-509.

391. Tavazoie, S.F., et al., *Endogenous human microRNAs that suppress breast cancer metastasis.* Nature, 2008. **451**(7175): p. 147-U3.

392. Korpal, M., et al., *Direct targeting of Sec23a by miR-200s influences cancer cell secretome and promotes metastatic colonization.* Nature Medicine, 2011. **17**(9): p. 1101-U108.

393. van Rooij, E., A.L. Purcell, and A.A. Levin, *Developing MicroRNA Therapeutics.* Circulation Research, 2012. **110**(3): p. 496-507.

394. Gumireddy, K., et al., *Small-molecule inhibitors of microRNA miR-21 function.* Angewandte Chemie-International Edition, 2008. **47**(39): p. 7482-7484.

395. Garzon, R., G. Marcucci, and C.M. Croce, *Targeting microRNAs in cancer: rationale, strategies and challenges.* Nature Reviews Drug Discovery, 2010. **9**(10): p. 775-789.

396. Krutzfeldt, J., et al., *Silencing of microRNAs in vivo with 'antagomirs'.* Nature, 2005. **438**(7068): p. 685-689.

397. Lanford, R.E., et al., *Therapeutic Silencing of MicroRNA-122 in Primates with Chronic Hepatitis C Virus Infection.* Science, 2010. **327**(5962): p. 198-201.

398. Janssen, H.L., et al., *Treatment of HCV infection by targeting microRNA.* N Engl J Med, 2013. **368**(18): p. 1685-94.

399. Bonci, D., et al., *The Mir-15a/Mir-16-1 Cluster Controls Prostate Cancer Progression Control by Targeting of Multiple Oncogenic Activities.* Journal of Urology, 2009. **181**(4): p. 188-188.

400. van Rooij, E., *The Art of MicroRNA Research.* Circulation Research, 2011. **108**(2): p. 219-234.

401. Huang, L. and Y. Liu, *In Vivo Delivery of RNAi with Lipid-Based Nanoparticles.* Annual Review of Biomedical Engineering, Vol 13, 2011. **13**: p. 507-530.

402. Bouchie, A., *First microRNA mimic enters clinic.* Nat Biotechnol, 2013. **31**(7): p. 577.

403. Boghaert, E.R., et al., *Immunohistochemical analysis of the proapoptotic protein Par-4 in normal rat tissues.* Cell growth & differentiation : the molecular biology journal of the American Association for Cancer Research, 1997. **8**(8): p. 881-90.

404. Sahai, E. and C.J. Marshall, *RHO-GTPases and cancer.* Nat Rev Cancer, 2002. **2**(2): p. 133-42.

405. Salvi, A., et al., *MicroRNA-23b mediates urokinase and c-met downmodulation and a decreased migration of human hepatocellular carcinoma cells.* Febs Journal, 2009. **276**(11): p. 2966-2982.

406. Pencheva, N. and S.F. Tavazoie, *Control of metastatic progression by microRNA regulatory networks.* Nat Cell Biol, 2013. **15**(6): p. 546-54.

407. Cline, M.S., et al., *Integration of biological networks and gene expression data using Cytoscape.* Nature Protocols, 2007. **2**(10): p. 2366-2382.

408. Geiger, B., J.P. Spatz, and A.D. Bershadsky, *Environmental sensing through focal adhesions.* Nature Reviews Molecular Cell Biology, 2009. **10**(1): p. 21-33.

409. Kreis, P. and J.V. Barnier, *PAK signalling in neuronal physiology.* Cell Signal, 2009. **21**(3): p. 384-93.

410. Ndlovu, N., et al., *Hyperactivated NF-{kappa}B and AP-1 transcription factors promote highly accessible chromatin and constitutive transcription across the*

interleukin-6 gene promoter in metastatic breast cancer cells. Molecular and cellular biology, 2009. **29**(20): p. 5488-504.

411. Patel, J.B., et al., *Control of EVI-1 oncogene expression in metastatic breast cancer cells through microRNA miR-22.* Oncogene, 2011. **30**(11): p. 1290-1301.

412. van Hove, E.R.A., et al., *Multimodal Mass Spectrometric Imaging of Small Molecules Reveals Distinct Spatio-Molecular Signatures in Differentially Metastatic Breast Tumor Models.* Cancer Research, 2010. **70**(22): p. 9012-9021.

413. Yu, R., et al., *Pituitary tumor transforming gene causes aneuploidy and p53-dependent and p53-independent apoptosis.* The Journal of biological chemistry, 2000. **275**(47): p. 36502-5.

414. Xu, G., et al., *Transcriptome and targetome analysis in MIR155 expressing cells using RNA-seq.* RNA, 2010. **16**(8): p. 1610-22.

415. Kim, H., et al., *Integrative genome analysis reveals an oncomir/oncogene cluster regulating glioblastoma survivorship.* Proc Natl Acad Sci U S A, 2010. **107**(5): p. 2183-8.

416. Pillai, R.S., et al., *Inhibition of translational initiation by Let-7 MicroRNA in human cells.* Science, 2005. **309**(5740): p. 1573-6.

417. Hsu, S.D., et al., *miRTarBase: a database curates experimentally validated microRNA-target interactions.* Nucleic Acids Res, 2011. **39**(Database issue): p. D163-9.

418. Kalsotra, A., et al., *MicroRNAs coordinate an alternative splicing network during mouse postnatal heart development.* Genes Dev, 2010. **24**(7): p. 653-8.

419. Huse, J.T., et al., *The PTEN-regulating microRNA miR-26a is amplified in high-grade glioma and facilitates gliomagenesis in vivo.* Genes & Development, 2009. **23**(11): p. 1327-1337.

420. Delorme, V., et al., *Cofilin activity downstream of Pak1 regulates cell protrusion efficiency by organizing lamellipodium and lamella actin networks.* Dev Cell, 2007. **13**(5): p. 646-662.

421. Ghosh, M., et al., *Cofilin promotes actin polymerization and defines the direction of cell motility.* Science, 2004. **304**(5671): p. 743-6.

422. Luo, D.Y., et al., *A systematic evaluation of miRNA:mRNA interactions involved in the migration and invasion of breast cancer cells.* Journal of Translational Medicine, 2013. **11**.

423. Nakagawa, H., et al., *N-WASP, WAVE and Mena play different roles in the organization of actin cytoskeleton in lamellipodia.* J Cell Sci, 2001. **114**(Pt 8): p. 1555-65.

424. Sun, T., M. Rodriguez, and L. Kim, *Glycogen synthase kinase 3 in the world of cell migration.* Dev Growth Differ, 2009. **51**(9): p. 735-42.

425. Delorme, V., et al., *Cofilin activity downstream of Pak1 regulates cell protrusion efficiency by organizing lamellipodium and lamella actin networks.* Dev Cell, 2007. **13**(5): p. 646-62.

426. Bernard, O., *Lim kinases, regulators of actin dynamics.* Int J Biochem Cell Biol, 2007. **39**(6): p. 1071-6.

427. Benseddik, K., et al., *ErbB2-dependent chemotaxis requires microtubule capture and stabilization coordinated by distinct signaling pathways.* PLoS One, 2013. **8**(1): p. e55211.

428. Jimenez, C., et al., *Role of the PI3K regulatory subunit in the control of actin organization and cell migration.* J Cell Biol, 2000. **151**(2): p. 249-62.

429. Stillfried, G.E., D.N. Saunders, and M. Ranson, *Plasminogen binding and activation at the breast cancer cell surface: the integral role of urokinase activity.* Breast Cancer Research, 2007. **9**(1).

430. Xia, D., J.T. Stull, and K.E. Kamm, *Myosin phosphatase targeting subunit 1 affects cell migration by regulating myosin phosphorylation and actin assembly.* Exp Cell Res, 2005. **304**(2): p. 506-17.

431. Hattori, M. and N. Minato, *Rap1 GTPase: functions, regulation, and malignancy.* J Biochem, 2003. **134**(4): p. 479-84.

432. Mizuno, K., *Signaling mechanisms and functional roles of cofilin phosphorylation and dephosphorylation.* Cell Signal, 2013. **25**(2): p. 457-69.

433. Le, X.F., et al., *Modulation of MicroRNA-194 and cell migration by HER2-targeting trastuzumab in breast cancer.* PLoS One, 2012. **7**(7): p. e41170.

434. Parsons, J.T., A.R. Horwitz, and M.A. Schwartz, *Cell adhesion: integrating cytoskeletal dynamics and cellular tension.* Nat Rev Mol Cell Biol, 2010. **11**(9): p. 633-43.

435. Burrows, C., et al., *The RNA binding protein Larp1 regulates cell division, apoptosis and cell migration.* Nucleic Acids Res, 2010. **38**(16): p. 5542-53.

436. van Delft, M.F., et al., *The BH3 mimetic ABT-737 targets selective Bcl-2 proteins and efficiently induces apoptosis via Bak/Bax if Mcl-1 is neutralized.* Cancer Cell, 2006. **10**(5): p. 389-399.

437. Henson, E.S., X. Hu, and S.B. Gibson, *Herceptin sensitizes ErbB2-overexpressing cells to apoptosis by reducing antiapoptotic Mcl-1 expression.* Clin Cancer Res, 2006. **12**(3 Pt 1): p. 845-53.

438. Fotiadou, P.P., et al., *Wild-type NRas and KRas perform distinct functions during transformation.* Mol Cell Biol, 2007. **27**(19): p. 6742-55.

439. Uechi, Y., et al., *Rap2 function requires palmitoylation and recycling endosome localization.* Biochem Biophys Res Commun, 2009. **378**(4): p. 732-7.

440. Fu, H., R.R. Subramanian, and S.C. Masters, *14-3-3 proteins: structure, function, and regulation.* Annu Rev Pharmacol Toxicol, 2000. **40**: p. 617-47.

441. Ooshio, T., et al., *Involvement of LMO7 in the association of two cell-cell adhesion molecules, nectin and E-cadherin, through afadin and alpha-actinin in epithelial cells.* J Biol Chem, 2004. **279**(30): p. 31365-73.

442. Bokoch, G.M., *Biology of the p21-activated kinases.* Annu Rev Biochem, 2003. **72**: p. 743-81.

443. Lei, M., et al., *Structure of PAK1 in an autoinhibited conformation reveals a multistage activation switch.* Cell, 2000. **102**(3): p. 387-97.

444. Cavalcanti-Adam, E.A., et al., *Cell spreading and focal adhesion dynamics are regulated by spacing of integrin ligands.* Biophysical Journal, 2007. **92**(8): p. 2964-74.

445. Dano, K., et al., *The Urokinase Receptor - Protein-Structure and Role in Plasminogen Activation and Cancer Invasion.* Fibrinolysis, 1994. **8**: p. 189-203.

446. Chanda, S.K., et al., *Genome-scale functional profiling of the mammalian AP-1 signaling pathway.* Proc Natl Acad Sci U S A, 2003. **100**(21): p. 12153-8.

447. Xu, L., et al., *MicroRNA-7-regulated TLR9 signaling-enhanced growth and metastatic potential of human lung cancer cells by altering the phosphoinositide-3-kinase, regulatory subunit 3/Akt pathway.* Mol Biol Cell, 2013. **24**(1): p. 42-55.

448. Baranwal, S., et al., *Molecular characterization of the tumor-suppressive function of nischarin in breast cancer.* J Natl Cancer Inst, 2011. **103**(20): p. 1513-28.

449. Vousden, K.H. and X. Lu, *Live or let die: the cell's response to p53.* Nat Rev Cancer, 2002. **2**(8): p. 594-604.

450. Abida, W.M., et al., *FBXO11 promotes the Neddylation of p53 and inhibits its transcriptional activity.* J Biol Chem, 2007. **282**(3): p. 1797-804.

451. Seoane, J., et al., *TGFbeta influences Myc, Miz-1 and Smad to control the CDK inhibitor p15INK4b.* Nature cell biology, 2001. **3**(4): p. 400-8.

APPENDICES

5400–5412 Nucleic Acids Research, 2013, Vol. 41, No. 10 Published online 10 April 2013
doi:10.1093/nar/gkt245

miR-23b regulates cytoskeletal remodeling, motility and metastasis by directly targeting multiple transcripts

Loredana Pellegrino[1], Justin Stebbing[1], Vania M. Braga[2], Adam E. Frampton[3], Jimmy Jacob[1], Lakjaya Buluwela[1], Long R. Jiao[3], Manikandan Periyasamy[1], Chris D. Madsen[4], Matthew P. Caley[5], Silvia Ottaviani[1], Laura Roca-Alonso[1], Mona El-Bahrawy[6], R. Charles Coombes[1], Jonathan Krell[1] and Leandro Castellano[1,*]

[1]Division of Oncology, Department of Surgery and Cancer, Imperial Centre for Translational and Experimental Medicine (ICTEM), Imperial College, Hammersmith Hospital campus, Du Cane Road, London, W12 0NN, UK, [2]Molecular Medicine, National Heart and Lung Institute, Faculty of Medicine, Imperial College, London, SW7 2AZ, UK, [3]HPB Surgical Unit, Department of Surgery and Cancer, Imperial College, Hammersmith Hospital campus, Du Cane Road, London, W12 0HS, UK, [4]Cancer Research UK, London Research Institute, 44 Lincoln's Inn Fields, London, WC2A 3PX, UK, [5]Blizard Institute Barts and The London School of Medicine and Dentistry, Centre for Cutaneous Research, 4 Newark Street, London, E1 2AT, UK and [6]Department of Histopathology, Imperial College, Hammersmith Hospital Campus, Du Cane Road, London, W12 0NN, UK

Received September 9, 2012; Revised March 17, 2013; Accepted March 18, 2013

ABSTRACT

Uncontrolled cell proliferation and cytoskeletal remodeling are responsible for tumor development and ultimately metastasis. A number of studies have implicated microRNAs in the regulation of cancer cell invasion and migration. Here, we show that miR-23b regulates focal adhesion, cell spreading, cell-cell junctions and the formation of lamellipodia in breast cancer (BC), implicating a central role for it in cytoskeletal dynamics. Inhibition of miR-23b, using a specific sponge construct, leads to an increase of cell migration and metastatic spread *in vivo*, indicating it as a metastatic suppressor microRNA. Clinically, low miR-23b expression correlates with the development of metastases in BC patients. Mechanistically, miR-23b is able to directly inhibit a number of genes implicated in cytoskeletal remodeling in BC cells. Through intracellular signal transduction, growth factors activate the transcription factor AP-1, and we show that this in turn reduces miR-23b levels by direct binding to its promoter, releasing the pro-invasive genes from translational inhibition. In aggregate, miR-23b expression invokes a sophisticated interaction network that co-ordinates a wide range of cellular responses required to alter the cytoskeleton during cancer cell motility.

INTRODUCTION

Deregulation of cell cycle progression genes is crucial to tumor growth, and additional genetic modifications are required to promote motile and invasive behaviors in cancer cells, leading to tumor dissemination and metastasis.

The cytoskeleton controls cell motility, invasion and adhesion. Three members of the Rho family of small GTPases, RhoA, Rac1 and cell division cycle 42, are crucial in regulating the molecular pathways implicated in cell migration (1,2), controlling cytoskeletal dynamics, cell adhesion, morphology and motility (1). This is achieved via effector proteins that regulate actin-based structures, and the p21-activated kinases (PAKs) are among the best characterized effectors of cell division cycle 42 and Rac1 (3). In addition, several growth factor receptor tyrosine kinases activate PAKs through Rho GTPases leading to cytoskeletal remodeling (4–6). Furthermore, in breast cancer (BC), the HER-2 pathway is able to regulate the actin cytoskeleton and cell motility via PAK1 and PAK2 activation and distinct downstream signaling mechanisms (7).

*To whom correspondence should be addressed. Tel: +44 2075 942823; Fax: +44 2083 835830; Email: l.castellano@imperial.ac.uk

The authors wish to be known that, in their opinion, the first two authors should be regarded as joint First Authors.

MicroRNAs (miRNAs) are small, single-stranded RNAs that regulate gene expression (8), and their dysregulation can therefore contribute to cell motility and metastasis by affecting relevant transcripts (9–13).

Using a bioinformatic approach, we identified miR-23b as a miRNA implicated in cytoskeletal remodeling and motility, and we further demonstrated this finding through a number of experimental techniques. In addition, using RNA-sequencing (RNA-seq) and luciferase reporter assays, we validated a subset of cytoskeletal genes as direct targets of miR-23b in BC, implicating a direct role of this miRNA in cytoskeletal remodeling and motility. Notably, when AP-1 is activated by growth factors, it binds directly to the miR-23b promoter, thereby reducing its expression, which indicates that this event contributes to motility and metastasis in BC.

MATERIALS AND METHODS

Cell culture

BC cell lines (MCF-7, MDA-MB-231 and MDA-MB-468) and colon cancer HCT116 cell lines were maintained in Dulbecco's modified Eagle's medium and McCoy's medium, respectively, supplemented with 10% FCS, 1% penicillin/streptomycin and 2% glutamine. MDA-MB-231 cells isolated from distant sites were maintained as previously described (14). Stable transfected MDA-MB-231 cell clones were expanded in G-418 (Roche Applied Science, Burgess Hill, UK).

Plasmid constructions

The miR-23b sponges were constructed by annealing, purifying and cloning oligonucleotides containing six tandem bulged miRNA binding motifs, into the HindIII and BamHI sites of the pEGFP-C1 plasmid (Contech, Saint-Germain-en-Laye, France), as 3′UTR of the EGFP mRNA. For 3′UTRs reporter construction, the 3′UTR of Pak2 or Pak1 were PCR-amplified from human genomic DNA and cloned into the pMIR-REPORT *Firefly* Luciferase vector. The miR-23b sensors were constructed as for miR-23b sponges, but into the SpeI and HindIII sites of the pMIR-REPORT *Firefly* Luciferase vector. The ANXA2, ARHGEF6, CFL2, LIMK2, PIK3R3, PLAU and TLN2 3′UTRs cloned into pLightSwitch_3′UTR GoClone vectors were used (Switch Gear Genomics, Menlo Park CA, USA). The indicated mutagenized miR-23b seed-containing luciferase reporter vector was created with a QuickChange II or II XL Site-Directed Mutagenesis Kit (Agilent Technology, Edinburgh, UK) according to the manufacturer's instructions. All plasmid sequences were verified to be free of mutations by direct sequencing. The sequences of all primers used for plasmid construction and site-directed mutagenesis are reported in Supplementary Table S1.

Transfections, reporter assays and cell treatments

Cells were plated in 6-well plates at 50% confluence and transfected with either the miRNA mimics (5 nM), miRNA inhibitors (100 nM) (Applied Biosystems, Warrington, UK) or siRNA oligonucleotides (40 nM) for 48 h using HiPerFect Transfection Reagent (Qiagen, Crawley, UK). For experiments of miRNA over-expression for 9 days, cells were plated in 6-well plates at 30% confluence and transfected with the miRNA mimics (5 nM); after 72 h of transfection, cells were split and re-transfected with additional miRNAs mimics; this protocol was repeated every 3 days for up to 9 days. Transfection of GFP-sponge-expressing plasmids was performed using Lipofectamine 2000 (Life Technologies Ltd, Paisley, UK). For 3′UTR reporter assays, cells were co-transfected with *Renilla* Luciferase vector, the indicated miRNA precursors or plasmids and 3′UTR-p-MIR REPORT *Firefly* Luciferase vectors in 24-well plates and analyzed as previously described (15). Cells co-transfected with pLightSwitch_3UTR GoClone vectors, and the indicated miRNA precursors or plasmids in 24 well plates were lysed using a passive lysis buffer (Promega, Southampton, UK) and processed with the LightSwitch Assay System (Switchgear Genomics Menlo Park CA, USA) according to manufacturer's instructions. Luciferase activity detection was performed using a GLOMAX 96 Microplate luminometer (Promega). For EGF treatment, MDA-MB-468 cells were plated in triplicate in normal growth medium. After 24 h, EGF (25 ng/ml) was added for the indicated time points in three independent biological replicates.

Immunofluorescence and cell–cell junction quantification

Cells were fixed with 4% paraformaldehyde and permeabilized in 0.2% Triton-X-100 for 30 min. F-actin was detected with phalloidin-Alexa Fluor® 488 (Invitrogen), and nuclei were visualized with TO-PRO-3 (Invitrogen). For E-cadherin and focal adhesion (FA) visualization, cells were stained either with anti-E-cadherin antibody (HECD-1) (M106, Takara Bio Inc.) or anti-Vinculin antibody (V9264, Sigma-Aldrich) and imaged using a confocal microscope. To analyze cell–cell junction linearity, the junction lenghts and distances between vertices were manually traced and measured by using LSM 5 Image Browser (Carl Zeiss MicroImaging, Inc.). To highlight the area of FAs, the images taken were inverted in black-and-white color and analyzed using NHI ImageJ software for FA area quantification. To study -lamellipodial formation, cells were imaged using ImageXpress Micro® microscope (Molecular Devices), and lamellipodia number was manually counted in a blind fashion (100 cells per each condition in the three independent experiments).

In vitro migration and invasion assays

For cell-tracking assays, cells were seeded in 24-well tissue culture plates at a final density of 1×10^4. After 48 h of transfection, time-lapse sequences were digitally recorded at intervals of 20 min for 24 h using the ImageXpress Micro® microscope (Molecular Devices). Cell trajectories were determined by following the centroid of the nuclei using the ImageJ plugin 'MTrackJ' (http://www.imagescience.org/meijering/software/mtrackj/), and speed of cell body movement was calculated for mean cell

migratory speed. A 50–100 cells per each condition were analyzed, and three independent experiments were performed. For transwell migration assays, 5×10^4 cells were seeded atop uncoated membranes with 8.0 µm pores (BD Biosciences). Cell were plated in serum free-medium and allowed to migrate toward a complete growth medium for 9 h. For 3D Collagen-I invasion assays, 7×10^4 cells were plated in black-walled 96-well plates and allowed to attach. Collagen-I gels ($n = 5$ gels per condition, 100 µl) were prepared as described (16) at a final concentration of 2.3 mg/ml and added atop the cells. After polymerization and equilibration for 1 h at 37°C and 5% CO_2, collagen gels were coated with 100 µl of cell culture medium supplemented with 10% FCS as chemoattractant, and cell invasion was allowed for 16–24 h. Collagen gels containing invaded cells were then fixed and stained, and z sections were taken by confocal microscopy. Invasion indexes were calculated as the number of cells at 40 µm divided by those at 0 µm. Three independent experiments were performed.

Cell growth and Annexin V-apoptotic assays

MCF7 and MDA-MB-231 cells growth was analyzed by performing an SRB assay. Cells were seeded in 96-well plates and transfected with the indicated molecules. The SRB cell viability assay was performed 48 h after transfections as described previously (17). To assay the apoptotic properties of miR-23b, MDA-MB-231 were transfected with the indicated microRNA precursor mimics and the cell death control siRNAs (20 nM) (Qiagen) used as positive control. After 48 h, detached cells were combined with adherent cells after lifting with trypsin-EDTA, stained with Annexin V/PE apoptosis detection kit (BD Biosciences) according to manufacturer's protocol and analyzed using a FACSCanto II flow citometer (BD Biosciences). Apoptotic cells were represented by high PE-Annexin V fluorescence signals.

Spreading assays

Spreading assays was performed as previously described (18).

Patients and samples

To investigate the potential role of miR-23b in BC metastasis, we prospectively measured their expression in primary BCs and corresponding lymph node metastasis from patients with lymph node positive BC. Between January 2008 and February 2010, we obtained primary breast tumors and corresponding lymph node metastases from 66 consecutive individuals eligible for chemotherapy at Imperial College Healthcare NHS Trust, London, UK. All 132 samples were formalin-fixed and paraffin-embedded. The clinico-pathologic characteristics are listed in Supplementary Table S2. Prospective written consent was obtained in accordance with ethical guidelines.

Statistical analysis

Data are presented as mean ± standard error of the mean calculated using Graph Prism software. Student's t-test and Chi-Square test were used for comparison, with $P < 0.05$ considered significant.

Sequence data were submitted to Gene Expression Omnibus database, accession number GSE37918.

RESULTS

Bioinformatic analyses reveal that miR-23b is involved in cytoskeletal remodeling and adhesion

Using a bioinformatic approach and an extensive literature review, we identified candidate miRNAs involved in cell motility and invasion. We selected miR-23b, as it reduces hepatocellular and cervical cancer cell motility through the regulation of PLAU and c-Met (19) and reduces experimental metastasis formation in colorectal cancer (20). However, its role in BC and the subsequent pathways regulated remain largely unknown. Nine hundred and thirty-eight randomly chosen genes and 938 potential miR-23b targets [identified using TargetScan (21)] were analyzed using DAVID (http://david.abcc.ncifcrf.gov/home.jsp) for gene ontology (GO) annotation and pathway enrichment analysis (22,23). This method suggested that miR-23b may regulate pathways involved in cancer, cytoskeletal remodeling, cell-cell junctions and cell adhesion (Supplementary Figure S1).

The miR-23b expression in cancer cell lines enhances cell–cell adhesion

We transfected epithelial-like (MCF-7) and mesenchymal-like (MDA-MB-231) BC cells with synthetic miR-23b precursor or a negative control (miR-n.c.). Ectopic expression of miR-23b increased epithelial characteristics in MCF-7 cells, as demonstrated by tighter colony morphology with marked cell–cell junctions (Figure 1A), independent of E-cadherin (CDH1) expression (Figure 1B). However, as miR-23b over-expression did not induce these characteristics in mesenchymal-like MDA-MB-231 cells (Figure 1C), and in addition, CDH1 expression did not change upon miR-23b over-expression, we hypothesized that such effects were unlikely to be due to re-expression of adhesion molecules during the mesenchymal-to-epithelial transition, but more likely due to miR-23b affecting the tension of existing cell–cell adhesions.

Next, we aimed to induce mesenchymal-to-epithelial transition via prolonged (9 days) miR-23b over-expression, using immunofluorescence to examine CDH1 and cell junction formation (24) (Figure 1D and E). The miR-23b over-expressing-MCF-7, but not MDA-MB-231 cells, overall showed more orderly and stable tight and adherens junctions compared with controls, confirming that miR-23b leads to an enhanced tension between existing cell–cell junctions (Figure 1D and E). The quantification of this effect is expressed as a linearity index, defined by the ratio of junction length to the distance between vertices (25), and supported that junctions in

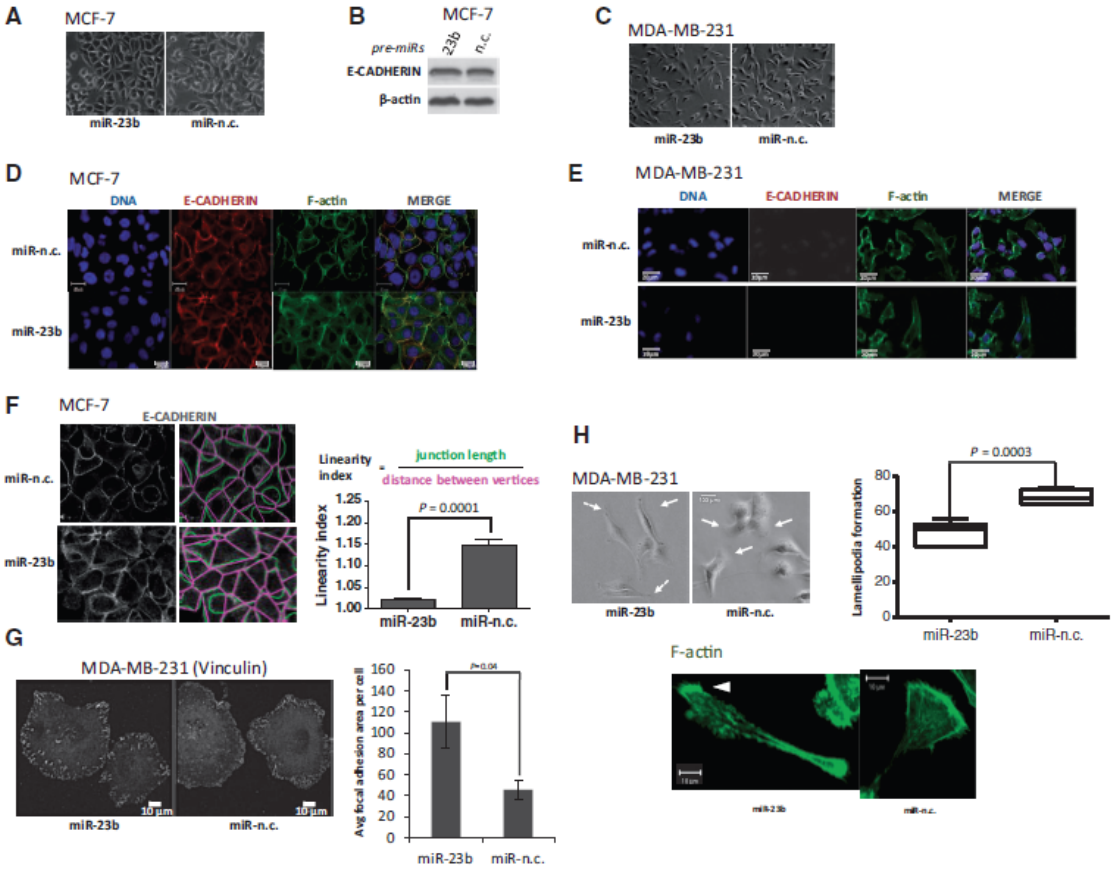

Figure 1. miR-23b expression affects cytoskeletal remodeling as predicted by bioinformatic analyses. (**A**) Phase-contrast images of MCF-7 cells upon transfection with miR-23b and miR-n.c. precursors (5 nM) for 48 h. (**B**) Western blot showing E-cadherin and β-actin expression in MCF-7 cells transfected with miR-23b and miR-n.c. precursors (5 nM) for 48 h. β-actin was used as a loading control. (**C**) Phase-contrast images of MDA-MB-231 cells upon transfection with miR-23b and miR-n.c. precursors (5 nM) for 48 h. (**D**) *From left to right*: TO-PRO-3 staining of DNA, immunofluorescence staining of E-cadherin (1:1000), Alexa Fluor 488 phalloidin (1:500) staining of F-actin and overlay of the three images of MCF-7 cells transfected with miR-23b and miR-n.c. precursors (5 nM) for 9 days. Scale bar = 20 µm (**E**) *From right to left*: TO-PRO-3 staining of nuclei, immunofluorescence staining of E-cadherin (1:1000), Alexa Fluor 488 phalloidin (1:500) staining of F-actin and overlay of the three images of MDA-MB-231 cells transfected with miR-23b and miR-n.c. precursors (5 nM) for 9 days. Scale bar = 20 µm. (**F**) Quantification of junction linearity. Junction length (green) and distance between vertices (pink) were measured and a linearity index was calculated by dividing the two measures (right). This index decreases in miR-23b over-expressing MCF-7 cells. Scale bar = 20 µm. 150–250 junctions per condition in two independent experiments were counted. Data are mean ± s.e.m. ($P = 0.0001$, Student's *t*-test). (**G**) Immunofluorescence staining of MDA-MB-231 using Vinculin antibody (1:400); images were false colored in a black-and-white fashion to highlight FAs. After transfection with miR-23b and miR-n.c. precursors (5 nM) for 48 h the cells were left to adhere on coverslips coated with 50 uM of collagen I for 1 h before staining. Scale bar = 10 µm. The bottom graph shows the FA size per treated cell. Quantification of FA size is represented as the average of FA area per cell. Data are shown as mean values ± s.e.m. from three independent experiments ($P = 0.04$, Student's *t*-test). (**H**) Phase-contrast images of MDA-MB-231 cells transfected with the indicated miRNA precursors (5 nM) for 48 h. Lamellipodial structures are indicated by continuous arrows; lack of lamellipodia is indicated by discontinuous arrows. The box plot on the right shows the number of lamellipodia formed after treating the cells with the indicated precursors. Scale bar = 100 µm. 50–150 cells per condition in three independent experiments were counted. Data are mean ± s.e.m. ($P = 0.0003$, Student's *t*-test). The image at the bottom shows typical lamellipodia in MDA-MB-231 cells transfected with the indicated precursors (5 nM) for 48 h and stained with Alexa Fluor 488 phalloidin.

miR-23b-expressing MCF-7 cells were straighter compared with controls (Figure 1F).

The miR-23b expression increases FA size and cell spreading and modulates the formation of lamellipodia

We stained MDA-MB-231 cells for the FA marker vinculin (26) to assess the effect of miR-23b over-expression on their ability to form FAs. FAs were significantly larger in cells after over-expressing miR-23b compared with miR-n.c.-transfected controls (Figure 1G). Remarkably, we also noticed that the number of cells forming lamellipodia was significantly less after miR-23b over-expression and at most these formed only small narrow protrusions (Figure 1H).

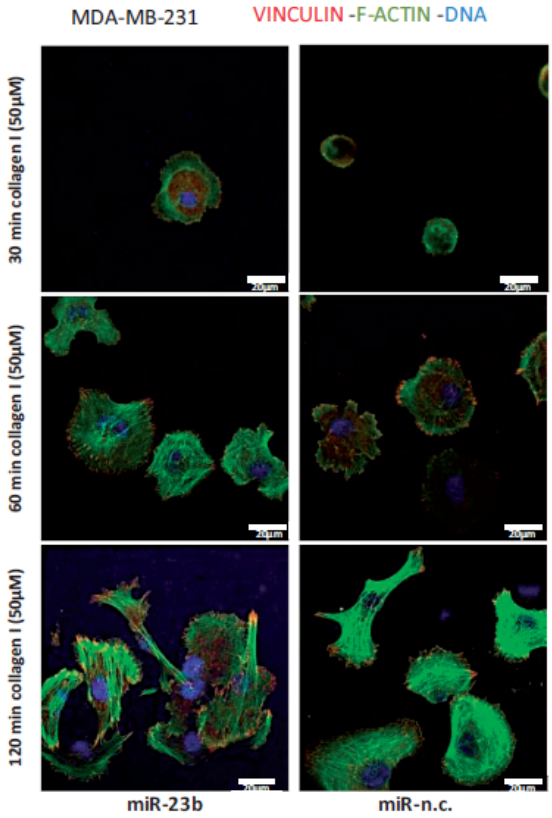

Figure 2. miR-23b expression modulate spreading capabilities on ECM in MDA-MB-231 cells. For spreading assays, MDA-MB-231 cells were transfected with miR-23b and miR-n.c. precursors (5 nM) for 48 h and seeded on collagen I (50 µM) matrices for 30, 60 and 120 min. Cells were than fixed and stained for anti-Vinculin and phalloidin to visualize FAs and F-actin, respectively. Nuclei are visualized with TO-PRO-3 stain (blue); scale bar = 20 µm.

To assess the effects of miR-23b on cell-spreading capacity, we plated MDA-MB-231 cells for 30, 60 and 120 min (Figure 2) on Type I collagen. The miR-23b-transfected cells spread more than controls and after 30 min contained lamellar protrusions, stress fiber-like actin bundles and punctate peripheral FAs, whereas the controls remained rounded with no FAs or F-actin bundles (Figure 2).

The miR-23b regulates breast cancer cell motility and invasion

We found that miR-23b over-expression did not affect the proliferation rate or promote apoptosis in cultured MDA-MB-231 or MCF-7 cells (Supplementary Figure S2A and B). However, miR-23b transfection markedly reduced *in vitro* migration of highly motile MDA-MB-231 cells compared with miR-n.c., effects which were similar to those seen in miR-31 over-expressing positive controls (Figure 3A). The miR-31 reduces MDA-MB-231 cell motility and experimental metastasis in BC (13) and accordingly miR-23b and miR-31 both reduced cell migratory speed (Figure 3B and Supplementary Movies S1–S3) and shortened migration trajectory lines (Figure 3C). Next, we developed MDA-MB-231 cell lines that stably expressed an EGFP-miR-23b sponge construct (Supplementary Figure S3A), enabling them to inhibit endogenous miR-23b. In particular, clone 10 reduced miR-23b levels by up to 70% (Supplementary Figure S3B). Co-expression of the sponge vector and a sensor vector [that contains six perfectly interacting sites for miR-23b (Supplementary Figure S3D)] increases luciferase activity compared with empty vector control (Supplementary Figure S3E), demonstrating the efficiency of the sponge vector in the inhibition of miR-23b activity. Notably, the inhibition of miR-23b significantly increased MDA-MB-231 cell migration (Figure 3D) and increased lamellipodia size (Supplementary Figure S3C), which was consistent with the effects of miR-23b over-expression on lamellipodia as described earlier in the text (Figure).

To evaluate invasive capacity, we tested MDA-MB-231 migration in 3D matrices. The miR-23b over-expression and silencing significantly reduced and increased cell invasion, respectively (Figure 3E and F).

The miR-23b directly targets PAK2 and increases myosin light chain II phosphorylation

We implicated miR-23b in cytoskeletal regulation and selected PAK2 as its candidate target based on our TargetScan analysis (Figure 4A and Supplementary Figure S4A) and its previously described role in cytoskeletal remodeling (7,27). Subsequently, we found that silencing PAK2 reduced motility and increased myosin light chain (MLC) II phosphorylation in MDA-MB-231 cells (Supplementary Figure S4C and D). Interestingly, PAK3 was not detected in three epithelial cancer cell lines (data not shown), consistent with its restricted tissue expression pattern (28). The miR-23b specifically reduced PAK2 levels in all tested cell lines, but not PAK1 (which is not a predicted miR-23b target; Figure 4B and Supplementary Figure S4B). Accordingly, MLC II phosphorylation was upregulated on miR-23b over-expression, which is important for regulating cytoskeletal reorganization and cell migration (Figure 4C). Furthermore, PAK2 levels increased in MCF-7 cells transiently transfected with miR-23b sponge construct and in MDA-MB-231 stably transfected with miR-23b sponge construct (i.e. after reduction of endogenous miR-23b levels; Figure 4D and Supplementary Figure S4E). Luciferase reporter assays next demonstrated that miR-23b regulates PAK2, but not PAK1, by direct interaction with its 3′UTR (Supplementary Figure S4F–I).

AP-1 directly interacts with the miR-23b promoter and transcriptionally suppresses its expression

The transcription factor AP-1 is activated through EGFR and HER-2 signaling pathways. It subsequently recognizes TPA-responsive elements (TREs) in promoter and enhancer regions of target genes involved in cell motility and growth (29) and is composed of c-JUN

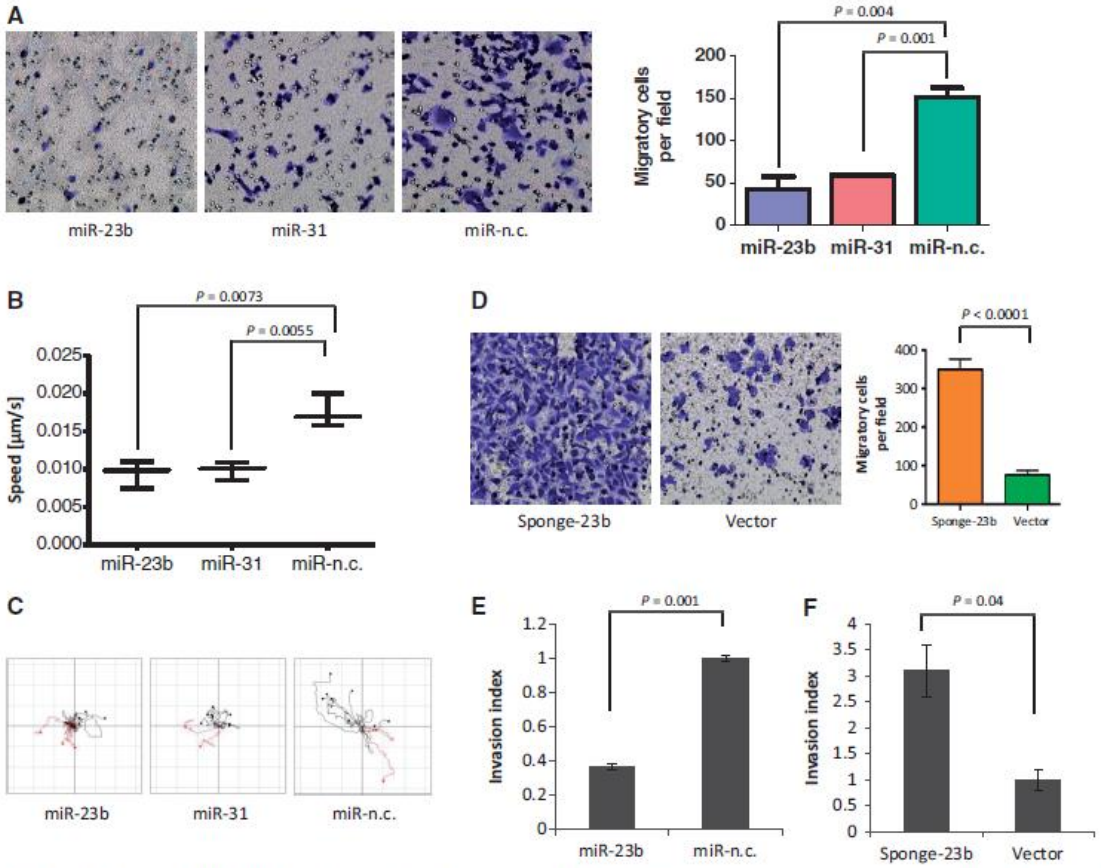

Figure 3. mir-23b inhibits MDA-MB-231 cell motility and invasion. (**A**) Transwell migration assays were performed for 9 h after transfecting MDA-MB-231 cells with the indicated precursors (5 nM) for 48 h. The graph on the right indicates cell migration expressed as percentage of the average of migratory cells per field ($n = 5$ fields per transfection). Data are mean of three experiments ± s.e.m. performed in triplicates ($P = 0.004$, $P = 0.001$, Student's t-test). (**B**) Motility of MDA-MB-231 cells expressing the indicated precursors was examined for 24 h by phase-contrast, time-lapse microscopy. Cell speed of 50–100 cells per condition was quantified and speed averages are presented as mean of three experiments ± s.e.m. ($P = 0.0001$, Student's t-test). (**C**) Plots show overlays of representative trajectories described by pre-miR-expressing MDA-MB-231 cells during time-lapse motility assays. (**D**) Transwell migration assays of MDA-MB-231 cells stably expressing the indicated constructs (Vector refers to pEGFP-C1 empty vector) were performed for 9 h. The graph on the right indicates cell migration expressed as a percentage of the average of migratory cells per field ($n = 5$ fields per transfection). Data are mean of three experiments ± s.e.m. performed in triplicates ($P < 0.0001$ Student's t-test). (**E**) Invasion of MDA-MB-231 cells transfected with miR-23b and miR-n.c. precursors (5 nM) for 48 h was assessed in collagen-I-3D-matrices (2.3 mg/ml) for 16 h. Confocal z sections were collected from each well at 0 µm (bottom of the well) and 40 µm and invasion indexes were calculated as the number of cells at 40 µm divided by those at 0 µm. Invasion indexes are mean of three experiments ± s.e.m. performed in quintuplicates ($P = 0.001$ Student's t-test). (**F**) Invasion assays using MDA-MB-231 cells stably expressing the miR-23b-sponge construct or the parental control pEGFP-C1 plasmid vector were performed as in (E). Invasion indexes are mean of three experiments ± s.e.m. performed in quintuplicates ($P = 0.04$, Student's t-test).

and c-FOS heterodimers (Supplementary Figure S5A) (30). Analysis of the transcription unit (TU) for transcription factors that may regulate this miRNA gene, revealed conserved and less conserved TREs along miR-23b TU (Figure 5A). The miR-23b is encoded in the complex TU, Chromosome 9 open reading frame 3 (*C9orf3*; Figure 5A), and c-MYC regulates its expression by directly interacting with its upstream transcriptional start site (31,32).

To determine whether AP-1 regulates miR-23b transcription, we next silenced c-FOS and c-JUN in MDA-MB-231 cells. Although individual gene silencing had little effect, co-silencing of both genes significantly increased primary (pri-) and mature miR-23b levels, thus implicating AP-1 in the regulation and reduction of miR-23b expression (Figure 5B and Supplementary Figure S5B). In addition, c-JUN-c-FOS co-silencing reduced PAK2 levels and greatly increased MLC II phosphorylation (Supplementary Figure S5C). Next, chromatin immunoprecipitation revealed that AP-1 is directly involved in the transcriptional inhibition of miR-23b, as c-JUN directly bound to at least two evolutionarily

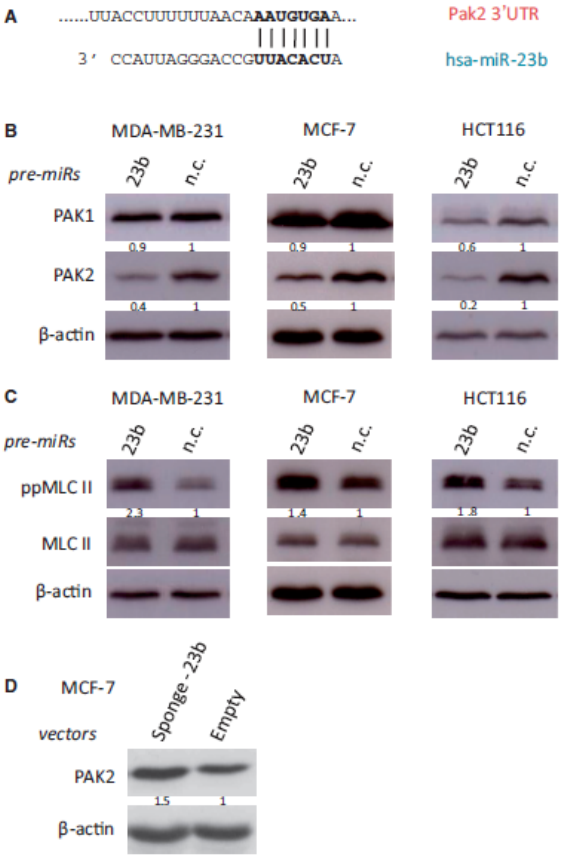

Figure 4. miR-23b targets PAK2 kinase, leading to induction of MLC II phosphorylation. (**A**) Predicted duplex formation between human Pak2 3′UTR (top) and has-miR-23b (bottom). (**B**) Western blots showing PAK1 and PAK2 levels after transfection for 48 h of the indicated miRNA precursors (5 nM) in breast cancer MDA-MB-231 and MCF-7 cells and colon cancer HCT116 cells. (**C**) Western blots showing MLC II levels and phosphorylation of MLC II at Thr18/Ser19 position, after transfection for 48 h of miR-23b and miR-n.c. precursors (5 nM) in the same cancer cell lines described in (B). (**D**) Western blots showing PAK2 levels after transient transfection of MCF-7 cells with mi-23b-sponge construct and pEGFP-C1 parental control (2 μg). β-actin was used as a loading control. Fold changes in protein expression levels were normalized for β-actin using ImageJ software are shown underneath each relative protein plot.

conserved TREs in the TU of *C9orf3* (Figure 5A and C). c-JUN also bound to the IL-6 gene promoter, used as positive control (33), but not a genomic DNA region that lacks the TREs (Figure 5C).

As *c-JUN* is transcriptionally activated by EGF (34), we exposed EGFR positive MDA-MB-468 BC cells to EGF. We found that c-Jun mRNA increased within 20 min and for up to 2 h (Supplementary Figure S5D), as expected (34), whereas miR-23b levels concomitantly decreased (Supplementary Figure S5E), thus indicating that EGF reduces miR-23b expression through c-JUN.

The action of miR-23b on the cytoskeleton is mediated by regulation of a subset of cytoskeletal genes

By treating BC cells with a siRNA against PAK2, we obtained ~94% silencing of the gene (Supplementary Figure S4D). On the other hand, we showed that miR-23b treatment reduced PAK2 levels to ~60% (Figure 4B). As miR-23b induced a stronger reduction of MDA-MB-231 motility compared with the silencing of PAK2 alone (Figure 3B and Supplementary Figure S4C), this miRNA must also mediate this effect through the regulation of other cytoskeletal genes. With this hypothesis in mind, we performed RNA-seq of miR-23b-over-expressing MCF-7 cells and MDA-MB-231 cells stably transfected with miR-23b sponge vector. The miR-23b expression in MCF-7 cells affected levels of 7.4% of transcripts, whereas in MDA-MB-231 cells stably transfected with the sponge vector, gene expression changed for 22.9% (Supplementary Table S3). As miRNAs repress gene expression, we selected downregulated genes from miR-23b-over-expressing MCF-7 and upregulated genes from miR-23b-sponge MDA-MB-231 (Supplementary Table S4) and performed GO term enrichment analysis (Supplementary Figure S6). Consistent with our findings, we observed enrichment in cytoskeletal organization genes in both cases (Supplementary Figure S6A and B). To further evaluate miR-23b targets, we intersected genes downregulated in MCF-7 cells over-expressing miR-23b with those genes upregulated in MDA-MB-231 cells containing sponge vectors that stably reduce miR-23b and combined them with those genes derived from a TargetScan analysis (Supplementary Table S4). We reasoned that the intersection would contain a highly enriched list of direct targets and considered a cutoff expression change of 1.2-fold sufficient, as miRNAs regulate transcripts by promoting destabilization through deadenylation (35,36), although mediating a stronger effect on protein translation (37). Higher fold changes may result in omitting many relevant targets. Furthermore, the impact of miRNAs on gene targets is variable and usually mild (38,39). Seventy percent of previously described miR-23b gene targets were among the intersection representing those genes downregulated in MCF-7 and/or upregulated in MDA-MB-231 and those in the TargetScan list (Supplementary Tables S4). Accordingly, we found that PAK2 is within this intersection (Supplementary Table S4). From this gene list, we selected a group of pro-metastatic genes for further validation.

Cytoskeletal genes are direct targets of miR-23b in BC

This finding was further validated performing RT-qPCR on 15 pro-metastatic genes involved in cytoskeletal remodeling from our RNA-seq analysis, that contain 'seeds' for miR-23b interaction (TargetScan analysis). Accordingly, these were all found to be downregulated in MCF-7 over-expressing miR-23b and upregulated in MDA-MB-231 stably transfected with miR-23b sponge vector (Supplementary Figure S7). Next, we selected seven genes (LIMK2, ARHGEF6, CFL2, PIK3R3, PLAU, ANXA2, TLN2) that are well described in the

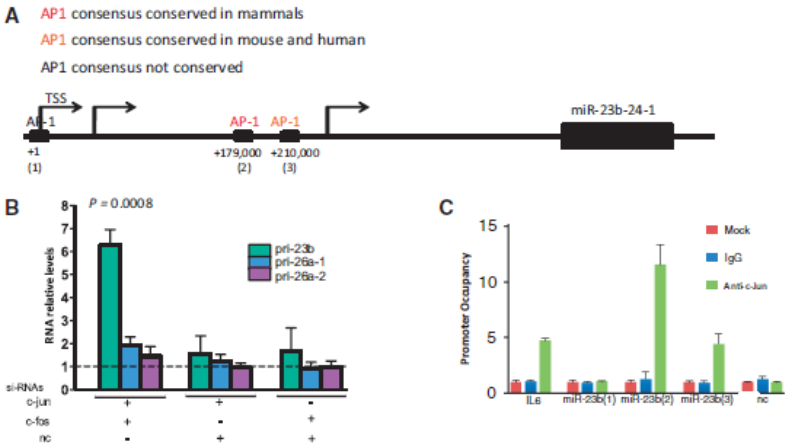

Figure 5. AP-1 transcriptionally suppresses miR-23b expression levels directly binding with its promoter. (**A**) Schematic representation of miR-23b TUs showing conserved, less conserved and non-conserved AP-1-specific TREs. TSS: transcription start site. (**B**) Relative levels of pri-mir-23b, pri-mir-26a-1 and pri-mir-26a-2 were measured by RT-qPCR after co-silencing of c-jun and c-fos, silencing of c-jun or c-fos by using siRNAs (20 nM) in MDA-MB-231 cells for 48 h. Data are presented relative to the siRNA-n.c. (40 nM) single transfection (dotted line). Data are mean of three experiments ± s.e.m. ($P = 0.0008$, Student's t-test). (**C**) MDA-MB-231 cells were processed for ChIP assays and RT-qPCR was performed. The c-JUN-interaction site genomic regions are presented, expressed as promoter occupancy. MiR-23b (1), (2), (3) represent each AP-1-specific TREs present in the TU of miR-23b promoter, respectively. IL6: interleuchin-6 promoter region; n.c.: a genomic region that does not contain AP-1-specific TREs. Data are mean of two independent experiments ± s.e.m.

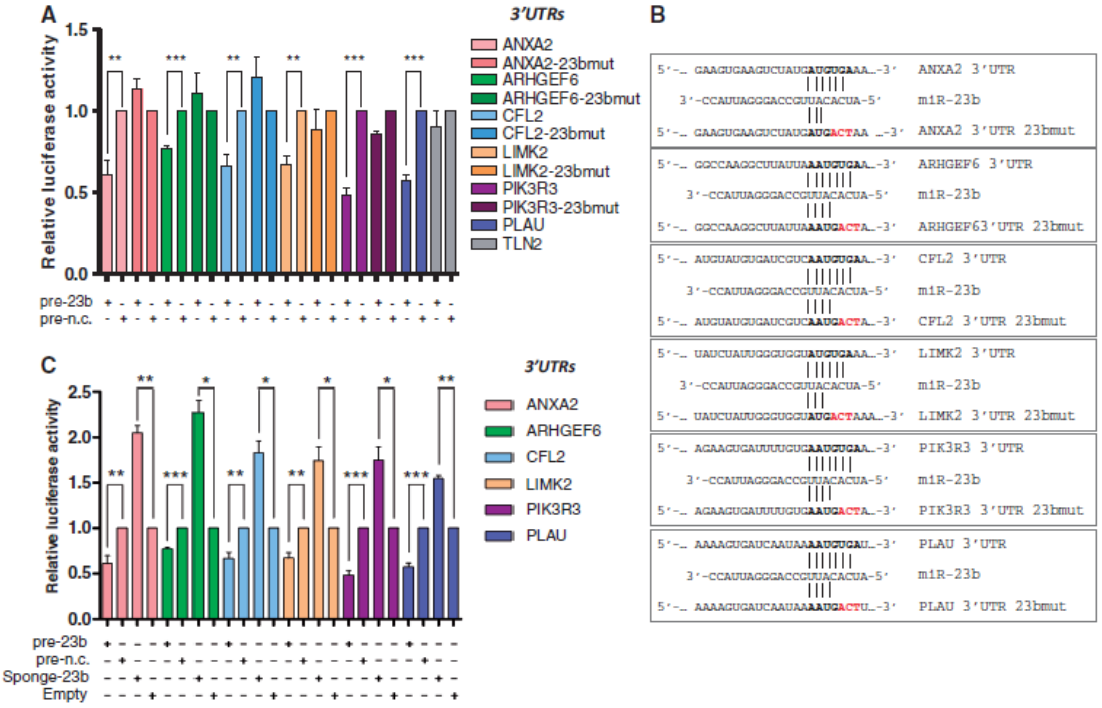

Figure 6. miR-23b targets ANXA2, ARHGEF6, CFL2, LIMK2, PIK3R3 and PLAU mRNAs by directly interacting with their relative 3′UTRs. (**A**) and (**C**), Relative luciferase activity levels were measured after 24 h from co-transfection of MCF-7 cells with the indicated 3′UTR-luciferase reporter constructs either with miR-23b or miR-n.c. precurors (5 nM) or with mi-23b-sponge construct or pEGFP-C1 parental control (150 ng). Data are mean of three independent experiments (each of them performed in triplicate) ± s.e.m (*$P < 0.05$; **$P \leq 0.006$; ***$P \leq 0.0005$). (**B**) Representation of miR-23b and the indicated target mRNA 3′UTR heteroduplexes: complementary nucleotides of the miR-23b seed sequence (in bold) and the mutant nucleotides of the miR-23b binding site (in red).

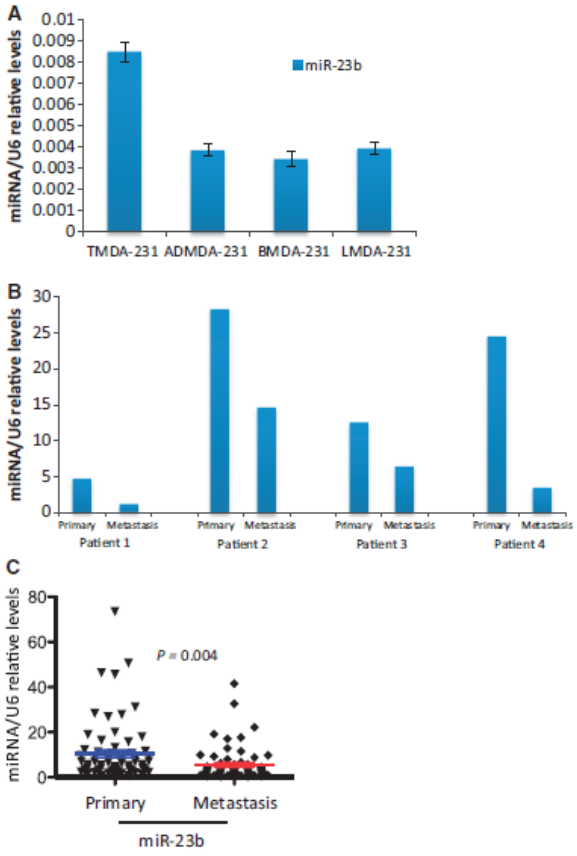

Figure 7. mir-23b expression is inversely correlated with metastasis. (**A**) RT-qPCR shows relative expression levels of miR-23b in MDA-MD-231 breast cancer cell lines that formed the primary tumor at the inoculation site (TMD-231) and cells that metastasized to the adrenal gland (AMD-231), bone (BMD-231) and lung (LMD-231) from the primary tumor in the fat pad of nude mice. Data are mean of triplicate samples in one experiment ± s.e.m. (**B**) miR-23b relative levels in four pairs of human primary breast cancer samples and their associated lymph-node metastasis. Data are relative levels of miR-23b in the primary tumor and matched lymph-node metastasis. (**C**) Scatter plot shows the mean miR-23b expression levels in 66 primary breast tumors and their corresponding metastatic specimens ($P = 0.004$, Student's *t*-test).

literature as promoters of cell motility through regulation of cytoskeletal remodeling pathways (19,40–43) and performed 3′UTR luciferase reporter assays (Figure 6). We could demonstrate the direct regulation by miR-23b of six of seven of these using both over-expression and inhibition of miR-23b (Figure 6A and C). In addition, site-directed mutagenesis precisely defined the sites of miR-23b interaction within their 3′UTRs (Figure 6A and B).

The miR-23b expression is inversely correlated with breast cancer metastases

We hypothesized that loss of miR-23b may be involved in BC spread and therefore examined miR-23b levels in MDA-MB-231 cells that had been inoculated into the mammary fat pads of nude mice and allowed to form metastatic deposits (44,45). We found higher miR-23b levels in the primary tumor cells at the inoculated sites, compared with metastatic cells at distant sites, such as the adrenal glands, bones and lungs (Figure 7A). Subsequently, we measured miR-23b levels in a small number of paired primary and metastatic BC patient samples. Accordingly, miR-23b levels were higher in primary tumors, compared with their corresponding lymph-node metastases (Figure 7B). We next validated this in a larger patient cohort ($n = 132$; 66 primary tumors and matching metastases) and again confirmed significantly higher mean expression of miR-23b in primary tumors than in the metastases (Figure 7C).

The miR-23b inhibition increases experimental metastasis and tumor growth *in vivo*

We further investigated the role of miR-23b in an experimental metastasis model. We injected MDA-MB-231 cells, stably transfected with miR-23b sponge or empty vector control constructs, into the mammary fat pad of BALB/c Nude mice and allowed tumor growth up to 300 mm^2 ($n = 7$ per treatment). We observed that local tumor invasion into the surrounding fat was dramatically increased by long-term miR-23b inhibition (Figure 8A). Extensive metastatic deposits were only detected in draining lymph nodes of mice injected with stably transfected miR-23b sponge cells, indicating that reduced miR-23b activity enhanced the ability of these cells to spontaneously metastasize (Figure 8B). Our *in vitro* findings showed that neither expression (Supplementary Figure S2A) nor inhibition of miR-23b (Supplementary Figure S8A) significantly altered cell growth, but miR-23b inhibition surprisingly increased tumor growth *in vivo* (Figure 7C). Normally, xenografts derived from MDA-MB-231 injection into the mammary fat pad of immunocompromised mice have extensive central necrotic areas (46); however, we saw that miR-23b downregulation dramatically reduced tumor necrosis without significantly affecting the number of tumor microvessels (Figure 8D and Supplementary Figure S8B). This could explain the discrepancies seen in cell growth rate *in vivo* and *in vitro* following miR-23b inhibition.

DISCUSSION

The current study focused on miR-23b because, although its involvement in some cancers is well-known, its global functions and role in BC are poorly defined. Using a pathway enriched analysis, we have suggested a role for miR-23b in cytoskeletal remodeling. We subsequently demonstrated this experimentally and validated a group of cytoskeletal genes as its direct targets.

The miR-23b over-expression increased epithelial characteristics in MCF-7 cells, but not in mesenchymal-like cells where CDH1 is not expressed. This is probably because miR-23b was unable to promote the formation of new junctions or increase CDH1 levels (Figure 1B), but rather enhanced the tension of existing ones. CDH1 is the principal mediator of adherens junction formation

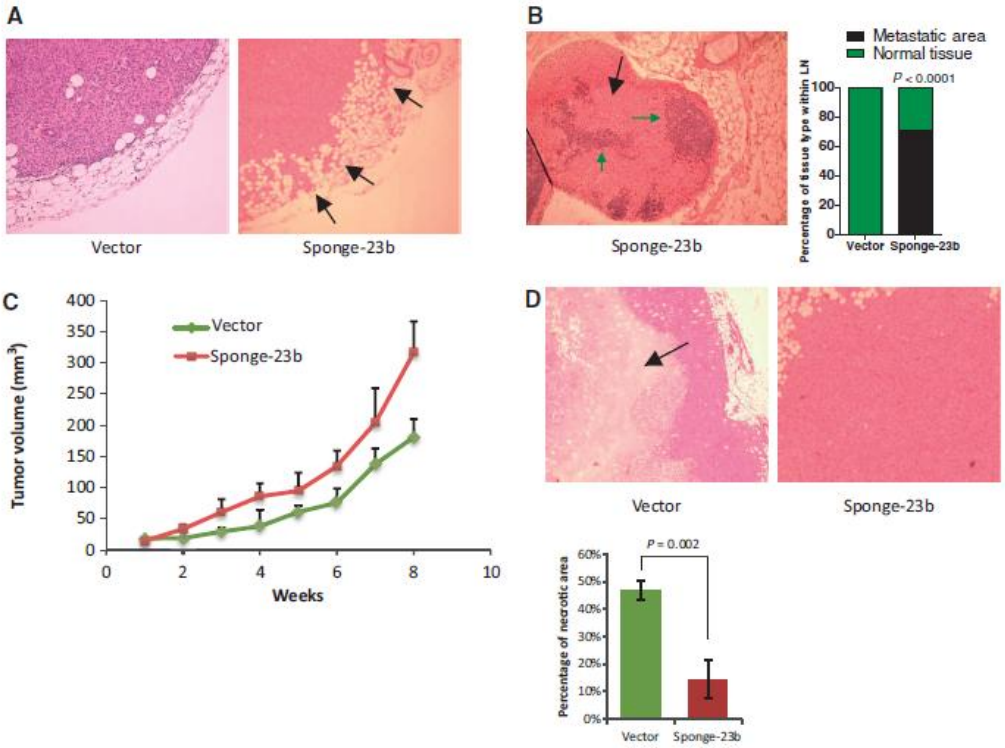

Figure 8. miR-23b inhibition increases tumor growth by reducing cell necrosis and increasing local invasion *in vivo*. (**A**) H&E stain of GFP-miR-23b-Sponge expressing- or GFP expressing-MDA-MB-231 cell primary tumors 2 months after orthotopic injection. Black arrows indicate regions of invasion into the surrounding fat. (**B**) Representation of a lymph node from a mouse injected with GFP-miR-23b-Sponge expressing-MDA-MB-231 cells H&E stained. The black arrow indicates metastatic areas whereas green arrows indicate residual normal tissue characterized by the presence of smaller nuclei ($n = 7$ per treatment). A quantification of the tissue type within the lymph nodes is shown in the graph on the right ($P = 0.0001$, Chi-Square test). (**C**) Line chart showing changes in tumor volume (mm^3) over time (weeks) after injection of 1×10^6 GFP-miR-23b-Sponge expressing- or GFP expressing-MDA-MB-231 cells into the mammary fat pad of BALB/c nude mice ($n = 7$ per treatment). (**D**) H&E stain of MDA-MB-231 cell primary tumors 2 months after orthotopic injection. Arrow indicates region of necrosis ($n = 7$ per treatment). The graph below shows a quantification of necrosis expressed as percentage of necrotic areas formed within the primary tumors ($P = 0.002$, Student's *t*-test).

between cells and although intracellular it is anchored to the actin cytoskeleton through α- and β-catenin (47). Recently, Zhang *et al.* (20) reported that miR-23b can inhibit migration and metastasis in colorectal cancer cells, indicating a similar role may exist for it in other tumor types. They showed that miR-23b increases epithelial characteristics through the upregulation of CDH1 (20). However, we could not demonstrate CDH1 upregulation on over-expression of miR-23b, neither at the RNA nor the protein level. This indicates that miR-23b probably confers epithelial characteristics in both tissues types by different pathways. Importantly, our RNA-seq analysis showed that miR-23b over-expression increased the expression of the cell–cell adhesion molecule *Nectin1*, which probably contributes to the formation of adherens junctions, as its downregulation in MCF-7 cells mediates EMT (48). In adition, *LMO7* is involved in the association between *CDH1* and *Nectin1* at the cell–cell junction level (49) and was upregulated by miR-23b expression (Supplementary Table S3).

The HER family of tyrosine kinase receptors is frequently over-expressed in breast and other types of cancers. Ligands such as EGF and heregulin can bind to them and increase the metastatic potential of cancer cells (50). AP-1 is a transcription factor formed by the interaction between c-FOS and c-JUN that is activated by HER-2 signaling and increases metastasis by regulating pro-metastatic genes (51). Here, we show that miR-23b is a miRNA transcriptionally suppressed by AP-1 (Figures 5 and 9). On the other hand, EGFR stimulation by EGF decreased the levels of mature miR-23b (Supplementary Figure S5 and Figure 9). The over-expression of miR-23b consequently regulates cytoskeletal dynamics and decreases cell motility and invasion *in vitro*. These results are consistent with the strong down-regulation of cell motility exerted by miR-23b over-expression in MCF-7 cells, recently shown by Zhang *et al* (20). This indicates that its downregulation by AP-1 is an important event that then leads to the acquisition of a more invasive phenotype for the cancer cells.

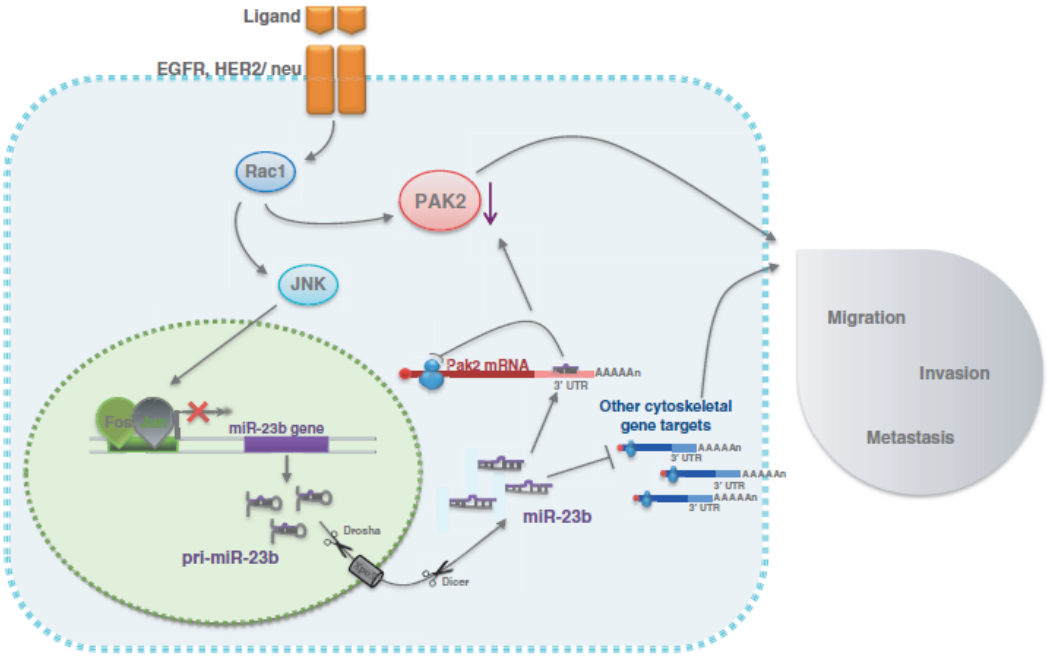

Figure 9. Schematic representation of the mechanism of action of miR-23b in BC cells.

Importantly, miR-23b is part of a cluster composed of miR-23b, miR-27b and miR-24-1 that are transcribed as a unique primary transcript (52). This may indicate that AP-1 mediates its effect by regulating all of the miRNA components of this cluster, but this observation requires further investigation.

Furthermore, the inhibition of miR-23b, by stably transfecting BC cells with a miR-23b sponge construct (i.e. loss-of-function), increases spontaneous metastasis in the lymph nodes of orthotopically injected nude mice. This demonstrated that the downregulation of miR-23b is an important event that mediates metastatic formation *in vivo*. Notably, miR-23b levels are reduced in MDA-MB-231 cells that have metastasized to distant organs (e.g. adrenal glands, bones and lungs; Figure 7A) after creation of orthotopic BC xenografts in nude mice. More importantly, we found miR-23b expression is significantly downregulated in lymph node metastases in a large patient cohort of paired BC samples (Figure 7B and C).

GO terms analysis of our RNA-seq data, obtained after miR-23b perturbation in BC cells, demonstrated that this miRNA regulates pathways involved in cytoskeletal remodeling, which is an essential mechanism that modifies tumor cells giving them more motile characteristics during the metastatic process. Accordingly, we showed here that miR-23b inhibits a large number of cytoskeletal genes, of which PAK2 (7,27), LIMK2 (40), ARHGEF6 (41), CFL2, PIK3R3 (42), PLAU (19) and ANXA2 (43) are regulated by direct interaction of miR-23b with their 3′UTRs (Figure 6 and Supplementary Figure S4). Moreover, in contrast to the other genes, luciferase levels of PAK2 3′UTR did not increase after the miR-23b sponge transfection. This suggests that the regulation exerted by miR-23b on PAK2, binding to the analyzed site, makes a minor contribution to the regulation of PAK2, indicating that other mechanisms, indirectly mediated by miR-23b, maybe involved. Interestingly, miR-23b over-expression dramatically reduced, and conversely its inhibition increased, lamellipodia size, which may explain changes in BC cell motility and invasiveness. Furthermore, miR-23b expression also increased FA size and the phosphorylation of MLC II, which regulates cell contractility. Importantly, these data indicate the mechanism of action of miR-23b in BC cells and demonstrate that its downregulation induces tumor growth, regulates cell–cell junctions and increases cell motility and invasion. Replacing miR-23b in BC patients may thus represent a novel therapeutic strategy to prevent tumor progression and metastatic spread.

SUPPLEMENTARY DATA

Supplementary Data are available at NAR Online. Supplementary Tables 1–6, Supplementary Figures 1–8, Supplementary Methods, Supplementary Movie 1–3 and Supplementary References [49–53].

ACKNOWLEDGEMENTS

The authors are indebted to the advice, expertise and time of Erik Sahai and Vikash Reebye. They thank Harikrishna Nakshatri for the MDA-MB-231 cells

derived from metastatic loci in nude mice. We would like to acknowledge support of the Imperial BRC and ECMC.

FUNDING

Association for International Cancer Research, the Rosetrees Trust, The Joseph Ettedgui Charitable Foundation, the Breast Cancer Campaign and the National Insitute for Health Research (in part). The authors are indebted to the support of Michael and Lotty Hunter. Funding for open access charge: Breast Cancer Campaign.

Conflict of interest statement. None declared.

REFERENCES

1. Hall,A. (1998) Rho GTPases and the actin cytoskeleton. *Science*, **279**, 509–514.
2. Michiels,F., Habets,G.G., Stam,J.C., van der Kammen,R.A. and Collard,J.G. (1995) A role for Rac in Tiam1-induced membrane ruffling and invasion. *Nature*, **375**, 338–340.
3. Molli,P.R., Li,D.Q., Murray,B.W., Rayala,S.K. and Kumar,R. (2009) PAK signaling in oncogenesis. *Oncogene*, **28**, 2545–2555.
4. Menard,R.E. and Mattingly,R.R. (2003) Cell surface receptors activate p21-activated kinase 1 via multiple Ras and PI3-kinase-dependent pathways. *Cell. Signal.*, **15**, 1099–1109.
5. Tsakiridis,T., Taha,C., Grinstein,S. and Klip,A. (1996) Insulin activates a p21-activated kinase in muscle cells via phosphatidylinositol 3-kinase. *J. Biol. Chem.*, **271**, 19664–19667.
6. Bagheri-Yarmand,R., Vadlamudi,R.K., Wang,R.A., Mendelsohn,J. and Kumar,R. (2000) Vascular endothelial growth factor up-regulation via p21-activated kinase-1 signaling regulates heregulin-beta1-mediated angiogenesis. *J. Biol. Chem.*, **275**, 39451–39457.
7. ConiglioS,J., Zavarella,S. and Symons,M.H. (2008) Pak1 and Pak2 mediate tumor cell invasion through distinct signaling mechanisms. *Mol. Cell. Biol.*, **28**, 4162–4172.
8. Bartel,D.P. (2009) MicroRNAs: target recognition and regulatory functions. *Cell*, **136**, 215–233.
9. Nicoloso,M.S., Spizzo,R., Shimizu,M., Rossi,S. and Calin,G.A. (2009) MicroRNAs—the micro steering wheel of tumour metastases. *Nat. Rev. Cancer*, **9**, 293–302.
10. Ma,L., Teruya-Feldstein,J. and Weinberg,R.A. (2007) Tumour invasion and metastasis initiated by microRNA-10b in breast cancer. *Nature*, **449**, 682–688.
11. Huang,Q., Gumireddy,K., Schrier,M., le Sage,C., Nagel,R., Nair,S., Egan,D.A., Li,A., Huang,G., Klein-Szanto,A.J. *et al.* (2008) The microRNAs miR–373 and miR-520c promote tumour invasion and metastasis. *Nat. Cell. Biol.*, **10**, 202–210.
12. Tavazoie,S.F., Alarcon,C., Oskarsson,T., Padua,D., Wang,Q., Bos,P.D., Gerald,W.L. and Massague,J. (2008) Endogenous human microRNAs that suppress breast cancer metastasis. *Nature*, **451**, 147–152.
13. Valastyan,S., Reinhardt,F., Benaich,N., Calogrias,D., Szasz,A.M., Wang,Z.C., Brock,J.E., Richardson,L. and Weinberg,R.A. (2009) A pleiotropically acting microRNA, miR-31, inhibits breast cancer metastasis. *Cell*, **137**, 1032–1046.
14. Patel,J.B., Appaiah,H.N., Burnett,R.M., Bhat-Nakshatri,P., Wang,G., Mehta,R., Badve,S., Thomson,M.J., Hammond,S., Steeg,P. *et al.* (2011) Control of EVI-1 oncogene expression in metastatic breast cancer cells through microRNA miR-22. *Oncogene*, **30**, 1290–1301.
15. Castellano,L., Giamas,G., Jacob,J., Coombes,R.C., Lucchesi,W., Thiruchelvam,P., Barton,G., Jiao,L.R., Wait,R., Waxman,J. *et al.* (2009) The estrogen receptor-alpha-induced microRNA signature regulates itself and its transcriptional response. *Proc. Natl Acad. Sci. USA*, **106**, 15732–15737.
16. Hooper,S., Marshall,J.F. and Sahai,E. (2006) Tumor cell migration in three dimensions. *Methods Enzymol.*, **406**, 625–643.
17. Zhao,D.H., Hong,J.J., Guo,S.Y., Yang,R.L., Yuan,J., Wen,C.Y., Zhou,K.Y. and Li,C.J. (2004) Aberrant expression and function of TCF4 in the proliferation of hepatocellular carcinoma cell line BEL-7402. *Cell Res.*, **14**, 74–80.
18. Medjkane,S., Perez-Sanchez,C., Gaggioli,C., Sahai,E. and Treisman,R. (2009) Myocardin-related transcription factors and SRF are required for cytoskeletal dynamics and experimental metastasis. *Nat. Cell. Biol.*, **11**, 257–268.
19. Salvi,A., Sabelli,C., Moncini,S., Venturin,M., Arici,B., Riva,P., Portolani,N., Giulini,S.M., De Petro,G. and Barlati,S. (2009) MicroRNA-23b mediates urokinase and c-met downmodulation and a decreased migration of human hepatocellular carcinoma cells. *FEBS J.*, **276**, 2966–2982.
20. Zhang,H., Hao,Y., Yang,J., Zhou,Y., Li,J., Yin,S., Sun,C., Ma,M., Huang,Y. and Xi,J.J. (2011) Genome—wide functional screening of miR-23b as a pleiotropic modulator suppressing cancer metastasis. *Nat. Commun.*, **2**, 554.
21. Lewis,B.P., Burge,C.B. and Bartel,D.P. (2005) Conserved seed pairing, often flanked by adenosines, indicates that thousands of human genes are microRNA targets. *Cell*, **120**, 15–20.
22. Ashburner,M., Ball,C.A., Blake,J.A., Botstein,D., Butler,H., Cherry,J.M., Davis,A.P., Dolinski,K., Dwight,S.S., Eppig,J.T. *et al.* (2000) Gene ontology: tool for the unification of biology. The gene ontology consortium. *Nat. Genet.*, **25**, 25–29.
23. Huang da,W., Sherman,B.T. and Lempicki,R.A. (2009) Systematic and integrative analysis of large gene lists using DAVID bioinformatics resources. *Nat. Protoc.*, **4**, 44–57.
24. Li,Y., VandenBoom,T.G. 2nd, Kong,D., Wang,Z., Ali,S., Philip,P.A. and Sarkar,F.H. (2009) Up-regulation of miR-200 and let-7 by natural agents leads to the reversal of epithelial-to-mesenchymal transition in gemcitabine-resistant pancreatic cancer cells. *Cancer Res.*, **69**, 6704–6712.
25. Otani,T., Ichii,T., Aono,S. and Takeichi,M. (2006) Cdc42 GEF Tuba regulates the junctional configuration of simple epithelial cells. *J. Cell Biol.*, **175**, 135–146.
26. Hynes,R.O. (2002) Integrins: bidirectional, allosteric signaling machines. *Cell*, **110**, 673–687.
27. Kumar,R., Gururaj,A.E. and Barnes,C.J. (2006) p21-activated kinases in cancer. *Nat. Rev. Cancer*, **6**, 459–471.
28. Kreis,P. and Barnier,J.V. (2009) PAK signalling in neuronal physiology. *Cell. Signal.*, **21**, 384–393.
29. Lamph,W.W., Wamsley,P., Sassone-Corsi,P. and Verma,I.M. (1988) Induction of proto-oncogene JUN/AP-1 by serum and TPA. *Nature*, **334**, 629–631.
30. Karin,M., Liu,Z. and Zandi,E. (1997) AP-1 function and regulation. *Curr. Opin. Cell Biol.*, **9**, 240–246.
31. Lundgren,P., Johansson,L., Englund,C., Sellstrom,A. and Mattsson,M.O. (1997) Expression pattern of glutamate decarboxylase (GAD) in the developing cortex of the embryonic chick brain. *Int. J. Dev. Neurosci.*, **15**, 127–137.
32. Gao,P., Tchernyshyov,I., Chang,T.C., Lee,Y.S., Kita,K., Ochi,T., Zeller,K.I., De Marzo,A.M., Van Eyk,J.E., Mendell,J.T. *et al.* (2009) c-Myc suppression of miR-23a/b enhances mitochondrial glutaminase expression and glutamine metabolism. *Nature*, **458**, 762–765.
33. Ndlovu,N., Van Lint,C., Van Wesemael,K., Callebert,P., Chalbos,D., Haegeman,G. and Vanden Berghe,W. (2009) Hyperactivated NF-{kappa}B and AP-1 transcription factors promote highly accessible chromatin and constitutive transcription across the interleukin-6 gene promoter in metastatic breast cancer cells. *Mol. Cell. Biol.*, **29**, 5488–5504.
34. Schaerli,P. and Jaggi,R. (1998) EGF-induced programmed cell death of human mammary carcinoma MDA-MB-468 cells is preceded by activation AP-1. *Cell. Mol. Life Sci.*, **54**, 129–138.
35. Chekulaeva,M., Mathys,H., Zipprich,J.T., Attig,J., Colic,M., Parker,R. and Filipowicz,W. (2011) miRNA repression involves GW182-mediated recruitment of CCR4-NOT through conserved W-containing motifs. *Nat. Struct. Mol. Biol.*, **18**, 1218–1226.
36. Fabian,M.R., Cieplak,M.K., Frank,F., Morita,M., Green,J., Srikumar,T., Nagar,B., Yamamoto,T., Raught,B., Duchaine,T.F. *et al.* (2011) miRNA-mediated deadenylation is orchestrated by GW182 through two conserved motifs that interact with CCR4-NOT. *Nat. Struct. Mol. Biol.*, **18**, 1211–1217.

37. Pillai,R.S., Bhattacharyya,S.N., Artus,C.G., Zoller,T., Cougot,N., Basyuk,E., Bertrand,E. and Filipowicz,W. (2005) Inhibition of translational initiation by Let-7 MicroRNA in human cells. *Science*, **309**, 1573–1576.
38. Selbach,M., Schwanhausser,B., Thierfelder,N., Fang,Z., Khanin,R. and Rajewsky,N. (2008) Widespread changes in protein synthesis induced by microRNAs. *Nature*, **455**, 58–63.
39. Baek,D., Villen,J., Shin,C., Camargo,F.D., Gygi,S.P. and Bartel,D.P. (2008) The impact of microRNAs on protein output. *Nature*, **455**, 64–71.
40. Johnson,E.O., Chang,K.H., Ghosh,S., Venkatesh,C., Giger,K., Low,P.S. and Shah,K. (2012) LIMK2 is a crucial regulator and effector of Aurora-A-kinase-mediated malignancy. *J. Cell Sci.*, **125**, 1204–1216.
41. Rosenberger,G., Gal,A. and Kutsche,K. (2005) AlphaPIX associates with calpain 4, the small subunit of calpain, and has a dual role in integrin-mediated cell spreading. *J. Biol. Chem.*, **280**, 6879–6889.
42. Xu,L., Wen,Z., Zhou,Y., Liu,Z., Li,Q., Fei,G., Luo,J. and Ren,T. (2013) MicroRNA-7-regulated TLR9 signaling-enhanced growth and metastatic potential of human lung cancer cells by altering the phosphoinositide-3-kinase, regulatory subunit 3/Akt pathway. *Mol. Biol. Cell*, **24**, 42–55.
43. Wu,B., Zhang,F., Yu,M., Zhao,P., Ji,W., Zhang,H., Han,J. and Niu,R. (2012) Up-regulation of Anxa2 gene promotes proliferation and invasion of breast cancer MCF-7 cells. *Cell Prolif.*, **45**, 189–198.
44. Helbig,G., Christopherson,K.W. 2nd, Bhat-Nakshatri,P., Kumar,S., Kishimoto,H., Miller,K.D., Broxmeyer,H.E. and Nakshatri,H. (2003) NF-kappaB promotes breast cancer cell migration and metastasis by inducing the expression of the chemokine receptor CXCR4. *J. Biol. Chem.*, **278**, 21631–21638.
45. Patel,J.B., Appaiah,H.N., Burnett,R.M., Bhat-Nakshatri,P., Wang,G., Mehta,R., Badve,S., Thomson,M.J., Hammond,S., Steeg,P. *et al.* Control of EVI-1 oncogene expression in metastatic breast cancer cells through microRNA miR-22. *Oncogene*, **30**, 1290–1301.
46. Amstalden van Hove,E.R., Blackwell,T.R., Klinkert,I., Eijkel,G.B., Heeren,R.M. and Glunde,K. Multimodal mass spectrometric imaging of small molecules reveals distinct spatio-molecular signatures in differentially metastatic breast tumor models. *Cancer Res.*, **70**, 9012–9021.
47. Fukata,M. and Kaibuchi,K. (2001) Rho-family GTPases in cadherin-mediated cell-cell adhesion. *Nat. Rev. Mol. Cell Biol.*, **2**, 887–897.
48. Vetter,G., Saumet,A., Moes,M., Vallar,L., Le Bechec,A., Laurini,C., Sabbah,M., Arar,K., Theillet,C., Lecellier,C.H. *et al.* (2010) miR-661 expression in SNAI1-induced epithelial to mesenchymal transition contributes to breast cancer cell invasion by targeting Nectin-1 and StarD10 messengers. *Oncogene*, **29**, 4436–4448.
49. Ooshio,T., Irie,K., Morimoto,K., Fukuhara,A., Imai,T. and Takai,Y. (2004) Involvement of LMO7 in the association of two cell-cell adhesion molecules, nectin and E-cadherin, through afadin and alpha-actinin in epithelial cells. *J. Biol. Chem.*, **279**, 31365–31373.
50. Png,K.J., Halberg,N., Yoshida,M. and Tavazoie,S.F. (2012) A microRNA regulon that mediates endothelial recruitment and metastasis by cancer cells. *Nature*, **481**, 190–194.
51. Ozanne,B.W., McGarry,L., Spence,H.J., Johnston,I., Winnie,J., Meagher,L. and Stapleton,G. (2000) Transcriptional regulation of cell invasion: AP-1 regulation of a multigenic invasion programme. *Eur. J. Cancer*, **36**, 1640–1648.
52. Chhabra,R., Dubey,R. and Saini,N. (2010) Cooperative and individualistic functions of the microRNAs in the miR-23a~27a~24-2 cluster and its implication in human diseases. *Mol. Cancer*, **9**, 232.
53. Fritah,A., Saucier,C., Mester,J., Redeuilh,G. and Sabbah,M. (2005) p21WAF1/CIP1 selectively controls the transcriptional activity of estrogen receptor alpha. *Mol. Cell. Biol.*, **25**, 2419–2430.

COMMENTARY

BioArchitecture 3:4, 119–124; July/August 2013; © 2013 Landes Bioscience

MicroRNA-23b regulates cellular architecture and impairs motogenic and invasive phenotypes during cancer progression

Loredana Pellegrino,* Jonathan Krell, Laura Roca-Alonso, Justin Stebbing, and Leandro Castellano

Division of Oncology; Department of Surgery & Cancer, Imperial College; Hammersmith Hospital Campus; Imperial Centre for Translational & Experimental Medicine; London, UK

The cytoskeleton is a dynamic three dimensional structure contained within the cytoplasm of a cell, and is important in cell shape and movement, and in metastatic progression during carcinogenesis. Members of the Rho family of small GTPases, RHO, RAC and cell cycle division 42 (Cdc42) proteins regulate cytoskeletal dynamics, through the control of a panel of genes. We have recently shown that the microRNA (miRNA) miR-23b represents a central effector of cytoskeletal remodelling. It increases cell-cell interactions, modulates focal adhesion and reduces cell motility and invasion by directly regulating several genes involved in these processes.

Keywords: miR-23b, microRNAs, miRNAs, cytoskeleton, motility, metastasis, adhesion, focal adhesion, tumor growth

Submitted: 08/07/13

Revised: 08/11/13

Accepted: 08/12/13

http://dx.doi.org/10.4161/bioa.26134

*Correspondence to: Loredana Pellegrino; Email: l.pellegrino@imperial.ac.uk

Commentary to: Pellegrino L, Stebbing J, Braga VM, Frampton AE, Jacob J, Buluwela L, Jiao LR, Periyasamy M, Madsen CD, Caley MP, et al. miR-23b regulates cytoskeletal remodeling, motility and metastasis by directly targeting multiple transcripts. Nucleic Acids Res 2013; 41:5400-12; PMID:23580553; http://dx.doi.org/10.1093/nar/gkt245

Introduction

Tumor progression often culminates in the development of metastasis, which usually results in the death of patients with solid malignancies.[1] After establishment of the primary tumor, cancer cells acquire aggressive traits that allow them to detach, migrate and invade, and these events denote the first steps of metastatasis.[2] Changes in the cellular cytoskeleton are central to the acquisition of a metastatic phenotyope. This generally requires the disruption of existing cell-cell contacts, the establishment of cell-matrix adhesions, the degradation or rearrangement of the extracellular matrix, and finally movement of the tumor cell. The actin cytoskeleton constitutes the structural support to cell morphology, polarity, adhesion and migration. Primary regulators of cytoskeletal dynamics are three members of the Rho family of small GTPases, RHO, RAC and cell cycle division 42 (Cdc42).[3] Under physiological conditions they ensure spatial and temporal cytoskeletal organization via the coordination of a plethora of effectors, including transcription factors. Conversely, aberrant activity of Rho GTPases has been significantly implicated in tumor aggressiveness and metastasis[4] Rho GTPases are activated in response to pro-migratory signals through various transmembrane receptors that are usually overexpressed or hyperactivated in cancer, thus leading to sustained Rho GTPase function. This results in dysregulation of the Rho GTPase cytoplasmic effectors and disruption of the actin cytoskeleton, leading to increased migration and invasion. In addition, aberrant activity of Rho GTPases induces changes in transcriptional activity, resulting in the expression of genes that further promote motility and invasion.[5] Accordingly, it is well-known that multigenic reprogramming events are necessary to promote the sustained expression of genes that initiate metastasis and coordinate the seeding of cancer cells to specific distant target organs.[6-8] In addition to the genetic and epigenetic alterations involved in malignant transformation, microRNAs (miRNAs) appear to play an important role in the establishment of the distinctive genetic signatures that characterize metastatic cells, owing to their ability to regulate the expression of multiple genes.[9]

MicroRNAs are a class of small, noncoding RNAs that function as post-transcriptional negative regulators in a wide range of physiological and pathological

processes. In malignant contexts, miRNAs play either oncogenic or tumor suppressor roles and deregulation of miRNA expression has been detected in many different human cancers.[10] Recently, it has been proposed that miRNA activity can promote or inhibit metastatic gene expression programs; this arises from the observation that specific miRNAs can control multigenic regulatory networks that operate at different steps of the metastatic process.[11] This is exemplified by miR-31, a miRNA that is preferentially downregulated during breast cancer progression, and that mediates coordinated repression of at least three pro-metastatic genes, *RhoA*, integrin α5 (*ITGA5*) and radixin (*RDX*) to suppress motility, invasion, resistance to anoikis and colonization of the lungs during breast cancer metastasis.[12]

Our group has recently identified miR-23b as a potent modulator of cytoskeletal dynamics via co-repression of a set of cytoskeleton specific genes, affecting motile and invasive properties necessary for breast cancer cells to metastatize.[13] Here, we attempt to unravel the molecular mechanisms employed by the miR-23b regulatory network in the inhibition of important features of cancer progression and metastasis.

Overlook of miRNA Biogenesis and Function

Most of mammalian miRNAs derive from intergenic or intronic genomic regions and go through a model of maturation events necessary for their ultimate function.[14,15] Mammalian single or clustered miRNA genes are generally transcribed by polymerase II, and less frequently by Polymerase III, into a primary miRNA transcript (pri-miRNA).[15] Owing to regions of imperfect complementarity, pri-miRNAs typically acquire double-stranded hairpin-like conformations flanked by single-stranded 5' and 3'ends that are typically capped and polyadenylated, respectively. The pri-miRNA hairpin structure is recognized and bound by the RNA-binding protein DGCR8, which allows the first cleavage event of the miRNA maturation process.[16] The binding of DGCR8to the ribonuclease Drosha enables it to process pri-miRNAs at the base of their hairpin region, thus releasing a ~70-nucleotide stem-loop intermediate, known as miRNA precursor (pre-miRNA).[16,17] Notably, a subclass of miRNAs undergo a noncanonical maturation pathway that does not require Drosha/DGCR8, but instead uses cellular splicing machinery for the formation of the pre-miRNA.[18] Completion of the miRNA maturation requires translocation of the pre-miRNA from the nucleus to the cytoplasm that is actively performed by exportin-5.[19] Once in the cytoplasm, the ribonuclease Dicer in complex with its cofactors, the RNA-binding proteins TARBP2 and PACT, cleaves off the loop of the pre-miRNA, yielding a 19–26-nucleotide-long double stranded miRNA-miRNA* duplex.[15,16,20] This miRNA duplex is then loaded onto the RNA-induced silencing complex (RISC), which consists of the Argonaute (Ago) protein family members and other proteins.[15,21] After strand separation, the guide strand or mature miRNA is preferentially retained into the active RISC, whereas the complementary strand (miRNA*) is discarded and degraded. The mature miRNA then guides Ago to selective recognition of a miRNA-specific target mRNA.[22] The specificity of target selection is generally determined by complementary matches between a "seed" sequence (positions 2 to 8 from the 5'end of the mature miRNA) and a miRNA-binding site usually embedded in the 3'untranslated region (3'UTR) of the target mRNA. Upon this interaction, the mature miRNA inhibits the expression of its target mRNA through Ago-mediated translational repression and/or deadenylation and decay of the messenger sequence.[23]

miR-23b Regulates the Actin Cytoskeleton and the Metastatic Process

miR-23b is encoded from a unique primary transcript that also contains miR-27b and miR-24–1. A few studies have implicated miR-23b in cancer progression, metastasis and cytoskeletal remodelling in several tumor types. In human colorectal cancer, miR-23b shows tumor suppressor functions by reducing in vitro migration and in vivo experimental metastatic formation, by inhibiting the expression of a cohort of pro-metastatic genes including uPA, c-MET, PAK2, FZD7, and MAP3K1.[24,25] MiR-23b-mediated repression of uPA has been shown to be critical in the regulation of migration in human cervical cancer cells.[26] In addition, this miRNA functions as an in vivo metastatic suppressor in prostate cancer, coordinating repression of the proto-oncogenes Src kinase and AKT, and inhibiting epithelial to mesenchymal transition (EMT) by reduction of the mesenchymal markers Vimentin and Snail and upregulation of E-cadherin.[27]

In our study, we showed that experimental suppression of miR-23b in breast cancer cell lines modulates cellular architecture and promotes in vivo tumor growth, invasion and lymph-node metastasis.[13] By combining bioinformatic and experimental analyses, we found that miR-23b is a master regulator of cytoskeletal dynamics in breast cancer cell models, with a robust impact on cell-cell interactions, cell-matrix adhesions, cell spreading and protrusion formation. We initially performed gain and loss of function experiments that revealed the ability of miR-23b to modulate in vitro migration and invasion of breast cancer cells.[13] Subsequently, we performed RNA-sequencing (RNA-seq) following miR-23b perturbation in cancer cell lines to investigate how its effect is mediated at the molecular level. This strategy allowed us to identify and validate a subset of cytoskeletal and pro-metastatic genes as direct miR-23b targets, namely the previously documented Pak2 and uPA, Arhgef6, Limk2, Cofilin-2 (Cfl2), and Annexin 2 (Anxa2). Coordinated repression of these targets along with mir-23b-mediated perturbation of the transcriptome state of breast cancer cells enabled our understanding of the molecular mechanism(s) that underpin the cellular phenotypes controlled by miR-23b.

We first showed that ectopic expression of miR-23b enhances epithelial characteristics of breast cancer MCF-7 cells, indicating that it may have a role in the inhibition of EMT during breast cancer progression[13]; this notion was supported by previous evidence in prostate and colorectal cancers where miR-23b

overexpression abolished features of EMT and upregulated the epithelial marker E-Cadherin.[24,27] Furthermore, under conditions of prolonged miR-23b administration we revealed that miR-23b failed to reverse EMT in- mesenchymal-like MDA-MB-231 cells and did not affect E-cadherin expression in either MDA-MB-231 or MCF-7 cells indicating that it specifically acts during EMT by improving the strength of existing junctions. In support of this hypothesis, sustained miR-23b ectopic expression improved the overall architecture of epithelia formed by 2-dimensional cultures of MCF-7 cells, which exhibited more orderly and stable cell-cell junctions compared with control-treated cells. Taken together, these data suggested that miR-23b activity confered enhanced tension between existing E-cadherin-mediated cell-cell junctions rather than inducing their de novo formation. Consistent with this hypothesis, analysis of our RNA-seq data revealed that prolonged overexpression of miR-23b in MCF-7 cells induced transcriptional upregulation of *Nectin1* and *LMO7*, which encode for cell-adhesion molecules that are highly involved in cell-cell junction formation. Nectin1 is a member of the Nectin family of transmembrane receptors that are involved in early establishment of cell-cell contacts, known as tight and adherens junctions.[28] Upon cell-cell interactions, clusters of Nectins on the lateral surface of the cell interact with similar clusters assembled on the membrane of the adjacent cell; simultaneously, on the intracellular side of both cells, Nectins recruit Afadin, an actin-binding protein that connects filamentous actin (F-actin) to the nectin-based adhesive structures. E-cadherin participates in the formation of adherens junctions following Nectin-mediated contacts.[29] Clusters of E-cadherin on the membrane of two adjacent cells connect to each other and are internally stabilized by interaction with F-actin via several actin-binding proteins. The interaction of additional adaptor molecules such as LMO7 with Afadin and E-cadherin-associated actin-binding proteins allows aggregation of Nectin and E-cadherin adhesive structures and strengthens the adhesive capabilities of E-cadherin.[30] Maturation of adherens junctions requires the assembly of additional E-cadherin-F-actin units and the accumulation of RHOA-activated myosin II. The latter generates a contractile force that brings two adjacent cadherin-based clusters together and maintains junctional tension.[31] This suggests that miR-23b may actually induce de novo formation of both tight and adherens junctions through a mechanism that requires Nectin1 upregulation and is independent of E-cadherin expression; in a later stage, miR-23b may stabilize existing and newly formed adherens junctions via upregulation of the adaptor molecule LMO7. Moreover, mir-23b likely contributes to enhance the junctional tension during assembly of the epithelia, as we detected increased myosin light chain II (MLCII) phosphorylation, indicative of myosin II activity, upon miR-23b overexpression in different cell lines, including MCF-7 cells.

In mesenchymal like breast cancer cells, miR-23b activity controls cytoskeletal dynamics to stimulate maturation of focal adhesions and cell spreading on the extracelluar matrix and impairs lamellipodia extension. The physiologic functions of the miR-23b targets identified in our study may elucidate the effects of miR-23b on the motile and invasive abilities of mesenchymal-like MDA-MB-231 cells.

During the migration process, a cell needs to acquire a polarized morphology, by extending membrane protrusions at the leading edge, such as lamellipodia and filopodia, that are stabilized by the formation of new focal adhesions (FAs). FAs are adhesive multiprotein complexes that connect the actin cytoskeleton to elements of the extracellular matrix.[32] Ectopic expression of a miR-23b mimic induced a significant increase of the FA area in MDA-MB-231 cells spreading on collagen I matrixes. Larger FA sites are caused by an excessive maturation of newly formed FAs, a process that requires local activity of myosin II.[32] At FA sites, myosin II activity is tightly regulated by the p21/RAC/Cdc42-activated kinases (PAKs). PAKs control the activation state of myosin II either by directly phosphorylating MLCII or by inhibiting the activity of MLCK, which results in reduced myosin II phosphorylation. PAK2, one of our identified miR-23b gene targets, has been shown to be crucial in limiting the size of FAs. Indeed, PAK2 depletion in breast cancer cells resulted in larger FA sizes and increased MLCII phosphorylation.[33] Accordingly, we observed that overexpression of miR-23b in MDA-MB-231 cells led to repression of PAK2 and enhanced phosphorylation of MLCII,. Conversely, inhibition of miR-23b activity using an in house sponge construct led to an increase of PAK2 levels which may explain the effect of miR-23b in inducing an increase in FA areas observed in these cells. Fully developed FAs promote cell spreading on the extracellular matrix and are associated with slower migration rates;[34,35] therefore a miR-23b-promoted increase of FA size may contribute to transient cell spreading and to the reduction in migratory phenotypes that we observed in miR-23b-overexpressing MDA-MB-231 cells.[13]

Localization of PAKs at FA sites is mediated by their direct interaction with αPIX (PAK-interacting exchange factor α), also known as COOL2 (Cloned out of library 2) or ARHGEF6 (RAC/Cdc42 guanine nucleotide exchange factor 6), strikingly, an additional miR-23b target validated in our study. ARHGEF6 is a well-described activator of RAC and Cdc42, which in turn activates PAKs.[36] ARHGEF6-mediated localization of PAKs at FA sites induces PAK activation through local stimulation of RAC and Cdc42. In this respect, along with repression of PAK2 expression, miR-23b may enhance FA maturation by limiting local PAK2 activity through downregulation of ARHGEF6.

It has been shown that ARHGEF6 overexpression dramatically promotes the formation of lamellipodia and filipodia protrusions, likely as a result of ARHGEF6-mediated activation of RAC and Cdc42.[37] Indeed, once activated, RAC and Cdc42 stimulate actin polymerization in order to support an extension of membrane protrusions, via a plethora of cytoplasmic effectors. Among them, activation of the PAK1/LIMK/cofilin pathway by both RAC and Cdc42 is crucial for actin polymerization dynamics and appropriate formation of lamellipodia at the leading edge.[38] RAC/Cdc42-activated PAK1 catalyzes phosphorylation and activation of LIMK which in turn

phosphorylates cofilin, resulting in its inhibition. Cofilin is an actin-binding protein responsible of F-actin severing; yet, it promotes lamellipodia assembly by inducing F-actin turnover that produces free barbed ends for the polymerization of new actin filaments.[39] Nevertheless, uncontrolled cofilin activity leads to accelerated F-actin turnover resulting in widening of the lamellipodium. PAK1-induced inactivation of cofilin ensures correct formation of lamellipodia by limiting their extent of expansion, that are under cofilin control.[40] We found that, miR-23b-overexpressing MDA-MB-231 cells exhibited significant impaired formation of lamellipodia protrusions at their leading edge and in contrast MDA-MB-231 stably expressing a sponge construct able to inhibit miR-23b activity showed larger lamellipodia. It is reasonable to infer that by coordinated repression of ARHGEF6, LIMK2 and CFL2, miR-23b disrupts crucial steps of the molecular pathway that supervises correct extension of lamellipodia. Notably, miR-23b-induced corruption of lamellipodia formation likely encompasses the suppressive effect of miR-23b on MDA-MB-231 cell migration as lamellipodia formation is crucial for cells to migrate. This effect can be also explained by the fact that downregulation of several miR-23b cytoskeletal targets, such as LIMK2, CFL2, and PAK2 inhibit migration and invasion of these cells.[13,41,42]

We also reported that overexpression of miR-23b greatly reduced invasion of MDA-MB-231 cells in three-dimensional collagen I matrixes; whereas inhibition of miR-23b activity strongly enhanced the invasive properties of these cells. Along with the role of miR-23b cytoskeletal targets in affecting breast cancer cell invasion, miR-23b seems to be closely implicated in the regulation of invasive processes, owing to its ability to directly target uPA and Annexin 2, two main components on the invasive machinery. Indeed, uPA and Annexin 2 play crucial roles in the extracellular cascade that converts plasminogen into plasmin, a serine protease largely implicated in invasion, neo-angiogenesis and metastasis. uPA directly catalyzes proteolytic cleavage of plasminogen, resulting in release of the active form plasmin.[43] Regulation of uPA by miR-23b has already been described in different tumor types[24,25] and we indicated that miR-23b is able to repress uPA expression in breast cancer. Moreover, it has been shown that inhibition of uPA activity abolishes breast cancer invasion and metastasis in vivo,[44] which is consistent with our data showing that miR-23b suppression promotes invasion and metastasis in animal models. On the other hand, we identified and validated Annexin 2 as a direct miR-23b target in breast cancer. Annexin 2 is a phospholipid-binding protein that promotes plasminogen activation and degradation of the extracellular matrix (ECM).[45] Annexin 2 localizes to the plasma membrane of invasive cells, where it is frequently found in heterotetramers known as AIIt. AIIt functions as a cell surface receptor for various secreted proteases, including tPA, Cathepsin B and plasminogen itself.[45] Docked on AIIt, both tPA and Cathepsin B mediate plasmin activation by direct proteolysis of plasminogen and by activating uPA, respectively.[45,46] By interacting with different components of the ECM, AIIt provides a structural linkage between the cellular proteolytic system and the ECM, thus promoting localized matrix degradation, and subsequently cell migration and invasion.[45,46] Overexpression of Annexin 2 is found in many tumors, including highly aggressive breast cancers where it correlates with increased invasiveness, neo-angiogenesis and metastasis; moreover, silencing of Annexin 2 reduced migration of MDA-MB-231 cells.[46,47] These observations suggest that miR-23b may further inhibit the metastatic potential of breast cancer cells through repression of Annexin 2.

By considering the overall role of miR-23b in breast cancer, we extrapolated a complex regulatory network that miR-23b imposes to impede acquisition of aggressive traits. This network employs mechanisms of post-transcriptional repression, transcriptomic changes and intracellular dynamics affecting multiple genes that differentially promote or inhibit breast cancer progression.

Notably, we found that miR-23b expression is inversely correlated with breast cancer metastasis. miR-23b is selectively downregulated in breast cancer cell lines that metastasized to different distal organs compared with cells derived from mammary primary tumors after inoculation in the mammary fat pads of nude mice. Accordingly, we found that, in a large cohort of paired primary-metastatic patient samples, miR-23b expression was significantly reduced in lymph-node metastasis compared with their matched primary tumors. In addition, we showed that AP-1 is a transcriptional suppressor of miR-23b expression in breast cancer and that breast cancer cells stimulated with EGF expressed lower levels of mature miR-23b. EGF is an extracellular ligand that specifically activates EGFR, a member of the HER2 family of receptor tyrosine kinases. Activated EGFR dimerizes with its preferred partner HER2 and triggers multiple signaling cascades leading to metastasis.[48] AP-1 is a transcription factor activated downstream of EGFR/HER2 signaling that controls a motogenic and invasive program that confers aggressive behaviors to tumor cells.[6,48] These data suggest that expression of miR-23b in breast cancer may be regulated by EGFR/HER2-activated signaling cascades involving AP-1 activity. Accordingly, miR-23b has been recently found to be downregulated together with miR-27a and miR-27b in HER2-transformed mammary epithelial cells.[49] Since overexpression of HER2 is detected in ~20% of breast cancers and correlates with increased metastatic potential of these tumors, we propose that a reduction in miR-23b expression and the subsequent disruption of its regulatory network are likely to be crucial events in the initiation of cancer progression and metastasis.

Disclosure of Potential Conflicts of Interest

No potential conflicts of interest were disclosed.

Acknowledgments

We would like to thank the support of Action Against Cancer (AAC, http://www.aacancer.org), the Rosetrees trust, and Mike and Lottie Hunter.

References

1. Chaffer CL, Weinberg RA. A perspective on cancer cell metastasis. Science 2011; 331:1559-64; PMID:21436443; http://dx.doi.org/10.1126/science.1203543
2. Entschladen F, Drell TL 4th, Lang K, Joseph J, Zaenker KS. Tumour-cell migration, invasion, and metastasis: navigation by neurotransmitters. Lancet Oncol 2004; 5:254-8; PMID:15050959; http://dx.doi.org/10.1016/S1470-2045(04)01431-7
3. Hall A. Rho GTPases and the actin cytoskeleton. Science 1998; 279:509-14; PMID:9438836; http://dx.doi.org/10.1126/science.279.5350.509
4. Sahai E, Marshall CJ. RHO-GTPases and cancer. Nat Rev Cancer 2002; 2:133-42; PMID:12635176; http://dx.doi.org/10.1038/nrc725
5. Buchsbaum RJ. Rho activation at a glance. J Cell Sci 2007; 120:1149-52; PMID:17376960; http://dx.doi.org/10.1242/jcs.03428
6. Ozanne BW, McGarry L, Spence HJ, Johnston I, Winnie J, Meagher L, Stapleton G. Transcriptional regulation of cell invasion: AP-1 regulation of a multigenic invasion programme. Eur J Cancer 2000; 36(13 Spec No):1640-8; PMID:10959050; http://dx.doi.org/10.1016/S0959-8049(00)00175-1
7. Minn AJ, Gupta GP, Siegel PM, Bos PD, Shu W, Giri DD, Viale A, Olshen AB, Gerald WL, Massagué J. Genes that mediate breast cancer metastasis to lung. Nature 2005; 436:518-24; PMID:16049480; http://dx.doi.org/10.1038/nature03799
8. Kang Y, Siegel PM, Shu W, Drobnjak M, Kakonen SM, Cordón-Cardo C, Guise TA, Massagué J. A multigenic program mediating breast cancer metastasis to bone. Cancer Cell 2003; 3:537-49; PMID:12842083; http://dx.doi.org/10.1016/S1535-6108(03)00132-6
9. Lewis BP, Burge CB, Bartel DP. Conserved seed pairing, often flanked by adenosines, indicates that thousands of human genes are microRNA targets. Cell 2005; 120:15-20; PMID:15652477; http://dx.doi.org/10.1016/j.cell.2004.12.035
10. Lujambio A, Lowe SW. The microcosmos of cancer. Nature 2012; 482:347-55; PMID:22337054; http://dx.doi.org/10.1038/nature10888
11. Pencheva N, Tavazoie SF. Control of metastatic progression by microRNA regulatory networks. Nat Cell Biol 2013; 15:546-54; PMID:23728460; http://dx.doi.org/10.1038/ncb2769
12. Valastyan S, Reinhardt F, Benaich N, Calogrias D, Szász AM, Wang ZC, Brock JE, Richardson AL, Weinberg RA. A pleiotropically acting microRNA, miR-31, inhibits breast cancer metastasis. Cell 2009; 137:1032-46; PMID:19524507; http://dx.doi.org/10.1016/j.cell.2009.03.047
13. Pellegrino L, Stebbing J, Braga VM, Frampton AE, Jacob J, Buluwela L, Jiao LR, Periyasamy M, Madsen CD, Caley MP, et al. miR-23b regulates cytoskeletal remodeling, motility and metastasis by directly targeting multiple transcripts. Nucleic Acids Res 2013; 41:5400-12; PMID:23580553; http://dx.doi.org/10.1093/nar/gkt245
14. Saini HK, Griffiths-Jones S, Enright AJ. Genomic analysis of human microRNA transcripts. Proc Natl Acad Sci U S A 2007; 104:17719-24; PMID:17965236; http://dx.doi.org/10.1073/pnas.0703890104
15. Winter J, Jung S, Keller S, Gregory RI, Diederichs S. Many roads to maturity: microRNA biogenesis pathways and their regulation. Nat Cell Biol 2009; 11:228-34; PMID:19255566; http://dx.doi.org/10.1038/ncb0309-228
16. Kim VN. MicroRNA biogenesis: coordinated cropping and dicing. Nat Rev Mol Cell Biol 2005; 6:376-85; PMID:15852042; http://dx.doi.org/10.1038/nrm1644
17. Lee Y, Ahn C, Han J, Choi H, Kim J, Yim J, Lee J, Provost P, Rådmark O, Kim S, et al. The nuclear RNase III Drosha initiates microRNA processing. Nature 2003; 425:415-9; PMID:14508493; http://dx.doi.org/10.1038/nature01957
18. Castellano L, Stebbing J. Deep sequencing of small RNAs identifies canonical and non-canonical miRNA and endogenous siRNAs in mammalian somatic tissues. Nucleic Acids Res 2013; 41:3339-51; PMID:23325850; http://dx.doi.org/10.1093/nar/gks1474
19. Lund E, Güttinger S, Calado A, Dahlberg JE, Kutay U. Nuclear export of microRNA precursors. Science 2004; 303:95-8; PMID:14631048; http://dx.doi.org/10.1126/science.1090599
20. Bernstein E, Caudy AA, Hammond SM, Hannon GJ. Role for a bidentate ribonuclease in the initiation step of RNA interference. Nature 2001; 409:363-6; PMID:11201747; http://dx.doi.org/10.1038/35053110
21. Gregory RI, Chendrimada TP, Cooch N, Shiekhattar R. Human RISC couples microRNA biogenesis and posttranscriptional gene silencing. Cell 2005; 123:631-40; PMID:16271387; http://dx.doi.org/10.1016/j.cell.2005.10.022
22. Bartel DP. MicroRNAs: target recognition and regulatory functions. Cell 2009; 136:215-33; PMID:19167326; http://dx.doi.org/10.1016/j.cell.2009.01.002
23. Ul Hussain M. Micro-RNAs (miRNAs): genomic organisation, biogenesis and mode of action. Cell Tissue Res 2012; 349:405-13; PMID:22622804; http://dx.doi.org/10.1007/s00441-012-1438-0
24. Zhang HS, Hao Y, Yang J, Zhou Y, Li J, Yin S, Sun C, Ma M, Huang Y, Xi JJ. Genome-wide functional screening of miR-23b as a pleiotropic modulator suppressing cancer metastasis. Nat Commun 2011; 2:554; PMID:22109528; http://dx.doi.org/10.1038/ncomms1555
25. Salvi A, Sabelli C, Moncini S, Venturin M, Arici B, Riva P, Portolani N, Giulini SM, De Petro G, Barlati S. MicroRNA-23b mediates urokinase and c-met downmodulation and a decreased migration of human hepatocellular carcinoma cells. FEBS J 2009; 276:2966-82; PMID:19490101; http://dx.doi.org/10.1111/j.1742-4658.2009.07014.x
26. Au Yeung CL, Tsang TY, Yau PL, Kwok TT. Human papillomavirus type 16 E6 induces cervical cancer cell migration through the p53/microRNA-23b/urokinase-type plasminogen activator pathway. Oncogene 2011; 30:2401-10; PMID:21242962; http://dx.doi.org/10.1038/onc.2010.613
27. Majid S, Dar AA, Saini S, Arora S, Shahryari V, Zaman MS, Chang I, Yamamura S, Tanaka Y, Deng G, et al. miR-23b represses proto-oncogene Src kinase and functions as methylation-silenced tumor suppressor with diagnostic and prognostic significance in prostate cancer. Cancer Res 2012; 72:6435-46; PMID:23074286; http://dx.doi.org/10.1158/0008-5472.CAN-12-2181
28. Rikitake Y, Mandai K, Takai Y. The role of nectins in different types of cell-cell adhesion. J Cell Sci 2012; 125:3713-22; PMID:23027581; http://dx.doi.org/10.1242/jcs.099572
29. Brieher WM, Yap AS. Cadherin junctions and their cytoskeleton(s). Curr Opin Cell Biol 2013; 25:39-46; PMID:23127608; http://dx.doi.org/10.1016/j.ceb.2012.10.010
30. Ooshio T, Irie K, Morimoto K, Fukuhara A, Imai T, Takai Y. Involvement of LMO7 in the association of two cell-cell adhesion molecules, nectin and E-cadherin, through afadin and alpha-actinin in epithelial cells. J Biol Chem 2004; 279:31365-73; PMID:15140894; http://dx.doi.org/10.1074/jbc.M401957200
31. Smutny M, Cox HL, Leerberg JM, Kovacs EM, Conti MA, Ferguson C, Hamilton NA, Parton RG, Adelstein RS, Yap AS. Myosin II isoforms identify distinct functional modules that support integrity of the epithelial zonula adherens. Nat Cell Biol 2010; 12:696-702; PMID:20543839; http://dx.doi.org/10.1038/ncb2072
32. Geiger B, Spatz JP, Bershadsky AD. Environmental sensing through focal adhesions. Nat Rev Mol Cell Biol 2009; 10:21-33; PMID:19197329; http://dx.doi.org/10.1038/nrm2593
33. Coniglio SJ, Zavarella S, Symons MH. Pak1 and Pak2 mediate tumor cell invasion through distinct signaling mechanisms. Mol Cell Biol 2008; 28:4162-72; PMID:18411304; http://dx.doi.org/10.1128/MCB.01532-07
34. Cavalcanti-Adam EA, Volberg T, Micoulet A, Kessler H, Geiger B, Spatz JP. Cell spreading and focal adhesion dynamics are regulated by spacing of integrin ligands. Biophys J 2007; 92:2964-74; PMID:17277192; http://dx.doi.org/10.1529/biophysj.106.089730
35. Friedl P, Wolf K. Plasticity of cell migration: a multiscale tuning model. J Cell Biol 2010; 188:11-9; PMID:19951899; http://dx.doi.org/10.1083/jcb.200909003
36. Baird D, Feng QY, Cerione RA. The Cool-2/alpha-Pix protein mediates a Cdc42-Rac signaling cascade. Curr Biol 2005; 15:1-10; PMID:15649357; http://dx.doi.org/10.1016/j.cub.2004.12.040
37. Rosenberger G, Gal A, Kutsche K. AlphaPIX associates with calpain 4, the small subunit of calpain, and has a dual role in integrin-mediated cell spreading. J Biol Chem 2005; 280:6879-89; PMID:15611136; http://dx.doi.org/10.1074/jbc.M412119200
38. Delorme V, Machacek M, DerMardirossian C, Anderson KL, Wittmann T, Hanein D, Waterman-Storer C, Danuser G, Bokoch GM. Cofilin activity downstream of Pak1 regulates cell protrusion efficiency by organizing lamellipodium and lamella actin networks. Dev Cell 2007; 13:646-62; PMID:17981134; http://dx.doi.org/10.1016/j.devcel.2007.08.011
39. Ghosh M, Song X, Mouneimne G, Sidani M, Lawrence DS, Condeelis JS. Cofilin promotes actin polymerization and defines the direction of cell motility. Science 2004; 304:743-6; PMID:15118165; http://dx.doi.org/10.1126/science.1094561
40. Delorme V, Machacek M, DerMardirossian C, Anderson KL, Wittmann T, Hanein D, Waterman-Storer C, Danuser G, Bokoch GM. Cofilin activity downstream of Pak1 regulates cell protrusion efficiency by organizing lamellipodium and lamella actin networks. Dev Cell 2007; 13:646-62; PMID:17981134; http://dx.doi.org/10.1016/j.devcel.2007.08.011
41. Johnson EO, Chang KH, Ghosh S, Venkatesh C, Giger K, Low PS, Shah K. LIMK2 is a crucial regulator and effector of Aurora-A-kinase-mediated malignancy. J Cell Sci 2012; 125:1204-16; PMID:22492986; http://dx.doi.org/10.1242/jcs.092304
42. Luo DY, Wilson JM, Harvel N, Liu J, Pei L, Huang S, Hawthorn L, Shi H. A systematic evaluation of miRNA:mRNA interactions involved in the migration and invasion of breast cancer cells. J Transl Med 2013; 11:57; PMID:23497265; http://dx.doi.org/10.1186/1479-5876-11-57
43. Danø K, Behrendt N, Høyer-Hansen G, Johnsen M, Lund LR, Ploug M, Rømer J. Plasminogen activation and cancer. Thromb Haemost 2005; 93:676-81; PMID:15841311
44. Rabbani SA, Gladu J. Urokinase receptor antibody can reduce tumor volume and detect the presence of occult tumor metastases in vivo. Cancer Res 2002; 62:2390-7; PMID:11956102

45. Kassam G, Choi KS, Ghuman J, Kang HM, Fitzpatrick SL, Zackson T, Zackson S, Toba M, Shinomiya A, Waisman DM. The role of annexin II tetramer in the activation of plasminogen. J Biol Chem 1998; 273:4790-9; PMID:9468544; http://dx.doi.org/10.1074/jbc.273.8.4790
46. Sharma M, Ownbey RT, Sharma MC. Breast cancer cell surface annexin II induces cell migration and neoangiogenesis via tPA dependent plasmin generation. Exp Mol Pathol 2010; 88:278-86; PMID:20079732; http://dx.doi.org/10.1016/j.yexmp.2010.01.001
47. Shetty PK, Thamake SI, Biswas S, Johansson SL, Vishwanatha JK. Reciprocal regulation of annexin A2 and EGFR with Her-2 in Her-2 negative and herceptin-resistant breast cancer. PLoS One 2012; 7:e44299; PMID:22957061; http://dx.doi.org/10.1371/journal.pone.0044299
48. Moghal N, Sternberg PW. Multiple positive and negative regulators of signaling by the EGF-receptor. Curr Opin Cell Biol 1999; 11:190-6; PMID:10209155; http://dx.doi.org/10.1016/S0955-0674(99)80025-8
49. Pincini A, Tornillo G, Orso F, Sciortino M, Bisaro B, Camacho-Leal MD, Lembo A, Brizzi MF, Turco E, De Pittà C, et al. Identification of p130Cas/ErbB2-dependent invasive signatures in transformed mammary epithelial cells. Cell Cycle 2013; 12; PMID:23839042; http://dx.doi.org/10.4161/cc.25415

EXPERT REVIEWS

Altered expression of the miRNA processing endoribonuclease Dicer has prognostic significance in human cancers

Expert Rev. Anticancer Ther. 13(1), 00–00 (2013)

Loredana Pellegrino*[1], Jimmy Jacob[1], Laura Roca-Alonso[1], Jonathan Krell[1], Leandro Castellano[1], and Adam E Frampton[2]

[1]Division of Oncology, Department of Surgery & Cancer, Imperial Centre for Translational and Experimental Medicine (ICTEM), Imperial College, Hammersmith Hospital Campus, Du Cane Road, London, W12 0NN, UK
[2]HPB Surgical Unit, Department of Surgery & Cancer, Imperial College, Hammersmith Hospital, Du Cane Road, London, W12 0HS, UK
*Author for correspondence: l.pellegrino@imperial.ac.uk

Evaluation of: Jafarnejad SM, Ardekani GS, Ghaffari M, Martinka M, Li G. Sox4-mediated Dicer expression is critical for suppression of melanoma cell invasion. *Oncogene* doi:10.1038/onc.2012.239 (2012) (Epub ahead of print).

Several studies have implicated miRNAs in the initiation and progression of human cancers. Examining the biogenesis pathways that generate these important regulatory molecules has revealed new mechanisms for tumor development. Altered expression of the endoribonuclease Dicer in many tumors has given new hope to unraveling the complex relationship between miRNA processing and cancer. This may provide further insight into mechanisms for targeting multiple genes that are critical for the malignant phenotype of several cancers. The evaluated article demonstrates that Dicer is transcriptionally regulated by Sox4 and reduced levels of this transcription factor consequently leads to a reduction in expression and therefore deregulation of cancer-related miRNAs in melanoma. Reduced Dicer expression in malignant melanoma is an independent predictor of poor survival. In this review, the authors assess the prognostic significance of Dicer expression in different tumor types.

Keywords: Dicer • melanoma • microRNA • prognostic marker • survival

MicroRNAs (miRNAs) are small noncoding RNAs that regulate the expression of target genes at the post-transcriptional level [1]. They are predicted to inhibit protein synthesis from >60% of human genes [2]. miRNAs plays an important role in almost all biological processes, including cancer. Although miRNAs can function as either tumor suppressors or oncogenes, an overall down-regulation of miRNA levels has been described in cancer [3]. Mechanisms that could sustain this reduction in miRNA abundance include genetic and epigenetic events affecting the expression of either the miRNA gene itself or members of the miRNA processing pathway [4,5]. Dicer is crucial for the maturation of miRNAs, therefore its altered expression may contribute to tumor initiation and progression. Several studies have associated aberrant Dicer expression with prognosis in various tumor types [6]. In the evaluated article, Jafarnejad *et al.* report for the first time that reduced Dicer expression is due to reduced transcription and correlates with poor survival in metastatic melanoma [7].

Summary of methods & results

The oncogenic and tumor suppressive effects of the Sox4 transcription factor are cell-type dependent and vary between tumors. In endometrial cancer, miR-129-2 down-regulates Sox4 expression leading to reduced cancer cell proliferation [8] and in colon cancer cells Sox4 has been shown to regulate cell-cycle arrest, apoptosis and tumor growth in a p53-dependent manner [9]. In prostate cancer, genome-wide promoter analysis revealed that Sox4 directly positively regulates the expression of three components of the RNA-induced silencing complex (Dicer, argonaute 1 and RNA helicase A) and other transcriptional targets involved in cancer progression and tumor metastasis [10]. Furthermore, Sox4 overexpression

 10.1586/ERA.12.150 ISSN 1473-7140

in bladder cancer cells impaired viability and high levels in tumor samples correlated with improved patient survival [11]. In melanoma, Jafarnejad *et al.* have previously shown that reduced Sox4 expression is associated with metastatic disease, compared with dysplastic nevi or primary melanoma [12]. In addition, reduced nuclear Sox4 expression was an independent prognostic factor for poor overall and disease-specific survival in metastatic melanoma and high-risk primary melanoma [12].

Sox4 transcription factor positively regulates Dicer expression in melanoma

The aims of the current study were to unravel the Sox4-associated Dicer-regulatory mechanisms in melanoma and assess the prognostic significance of altered Dicer expression in tumor samples [7]. The authors initially demonstrate that knockdown of Sox4 by siRNA or overexpression of Sox4 by POTB7-Sox4 decreases or increases Dicer mRNA levels respectively. Sox4 binding to and activation of the Dicer promoter region was then confirmed, as was its ability to regulate Dicer transcription.

Melanoma cell invasion is inhibited by Sox4 in a Dicer-dependent manner

The authors had previously demonstrated that Sox4 knockdown increased cell invasion by threefold and in the present study they showed that Dicer knockdown increases cell invasion in melanoma cell lines by 1.7- to two fold compared with controls. To investigate the relationship between Sox4 and Dicer expression on cell invasiveness, Flag-Dicer was overexpressed in Sox4-KD (knockdown) cells leading to a partial reduction in cell invasion.

Reduced Dicer cytoplasmic staining correlates with disease progression & poor survival in melanoma patients

Next, a large tissue microarray containing scores from 514 patients (30 normal nevi, 87 dysplastic nevi, 262 primary melanomas and 135 metastatic melanomas) was used to evaluate the relationship between cytoplasmic staining of Dicer and clinicopathologic characteristics and survival outcomes. Reduced Dicer expression was found in metastatic melanoma compared with the other tissue types ($p = 0.003$). However, they were no differences in Dicer expression between normal nevi, dysplastic nevi and primary melanomas. Interestingly, there was an inverse correlation between Dicer expression and AJCC disease stage (i.e. negative-weak staining associated with more advanced disease). Multivariate Cox regression was then performed for primary and metastatic melanoma cases using cytoplasmic Dicer staining, age and sex as covariates. This demonstrated that negative-weak Dicer cytoplasmic staining was an independent predictor of poor overall ($p = 0.002$) and disease-specific survival ($p = 0.007$). It would have been appropriate to show the results for other univariate factors (e.g. Breslow thickness) to examine their influence on patient survival and perhaps include this in the multivariate model. Some of the results were validated using a second anti-Dicer antibody, including the correlations between reduced Dicer cytoplasmic staining and metastatic melanoma ($p = 0.001$) and poor disease-specific survival ($p = 0.037$). Furthermore, comparison with a previous Sox4 tissue microarray revealed that patients with strong Sox4 immunostaining also had higher Dicer expression ($p = 0.004$).

Cancer & melanoma-related miRNAs are regulated by Sox4

Sox4-KD cells (that have reduced Dicer expression) were found to have >twofold downregulation of 34.9% and >twofold upregulation of 26.5% of miRNAs compared with control transfected cells. Rescue of Dicer expression in Sox4-KD cells was able to increase 64.5% (198/307) of downregulated miRNAs back to either control or higher than control levels. These data indicate that Sox4 also plays a critical role in miRNA biogenesis. Ingenuity pathway analysis indicated that 61 cancer-related miRNAs were deregulated in Sox4-KD cells compared with controls and rescue of Dicer was able to specifically correct their expression.

Discussion

Dicer is a cytoplasmic endoribonuclease Type III essential for the final step of miRNA maturation [13]. Based on large-scale profiling, a general downregulation of miRNAs has been highlighted in cancer. A single mutation in the *Dicer1* locus is potentially deleterious for the normal miRNA profile inside a particular cell; it is therefore unsurprising that an altered expression of Dicer is associated with tumorigenesis. For this reason, several studies have focused on the potential significance of aberrant Dicer expression in cancer patients and investigated it as a prognostic marker.

In the present study, Jafarnejad *et al.* found that Dicer expression is positively regulated by the transcription factor Sox4 in melanoma cell lines [7]. Although Sox4 has already been shown to induce Dicer promoter activity in prostate cancer cells [10], the authors have been able to link their previous evidence of decreased expression of Sox4 in malignant melanoma and its ability to suppress melanoma cell invasion [12] with the Sox4-dependent modulation of Dicer expression. They reveal for the first time that Dicer silencing enhances the invasive capabilities of melanoma cells and restored levels, upon Sox4 knockdown, can reverse this. Although *in vivo* Dicer knockdown experiments are required, these data validate the finding that Dicer downregulation promotes tumor metastasis in melanoma, as well as in other tumor types [14,15]. Furthermore, they report that a reduction in Dicer immunostaining is associated with poorer overall and disease-specific 5-year survival in a large cohort of melanoma patients ($n = 514$). These results were confirmed by using a second anti-Dicer antibody, mentioned in a recent report in which Ma *et al.* actually observed the opposite in that Dicer staining was upregulated in melanoma cases compared with melanocytic nevi ($n = 223$) [16]. To further address this discrepancy, the authors could have used quantitative real-time reverse-transcription PCR to validate Dicer expression at the mRNA level, as immunohistochemical data and semi-quantitative at best. In fact, no correlation between Dicer mRNA and immunostaining levels in FFPE samples has been observed for many of the available antibodies against Dicer [17]. The different techniques of assaying Dicer expression, along with the variability in sample-sizes and the heterogeneity in the source of sample populations, may reflect the variations in the aberrant expression of Dicer that have been

Table 1. Association of Dicer expression with clinicopathological features in different human cancers.

Study (year)	Tumor type	Methods/sample size	Dicer expression	Findings	Ref.
Karube *et al.* (2005)	Lung	Real-time RT-PCR/n = 67 NSCLC cases	Low in a fraction of NSCLC cases	Correlated with poor tumor differentiation ($p = 0.01$) Associated with shorter post-operative survival ($p = 0.0001$) Can be used as predictive factor for disease stage ($p = 0.003$) and poor prognosis ($p < 0.001$)	[21]
Merritt *et al.* (2008)		Real-time RT-PCR/n = 91 tumor patients		High Dicer levels are associated with increased survival ($p = 0.008$)	[22]
Wu *et al.* (2011)	Liver	Real-time RT-PCR/n = 36 HCC and relative adjacent non-neoplastic tissues	Low in malignant tissues compared with non-neoplastic ones in 94.4% of the HCC cases (34 out of 36 patients)	No association between Dicer expression and any clinical characteristics, such as age, sex, tumor number, tumor stage, tumor size and distant metastasis	[23]
Faber *et al.* (2011)	Colorectal	IHC-TMA/n = 237 samples from patients with colorectal adenocarcinoma (no evidence of metastasis)	Null (IHC-score: 0) in n = 15 Low (IHC-score: 1) in n = 126 Moderate (IHC-score: 2) in n = 78 Strong (IHC-score: 3) in n = 18	Strong Dicer expression is associated with poor survival (CSS, $p < 0.001$) and reduced PFS ($p < 0.001$) Null cases for Dicer staining showed no relapse (0/15) compared with 10/18 relapses in the strong Dicer staining group	[24]
Stratmann *et al.* (2011)		Real-time RT-PCR/n = 162 normal mucosa, n = 162 primary CRC, n = 37 liver metastasis tissues	Higher in rectal cancer than in CRC ($p = 0.018$) Higher in primary rectal tumor compared with normal mucosa ($p < 0.034$) (not in CRC patients) Decreased in liver metastases compared with normal and primary tumour tissues (for rectal and colon cancer; $p < 0.05$)	Increased expression of Dicer mRNA in normal mucosa from CRC patients is related to poor survival ($p < 0.001$)	[25]
Papachristou *et al.* (2011)		Real-time RT-PCR/n = 76 primary CRC and n = 27 normal paired specimens	Higher mRNA levels in stage III compared with stage II tumors ($p = 0.032$)	No association between Dicer mRNA levels and overall survival or time to tumor progression	[26]
Faggad *et al.* (2012)		IHC-TMA/n = 331 samples from patients with primary colorectal carcinoma	Negative in 19.4% of tissue samples	Inversely associated with disease stage ($p = 0.029$), tumor grade ($p = 0.001$), tumor stage ($p = 0.022$) and nodal metastasis ($p = 0.004$) Correlates with shortened overall survival ($p = 0.007$)	[27]
Ma *et al.* (2011)	Melanoma	IHC-TMA/n = 404 samples (n = 71 melanocytic nevi, n = 223 melanomas, n = 73 carcinomas, n = 12 sarcomas)	Higher in melanomas compared with benign melanocytic nevi ($p < 0.0001$)	Dicer upregulation is associated with increased tumor mitotic index ($p = 0.04$), Breslow's depth of invasion ($p = 0.03$), nodal metastasis ($p = 0.04$) and AJCC clinical stage ($p = 0.009$)	[16]
Jafarnejad *et al.* (2012)		IHC-TMA/n = 514 FFPE tissues (n = 30 normal nevi, n = 87 dysplatic nevi, n = 262 primary melanomas, n = 135 metastatic melanomas)	Lower in metastatic melanoma compared with other stages of melanocytic lesions ($p = 0.003$) Lower in male individuals compared with their female counterparts ($p = 0.003$)	Is associated with AJCC stages ($p = 0.003$) Is positively correlated with lymphocytic response in primary melanomas ($p = 0.0036$) No correlation between Dicer expression and patient age, tumor thickness, location, subtype or ulceration status Reduced expression is an independent predictor of poor survival	[7]

AJCC: American Joint Committee on Cancer; AML: Acute myeloid leukemia; AR: Androgen receptor; BRCA1: Breast cancer 1 susceptibility protein; CLL: Chronic lymphocytic leukemia; CRC: Colorectal cancer; CSS: Cancer specific survival; ER: Estrogen receptor, HCC: Hepatocarcinoma; IGHV: Immunoglobulin heavy chain variable gene; IHC: Immunohistochemistry; INT: Istituto Nazionale Tumori; LN: Lymph node; MBL: Monoclonal B-cell lymphocytosis; NSCLC: Nonsmall cell lung cancer; PFS: Progression-free survival; PR: Progesterone receptor; PSA: Prostate-specific antigen; RT-PCR: Reverse-transcription PCR; TMA: Tissue microarray.

Table 1. Association of Dicer expression with clinicopathological features in different human cancers (cont.).

Study (year)	Tumor type	Methods/sample size	Dicer expression	Findings	Ref.
Grelier *et al.* (2009)	Breast	Real-time RT-PCR/n = 104 cancer patients vs n = 4 normal tissue samples, IHC-TMA/n = 86 invasive cancer patients vs n = 8 normal tissue samples	Protein staining intensity 0: n = 7; 1: n = 58; 2: n = 21	Lower protein levels (intensity of 0 or 1) are associated with ER and PR positive tumors (p = 0.008 and p = 0.019, respectively) and with luminal A cancer subtype (p = 0.0174) Lower mRNA levels in cases with LN metastasis (p = 0.02) and in tumors not classified as luminal A cancer subtype (p = 0.0481) Only mRNA expression is associated with metastasis-free survival (p = 0.0032)	[28]
Dedes *et al.* (2010)		Real-time RT-PCR, IHC/n = 245 patients receiving adjuvant anthracycline-based chemotherapy vs n = 10 normal tissue samples	Lower in 46% of cases Poor correlation between Dicer mRNA and protein levels	Associated with lack of ER (p < 0.001), PR (p = 0.040) and Bcl2 (p = 0.002) expression, with high grade (p = 0.013), high Ki-67 (p = 0.002), triple negative (p = 0.001) and basal-like phenotypes (basal keratins, p = 0.001; basal markers, p < 0.001; molecular subtypes, p = 0.001) No association between Dicer down-regulation and metastasis-free, disease-free or disease-specific survival	[17]
Martello *et al.* (2010)		IHC/Milan INT dataset: n = 69 breast cancer patients (no distant metastasis), Real-time RT-PCR/London dataset: n = 164, Uppsala dataset: n = 249, New York dataset: n = 82, TransBIG dataset: n = 198, Rotterdam dataset: n = 313	Lower protein levels in 80% of Milan INT dataset cases (n = 20) Lower mRNA levels in n = 41, 85, 17, 56, 69 for London, Uppsala, New York, TransBIG and Rotterdam datasets, respectively	No significant association between Dicer mRNA levels and metastasis or outcome	[15]
Yan *et al.* (2012)		Real-time RT-PCR/n = 49 pairs tissues	Lower in 53.1% of cases	No association with age, tumor grade, hormonal receptor status, Her-2 status or subtype	[29]
Khoshnaw *et al.* (2012)		IHC/n = 24 FFPE specimens (normal parenchymal tissue, *in situ* DCIS, invasive tissue adjacent to DCIS and LN metastasis) IHC-TMA/n = 1174 invasive tissue samples	IHC-scores: 250, 180, 150 and 100 in normal, DCIS, invasive and metastatic tissues, respectively (n = 24) Lower (IHC-score ≤157) in 617 cases (negative in 91 cases), stronger (IHC-score ≥157) in 557 cases	Dicer down-regulation is associated with cancer progression (n = 24; higher in normal vs DCIS, p < 0.001; higher in DCIS vs invasive tissue, p = 0.033; higher in invasive vs metastasis, p < 0.001) Loss of Dicer is associated with loss of tubule formation (p = 0.009) loss of ER (p = 0.038), PR (p = 0.023), AR (p = 0.001),BRCA1 (p = 0.003) and p27 expression (p < 0.001) in TMA set Lower Dicer expression is correlated to reduced recurrence at 5-years (p = 0.002) in TMA set	[30]
Merritt *et al.* (2008)		Real-time RT-PCR/n = 129 tumor patients		High Dicer expression is associated with increased disease-free survival (p = 0.006)	[22]

AJCC: American Joint Committee on Cancer; AML: Acute myeloid leukemia; AR: Androgen receptor; BRCA1: Breast cancer 1 susceptibility protein; CLL: Chronic lymphocytic leukemia; CRC: Colorectal cancer; CSS: Cancer specific survival; ER: Estrogen receptor, HCC: Hepatocarcinoma; IGHV: Immunoglobulin heavy chain variable gene; IHC: Immunohistochemistry; INT: Istituto Nazionale Tumori; LN: Lymph node; MBL: Monoclonal B-cell lymphocytosis; NSCLC: Nonsmall cell lung cancer; PFS: Progression-free survival; PR: Progesterone receptor; PSA: Prostate-specific antigen; RT-PCR: Reverse-transcription PCR; TMA: Tissue microarray.

Table 1. Association of Dicer expression with clinicopathological features in different human cancers (cont.).

Study (year)	Tumor type	Methods/sample size	Dicer expression	Findings	Ref.
Martin *et al.* (2009)	Leukemia	Affymetrix GeneChip HG U133 Plus 2.0 array/n = 71 non M3 AML cases and n = 5 CD34+ normal bone marrows	Higher in 86% of AML samples	No association between Dicer levels and percent attaining complete response to induction therapy, event-free survival and overall survival	[31]
Zhu *et al.* (2012)	Leukemia	Real-time RT-PCR/n = 165 CLL patients, n = 8 MBL cases, n = 10 age-matched normal controls	Lower in CLL patients compared with normal controls ($p = 0.0055$) and MBL cases ($p = 0.0126$)	Lower Dicer expression correlates with more aggressive Binet stage ($p = 0.001$) Lower Dicer levels in patients with unmutated *IGHV* genes compared with patients with *IGHV* mutations ($p < 0.0001$), in CD-38-positive group than in CD-38 negative one ($p = 0.0304$), in ZAP-70-positive patients than ZAP-70 negative ones ($p = 0.0075$), in patients with deletion in 17p13 or 11q22.3 in contrast to patients with good risk cytogenetics ($p = 0.011$) Lower Dicer expression is associated with shorter overall survival ($p = 0.0046$) and reduced treatment free survival ($p = 0.0046$)	[32]
Zighelboim *et al.* (2011)	Endometrial	qRT-PCR/n = 169 endometrioid endometrial tumors (n = 57 recurrent, n = 112, non-recurrent [controls])	Lower in primary endometrial cancers with subsequent recurrence	Is not associated with age, race or surgical stages Lower Dicer mRNA levels are associated with lower grade tumors ($p = 0.02$) and decreased disease-free survival ($p = 0.01$)	[33]
Flavin *et al.* (2008)	Ovary	IHC-TMA/n = 66 FFPE ovarian serous adenocarcinoma tumors vs n = 40 age-matched normal ovaries Real-time RT-PCR/n = 50 independent FFPE ovarian serous adenocarcinoma cases	Higher mRNA levels in ovarian serous adenocarcinomas vs normal whole ovary ($p = 0.054$) Higher protein levels (stronger in 74% of cases) in ovarian serous adenocarcinomas vs normal whole ovary ($p < 0.0001$)	Modest correlation between Dicer mRNA and protein levels ($p = 0.03$) Higher Dicer expression correlates with absence of LN metastasis ($p = 0.02$), Ki-67 proliferation index less than 50% ($p = 0.03$) compared with low Dicer expression No significant association between Dicer expression and disease-free or overall survival	[34]
Merritt *et al.* (2008)		Real-time RT-PCR/n = 111 patients with invasive epithelial ovarian cancer vs n = 11 benign ovarian epithelial samples IHC/n = 32 subgroup of ovarian tumors	Lower mRNA levels in 60% of tumor cases	Correlation between mRNA and protein levels Lower Dicer expression is associated with advanced tumor stage ($p = 0.007$) High Dicer expression is associated with increased median survival ($p < 0.001$) Decreased mRNA level was and indicator of poor survival ($p = 0.02$)	[22]
Chiosea *et al.* (2006)	Prostate	Affymetrix Chip Hybridization/n = 104 prostate samples (n = 16 normal, n = 64 organ-confined prostate cancer tissues, n = 24 metastatic tissues) IHC-TMA/n = 232 specimens from 166 patients	Higher mRNA levels in metastatic tissues compared with organ-confined tumors	Association between increased Dicer protein expression and clinical stage ($p = 0.001$) and pathological T stage ($p < 0.009$)	[35]

AJCC: American Joint Committee on Cancer; AML: Acute myeloid leukemia; AR: Androgen receptor; BRCA1: Breast cancer 1 susceptibility protein; CLL: Chronic lymphocytic leukemia; CRC: Colorectal cancer; CSS: Cancer specific survival; ER: Estrogen receptor, HCC: Hepatocarcinoma; IGHV: Immunoglobulin heavy chain variable gene; IHC: Immunohistochemistry; INT: Istituto Nazionale Tumori; LN: Lymph node; MBL: Monoclonal B-cell lymphocytosis; NSCLC: Nonsmall cell lung cancer; PFS: Progression-free survival; PR: Progesterone receptor; PSA: Prostate-specific antigen; RT-PCR: Reverse-transcription PCR; TMA: Tissue microarray.

Table 1. Association of Dicer expression with clinicopathological features in different human cancers (cont.).

Study (year)	Tumor type	Methods/sample size	Dicer expression	Findings	Ref.
			Increased protein levels in 81% of prostate cancers specimens ($p = 0.006$)	No correlation between Dicer protein expression and PSA relapse	
Tchernitsa *et al.* (2010)	Gastric	IHC-TMA/n = 332 patients	Higher in tumors than in non-neoplastic faveolar epithelium ($p < 0.001$)	Higher Dicer levels are associated with tumor type (intestinal vs diffuse type, $p < 0.001$) and with local tumor growth ($p = 0.007$) No correlation between Dicer expression and survival	[36]

AJCC: American Joint Committee on Cancer; AML: Acute myeloid leukemia; AR: Androgen receptor; BRCA1: Breast cancer 1 susceptibility protein; CLL: Chronic lymphocytic leukemia; CRC: Colorectal cancer; CSS: Cancer specific survival; ER: Estrogen receptor, HCC: Hepatocarcinoma; IGHV: Immunoglobulin heavy chain variable gene; IHC: Immunohistochemistry; INT: Istituto Nazionale Tumori; LN: Lymph node; MBL: Monoclonal B-cell lymphocytosis; NSCLC: Nonsmall cell lung cancer; PFS: Progression-free survival; PR: Progesterone receptor; PSA: Prostate-specific antigen; RT-PCR: Reverse-transcription PCR; TMA: Tissue microarray.

detected within the same tumor type and across different cancers (Table 1). This lack of consistency could make validating Dicer as a novel prognostic cancer biomarker difficult.

Five-year view

Melanoma is phenotypically aggressive and associated with high mortality. Our understanding of the tumor biology of melanoma is relatively poor compared with many other cancers, but recent progress has been made in the identification of specific prognostic and predictive biomarkers, such as BRAF and AKT3, which has led to the design and clinical implementation of new targeted agents. Despite this, there is a clear need for the identification of further biomarkers and therapeutic targets in melanoma. Although Dicer itself is not a tumor suppressor gene, its expression is often reduced in melanoma and the associated reduction in processing and production of mature tumor suppressing miRNAs can contribute greatly to disease proliferation, invasion and metastasis. Therefore Dicer replacement or methods to increase Dicer expression in these tumors may improve outcome in this disease. Different accessory proteins that modulate the rate of Dicer processing can have far reaching effects on the production of specific subsets of miRNAs. Dicer-interacting proteins, such as Sox4, therefore represent a crucial window in the deregulation of gene expression present in many cancers. This study [7] is the first to show a positive correlation between Sox4 and Dicer in melanoma patients, and it demonstrates a significant positive correlation between increased expression of these proteins and better patient survival. This suggests a potentially important role for both Dicer and Sox4 as prognostic biomarkers in melanoma in the coming years, although larger studies encompassing protocols outlined by the REMARK group are required to validate this [18]. Furthermore, it provides further evidence that maintaining Dicer expression levels in melanoma may improve patient outcome. Based on the results of this study the authors propose that this could potentially be achieved by upregulating Sox4 expression in tumors, perhaps by using small activating RNAs [19] or gene therapy. Although the *in vivo* delivery of miRNA, small activating RNA and siRNA to tumors has proved challenging, predominantly due to difficulties with drug delivery and tissue-targeting, there have been significant advances recently, most notably the use of a nanoparticle system to successfully deliver an siRNA to the M2 subunit of ribonucleotide reductase in melanoma [20]. This suggests that the design of a similar system to deliver Sox4 may not be beyond the realms of possibility in the future. This study also provides a brief insight into a Sox4-regulated miRNA biogenesis pathway. Although further studies are necessary to elucidate the precise role of Sox4-regulated miRNAs, this could provide even further therapeutic opportunities by replacing Sox4-regulated tumor suppressing miRNAs in tumors with reduced Sox4 or Dicer expression. Additionally, if miRNAs that target Sox4 are identified then RNAi based therapies could be designed to reduce miRNA-induced repression of Sox4 expression. Although the authors are far from achieving these goals, this study provides new insight into potentially novel therapies for this aggressive disease.

Financial & competing interests disclosure

The authors have no relevant affiliations or financial involvement with any organization or entity with a financial interest in or financial conflict with the subject matter or materials discussed in the manuscript. This includes employment, consultancies, honoraria, stock ownership or options, expert testimony, grants or patents received or pending, or royalties.

No writing assistance was utilized in the production of this manuscript.

Key issues

- Sox4 positively regulates Dicer expression at the transcriptional level in melanoma.
- Sox4-dependent deregulation of a subset of cancer-related miRNAs appears important in melanoma.
- Low Dicer expression correlates with melanoma progression and is an independent predictor of poor survival.
- Although many studies have suggested Dicer as a novel marker for prognosis in different human cancers, further investigation of the underlying mechanisms are required.

References

1 Bartel DP. MicroRNAs: target recognition and regulatory functions. *Cell* 136(2), 215–233 (2009).

2 Friedman RC, Farh KK, Burge CB, Bartel DP. Most mammalian mRNAs are conserved targets of microRNAs. *Genome Res.* 19(1), 92–105 (2009).

3 Lu J, Getz G, Miska EA *et al.* MicroRNA expression profiles classify human cancers. *Nature* 435(7043), 834–838 (2005).

4 Garzon R, Calin GA, Croce CM. MicroRNAs in Cancer. *Annu. Rev. Med.* 60, 167–179 (2009).

5 Davalos V, Esteller M. Rolling the dice to discover the role of DICER in tumorigenesis. *Cancer Cell* 21(6), 717–719 (2012).

6 Bahubeshi A, Tischkowitz M, Foulkes WD. miRNA processing and human cancer: DICER1 cuts the mustard. *Sci. Transl. Med.* 3(111), 111ps46 (2011).

7 Jafarnejad SM, Ardekani GS, Ghaffari M, Martinka M, Li G. Sox4-mediated Dicer expression is critical for suppression of melanoma cell invasion. *Oncogene* doi:10.1038/onc.2012.239 (2012) (Epub ahead of print).

8 Huang YW, Liu JC, Deatherage DE *et al.* Epigenetic repression of microRNA-129-2 leads to overexpression of SOX4 oncogene in endometrial cancer. *Cancer Res.* 69(23), 9038–9046 (2009).

9 Pan X, Zhao J, Zhang WN *et al.* Induction of SOX4 by DNA damage is critical for p53 stabilization and function. *Proc. Natl Acad. Sci. U.S.A.* 106(10), 3788–3793 (2009).

10 Scharer CD, McCabe CD, Ali-Seyed M, Berger MF, Bulyk ML, Moreno CS. Genome-wide promoter analysis of the SOX4 transcriptional network in prostate cancer cells. *Cancer Res.* 69(2), 709–717 (2009).

11 Aaboe M, Birkenkamp-Demtroder K, Wiuf C *et al.* SOX4 expression in bladder carcinoma: clinical aspects and *in vitro* functional characterization. *Cancer Res.* 66(7), 3434–3442 (2006).

12 Jafarnejad SM, Wani AA, Martinka M, Li G. Prognostic significance of Sox4 expression in human cutaneous melanoma and its role in cell migration and invasion. *Am. J. Pathol.* 177(6), 2741–2752 (2010).

13 Tijsterman M, Plasterk RH. Dicers at RISC; the mechanism of RNAi. *Cell* 117(1), 1–3 (2004).

14 Su X, Chakravarti D, Cho MS *et al.* TAp63 suppresses metastasis through coordinate regulation of Dicer and miRNAs. *Nature* 467(7318), 986–990 (2010).

15 Martello G, Rosato A, Ferrari F *et al.* A MicroRNA targeting dicer for metastasis control. *Cell* 141(7), 1195–1207 (2010).

16 Ma Z, Swede H, Cassarino D, Fleming E, Fire A, Dadras SS. Up-regulated Dicer expression in patients with cutaneous melanoma. *PLoS ONE* 6(6), e20494 (2011).

17 Dedes KJ, Natrajan R, Lambros MB *et al.* Down-regulation of the miRNA master regulators Drosha and Dicer is associated with specific subgroups of breast cancer. *Eur. J. Cancer* 47(1), 138–150 (2011).

18 McShane LM, Altman DG, Sauerbrei W, Taube SE, Gion M, Clark GM; Statistics Subcommittee of the NCI-EORTC Working Group on Cancer Diagnostics. REporting recommendations for tumor MARKer prognostic studies (REMARK). *Nat. Clin. Pract. Urol.* 2(8), 416–422 (2005).

19 Place RF, Wang J, Noonan EJ *et al.* Formulation of Small Activating RNA Into Lipidoid Nanoparticles Inhibits Xenograft Prostate Tumor Growth by Inducing p21 Expression. *Mol. Ther. Nucleic Acids* 1, e15 (2012).

20 Davis ME, Zuckerman JE, Choi CH *et al.* Evidence of RNAi in humans from systemically administered siRNA via targeted nanoparticles. *Nature* 464(7291), 1067–1070 (2010).

21 Karube Y, Tanaka H, Osada H *et al.* Reduced expression of Dicer associated with poor prognosis in lung cancer patients. *Cancer Sci.* 96(2), 111–115 (2005).

22 Merritt WM, Lin YG, Han LY *et al.* Dicer, Drosha, and outcomes in patients with ovarian cancer. *N. Engl. J. Med.* 359(25), 2641–2650 (2008).

23 Wu JF, Shen W, Liu NZ *et al.* Down-regulation of Dicer in hepatocellular carcinoma. *Med. Oncol.* 28(3), 804–809 (2011).

24 Faber C, Horst D, Hlubek F, Kirchner T. Overexpression of Dicer predicts poor survival in colorectal cancer. *Eur. J. Cancer* 47(9), 1414–1419 (2011).

25 Stratmann J, Wang CJ, Gnosa S *et al.* Dicer and miRNA in relation to clinicopathological variables in colorectal cancer patients. *BMC Cancer* 11, 345 (2011).

26 Papachristou DJ, Korpetinou A, Giannopoulou E *et al.* Expression of the ribonucleases Drosha, Dicer, and Ago2 in colorectal carcinomas. *Virchows Arch.* 459(4), 431–440 (2011).

27 Faggad A, Kasajima A, Weichert W *et al.* Down-regulation of the microRNA processing enzyme Dicer is a prognostic factor in human colorectal cancer. *Histopathology* doi:10.1111/j.1365-2559.2011.04110.x (2012) (Epub ahead of print).

28 Grelier G, Voirin N, Ay AS *et al.* Prognostic value of Dicer expression in human breast cancers and association with the mesenchymal phenotype. *Br. J. Cancer* 101(4), 673–683 (2009).

29 Yan M, Huang HY, Wang T *et al.* Dysregulated expression of dicer and drosha in breast cancer. *Pathol. Oncol. Res.* 18(2), 343–348 (2012).

30 Khoshnaw SM, Rakha EA, Abdel-Fatah TM *et al.* Loss of Dicer expression is associated with breast cancer progression and recurrence. *Breast Cancer Res. Treat.* 135(2), 403–413 (2012).

31 Martin MG, Payton JE, Link DC. Dicer and outcomes in patients with acute myeloid leukemia (AML). *Leuk. Res.* 33(8), e127 (2009).

32 Zhu DX, Fan L, Lu RN *et al.* Downregulated Dicer expression predicts poor prognosis in chronic lymphocytic leukemia. *Cancer Sci.* 103(5), 875–881 (2012).

33 Zighelboim I, Reinhart AJ, Gao F *et al.* DICER1 expression and outcomes in endometrioid endometrial adenocarcinoma. *Cancer* 117(7), 1446–1453 (2011).

34 Flavin RJ, Smyth PC, Finn SP *et al.* Altered eIF6 and Dicer expression is associated with clinicopathological features in ovarian serous carcinoma patients. *Mod. Pathol.* 21(6), 676–684 (2008).

35 Chiosea S, Jelezcova E, Chandran U *et al.* Up-regulation of dicer, a component of the MicroRNA machinery, in prostate adenocarcinoma. *Am. J. Pathol.* 169(5), 1812–1820 (2006).

36 Tchernitsa O, Kasajima A, Schäfer R *et al.* Systematic evaluation of the miRNA-ome and its downstream effects on mRNA expression identifies gastric cancer progression. *J. Pathol.* 222(3), 310–319 (2010).